

AMPK controls the regenerative programme of DRG sensory neurons after injury

Dissertation

Zur Erlangung des Grades eines
Doktors der Naturwissenschaften

der Mathematisch-Naturwissenschaftlichen Fakultät
und
der Medizinischen Fakultät
der Eberhard-Karls-Universität Tübingen

vorgelegt von
Guiping Kong
aus V.R. China

Tübingen
February - 2018

Tag der mündlichen Prüfung:

Dekan der Math.-Nat. Fakultät:

Prof. Dr. W. Rosenstiel

Dekan der Medizinischen Fakultät:

Prof. Dr. I. B. Autenrieth

1. Berichterstatter:

Prof. Dr. Simone Di Giovanni

2. Berichterstatter:

Prof. Dr. Philipp Kahle

Prüfungskommission:

Prof. Dr. Simone Di Giovanni

Prof. Dr. Philipp Kahle

Dr. Jonas Neher

PD Dr. Andrea Wizenmann

Erklärung / Declaration:

Ich erkläre, dass ich die zur Promotion eingereichte Arbeit mit dem Titel:

„ AMPK controls the regenerative programme of DRG sensory neurons after injury “

selbständig verfasst, nur die angegebenen Quellen und Hilfsmittel benutzt und wörtlich o- der inhaltlich übernommene Stellen als solche gekennzeichnet habe. Ich versichere an Eides statt, dass diese Angaben wahr sind und dass ich nichts verschwiegen habe. Mir ist bekannt, dass die falsche Abgabe einer Versicherung an Eides statt mit Freiheitsstrafe bis zu drei Jah- ren oder mit Geldstrafe bestraft wird.

I hereby declare that I have produced the work entitled “AMPK controls the regenerative programme of DRG sensory neurons after injury”, submitted for the award of a doctorate, on my own (without external help), have used only the sources and aids indicated and have marked passages included from other works, whether verbatim or in con- tent, as such. I swear upon oath that these statements are true and that I have not concealed anything. I am aware that making a false declaration under oath is punishable by a term of imprisonment of up to three years or by a fine.

Tübingen, den

Datum / Date

.....

Unterschrift /Signature

Index of Contents

Abstract	1
1. Introduction.....	2
1.1 Axon Regeneration in the Peripheral Nervous System.....	2
1.1.1 Anatomy of Peripheral Nerve.....	2
1.1.2 Peripheral Nervous System Regeneration	4
1.1.3 Summary of cell intrinsic mechanisms of axonal regeneration in the PNS.....	5
1.2 Dorsal Root Ganglion (DRG) - an experimental model for axonal regeneration	6
1.3 Axon Regeneration in the Central Nervous System.....	8
1.3.1 Central Nervous System Regeneration	8
1.3.2 The structure differences between peripheral and central nervous system neurons....	8
1.3.3 Extrinsic inhibitors of the CNS regeneration.....	10
1.3.4 Inflammation	12
1.3.5 Intrinsic regeneration mechanisms in CNS	13
1.5 Hypothesis.....	17
1.6 Experimental Strategy.....	18
2. Methods	19
3. Results	29
3.1 L4-6 DRG RNAseq and proteomics from sciatic or central projecting branches of DRG axoplasm following sciatic versus spinal injury identify AMPK as a signaling hub	29
3.2 AMPK α 1 expression, phosphorylation and activity are downregulated following SNA...	36
3.3 Pharmacological inhibition of AMPK promotes DRG regenerative growth	38
3.4 AMPK α immunoprecipitation followed mass spectrometry identifies differential AMPK proteosomal degradation.....	39
3.4.1 AMPK α forms a preferential protein complex with the proteasome after SNA, which controls AMPK α 1 expression.	39
3.4.2 AMPK α 1 protein degradation is regulated by proteasome activity.....	41
3.5 PSMC5 forms a protein complex with AMPK α 1 to regulate AMPK α 1 expression	42
3.6 CaMKII α activation is required for SNA-dependent AMPK α 1 degradation.....	46
3.7 The E3 ligase Trim28 is involved AMPK α 1 degradation in DRG neurons after SNA.....	47
3.8 AMPK α 1 deletion promotes axonal regeneration and sensory recovery after SCI.....	49
3.9 L4-6 DRG AMPK α 1 conditional deletion in sensory neurons enhances key regenerative signaling molecules	53
4. Discussion	56
4.1 Combined RNAseq in DRG and axoplasm proteomics bioinformatics analysis reveals a distinct injury response between peripheral and central axons injuries	56
4.2 AMPK is a novel regulator contributing to axonal regeneration	56
4.3 SNA induced AMPK α 1 degradation is dependent upon the proteasome	59
4.4 Calcium activated CaMKII α is necessary for SNA induced AMPK α 1 degradation	61
4.5 The E3 ligase Trim28 is involved in AMPK α 1 degradation via ubiquitination-proteasome system.....	62
4.6 Conditional deletion of AMPK α 1 promotes axonal regeneration and functional recovery after SCI	62
4.7 A novel mechanism that involved in AMPK α 1 degradation after SNA in DRGs.....	64
5. Outlook.....	66
6. References.....	67
7. Appendix	82

7.1 List of Figures	82
7.2 List of Abbreviations	84
8. Supplementary files.....	85
Supplementary file 1.....	85
Supplementary file 2.....	101
Supplementary file 3.....	105
Supplementary file 4.....	106
Supplementary file 5.....	128
Supplementary file 6.....	135
Supplementary file 7.....	135
Supplementary file 8.....	136
Supplementary file 9.....	137
Supplementary file 10.....	137
Supplementary file 11.....	138
Acknowledgements	144
Curriculum Vitae.....	145

Abstract

Regeneration after injury occurs in axons that lie in the peripheral nervous system but it fails in the central nervous system limiting functional recovery. Despite recent progress, to date we ignore the molecular identity of peripheral versus central projecting axons that might underpin this differential regenerative ability. To fill this knowledge gap, here we combined axoplasmic proteomics from sciatic or centrally projecting branches of L4-6 DRG with RNAseq to compare axonal and cell body responses between a regeneration-incompetent central spinal versus regeneration-competent peripheral sciatic nerve injury. This allowed identifying for the first time signalling pathways uniquely represented in peripheral versus central projecting L4-6 DRG axons, including prior and subsequent to an injury. Next, RNAseq and proteomics network and pathway analysis suggested AMPK as master regulator controlling axonal regenerative signalling pathways. AMPK immunoprecipitation followed by mass spectrometry from DRG suggested that the 26S proteasome and the 26S regulatory subunit PSMC5 are preferentially bound to AMPK α for proteasomal degradation following sciatic axotomy. Mechanistically, we found that phosphorylation of proteasomal subunit PSMC5 and injury activated CaMKII α are required for AMPK α 1 degradation after sciatic injury. Moreover, ubiquitin E3 ligase Trim28 regulates AMPK α 1 expression. Finally, conditional deletion of AMPK α 1 promotes multiple regenerative signals, axonal regeneration and functional recovery of sensory axons across the injured spinal cord, suggesting inhibition of AMPK as novel regenerative target following spinal injury.

1. Introduction

In adult mammalian central nervous system (CNS), axons do not spontaneously regenerate after injury, which contributes to extremely limited functional recovery after trauma. In contrast, adult peripheral nervous system (PNS) axons can regenerate following functional recovery after peripheral nerve injury. Studies by Aguayo and his colleagues demonstrated that some injured mature CNS axons can regrow into the grafted permissive peripheral nerve (Benfey and Aguayo, 1982; David and Aguayo, 1981; Richardson et al., 1984; Richardson et al., 1980). This research revealed that the PNS environment is permissive but the CNS environment is inhibitory for the axon growth. Based on this hypothesis, numerous studies have focused on searching molecules and signaling mechanisms of the extrinsic inhibitory environment for axon regrowth. As a consequence, a number of inhibitory factors including of molecules associated with glial scar, specific protein in myelin debris and even axonal components have been found in CNS (Case and Tessier-Lavigne, 2005; Schwab and Strittmatter, 2014; Silver et al., 2015). While later studies suggested that removing or blocking of extrinsic inhibitory molecules activity resulted in some types of axons regrowth, however, in most cases, these treatments were not sufficient for the axon regeneration. Meanwhile, Tuszynski group found that implanted human induced pluripotent stem cells (iPSCs) can survive and differentiate into neurons and glia and are shown extending axons throughout white and grey matter with new synapses formation after spinal cord injury (Lu et al., 2012) (Lu et al., 2014). These studies also serve as a proof that neurons with high growth capacity can regrow in the injured CNS despite the presence of inhibitory environment. Therefore, the intrinsic regenerative capacity decline following development more likely contributes to the regeneration failure in the adult CNS after injury.

1.1 Axon Regeneration in the Peripheral Nervous System

1.1.1 Anatomy of Peripheral Nerve

The peripheral nervous system consists of three types of cells: neuronal, glial, and stromal cells. Nerves are formed from various combinations of motor, sensory, and autonomic neurons. Efferent neurons (motor and autonomic) receive signals through their dendrites from central nervous system neurons, mainly using the neurotransmitter acetylcholine among others.

Afferent (sensory) neurons receive their signals through their dendrites from specialized cell types, such as Dorsal Root Ganglion (DRG) for nociception, mechanoreception and proprioception. These signals are sent to the CNS to provide sensory information to the brain or interneurons in the spinal cord when a reflex response is necessary (Menorca et al., 2013).

Besides neurons, non-neuronal cells play a key role in the maintenance and function of peripheral nerve. Schwann cells form a layer of myelin enveloping the myelinated axons and provide trophic support through releasing important neurotrophins such as Nerve Growth Factor (NGF) (Taniuchi et al., 1988). The myelin sheath is laid down in small segments which are called internodes and each segment is formed by one Schwann cell. The gap between segments is termed as the node of Ranvier. Ranvier forms between each individual Schwann cells that allows the action potentials jump from node of Ranvier to node of Ranvier which is termed as saltatory conduction that improves the conduction velocity (Figure1)(Hille, 2001; Salzer, 1997; Vabnick and Shrager, 1998).

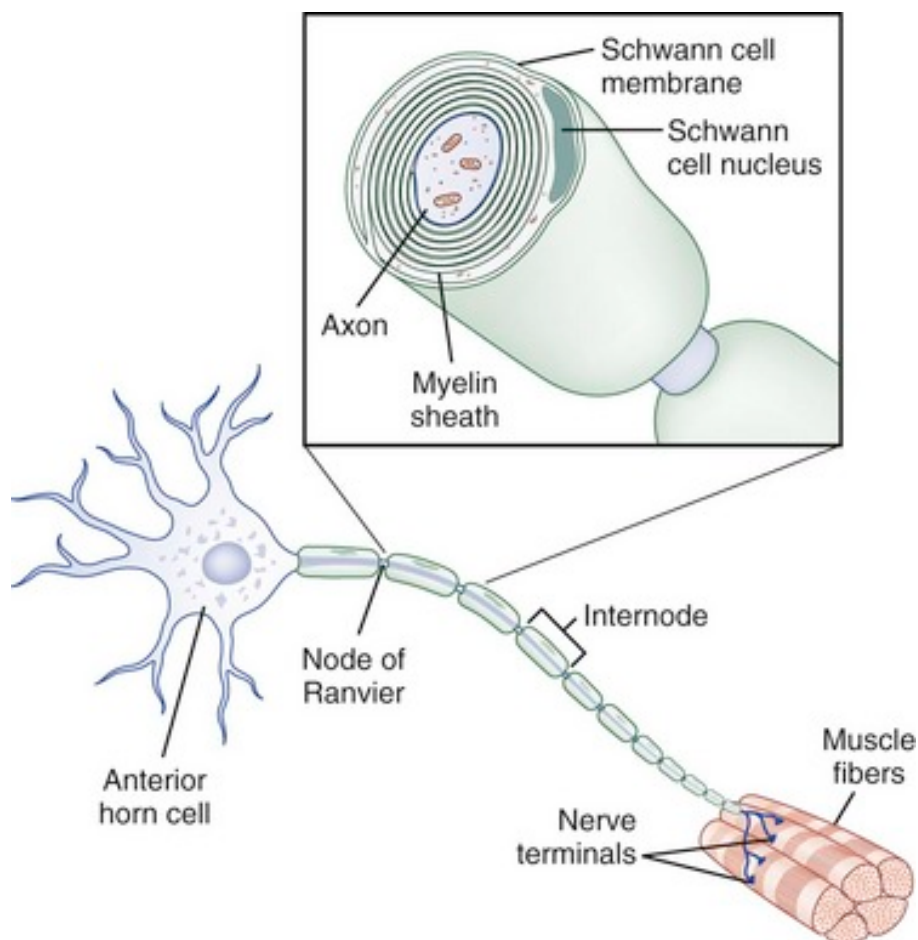


Figure 1. The anatomical diagram of a peripherals nerve. The motor neuron lies in the anterior horn of spinal cord. Axons extend from the anterior horn cell body and contact with their target muscles. Schwann cells which are termed as the local support cells form a myelin sheath that is paved in segments called internodes and each internode is derived from one Schwann cell. The gap between internode is called node of Ranvier (Tsao et al., 2012).

1.1.2 Peripheral Nervous System Regeneration

Adult PNS neurons are able to regenerate after injury, which serves as a useful model to study how the regenerative program is initiated after injury. After peripheral nerve injury, the axon is divided into two segments: the proximal part which contacts the cell body and the distal part of the axon, which is disconnected from the cell body, which undergoes Wallerian degeneration. Schwann cells divide and initiate to phagocytize myelin and axonal debris on their own before the recruitment of macrophages that complete the destruction and phagocytosis of all debris (Fu and Gordon, 1997; Sulaiman and Gordon, 2003). The proximal part of the axon attached to the cell body retains intact myelin although the diameter declines. The regenerating axons sprout form growth cones from the cut end and grow into Schwann cell-lined endoneurial tubes (Büngner) where they are attracted by neurotrophic factors secreted by Schwann cells. Meanwhile, the neuronal cell body undergoes chromatolysis that is followed by metabolic changes and synthesis of proteins required for regeneration which are transported to the growth cones (Deumens et al., 2010; Navarro et al., 2007). When the regenerated axons reach their target muscles and sense organs, they make functional connections to restore movement and sensation (Gordon and Stein, 1982). Following axonal regeneration, Schwann cells progressively remyelinate axons and the size of nerves return to normal after they make functional connections with their targets (Gordon and Stein, 1982) (Figure 2).

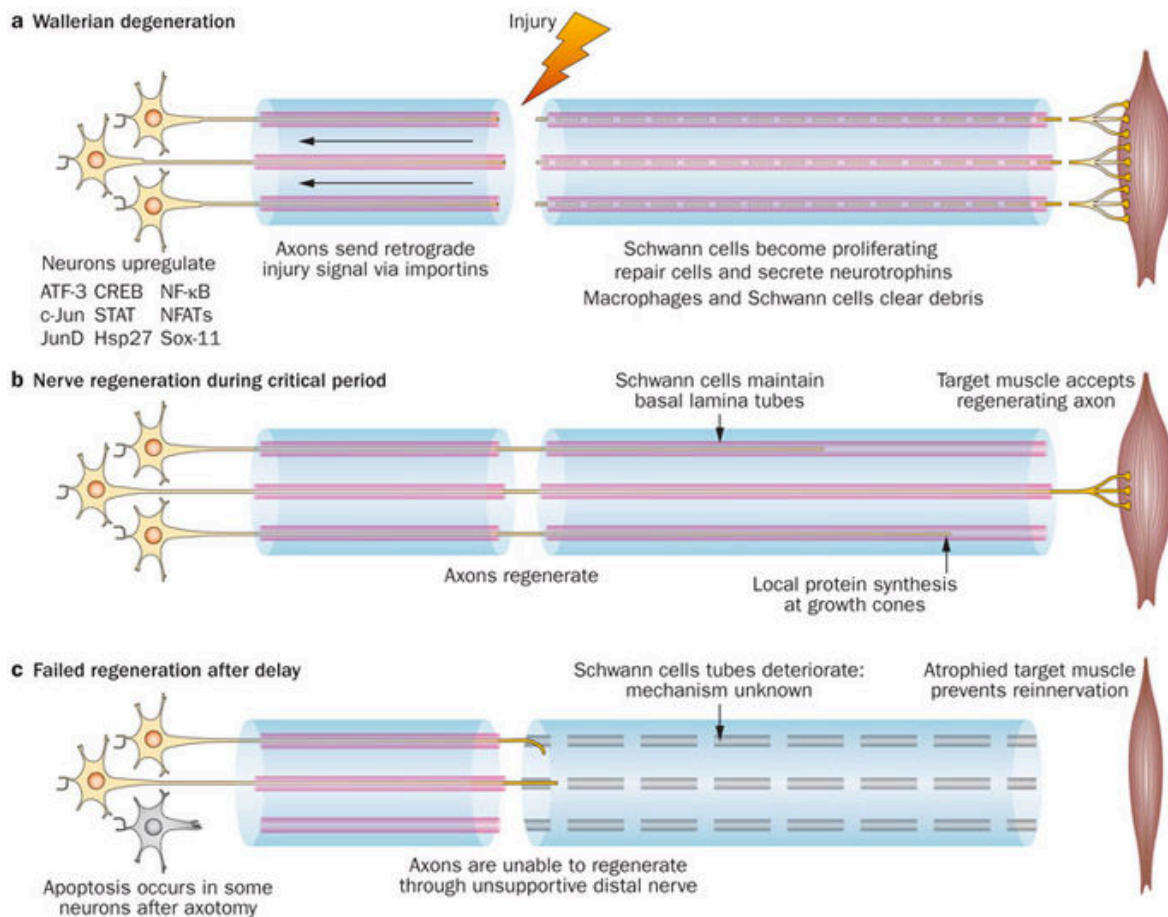


Figure 2. A schematic diagram of peripheral nervous regeneration. After injury, a retrograde signal is sent to the cell body and growth associated gene are upregulated. The distal part of axons and myelin sheath begin to degenerate. After, macrophages are recruited to the injury site and clear myelin debris and Schwann cells start to proliferate, meanwhile, neuron cell body undergoes the process of chromatolysis. This process involves breakup of the endoplasmic reticulum; the nucleus's displacement and the transcription changes which switch the gene expression pattern from axon maintenance to protein synthesis. Then, the new formed proteins which are necessary for regrowth are transported to the axon sprout tip of growth corn and Schwann cells line up in bands of Büngner which facilitates the sprouting of the new nerve branches from the proximal injured axon terminus. However, if reinnervation is delayed, Schwann cells tubes will degenerate and target muscle becomes atrophy. (Scheib and Höke, 2013).

1.1.3 Summary of cell intrinsic mechanisms of axonal regeneration in the PNS

Previous studies have revealed that in order to initiate a regenerative response to the injury in the PNS, neurons must shift their physiology from synaptic transmission and maintenance of their structure to axon growth (Benowitz and Yin, 2007). A series of molecular responses take place in response to injury for successful nerve regeneration and functional recovery (Figure 3). Extracellular calcium enters into the axoplasm as one of the first signals caused by injury.

Injury induced calcium influx into axoplasm activates cAMP and PKA thereby promoting growth cone formation, local protein synthesis and resealing of the axonal membrane (Chierzi et al., 2005; Kamber et al., 2009; Krause et al., 1994). The intracellular calcium wave propagates back to the cell body, which leads to HDAC5 nuclear export, activating the pro-regenerative transcriptional program (Cho et al., 2013). Following calcium mediated signaling, a retrograde injury signaling including ERK, JNK, STAT3 transports to the neuronal cell body (Ben-Yaakov et al., 2012; Cavalli et al., 2005; Perlson et al., 2005). This process is mediated by importin and dynein proteins (Hanz et al., 2003; Schnapp and Reese, 1989; Yudin et al., 2008). Afterwards, a number of RAGs (regeneration associated genes) such as GAP-43, CAP-23, Arg1, IL6, SPRR1A are synthesized in the cell body and anterogradely transported to the injury site (Bomze et al., 2001; Bonilla et al., 2002; Cao et al., 2006; Deng et al., 2009) activating the pro-regenerative program and axonal regrowth.

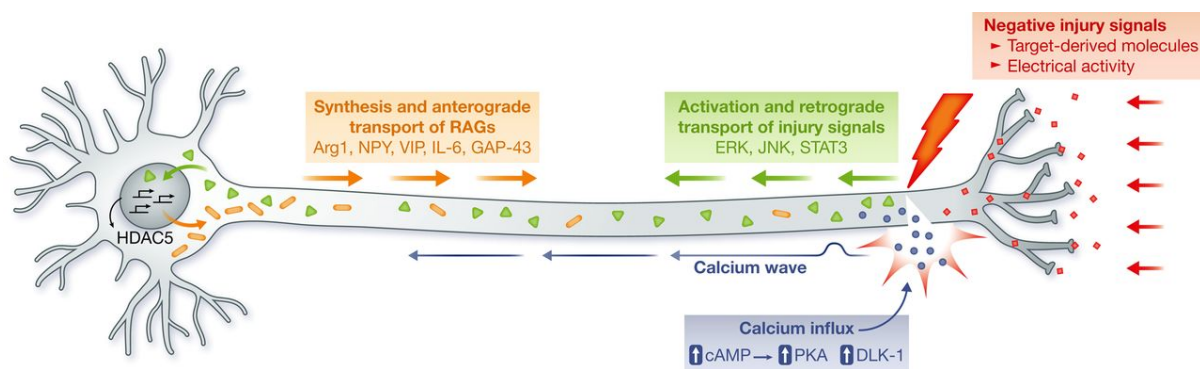


Figure 3. The response of a PNS neuron after injury. After injury, in the injury site, local calcium influx activates cAMP, PKA and DLK-1 to initiate local protein synthesis, growth cone formation and reseal the injured axon membrane. In cell body, the back-propagated calcium induces HDAC5 nuclear export to activate the regenerative programme. After, the retrograde signalling including ERK, JNK, STAT3 transports into cell body, which will induce a number of RAGs synthesis (Mar et al., 2014).

1.2 Dorsal Root Ganglion (DRG) - an experimental model for axonal regeneration

Dorsal root ganglion (DRG) neurons are pseudo-unipolar since they possess one peripheral branch innervating targets such as skin and muscles and one central branch extending into spinal cord conveying sensory information into the dorsal column to relay the sensory signal to the brain. Based on their location, DRGs are grouped into cervical, thoracic and lumbar DRGs. DRG contains a diverse group of sensory neurons that can be classified into three types based on their soma size and the status of the myelination of their axons: larger diameter (>

45µm in diameter) with heavily myelinated fibers ($A\alpha$ and $A\beta$), which project to the dorsal column nuclei and deeper spinal cord layers, medium diameter (15-45µm in diameter) with thinly myelinated fibers ($A\delta$) and unmyelinated C fibers which project to the superficial layers of the spinal cord (Caspary and Anderson, 2003; Mantyh, 2006; Todd, 2002). These fibers that arise from DRG neurons are involved in detecting and relaying sensory information including mechanoreception and proprioception ($A\alpha$ and $A\beta$), nociception ($A\delta$ and C) such as thermal, chemical stimuli (D'mello and Dickenson, 2008) (Figure 4).

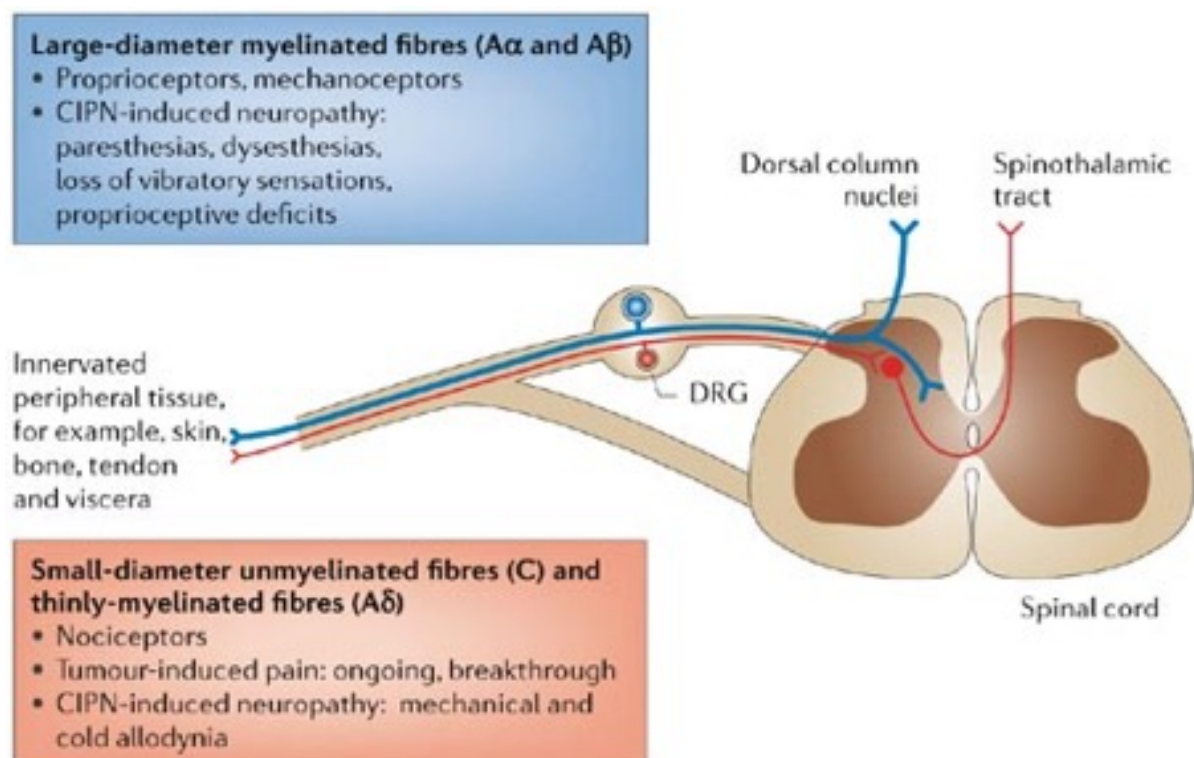


Figure 4. Schematic of Dorsal Root Ganglion (DRG). Afferent neurons' cell bodies are in dorsal root ganglion (DRG). The sensory information is transmitted from peripheral tissues to spinal cord and brain via DRG. Specially, nociception including thermal, chemical and mechanical stimuli projects to the superficial layer of the spinal cord, in contrast, the non-noxious sensation including light touch, vibration and proprioceptive stimuli projects into dorsal column nuclei and deeper spinal cord layer (Mantyh, 2006).

The DRG peripheral branches can regenerate while the central branches do not after an injury (Ramon y Cajal, 1991). A peripheral injury prior to the spinal cord injury (called conditioning

lesion) will allow the central branch to regain some regrowth ability (Neumann and Woolf, 1999; Richardson and Issa, 1984). Therefore, the DRG system is a good model to investigate the mechanisms that modulate axon regeneration after injury thereby helping to develop strategies to promote axonal regeneration after the central nervous system injury.

Sensory neurons extending into the sciatic nerve are located in L4-L6 DRGs. Sciatic nerve injury can be easily performed, normally at mid-thigh level. The central projection of the same neurons can be injured at the same distance from the cell body by a dorsal column crush or dorsal hemi-section injury as a spinal cord injury model. These injury models will allow us to compare the cell responses in the same neurons after peripheral and central injuries with different extrinsic environments but with the same cell body. This allows investigating signaling pathways that are activated or repressed to initiate or block the regenerative program.

1.3 Axon Regeneration in the Central Nervous System

1.3.1 Central Nervous System Regeneration

Previous research by Aguayo and colleagues proved that the adult mammalian CNS neurons that cannot regenerate are capable of growing into the permissive environment of a peripheral nerve graft (Benfey and Aguayo, 1982; David and Aguayo, 1981; Richardson et al., 1984; Richardson et al., 1980). This finding suggested that the environment is an important factor for CNS axonal regeneration. There are two classic types of CNS barriers to regeneration, extrinsic and neuronal intrinsic. The extrinsic inhibitors include the myelin-associated inhibitors (Berry, 1982; Schwab and Caroni, 1988a; Schwab and Thoenen, 1985) and the chondroitin sulfate proteoglycans (CSPGs) (Morgenstern et al., 2002). Besides the inhibitory extrinsic environment, limited intrinsic growth ability is another pivotal factor for limited CNS axonal regeneration (Liu et al., 2011).

1.3.2 The structure differences between peripheral and central nervous system neurons

Better understanding of the differences between peripheral and central nervous system after injury will give us more detailed information about regeneration failure of the CNS. The nervous system is mainly composed of neurons and glia cells. Schwann cells are glia cells in the PNS, whereas oligodendrocytes, astrocytes and microglia are glia cells in the CNS. In the PNS, Schwann cells form myelin sheath and myelinate one internode in one axon. In contrast, each oligodendrocyte can myelinate several axons and several internodes per axon in CNS. Moreover, Schwann cells are surrounded by the basal lamina which is not found in CNS axons

(Poliak and Peles, 2003)(Figure 5). Lack of the basal lamina surrounding the axons may contribute to the regenerative failure in CNS as the basal lamina is not only rich in extracellular matrix proteins promotes axon growth, such as laminin and collagen IV (Ard et al., 1987; Bunge et al., 1986; Cornbrooks et al., 1983) but may also shelters the axons from inhibitory molecules (Höke, 2006).

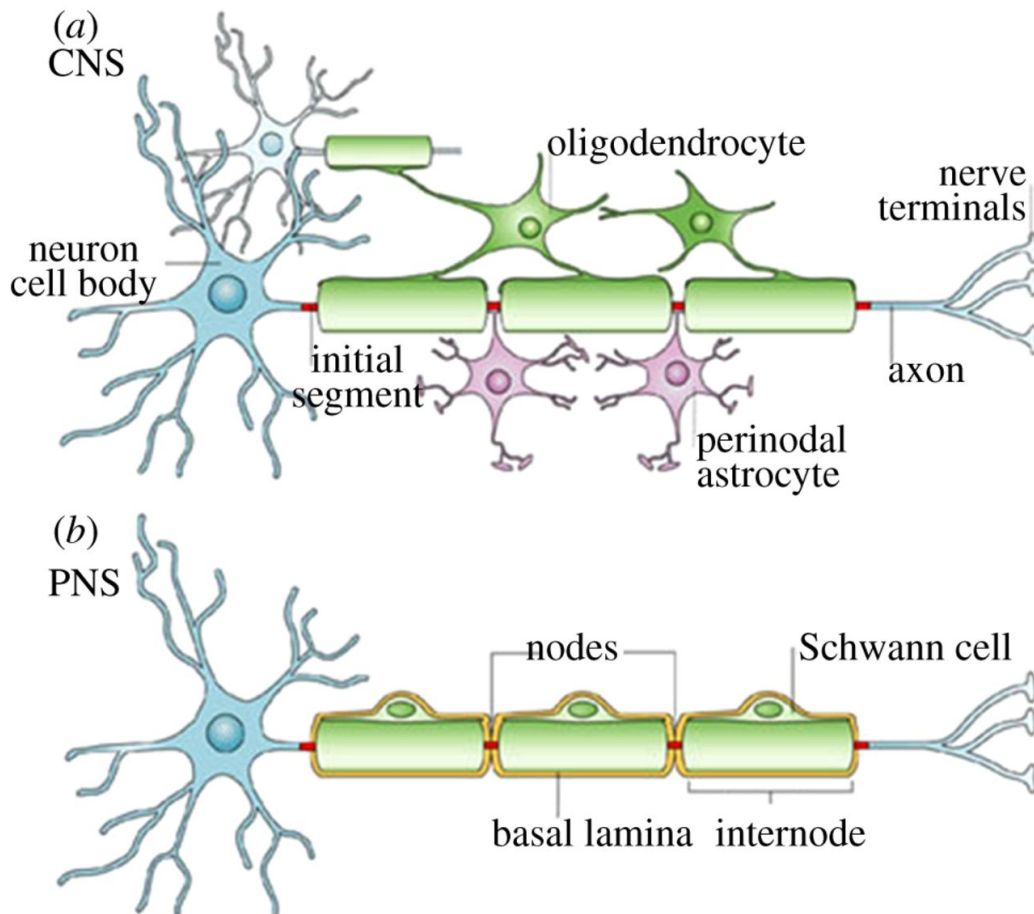


Figure 5. The structure of myelinated axons in PNS and CNS. Schwann cells in PNS and oligodendrocytes in CNS form myelin sheath around axons. Schwann cells myelinate one internode in one axon in PNS, whereas oligodendrocytes can myelinate different axons and several internodes per axon in CNS. (Poliak and Peles, 2003)

The peripheral branch of DRG neurons terminates in sensory receptors while the central branch enters into the spinal cord and the two lie at the interface between the central and the peripheral nervous system. DRG central axons must pass through the dorsal root entry zone (DREZ) to enter into the spinal cord, transitioning between a permissive and a non-permissive regenerative environment. Schwann cells that promote regeneration in the PNS, are juxtaposed

by oligodendrocytes in the CNS when DRG central branch axons pass through the DREZ and astrocytes are supportive glia cells (Figure 6).

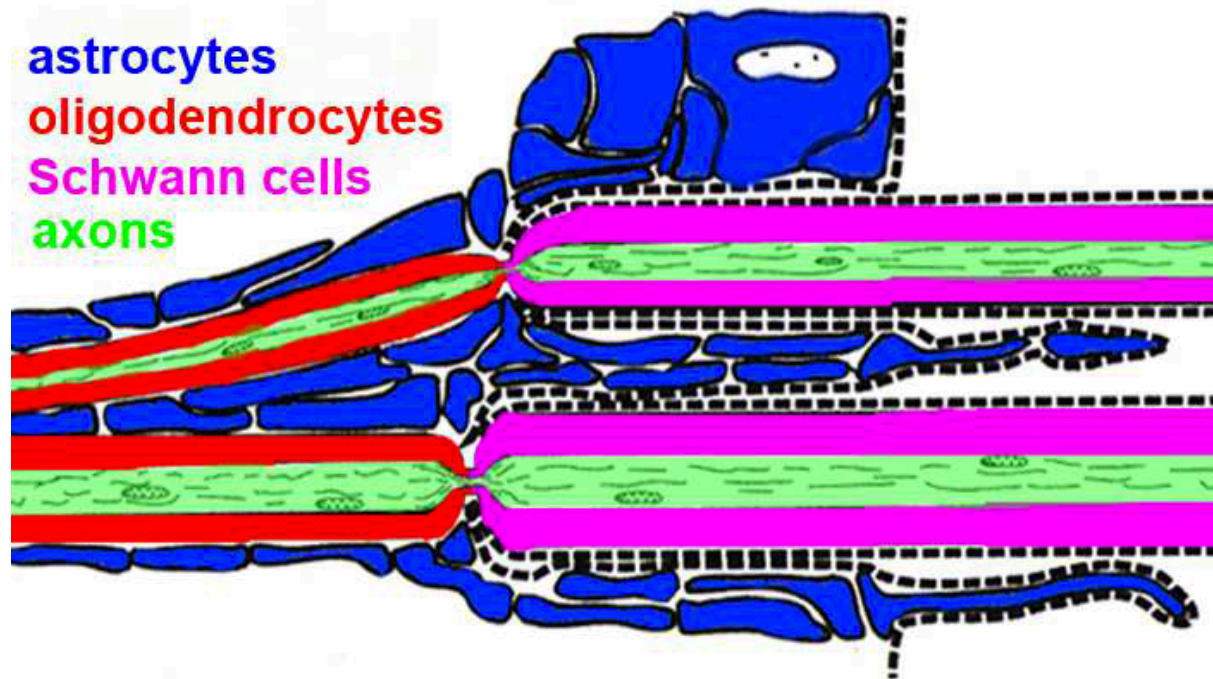


Figure 6. Glia organization of peripheral and central branches of DRG at dorsal root entry zone (DREZ). Peripheral to the DREZ, sheaths are formed by Schwann cells (Pink) enveloped in endoneurial tubes, central to it, myelin sheaths are formed by oligodendrocytes (Red) and the supporting tissues are astrocytic (Blue) (Tang et al., 2012b).

1.3.3 Extrinsic inhibitors of the CNS regeneration

1.3.3.1 Myelin-associated inhibitors

Myelin associated inhibitors are expressed by oligodendrocytes that are components of CNS myelin. Myelin in the CNS was first found as a major source of inhibition for axon outgrowth over 30 years ago (Schwab and Thoenen, 1985). With the development of subsequent studies which mainly focused on looking for individual molecules, myelin-associated glycoprotein (MAG) (McKerracher et al., 1994), Nogo-A (Chen et al., 2000; GrandPre et al., 2000), oligodendrocyte myelin glycoprotein (OMgp) (Kottis et al., 2002), Semaphorin4D(Sema4D)(Moreau-Fauvarque et al., 2003) and ephrin-B3 (Benson et al., 2005) were identified.

However, Nogo-A that is highly expressed by CNS oligodendrocytes is the best-characterized member of MAIs. Nogo is a member of Reticulon family of membrane proteins. There are at least 3 isoforms of Nogo family: Nogo-A, -B and -C. Structure-function analyses found two inhibitory domains: a Nogo-66 amino acid loop which is a common part in these isoforms and interacts with the NgR1 receptor on the neuronal membrane (Fournier et al., 2001) and a fragment (called Nogo- Δ 20) in the amino terminal of extracellular domain, only found in Nogo-A. Both inhibitory domains are associated with neurite outgrowth inhibition (Chen et al., 2000; Fournier et al., 2001; Oertle et al., 2003; Simmons and Walsh, 2000). Later research revealed that genetic deletion of Nogo-A promotes corticospinal and raphe spinal tract regeneration and functional recovery after spinal cord injury (Dimou et al., 2006; Kim et al., 2003; Simonen et al., 2003; Zheng et al., 2003). An anti-Nogo antibody treatment for SCI is in currently in phase 2 clinical trials.

MAG was the first described myelin inhibitor (McKerracher et al., 1994). But interestingly, while MAG inhibits postnatal neurons neurite outgrowth, it promotes axonal growth of embryonic and newborn neurons and this promotion role will sharply change to inhibition at postnatal day 3 (DeBellard et al., 1996; Johnson et al., 1989; Turnley and Bartlett, 1998), which suggests that this protein seems to be bifunctional. So far, there is no evidence showing that MAG knockout promotes cortical spinal tract or optic nerve regeneration after injury (Bartsch et al., 1995), suggesting that MAG is not as important as Nogo-A in inhibiting axonal regeneration in the adult CNS.

OMgp is a GPI (glycosylphosphatidylinositol)-anchored protein expressed not only in oligodendrocytes but also in neurons CNS (Habib et al., 1998). In vitro experiments found that OMgp participates in growth cone collapse and inhibits neurite outgrowth through its interaction with the Nogo receptor-NgR (Kottis et al., 2002; Wang et al., 2002).

In addition to these three myelin components, Semaphorin4D and ephrin-B3 are also found in CNS myelin as inhibitors for axon growth in the adult. Semaphorin4D is selectively expressed in myelinating oligodendrocytes and its expression can be upregulated by injury (Moreau-Fauvarque et al., 2003). Semaphorin4D- deficient mice show improved motor behavior than wild-type (Yukawa et al., 2009). Ephrin-B3 is also expressed in postnatal myelinating oligodendrocytes, it functions as a midline repellent for the corticospinal tract axons during development and is a myelin-based inhibitor for neurite outgrowth (Benson et al., 2005).

1.3.3.2 The glial scar and CSPGs

Reactive astrocytes are the main cellular response to spinal cord injury. The astrocytic response to injury is referred as gliosis which includes: proliferation and hypertrophy. But in most injury types, the amount of glial cells proliferation is relatively small. The main reaction to injury is hypertrophy with increased production of GFAP (glial fibrillary acidic protein) (Eng, 1985) other intermediate filament proteins, such as vimentin (Yang et al., 1994). The reactive astrocytes form an extremely dense physical wall at the lesion site which inhibits axonal regeneration while it can also provide partial support to regrowing axons (Anderson et al., 2016).

Chondroitin sulphate proteoglycans (CSPGs) are known to be upregulated in the glia scar in the brain and spinal cord of mature animals after injury when they are secreted very rapidly (within 24 hours) and can persist for many months (Jones et al., 2003; McKeon et al., 1999; Tang et al., 2003). Reactive astrocytes have been regarded as the main source of CSPGs around the lesion. Previous in vitro experiments indicated that CSPGs inhibited neurite outgrowth (Canning et al., 1993; Dou and Levine, 1994; McKeon et al., 1991; Smith-Thomas et al., 1994) and CSPGs in the glia scar are inhibitors for axon growth in vivo (McKeon et al., 1999). Several studies showed that local application of ChABC which is a bacterial enzyme and can digest CSPGs, promoted dorsal column and corticospinal tract regeneration (Bradbury et al., 2002b) including promoting recovery of respiratory pathways (Alilain et al., 2011). However, applying ChABC to SCI patients has a number of limitations such as incomplete digestion ability of CSPGs, the enzyme activity can only last for a short time at body temperature and it cannot cross the blood-brain barrier. Several CSPGs receptors have been found, including: LAR phosphatase, PTP σ , Nogo receptors 1 and 3 (NR1 and NR3) (Dickendesher et al., 2012; Fisher et al., 2011; Shen et al., 2009). Previous research reported that LAR, NR1 and NR3 participate in CSPGs suppression of neuronal outgrowth (Dickendesher et al., 2012) (Fisher et al., 2011). Recent studies found that systemic delivery of a mimetic peptide of the PTP σ wedge domain restored serotonergic innervation caudal to the spinal cord lesion and promoted functional recovery of both locomotion and urinary system (Lang et al., 2015).

1.3.4 Inflammation

Another extrinsic factor influencing CNS regeneration is inflammation. In mammals, the acute inflammatory response takes place after CNS trauma. Firstly, microglia cells become activated and migrate to the injury site and then start to produce all kinds of pro- and anti-inflammatory

cytokines (Czeh, 2011). Moreover, macrophages and neutrophils from the periphery infiltrate the injury site and then together with microglia/macrophages and astrocytes facilitate the formation of the glia scar (Benowitz and Yin, 2010; Lee-Liu et al., 2013). Alternatively, the microglia/macrophages have also been deemed to exert beneficial effect at the lesion site, such as phagocytosis of myelin debris and protection against glutamate excitotoxicity. Therefore, the role of neuroinflammation is controversial. It has been proposed that the phenotypic differences of macrophages determined by the spinal microenvironment (Stout and Suttles, 2004) affect their role in repair after spinal cord injury (Gensel and Zhang, 2015). Pro-inflammatory macrophages M1 (classical activation) and anti-inflammatory macrophages M2 (alternative activation) are regarded as the two main macrophage subsets at the injury site and have been shown to have a neurotoxic and regeneration-promoting role respectively. As reported, both M1 (CD68 positive) and M2 (arginase-1 positive) exist in the lesion center during the first week after SCI, but only M1 persist until day-28 after injury in mice (Kigerl et al., 2009). Moreover, a transit from M1 to M2 induced by transplanted stem cells in the injury spinal cord prevents the secondary tissue damage (neuronal loss, axon retraction and demyelination) and promotes regrowth (Busch et al., 2011; Cusimano et al., 2012). Furthermore, the acute inflammation in cell body of the axotomised neurons after spinal cord injury cannot be overlooked. Recent research revealed that overexpression of chemokine CCL2 in DRGs mobilizes M2-like macrophages and promotes sensory axonal regeneration in rat (Kwon et al., 2015).

1.3.5 Intrinsic regeneration mechanisms in CNS

The regenerative capacity of CNS neurons declines during development. Thus, one hypothesis proposes that the loss of regenerative ability is partially due to neurons transitioning from a growing (embryonic) to phase where they have to communicate via synaptic activity (mature). Gene screening approaches found that several Krüppel-like transcription factors (KLFs) are developmentally regulated, such as KLF4 and KLF6 /7 that inhibit or promote axon regeneration respectively (Blackmore et al., 2012; Moore et al., 2009). Recently, Calcium Channel Subunit $\alpha 2\delta 2$ (Cacna2d2) was found as a developmental regulated protein which inhibits axon growth. Pharmacological inhibition of Cacna2d2 enhances axon regeneration in adult mice after spinal cord injury (Tedeschi et al., 2016).

Many studies in peripheral DRG neurons identified a series of RAGs which are activated by peripheral injury, but not by the damage of their central axons, such as CAP23, GAP-43,

SPRR1A (Bosse et al., 2006; Bosse et al., 2001; Schmitt et al., 2003; Skene and Willard, 1981). In addition, transcription-dependent gene expression changes have been found after peripheral but not after central branch injury of sensory DRG neurons (Bareyre and Schwab, 2003; Costigan et al., 2002; Hoffman, 2010; Xiao et al., 2002). Importantly, conditioning lesion upregulates the pro-growth transcription factors including c-Jun, ATF3, HIF-1 α , SOX11, Smad1, Stat3, cAMP and arginase-1 (Cho et al., 2015; Enes et al., 2010; Hannila and Filbin, 2008; Hoffman, 2010). All of these genes can be used as potential modulators for CNS regeneration. The classical transcriptional pathways, which are involved in peripheral nerve regeneration, are shown in Figure 7.

After peripheral nerve injury, the upregulation of cAMP leads to the activation of PKA, which phosphorylates CREB (Gao et al., 2004; Hannila and Filbin, 2008; Qiu et al., 2002; Teng and Tang, 2006). Overexpression of constitutively active CREB promotes axonal regeneration of dorsal column axons (Gao et al., 2004). The phosphorylation of CREB upregulates Arginase-1, which in turn promotes the polyamines synthesis, which is reported to effect axonal growth (Abe et al., 1997; Dornay et al., 1986). Later studies have identified daidzein as a novel activator of Arginase-1 that can promote regeneration via a cAMP-independent pathway (Ma et al., 2010).

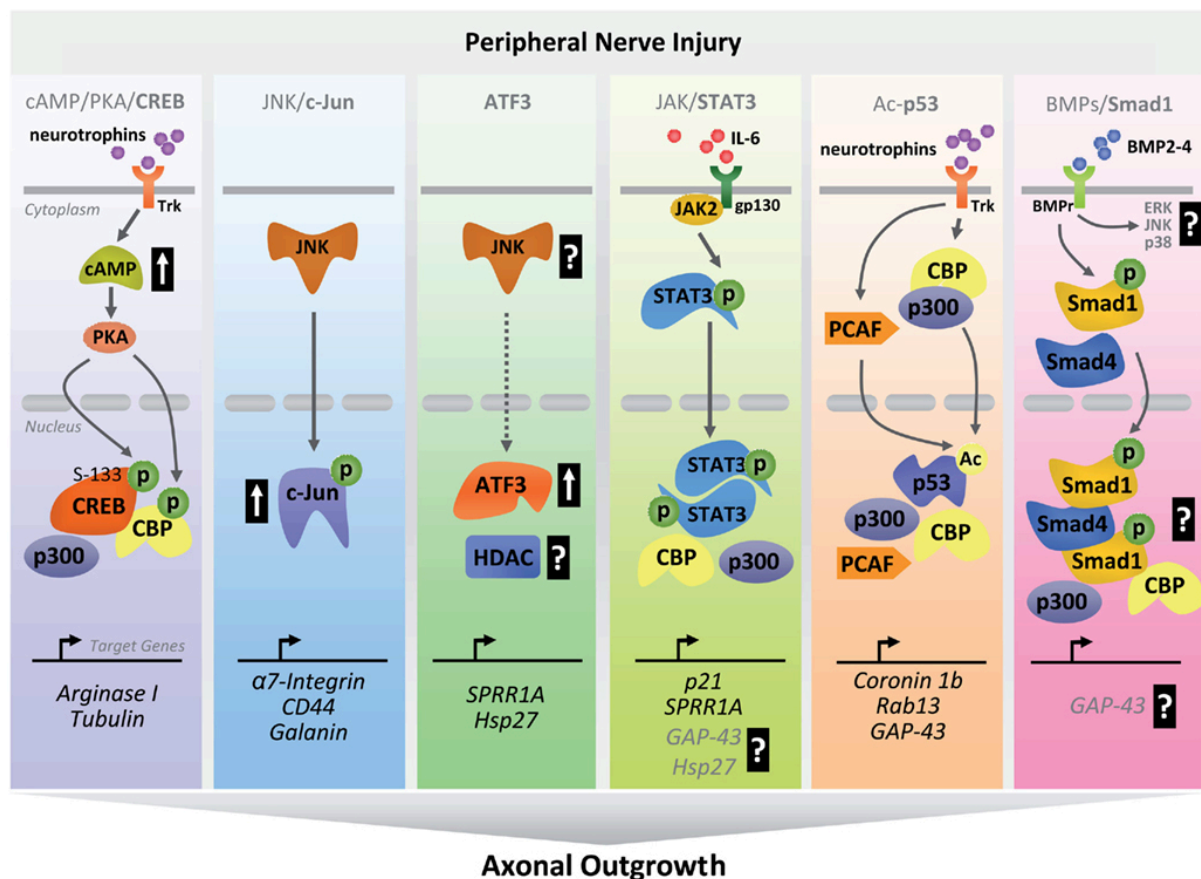


Figure 7. A diagram of transcriptional pathways involved in peripheral nerve regeneration. After peripheral nerve injury, activated transcriptional factors and co-factors translocate into nucleus and drive their targets regeneration-associated genes expression (Tedeschi, 2011).

While upregulation of c-Jun has been shown to be critical for regeneration in several injury models (Herdegen et al., 1991; Jenkins and Hunt, 1991; Lindwall and Kanje, 2005), its deletion impairs axon regeneration and results in cell death after peripheral nerve injury in mice (Raivich et al., 2004). c-Jun is activated by JNK-dependent phosphorylation. After injury, JNKs can be activated and retrogradely transported in to cell body, inducing c-Jun phosphorylation and translocation into the nucleus. Furthermore, c-Jun has been reported to regulate the expression of PNS regeneration associated genes, such as CD44, Galanin, and $\alpha 7\beta 1$ integrin (Herdegen et al., 1997; Lindwall and Kanje, 2005; Raivich et al., 2004; Teng and Tang, 2006).

Similarly to c-Jun, peripheral axonal injury induces the transcription factor 3 (ATF3) activation via phosphorylation, which doesn't occur after central axonal injury (Tsujino et al., 2000). While constitutive overexpression of ATF3 in DRG neurons promotes peripheral axonal regeneration to a similar extent as that of a conditioning lesion, ATF3 overexpression is not sufficient to overcome the inhibitory effects of myelin or promotes axonal regeneration after spinal cord injury (Seijffers et al., 2007). Facial nerve regeneration and the neurite growth of adult DRG neurons are decreased in ATF3 mutant mice and a number of ATF3 regulated RAGs (vasoactive intestinal peptide (Vip), Ngf, Grp, Gal, Pacap) are found by transcriptomics analysis (Gey et al., 2016). After peripheral axotomy, Hsp27, one of the identified of ATF3 target gene in neurons, is upregulated in DRG, dorsal horn and motor neurons of spinal cord (Costigan et al., 1998). Moreover, Hsp27 has been reported to promote axonal growth and motor function recovery after peripheral nerve injury in mice (Ma et al., 2011). Notably, ATF3 transgenic mice show upregulated SPRR1A (well-known RAG) expression in non-injured DRG neurons (Seijffers et al., 2007). Network analysis revealed that ATF3 interacts with some transcription factors that are known involved in axonal regeneration including members of AP1 (Fos, c-Jun, Junb) and NF- κ B (Gilchrist et al., 2006). But the mechanism of how these interactions affect transcription after peripheral nerve injury is still unknown.

In addition, ATF3 has been predicted to interact with HDACs (Gilchrist et al., 2006) to regulate gene transcription via chromatin remodeling, although the function of this interaction is unclear and deserves further research in neurons.

The JAK-STAT signaling is a main transduction pathway of cytokines and growth factors, which participates in many biological processes including cell proliferation, inflammation, axon regeneration, and apoptosis. STAT3 is activated by JAK family proteins via phosphorylation by ligand-receptor coupling. IL6 cytokine family, such as IL6, LIF, CTNF, are the main cytokines that regulate STAT3 activity (Heinrich et al., 1998). Importantly, peripheral injury induced phosphorylated STAT3 in axons that intrinsically regulates peripheral axon regeneration by regulating its target genes expression, such as SPRR1A, p21/Cip1/Waf1 (Bellido et al., 1998; Chin et al., 1996; Lee et al., 2004; Smith et al., 2011).

After peripheral injury, the tumor suppressor p53 is activated by acetylation on its C-terminal domain and acetylated p53 is required for axonal regeneration (Di Giovanni et al., 2006; Tedeschi et al., 2009). Moreover, acetylated p53 forms a transcriptional complex with CBP/p300 and PCAF occupying the promoter of Coronin 1b, Rab13 and GAP43 that are necessary for axonal regeneration (Di Giovanni et al., 2006; Gaub et al., 2010; Tedeschi et al., 2009). Another p53 post-translational modification is phosphorylation, which is required during neurite outgrowth and growth cone remodeling. Phosphorylated p53 has been reported to inhibit Rho kinase (ROCK) activity at the growth cone and to reduce growth cone collapse (Qin et al., 2009). In addition, the p53 acetylation at lysine 320 by PCAF increases its binding with the promoter of e p21Cip1/Waf1 (Liu et al., 1999). Similarly to GAP-43, p21Cip1/Waf1 is upregulated following peripheral axotomy (Bonilla et al., 2002) and it has been shown to regulate growth cone remodeling via inhibiting ROCK activity (Tanaka et al., 2002). Furthermore, recent research in our lab found that conditional deletion or pharmacological inhibition of MDM4 to disrupt the interaction of MDM2/p53 promotes optic nerve regeneration and cortical spinal tract sprouting after injury. However, double deletion of MDM4-p53 or inhibition of MDM2 in p53 null mice abolishes this regenerative phenotype, which prove that this phenotype depends upon p53 (Joshi et al., 2015).

Gene expression profiling analysis revealed that Smad1 is upregulated by sciatic nerve axotomy in DRGs (Zou et al., 2009). Smads are the intracellular mediators of BMP signaling and intraganglionic injection of BMP2/4 induce Smad1 phosphorylation and nuclear translocation (Zou et al., 2009). Moreover, AAV-mediated activation of Smad1-BMP signaling pathway increases the intrinsic growth ability of adult DRG neurons in vitro and promotes sensory axonal regeneration in vivo (Parikh et al., 2011). Importantly, previous studies have shown that Smad1 and Smad4 activated by BMP to interact with coactivator CBP/p300 to activate transcription (Feng et al., 1998; Pouponnot et al., 1998).

Several studies have shown that epigenetic changes such as histone modifications also regulate axonal regeneration. Histone deacetylase 5 (HDAC5) nuclear export induced by injury was found to be required for axonal regeneration in DRG neurons by enhancing histone acetylation and a pro-regenerative program (Cho et al., 2013). Overexpression of the histone acetyltransferase P300 was also found to promote optic nerve regeneration (Gaub et al., 2011). Furthermore, the histone acetyltransferase p300/CBP-associated factor (PCAF) which promotes the acetylation of H3K9 at the promoters of well-known RAGs such as GAP-43, Galanin and BDNF is necessary for the conditioning lesion induced regeneration (Puttagunta et al., 2014).

Recent research found that ten-eleven translocation methylcytosine dioxygenases 3 (Tet3) and 5-hydroxymethylcytosine (5hmC) are upregulated following sciatic nerve injury in DRG neurons and Tet3 is required for sciatic nerve regeneration by regulating ATF3, Smad1, STAT3 (Weng et al., 2017).

1.5 Hypothesis

While axonal regeneration and partial functional recovery in the injured PNS occur, axonal regeneration fails in the CNS such as after a spinal cord injury (SCI), strongly contributing to unsuccessful functional recovery. The bipolar sensory fiber tracts belonging to the dorsal root ganglia (DRG) system extending one branch in the periphery and one into the spinal cord represent an ideal model to directly compare the differential regenerative ability of PNS vs CNS axons within a single cell body. Although only leading to limited axonal regeneration beyond the lesion site, the gold standard for regeneration of sensory fibers across the injured spinal cord remains the conditioning lesion of L4-L6 DRG peripheral sciatic nerve preceding a spinal cord injury. However, despite recent progress in the molecular understanding of the conditioning effect, we are still uncovering the nature of these contrasting molecular signatures associated with successful PNS versus failed CNS regeneration, limiting the identification of effective targets for nerve regeneration and functional recovery. We hypothesize that key axonal signaling following peripheral but not central axonal injury regulates pathways that control the regenerative phenotype. These axonal signals together with changes in gene expression might modulate long-term regenerative reprogramming. Therefore, we believe that the combined investigation of protein as well as gene expression changes in the “DRG-axonal signaling unit” after central versus peripheral nerve injury will be critical to identify regenerative pathways.

1.6 Experimental Strategy

To this end we planned to perform combined RNAseq from DRG and proteomics from sciatic axoplasm in mice following an equidistant sciatic or spinal cord (dorsal column) axotomy to investigate differential molecular responses associated with regeneration versus regenerative failure. Then integrated bioinformatics analysis of the RNAseq and proteomics data was done to identify candidate central nodes that are involved in axonal regeneration in peripheral branch but not in the central branch. Finally, specific pathways were investigated in spinal cord injury models to assess their ability to control axonal regeneration.

2. Methods

Animals

All animal procedures used for this study were performed in accordance to The Animal Welfare Act and the guidelines of the University of Tübingen. Three mouse germ-lines were used for this study: C57BL6/J (Charles River Laboratories), Prkaa1^{fl} (Stock No: 014141) and Prkaa2^{fl} (Stock No: 014142) mice (purchased from The Jackson Laboratory). Equal number of male and female animals were used for all the experiments.

AAVs

AAV-GFP and AAV-Cre-GFP were purchased from SignaGen Laboratories.

Chemical reagents

Compound C was purchased from Sigma (866405-64-3). Bortezomib was obtained from Selleckchem (PS-341). KN-93 and KN-92 phosphate were purchased from MedChem Express (HY-15465B, HY-15517A).

Plasmids

The PSMC5 WT, phospho-dead (S120A) phospho-mimetic (S120D) and CaMKII phospho-mimetic (T286D) plasmids were obtained from Prof. Gentry Patrick, University of California, San Diego. The blank vector, CaMKII WT and phospho-dead (T286A) plasmids were purchased from Addgene.

siRNA

The control siRNA (sc-37007), PSMC5 siRNA (SC-76604) and Trim28 siRNA (sc-38551) were purchased from Santa Cruz.

Axoplasm preparation for Proteomics

Axoplasm preparation was done in Hertie Institute, University of Tübingen.

6-8-week old mice were performed with bilateral sciatic nerve axotomy or sham injury. The axotomy injury was applied about 1.5cm distally to the L4-L6 DRG neurons. 24h later, animals were sacrificed and the proximal nerve segments were collected in 500 μ L 0.2X PBS on ice and then processed for the axoplasm extraction as described previously (Rishal et al., 2010).

Briefly, nerve fascicles were separated carefully by using fine forceps, then once they became cloudy, they were transferred to a fresh eppendorf tube containing 500 μ L 0.2X PBS for incubation at room temperature for 2 hours. After 2h incubation, the fascicles were washed 3 times using the same solution by transferring them from one eppendorf tube to one eppendorf tube following 5 min shaking every time. After that, removing the fluid as much as possible by putting the fascicles to a new empty eppendorf tube, then the axoplasm was extracted by using 300 μ L 1X PSB for 30 min incubation at room temperature with subsequent centrifugation at 10,000 x g for 10 min at 4°C. Protease (Roche, catalog number: 04693116001) and phosphatase inhibitors (Roche, catalog number: 04906837001) were added into all solutions used in the purification procedure. Finally, purified axoplasm was concentrated by centrifugation at 4,000 x g for 30 min at 4°C using the Amicon Pro Affinity Concentrator (Millipore, ACS500312), afterwards, 500 μ L denaturation buffer (6M urea, 2M thiourea in 10mM Tris pH 8.0) was added into the same concentrator for buffer exchange. After centrifugation at 4,000 x g for 2h at 4°C, the total volume was concentrated to about 30 μ L for future Mass Spectrometry analysis.

15 mice were used for each group and biological triplicated were performed with each condition. As for the central part of axoplasm collection and purification, we used the same number of mice and protocol as we did for the peripheral part.

Mass Spectrometry Sample Preparation

Samples preparation was carried out in the Proteomics Core Facility, Institute of Molecular Biology, Johannes Gutenberg University of Mainz.

Samples were boiled at 70°C for 10 minutes in 1x NuPAGE LDS Sample Buffer (Life technologies) containing 100mM DTT and separated on a 10% NuPAGE Bis-Tris gel (Life technologies) for 10 or 20 minutes at 180V in MES running buffer (Life technologies). After fixation in 7% acetic acid containing 40% methanol and subsequently staining for 30 minutes using Colloidal Blue staining kit (Life technologies) protein lane was excised from the gel (for the axoplasm proteome analysis samples was separated in six slices), chopped and destained (50% ethanol in 25 mM NH_4HCO_3) for 15 minutes rotating at room temperature and dehydrated for 10 minutes rotating in 100% acetonitrile. Vacuum dried samples were rehydrated and reduced for 60 minutes in reduction buffer (10mM DTT in 50mM NH_4HCO_3 pH 8.0) at 56°C and subsequently alkylated in 50 mM iodoacetamide in 50mM NH_4HCO_3 pH 8.0 for 45 minutes at room temperature in the dark. Dehydrated and vacuum dried samples were trypsin digested (1 μ g trypsin/sample in 50mM Triethylammonium bicarbonate buffer pH

8.0) at 37°C over night. Stepwise peptide extraction was done as follows: twice extraction solution (30% acetonitrile) and 100% acetonitrile for 15 minutes at 25°C shaking at 1,400 rpm. Reductive methylation for quantification was performed as described in (Hsu et al., 2003). After purification and desalted using C18 stage tips (Rappsilber et al., 2007) 3.5 µL peptides were loaded and separated on C18 column (New Objective) with 75 µm inner diameter self-packed with 1.9µm Reprisil beads (Dr. Maisch) which was mounted to an EasyLC1000 HPLC (Thermo).

Mass Spectrometry Measurement and Data Analysis

MS and data analysis were performed in the Proteomics Core Facility, Institute of Molecular Biology, Johannes Gutenberg University of Mainz. Reversed-phase chromatography gradient (Buffer A: 0.1% formic acid, Buffer B: 80% acetonitrile and 0.1% formic acid, Gradient: 0-67 min 0-22% Buffer B, 67-88 min 22-40% Buffer B, 89-92 min 40-95% Buffer B) was applied and peptides eluted and directly sprayed into a Q Exactive Plus mass spectrometer from Thermo operating in positive scan mode with a full scan resolution of 70,000; AGC target 3×10^6 ; max IT = 20ms; Scan range 300 - 1650 m/z and a Top10 MSMS method. Normalized collision energy was set to 25 and MSMS scan mode operated with resolution of 17,000; AGC target 1×10^5 ; max IT = 120 ms.

Database search was performed using MaxQuant Version 1.5.2.8 (Cox and Mann, 2008) against Mus Musculus Ensembl database (release-81; 3rd July 2015; 53819 entries) for Axoplasmn proteome analysis and Mouse Uniprot database (downloaded 8th of January 2015; 83,429 entries) for AMPK immunoprecipitation analysis, with Trypsin/P as digestion enzyme allowing 2 missed cleavages. As settings the following was applied: variable modification: Acetyl (Protein N-term); Oxidation (M), fixed modifications: Carbamidomethyl (C), FDR of 1% on peptide and protein level was applied.

As light label: DimethylLys0 and DimethylNter0 and heavy label: DimethylLys4 and DimethylNter4 were set with max. 3 labeled amino acids.

Proteins with at least two peptides (one of them unique) were considered as identified. Proteins matching reverse database or common contamination list as well as proteins with peptides only identified by peptides with modification were filtered out. Normalized MaxQuant ratios were used for further analysis.

Statistical calculation and visual presentation was done in R version 3.3.1 (2016-06-21) (Team, 2016). Package “biomaRt” was used to convert Ensemble identifiers into gene names.

AMPK α Immunoprecipitation(IP) for Mass Spectrometry

The preparation of AMPK α IP samples for MS was done in Hertie Institute, University of Tübingen.

Adult mice were performed with bilateral sciatic nerve axotomy or sham injury. 6h later, L4-L6 DRG neurons were harvested and lysed in IP lysis buffer (25mM Tris•HCl pH 7.4, 150mM NaCl, 1% NP-40, 1mM EDTA, 5% glycerol) containing cocktail of protease and phosphatase inhibitors on ice for 30min. After centrifuging at 12,000 x g for 10 min at 4°C, protein concentration was measured by BCA protein assay kit (Thermo Fisher, 23227).

1.2 mg protein per group was used for the AMPK α immunoprecipitation experiment. 5 μ g AMPK α antibody (Abcam, ab80039) was added into each sample for overnight incubation at 4°C on a rotary device. And normal rabbit IgG immunoprecipitation was applied as the negative control. On the secondary day, 50 μ L protein A Dynabeads was washed 2 times with 500 μ L IP lysis buffer and incubated with the protein and AMPK α antibody mixed solution for 1h at 4°C. After, the nonspecific proteins were separated by the Magna Grip Rack (Millipore, 20-400). The Dynabeads complex were washed 3 times with 1ml IP lysis buffer. Then Dynabeads were re-suspended by 30 μ L 1XSDS loading buffer containing reducing agent and mixed gently. After boiled 10min at 70°C, the SDS loading buffer was separated from the beads mixture and collected for the future mass spectrometry analysis. All samples were prepared with biological duplicates.

RNA-seq

The DRG samples for RNAseq were prepared in Division of Brain Sciences, Department of Medicine, Imperial College London. Sequencing was done at Imperial MRC Genomic Facility. Sciatic L4-L6 DRGs (3 biological replicates, 2 mice/condition) were extracted 24h after injury and collected in RNAlater (Qiagen) to prevent RNA degradation. RNA extraction and library preparation were performed as previously reported (Hervera et al.) Briefly, tissue was crushed in RLT Lysis buffer (Qiagen), and RNA was isolated with RNeasy mini kit and DNase on column digestion (Qiagen) following manufacturer’s guidelines. RNA quality was assessed with Agilent 2100 Bioanalyzer (Agilent). RNA with RIN factor above 7.5 was used for library preparation. cDNA libraries for each sample were generated using the TruSeq stranded mRNA

Sample Preparation Kit A (Illumina, San Diego CA) according to the low-sample TruSeq RNA Sample Preparation Guide protocol. Libraries were verified using a DNA chip on the Agilent 2100 Bioanalyzer (Agilent) with clean elution profiles at the size peak of about 260 bp, quantified using Qbit (ThermoFisher) and multiplexed for Illumina HiSeq 2000 sequencing, using 100-cycle, single end sequencing.

Bioinformatics analysis

For creating modified volcano plots normalized ratio of triplicates were averaged and standard deviation calculated. Those ones which were up- or down-regulated 1.5-fold in 2 out of 3 replicates were plotted against the $-\log_{10}$ standard deviation. Plottings were done using function “ggplot” provided in package “ggplot2”.

Gene Ontology (GO) and KEGG Pathway analysis were performed using DAVID (<https://david.ncifcrf.gov/>) and setting all the expressed genes/proteins in our dataset as background.

Protein-protein interaction network were visualized using Cytoscape (<http://www.cytoscape.org/>). The AMPK interaction network was produced by generating a protein-protein interaction network using String (<https://string-db.org/>), integrating all genes assigned to significantly enriched pathways in the combined (Proteomics and RNAseq) KEGG analysis ($p < 0.05$). Genes were jointly organized in a circular layout according to their KEGG affiliation by using Cytoscape.

Western Blot analysis

The bilateral L4-L6 DRG neurons were collected in 1xPBS and lysed in RIPA buffer at different time points after sciatic nerve axotomy. All the buffers used in the above steps contain protease and phosphatase inhibitors. Protein samples from all conditions were loaded on 10% SDS-PAGE gel and transferred on the nitrocellulose membrane (Thermo Fisher, IB301001) using the iBlot® Gel Transfer Device (Thermo Fisher, IB1001EU). The membrane was blocked with 5% milk for 1h at RT and incubated with primary antibodies diluted with 5% milk overnight at 4°C followed by incubation of HRP-conjugated Amersham ECL Rabbit IgG (GE Healthcare Life Sciences, NA934, 1: 2000) or Amersham ECL Mouse IgG (GE Healthcare Life Sciences, NA931, 1: 2000) on the second day.

For the F11 cell lysate used in this experiment, we followed the similar protocol as we did for the DRG tissue. Cells were washed 2 times with cold 1X PBS and lysed in RIPA buffer after

siRNA and plasmid transfection at 48h. Collected protein samples were used for the following steps as we mentioned above.

The primary antibodies used for this experiment are: anti-AMPK α 1 (Abcam, ab32047, 1: 500), anti-AMPK α 2 (Abcam, ab3760, 1: 500), anti-phospho-AMPK α (Cell Signaling Technology, #2535, 1: 1000), anti-PSMC5 (Abcam, ab178681, 1: 5000), anti-phospho-CaMKII (Cell Signaling Technology, #3361, 1: 1000), anti-CaMKII α (Thermo Fisher, MA1-048, 1: 1000), anti-GAPDH (Cell Signaling Technology, #2118S, 1: 10000), anti-Trim28 (Abcam, ab10484, 1: 500).

AMPK Activity Assay

Adult mice were performed with bilateral sciatic nerve axotomy or sham injury. 24h later, L4-L6 DRG neurons were collected and then lysed in lysis buffer (25mM Tris•HCl pH 7.4, 150mM NaCl, 1% NP-40, 1mM EDTA, 5% glycerol) containing cocktail of protease (Roche, catalog number: 04693116001) and phosphatase inhibitors (Roche, catalog number: 04906837001). 1 μ g DRG protein was used for the activity assay by using the CycLex® AMPK Kinase Assay Kit (MBL, CY-1182) according to the manufacture's protocol. Measurement was performed in biological triplicates.

Dorsal Root Ganglion (DRG) culture and Electroporation

Adult mice (6-8weeks) were used for this experiment. DRGs were dissected and collected in HBSS on ice. Collected DRGs after centrifugation were digested in a solution of DispaseII 10mg/ml (Sigma) and Collagenase II 20mg/ml (sigma) in DMEM GlutaMAX Supplement at 37°C for 35 min. Then DRG tissues were transferred in DRG media (10% FBS, 2% B27 in DMEM/F12, GlutaMAX Supplement) and mechanically dissociated into cell suspension by gentle trituration with a fire-polished sigmacote coated pipette. After cell counting, DRG cells were spun down and re-suspended in DRG culture media (1% Penicillin/Streptomycin, 2% B27 in DMEM/F12, GlutaMAX Supplement). Cells were plated 3,000-5,000 per laminin pre-coated coverslip (laminin 2.4 μ g/ μ L (1.2 mg/mL, millipore) or myelin 1.3 μ g/cm²). For neurite outgrowth analysis, the culture plate was put into the incubator (37°C, 5% CO₂) for 18-24h.

For electroporation experiment, dissociated cells were spun down after counting at 800g for 5min. During this period, the transfection solution was prepared by mixing the Lonza nucleofector solution with GFP (0.4 μ g), siRNA (6 pmol) or DNA (3-4 μ g) to a final volume of 20 μ L for each transfection. Then the nucleofector solution was gently mixed with cell pellet

and transferred to the electroporation cuvette. After electroporation, pre-warmed DRG culture media was added into cuvette and cells were plated on coverslip. The culture plate was put into the incubator (37°C, 5% CO₂) for 36-48h.

DRG neurite length analysis

Cultured DRG neurons were fixed using 4%PFA for 20min at room temperature. Cell were stained with different antibodies based on different experimental purpose. Immunofluorescence pictures were taken at 10X magnification using a CDD camera (Axiocam MRm, Zeiss). The neurite length of cultured DRG cells was measured by using Neurite J plugin for Image J software (Image J) with at least 200 cells per condition. All analyses were performed in blind.

Immunocytochemistry

Cultured DRG cells were fixed with 4%PFA for 20min at room temperature and washed with PBS for 3 times. Then cells were treated with 0.25% TritonX-100 for 10 min following with washing once with PBS. After, cells were incubated with primary and Alexa Fluor secondary antibodies at room temperature in 1h successively. All coverslips were mounted with VECTASHIELD anti-fade mounting medium. The primary antibodies used in this study are: anti- β III Tubulin (Promega, G712A, 1: 1000), anti- β IIITubulin (BioLegend, 802001, 1: 1000), anti-GFP (Abcam, ab13970, 1: 500), anti-PSMC5 (Abcam, ab178681, 1: 200), anti-Trim28 (Abcam, ab10484, 1: 400).

Immunohistochemistry

Mice were anaesthetized and perfused with 4% PFA in PBS. DRGs and spinal cords were dissected and post-fixed in PFA on ice for 2h and then cryoprotected in 30% sucrose for 72h at 4°C. The DRGs and spinal cords were sectioned in 10 μ m and 18 μ m thickness respectively. The slides were block with 5%NGS with 0.3% TritonX-100 and then incubated with primary antibodies at 4°C overnight. In the next day, slides were washed with PBST for 3 times and then incubated with Alexa Fluor secondary antibodies for 1h followed by PBST washing. All slides were mounted with VECTASHIELD anti-fade mounting medium. The primary antibodies used in this study are: anti-GFAP (Millipore, AB5804, 1:500), anti-AMPK α 1 (Abcam, ab32047, 1:100), anti-Neurofilament 200 (Sigma, N5389, 1:400), anti-GFP (Abcam, ab13970, 1:500), anti-p-ACC (Cell Signaling, 11818, 1:100), anti-c-Jun (Cell Signaling, 9165S, 1:100), anti-p-ERK (Cell Signaling, 4370, 1:100).

Cell Culture and Transfections

F11 cells were cultured in DMEM GlutaMAX supplement with 10% FBS, 2 mM L-Glutamine and 1% Penicillin/Streptomycin. The day before transfection, cells were seeded into 24-well plate and the cell confluency was 70%-90% at the time of transfection. The siRNA and plasmids transfection were performed using Lipofectamine RNAiMAX (Thermo Fisher) and Lipofectamine 3000 (Thermo Fisher) respectively, according to the manufacture's protocol. After 48-72h incubation, cells were harvested for the Western Blot analysis.

RNA Isolation and Reverse Transcription

Bilateral L4-L6 DRG neurons were harvested in RNAlater Stabilisation Solution and total RNA was extracted according to the manufacture's protocol of the Rneasy Mini Kit from QIAGEN. RNA quality was assessed by measuring the ratio of absorbance at 260 nm and 280 nm using a NanoDrop 2000 spectrometer (Thermo Fisher). The reverse transcription was performed using SuperScript™ II Reverse Transcriptase (Thermo Fisher), according to the manufacture's protocol.

Quantitative real-time PCR

qRT-PCR was performed using KAPA SYBR® FAST qPCR kit (Sigma, KK4601) in Applied Biosystems® 7500 Real-Time PCR System. The gene expression level was normalized by the housekeeping gene GAPDH. Primers used in qPCR were as follows:

Gene name	Forward 5'-3'	Reverse 5'-3'
AMPK α 1	AGAACATTCGGAGCCTTGACG	AGGATCTGCTGGAACAGACGG
Lgals	TCAAACCTGGGGAATGTCTC	ATGCACACCTCTGTGATGCT
Myc	TGAGCCCCTAGTGCTGCAT	AGCCCGACTCCGACCTCTT
BDNF	AGTCTCCAGGACAGCAAAGC	TCGTCAGACCTCTCGAACCT
P53	AGAGACCGCCGTACAGAAGA	CTGTAGCATGGGCATCCTTT
NGF	GGGAGCGCATCGAGTTTTG	TACGCTATGCACCTCACTGC
c-Jun	TGGTGTGGTGTTCCTTAAGGC	CCTGCTTTGAGAATCAACAGC
IGF-1	ACCGAGGGGCTTTTACTTCA	TGGCTCACCTTTCCTTCTCC
Gal	GTGACCCTGTCAGCCACTCT	GGTCTCCTTTCCTCCACCTC
P21	CGGTGGAACCTTTGACTTCGT	AGAGTGCAAGACAGCGACAA
Sprr1a	CCCCTCAACTGTCACCTCCAT	CAGGAGCCCCTTGAAGATGAG
IL6	GAGGATACTACTCCCAACAGACC	AAGTGCATCATCGTTGTTTCATACA
CCL2	GCAGGTCCCTGTCATGCTTC	CAGGTGAGTGGGGCGTTAA
Fos	GAAACGGAGAATCCGAAGGG	CTCAGGGTCGTTGAGAAGGG
Arg1	CTCCAAGCCAAAGTCCTTAGAG	AGGAGGTGTCATTAGGGACATC
ATF3	CTTCCCAGTGGAGCCAATC	CCTGGCCTGGATGTTGAAGC
HIF1 α	CTGCACGGGCCATATTCATG	AGCGGCCCAAAAGTTCTTCC
HDAC5	TAGTCTCCGCTGGGTTTTGATG	ATTGACGCTGGGCTTTTGC

CXCL12	GTCAGCCTGAGCTACCGATG	TTCTTCAGCCGTGCAACAATC
GAPDH	TCAACAGCAACTCCCCTCTTCCA	ACCCTGTTGCTGTAGCCGTATTCA

Peripheral nerve crush

Mice were anaesthetized with xylazine (10 mg/kg of body weight) and ketamine (100 mg/kg of bodyweight). After shaving, the sciatic nerve was exposed at the middle thigh level and crushed 15 seconds using #2 forceps (Dumont, FST). L4-L6 DRGs were isolated for different experiments at different time points.

Viral injections and Dorsal column crush

Four-week old AMPK α 1 (prkaa1)^{fl/fl} and AMPK α 2 (prkaa2)^{fl/fl} mice were anaesthetized with xylazine (10 mg/kg of body weight) and ketamine (100 mg/kg of bodyweight) and the bilateral sciatic nerves were injected with 2 μ L AAV-GFP or AAV-Cre-GFP using a Hamilton syringe attached with a glass-pulled micropipette.

Four weeks after AAV injection, mice were performed with T9 dorsal column crush. Specially, a T9-T10 laminectomy was performed and a dorsal column crush lesion was made to a depth of 0.5mm for 5s with forceps (Dumont #5, FST).

Dextran tracing

In order to retrogradely label ascending regenerative axons of dorsal column, four weeks after injury (5 days before sacrificing mice), 2 μ L of dextran (Thermo Fisher, D34679) was injected into sciatic nerve.

Evaluation of the dorsal column regenerating axons

Sagittal spinal cord sections were stained with GFAP and then mounted with VECTASHIELD anti-fade mounting medium. At least three sections with dextran tracing of each mouse were quantified for the analysis. The number of regenerating axons at different distances to the lesion center was normalized to the number of dextran labeled axons at 600 μ m caudal to the lesion center. Coronal section of spinal cord at 1mm rostral to the lesion was used to certify that the dextran positive axons pass through the lesion center were the regenerated axons but not spared ones.

Manual Von Frey tests

Mice were treated with sciatic nerve injection of AAV-GFP or AAV-Cre-GFP for four weeks before surgery. The first Von Frey test was taken on one day before the surgery as the baseline and the following tests were taken on day 1, 3, 7, 14, 21, 28, 35 after injury. Mice were put on the test chamber 30min for the acclimation before starting behavior tests. The mechanical sensitivity was determined by probing the plantar surface of the hind paw with the calibrated von Frey filaments that range from 0.4g to 4g. In order to give the sensory receptors enough time to back to baseline, the interval time was at least 30 seconds between each trial. A quick hind paw withdraw was considered as a positive response. Five trials were taken for each mouse and three values with the least deviating were selected to calculate the average. The threshold was determined as the lowest level of monofilament.

Grid walk

The grid walk test was performed at day 0, +1, +7 and +35 days after dorsal column crush. Mice were put on a metal grid (50 cm × 5 cm) placed between two 40cm vertical high wood blocks. A foot slip was counted when the hind paws protruded through the grid. One valid run was selected when mouse run through the full length of the grid.

Three times of valid run were used to calculate the average foot slips per run.

Hargreaves tests

Hargreaves test was performed as described previously (Schildhaus et al., 2014). Briefly, mice were put on a glass floor and separated by plastic chambers. Mice were given 30 minutes for the acclimation. The thermal heat stimuli (infrared radiation source, intensity=80) was carefully put under the plantar surface of the hind paw no more than 12 seconds. The hind paw withdrawal time was recorded automatically. Five trials were taken on each paw and average was calculated with the longest and shortest time removed.

Statistical Analysis

All statistical analyses were performed using Graphpad Prism 6.0 (Graphpad Software Inc., La Jolla, CA). All data are presented as group mean ± SEM unless otherwise noted.

3. Results

3.1 L4-6 DRG RNAseq and proteomics from sciatic or central projecting branches of DRG axoplasm following sciatic versus spinal injury identify AMPK as a signaling hub

Our initial experiments aimed to systematically investigate previously unknown axonal signalling pathways associated with differential regenerative vs non-regenerative axonal injury in the DRG system. To this end, we performed protein mass spectrometry from axoplasmic extracts of L4-6 DRG peripheral sciatic nerve and L4-6 DRG central branches following sciatic axotomy or spinal dorsal column axotomy respectively (see cartoon, Figure 8). In parallel experiments, we carried out RNAseq from DRG *ex vivo* following the same dual injury paradigm. In fact, the combination of axoplasmic proteomics and DRG transcriptomics would allow the identification of axonal and soma post-injury signalling pathways within the “DRG axonal signalling unit” that may be relevant for the regeneration programme.

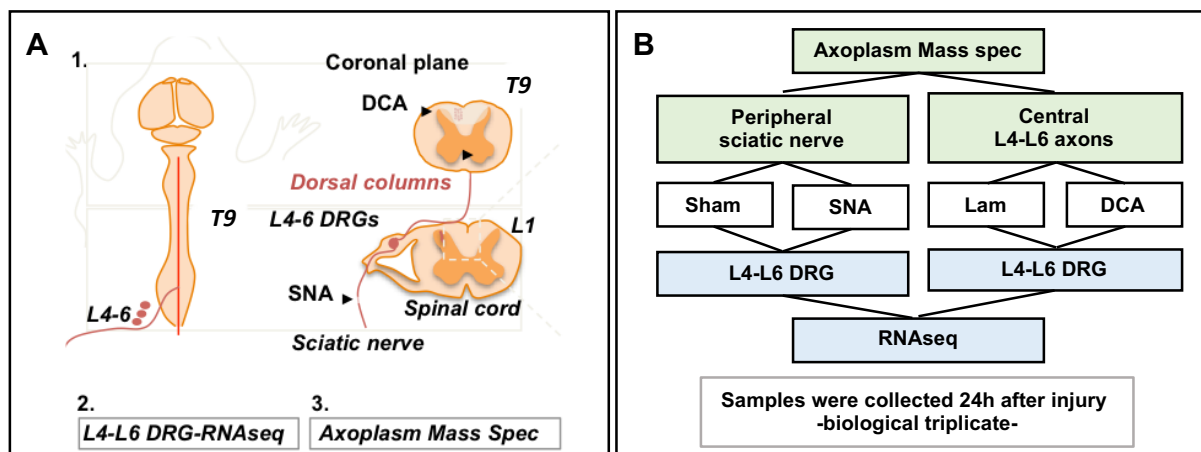


Figure 8. Schematic of experimental diagram

(A) Diagram of sciatic nerve and T9 dorsal column axotomy.

(B) Schematic diagram of experimental paradigm.

First, we measured the expression of axoplasmic proteins comparing peripheral vs central L4-6 DRG projections in the mock control (without injury). This would allow the detection of possible molecular differences in the two compartments, prior of the injury. Interestingly, the peripheral and central axonal projections seemed to have a very distinct molecular profile (Figure 9A) with 821 and 563 proteins being enriched in the peripheral and central projections, respectively (Figure 9B and Supplementary file 1). Importantly, functional classification of these protein groups showed that peripheral nerve proteins are involved in cytoplasmic carbohydrates and amino acid and vitamin metabolism (Figure 9C and Supplementary file 6)

while the central branch proteins include proteins involved in energy production, mitochondrial metabolism (mainly TCA cycle), protein folding, cytoskeleton regulation (Figure 9D and Supplementary file 7). This might suggest for the first time that the peripheral and central DRG branch represent two very different compartments, relying on different metabolic regulation for energy production.

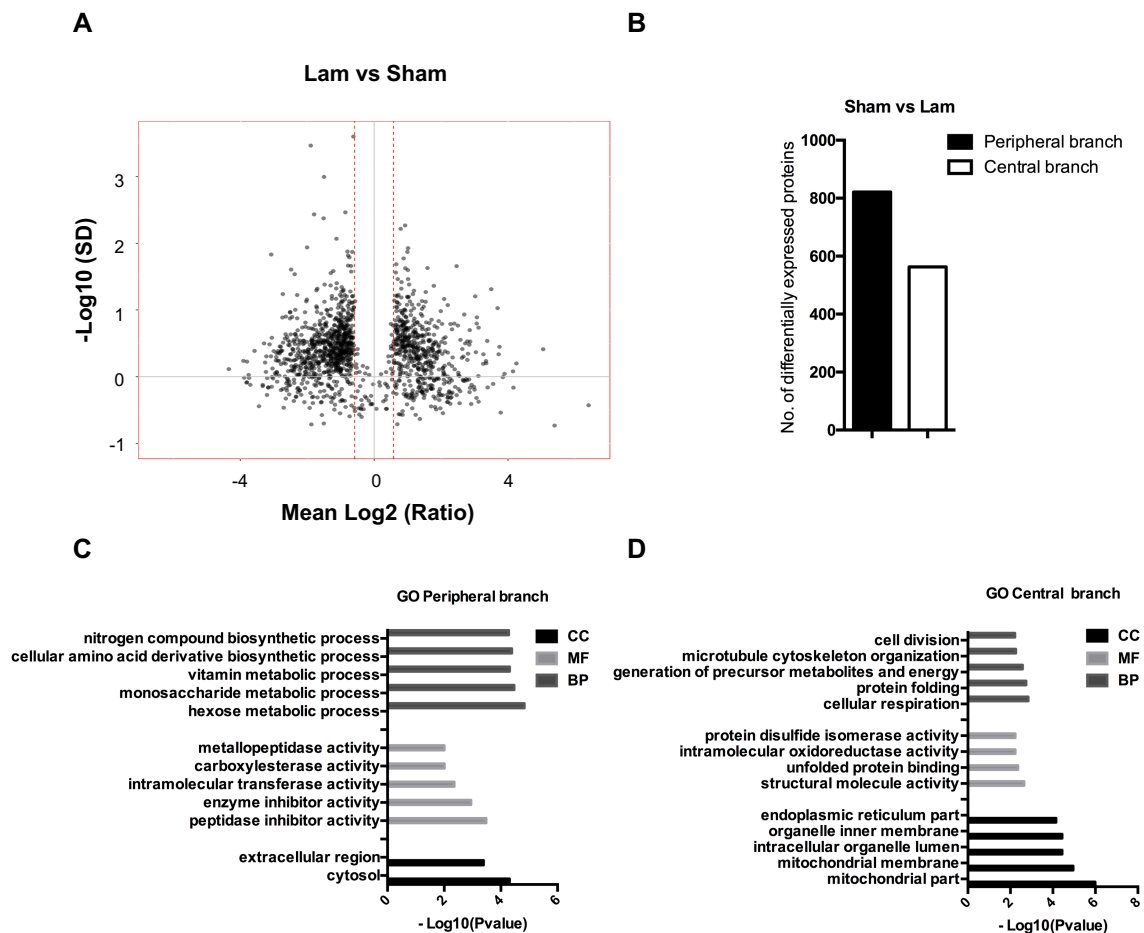


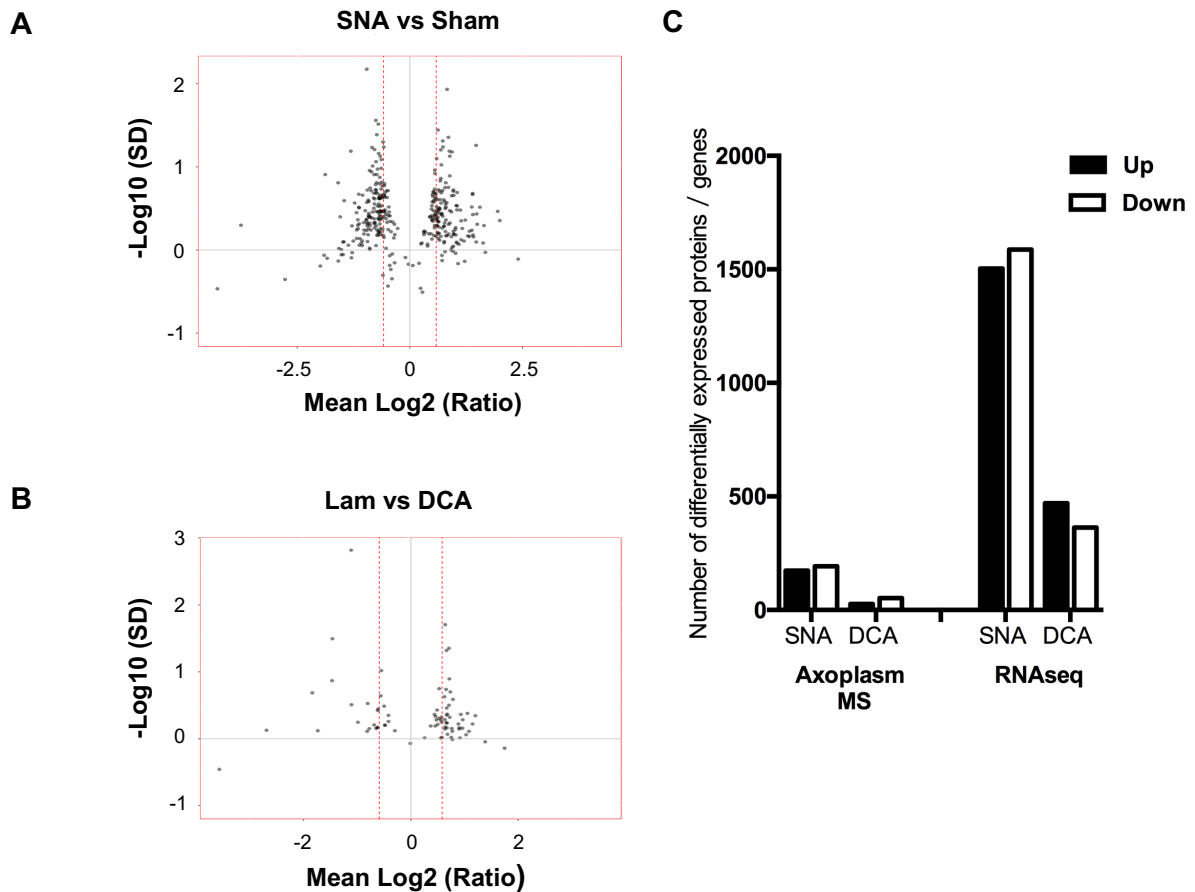
Figure 9. The peripheral and central axonal projections have a very distinct molecular profile without lesion

(A) Volcano plot of the differentially expressed proteins in the axoplasmic extract from central (Lam) branch vs peripheral (Sham) nerve. The average ratio is plotted against the standard deviation (SD). The dashed red lines represent \log_2 threshold=0.58. The grey dots represent proteins with a concordance of at least 2 replicates out of 3.

(B) Histogram shows the number of differentially expressed proteins in the axoplasmic extract from central (Lam) branch vs peripheral (Sham) nerve.

(C-D) Histograms show the first 5 ranked GO categories (BP: Biological Process; MF: Molecular Function; CC: Cellular Component, p-value < 0.01) of the proteins enriched in the peripheral branch and central branch.

Therefore, not surprisingly, when we compared proteomics expression data of injured peripheral vs central axons to their respective control, we found a very distinct injury response. While injury-responsive proteins in the sciatic nerve were numerous, differential protein expression in central axons was more modest (Figure 10A-C and Supplementary file 2, 3). Functional classification of the differential expressed proteins showed that injury-responsive proteins in the sciatic were mainly belonged to functional classes representing transcription, translation, response to injury and nucleotide binding process (Figure 10D and Supplementary file 8). However, represented functional classes of differential protein expression in central axons included regulation of translation and mitochondrial structure (Figure 10D and Supplementary file 8).



D

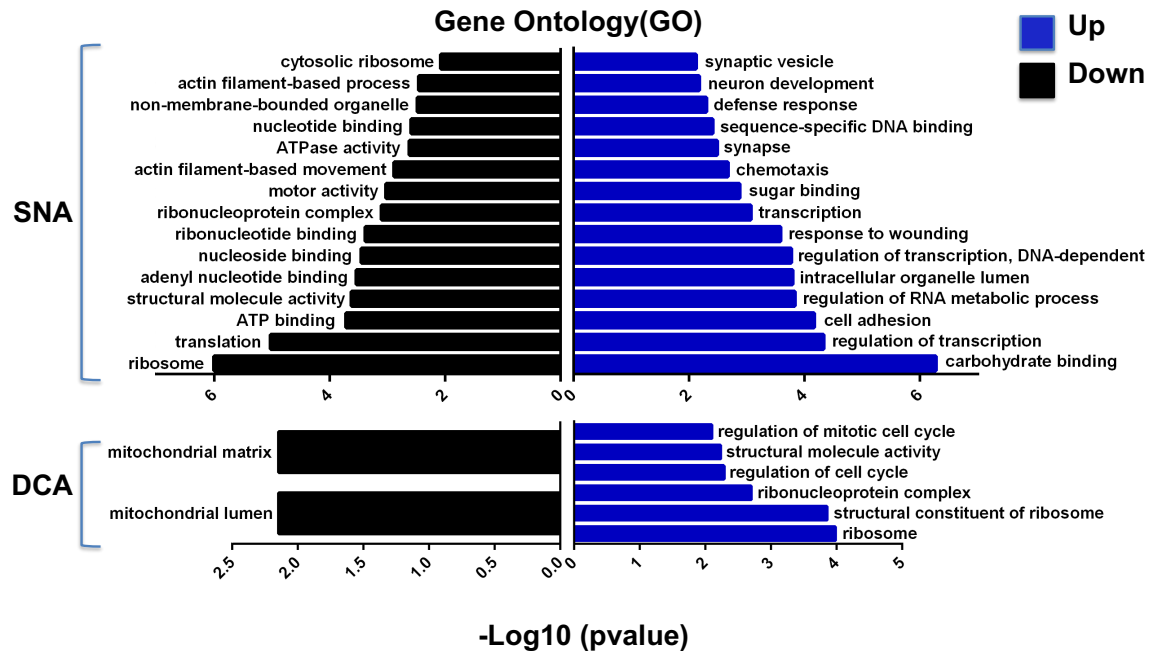


Figure 10. Injuries to the peripheral and central branch of DRG elicit different response

(A-B) Volcano plots of the differentially expressed proteins in the axoplasmic extract from peripheral nerve after sciatic nerve axotomy (SNA) vs Sham (control injury) and from the central branch's axoplasmic extract after dorsal column axotomy (DCA) vs Lam (control injury). The average ratio is plotted against the standard deviation (SD). The dashed red lines represent \log_2 threshold=0.58. The grey dots represent proteins with a concordance of at least 2 replicates out of 3.

(C) Histogram shows the number of differentially expressed proteins in both peripheral and central branch axoplasm and genes in L4-L6 DRGs following sciatic nerve and dorsal dorsal column axotomy.

(D) Gene ontology analysis of differentially expressed proteins elicited by SNA and DNA. Differentially expressed proteins were selected with cut off $\log_2(FC) > 0.58$ (Blue) or $\log_2(FC) < -0.58$ (Black). Gene ontology was performed by DAVID. Only enriched GO items with $p\text{-value} < 0.01$ were selected.

In line with proteomics analysis, RNAseq data revealed a similarly highly unique post-injury pattern of gene expression in DRG between sciatic and dorsal column axotomies (Figure 10C and Supplementary file 4, 5). Protein-protein interaction network of the differentially expressed proteins in the peripheral axoplasm after nerve injury (Figure 11A) revealed that proteins are highly interconnected, with a higher prevalence for proteins involved in transcription/translation and metabolic regulation, and the protein AMPK seems to be a central node in such networks. On the contrary, proteins differentially expressed after DCA do not seem to be organized in relevant functional networks (Figure 11B).

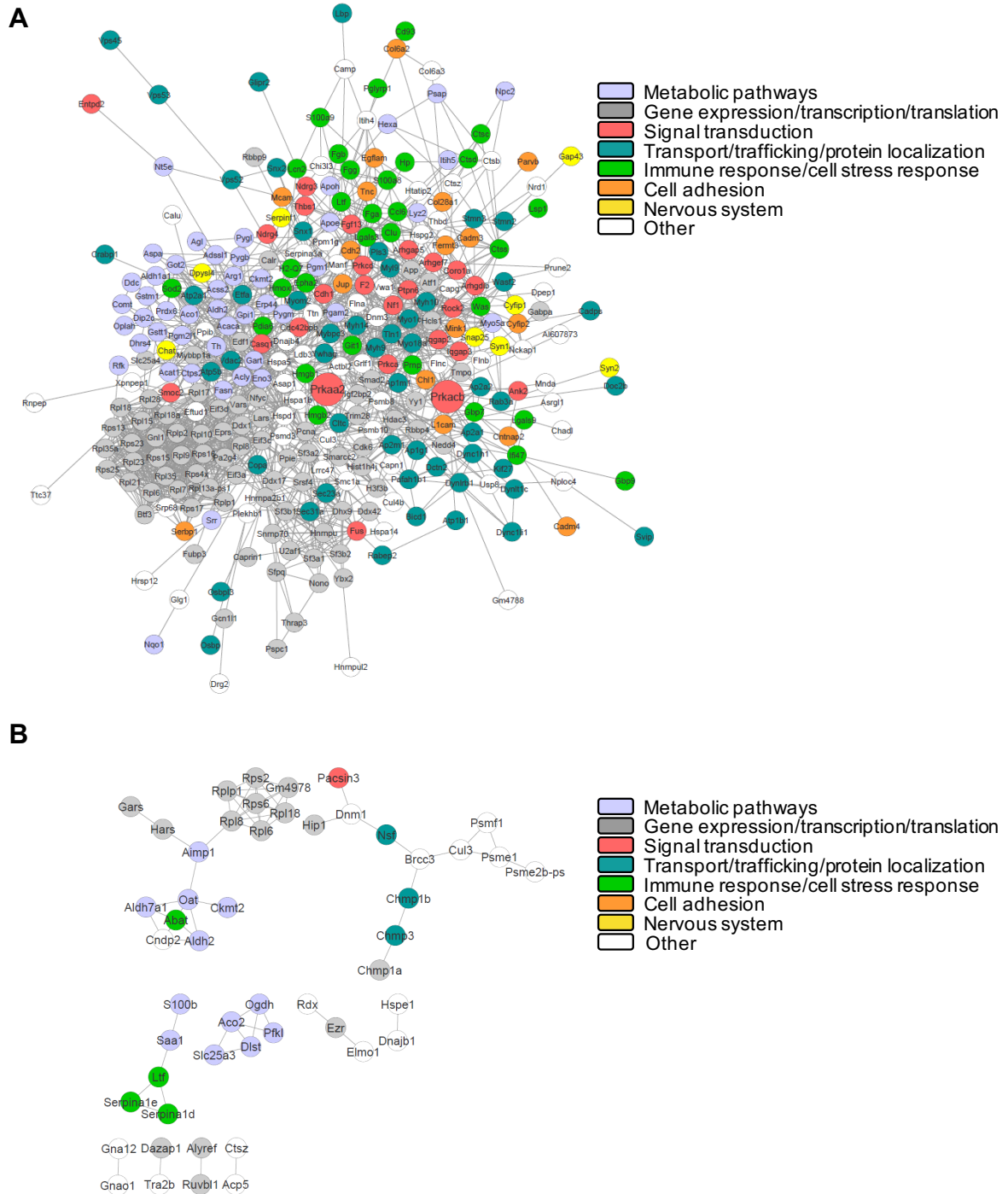


Figure 11. Protein network analysis shows that AMPK seems as the hub protein in the network after SNA (A-B) Protein-protein interaction network of the differentially expressed proteins after SNA and DCA visualized with Cytoscape. The nodes represent different proteins, while edges represent interaction score. Node color represents Gene Ontology annotation of the proteins.

In order to have a better understanding of the signalling pathways within the “DRG axonal signalling unit” that may be relevant for the regeneration programme, we decided to combine the axoplasmic proteomics and DRG transcriptomics. The KEEG pathway analysis of the combined dataset after SNA revealed enrichment of proteins were involved in actin regulation, ribosome components, insulin signalling pathway and other metabolic pathways (Figure 12A and Supplementary file 9), while after DCA proteins mainly involved in amino acid metabolism were regulated (Figure 12B and Supplementary file 10).

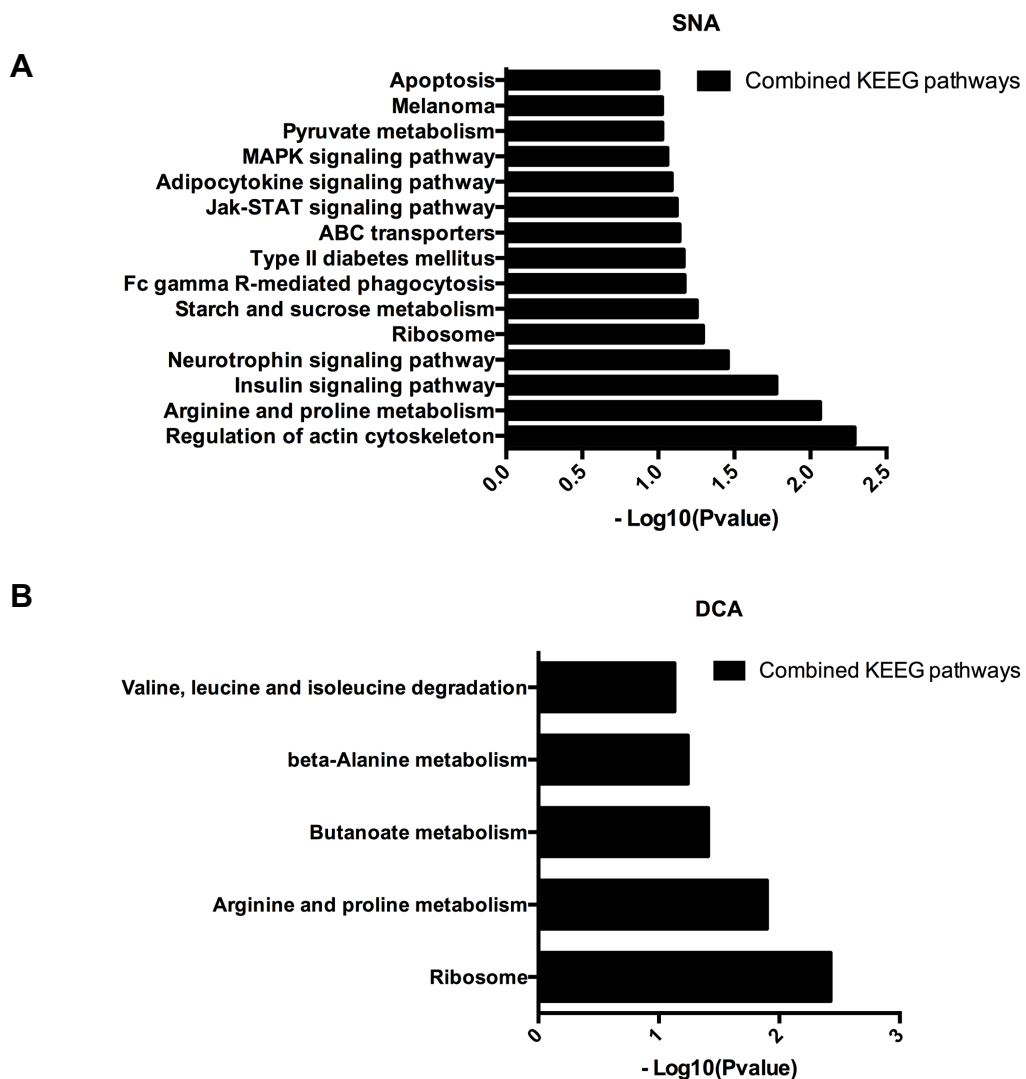


Figure 12. Combined KEEG pathways following SNA and DCA in both axoplasm and DRG

Histograms show the enriched KEGG pathways (p-value < 0.1) of the differentially expressed genes and proteins, in DRG and axoplasm respectively, after SNA (A) or DCA (B).

Moreover, we performed protein-protein interaction network using the all genes assigned to significantly enriched in the combined (RNAseq and proteomics) KEGG pathways (p-value < 0.1) after SNA. Data showed that AMPK controls many signaling pathways that are involved in axonal regeneration (Figure 13).

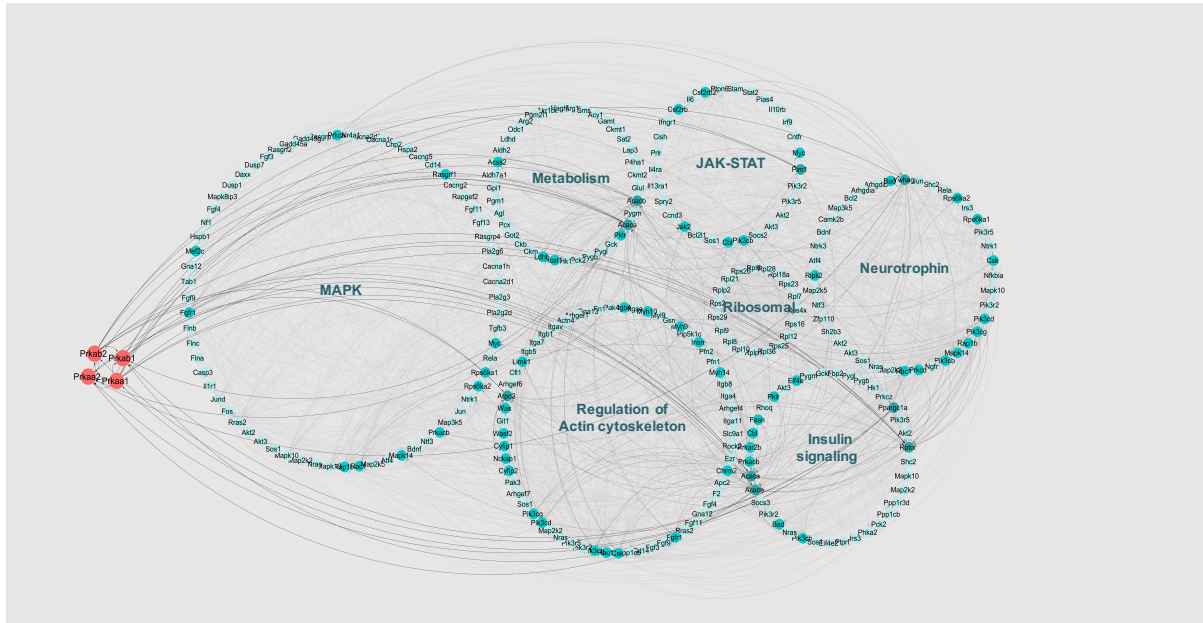


Figure13. Cytoscape visualization of the protein network under AMPK control after SNA

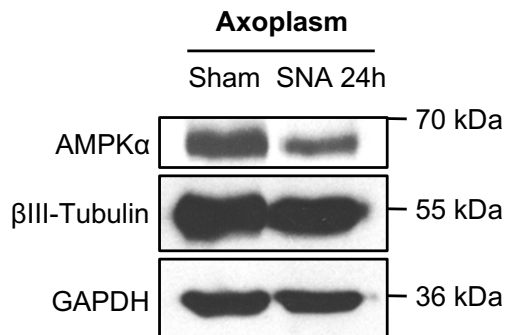
Protein-protein interaction network was analyzed by String and visualized by Cytoscape. The nodes represent different proteins, while Edges represent protein interaction score according to String database. Genes were jointly organized in a circular layout according to their KEGG affiliation by using Cytoscape. Red nodes represent the four AMPK subunits.

Importantly, while AMPK α mRNA level did not change in DRGs after SNA and DCA, our proteomics data revealed that the protein level of AMPK α was significantly reduced in the axoplasm following SNA but not DCA which is validated by peripheral axoplasm WB (Figure 14), suggesting that down-regulation of AMPK signaling via AMPK α degradation may play a role in the differential regenerative response to central vs peripheral injury. The validation of AMPK expression in axoplasm of central branch after DCA will be performed in further experiments.

A

AMPK α	SNA vs Sham	DCA vs Lam
Axoplasm MS (Protein)	Mean Log2 (Ratio) = -0.699	No change
RNAseq (mRNA)	No change	No change

B



C

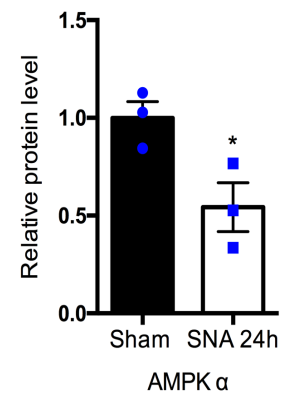


Figure 14. AMPK α protein expression is downregulated in axoplasm after SNA but does not change after DCA

(A). Table shows the AMPK α protein (in axoplasm) and mRNA (in DRG) changes following SNA and DCA at 24h.

(B). Immunoblot shows AMPK α 1 expression in axoplasm under sham and SNA at 24h.

(C). Quantification of (B). n=3 independent experiments. The relative protein expression level is normalized by GAPDH following versus Sham. Values represent means \pm SEM (*p < 0.05; paired t test).

3.2 AMPK α 1 expression, phosphorylation and activity are downregulated following SNA

Next, we aimed to establish the expression levels of AMPK α 1 and AMPK α 2 following central dorsal column axotomy (DCA) versus peripheral sciatic nerve axotomy (SNA) in DRG. Immunoblots revealed that the expression of AMPK α 1 but not α 2 is reduced following SNA but not DCA (Figure 15A-D). The expression of the overall active phosphorylated AMPK α (pAMPK α) is also reduced following SNA in a similar tendency as AMPK α 1 (Figure 15A-B), suggesting that sciatic axotomy is followed by inhibition of AMPK α 1 protein expression rather than specific changes in phosphorylation. However, the p-AMPK α antibody recognizes both phosphorylated AMPK α 1 and AMPK α 2, so the reduced level of p-AMPK α observed in WB is not totally the same as AMPK α 1 reduction level. Importantly, we found by

immunohistochemistry that AMPK α 1 expression was inhibited specifically in DRG neurons following SNA (Figure 15E-F). An extra immunostaining experiment will be done aimed to evaluate AMPK α 1 reduction in different type of DRG neurons. In order to detect whether AMPK activity was affected by SNA, we measured AMPK activity from DRG *ex vivo* subsequently to SNA and found that it is significantly reduced (Figure 15G), in line with the inhibition of AMPK α 1 and p-AMPK α protein expression. Also, the activity assay cannot distinguish AMPK α 1 and AMPK α 2 as they have the same phosphorylation site, so the reduced level of AMPK activity is not the same as AMPK α 1 degradation level after SNA.

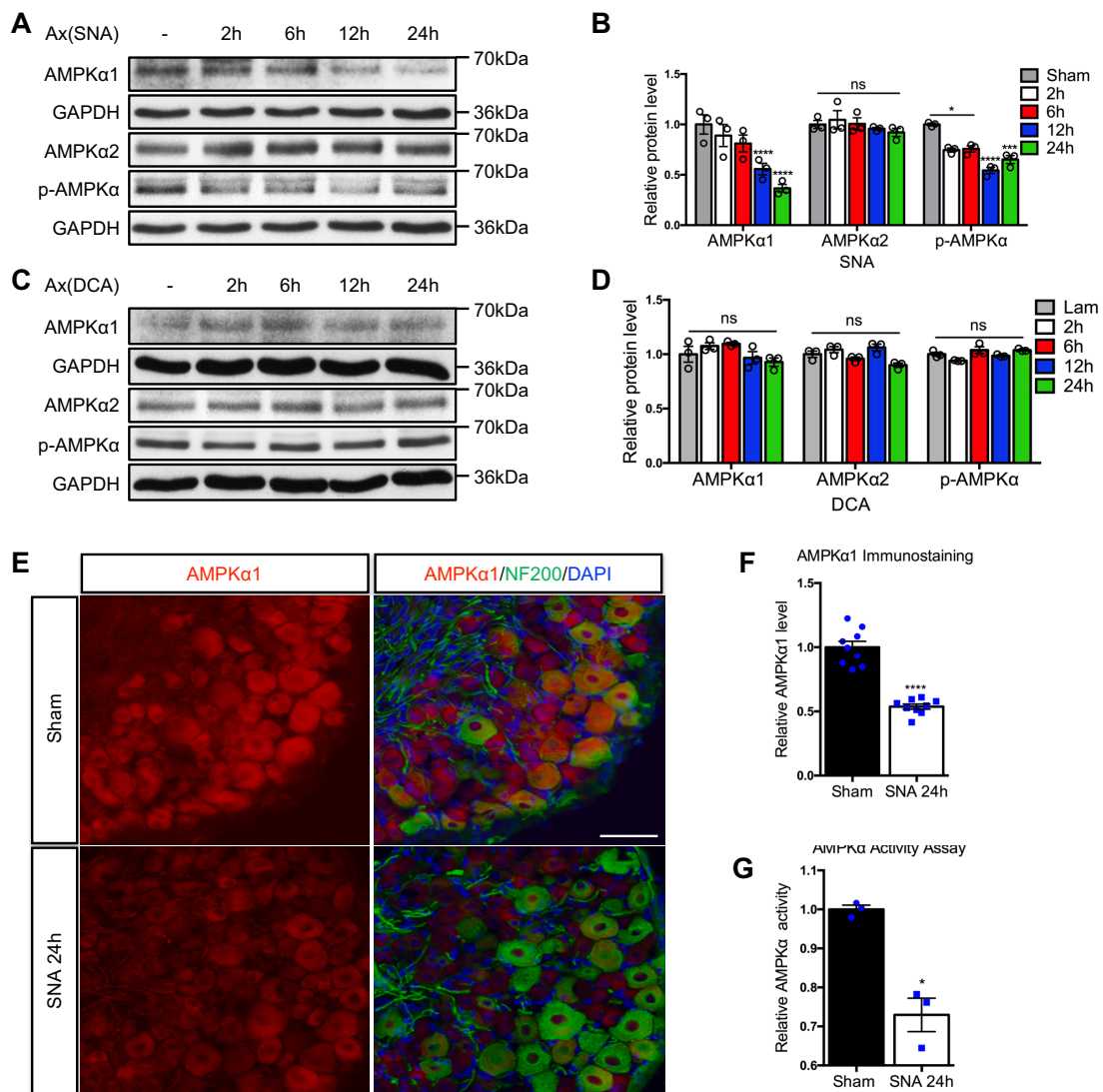


Figure 15. DRG immunoblotting and immunostaining show that AMPK α 1 is downregulated after SNA

(A) Immunoblot shows AMPK α 1; AMPK α 2 and p-AMPK α expression under sham and SNA at different time points.

(B) Quantification of AMPK α 1; AMPK α 2 and p-AMPK α expression of (A). n=3 independent experiments. The relative expression level of each protein at different time point is normalized by GAPDH following versus Sham. Values represent means \pm SEM (*p < 0.05; ***p < 0.001; ****p < 0.0001; ns: no significant; Two-Way ANOVA followed by Bonferroni test).

(C) Immunoblot shows AMPK α 1; AMPK α 2 and p-AMPK α expression under lam and DCA at different time points.

(D) Quantification of AMPK α 1; AMPK α 2 and p-AMPK α expression of (B). n=3 independent experiments. The relative expression level of each protein at different time point is normalized by GAPDH following versus Lam. Values represent means \pm SEM (ns: no significant; Two-Way ANOVA followed by Bonferroni test).

(E) Representative fluorescence images of immunostaining for AMPK α 1; neurofilament 200 (NF-200) and DAPI in DRG neurons under Sham and 24h SNA. Scale Bar, 50 μ m.

(F) Quantification of AMPK α 1 expression level of (C). n=3 mice, 9 DRGs in total of each group. Values represent means \pm SEM (****p < 0.0001; paired t test).

(G) AMPK activity assay in DRG neurons. n = 3 independent experiments. The assay was performed with samples under sham and 24h SNA. Values represent means \pm SEM (*p < 0.05; paired t test).

3.3 Pharmacological inhibition of AMPK promotes DRG regenerative growth

Next, to investigate whether AMPK inhibits axon growth, we used the AMPK inhibitor compound C (an ATP competitor) in cultured DRG neurons. We found that pharmacological inhibition of AMPK activity with compound C (10nM) significantly enhanced neurite outgrowth in cultured DRG neurons on both PDL/laminin growth permissive and myelin inhibiting substrates (Figure 16A-B). It has been reported that AMPK regulates cell growth via suppression the mammalian target of rapamycin complex1 (mTORC1) pathway (Shaw, 2009). To confirm whether treatment of compound C activates mTOR signalling, we tested the phosphorylation of ribosomal protein S6 kinase (p70S6K), which is a downstream target of mTOR (Hay and Sonenberg, 2004). We found that treatment with 10nM compound C increased p70S6K phosphorylation level at 24h (Figure 16C). Moreover, mTOR pathway has been reported as an important pathway for axonal regeneration (Park et al., 2008; Sun et al., 2011). Besides inhibits AMPK activity, compound C is also found to inhibit other kinases (Bain et al., 2007; Vogt et al., 2011) and play an anti-glioma role in an AMPK-independent manner (Liu et al., 2014). However, our bioinformatics analysis has predicted that AMPK as a key node to control multiple regenerative pathways, so we do believe that inhibition of AMPK activity plays a pivotal role in neurite outgrowth compared with other kinases in our in vitro experiment.

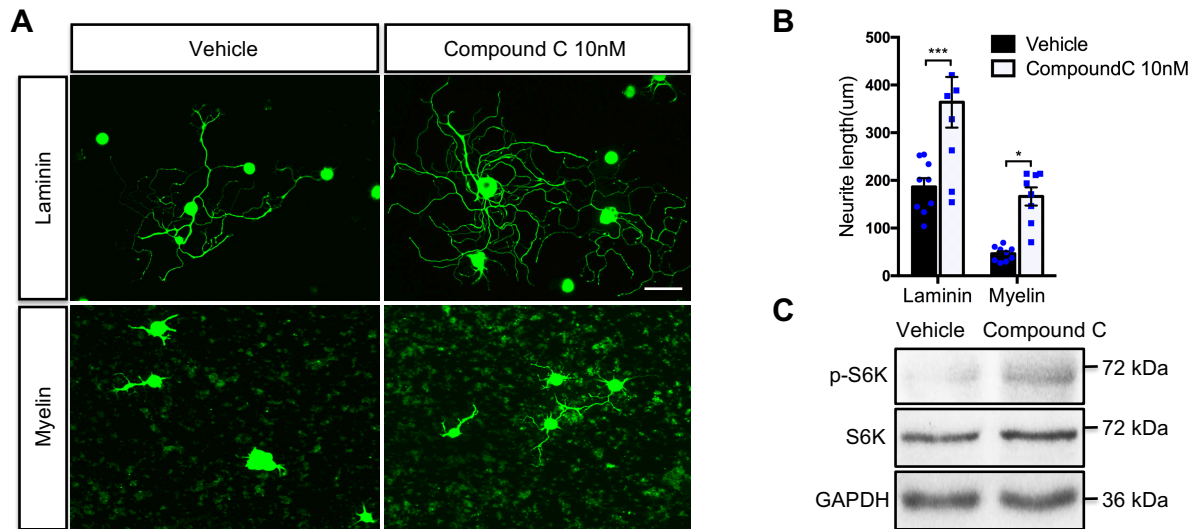


Figure 16. AMPK inhibition promotes DRG neurite outgrowth

(A) Representative neurite outgrowth images of cultured DRG neurons at 24h after delivery of vehicle or compound C (AMPK activity inhibitor). Compound C promotes DRG regenerative growth. Scale Bar, 20 µm.

(B) Quantification average neurite length of (A). n=3 independent experiments in triplicate. Values represent means ± SEM (*p < 0.05; ***p < 0.001; Two-Way ANOVA followed by Bonferroni test).

(C) Immunoblot shows that p-S6K and S6K expression in cultured DRG neurons treated with Vehicle or compound C (10nM).

Together, our data so far suggest that AMPK activity and AMPK signalling pathways are negatively regulated by regenerative SNA while they remain unresponsive following non-regenerative DCA. Furthermore, inhibition of AMPK activity promotes DRG regenerative growth on both growth permissive and inhibitory substrates.

3.4 AMPK α immunoprecipitation followed mass spectrometry identifies differential AMPK proteosomal degradation

3.4.1 AMPK α forms a preferential protein complex with the proteasome after SNA, which controls AMPK α 1 expression.

To investigate the molecular mechanisms underpinning the SNA-dependent reduction of AMPK α 1 protein expression, we performed immunoprecipitation of AMPK α followed by mass spectrometry from DRG ex vivo following sham or sciatic axotomy at 6h. IgG was used as the negative control to exclude the non-specifically bound proteins. We found 117 and 91 proteins were immunoprecipitated with AMPK α in sham and after sciatic injury respectively (Supplementary file 11). To gain functional insight into the differentially expressed protein profiles, we performed a protein-protein interaction network analysis (using String followed

Specially, the proteasome 19S regulatory subunit PSMC5, also known as RPT6, shows a putative direct connection with AMPK α and it was therefore predicted to interact with AMPK α . RPT6 has been reported as the crucial subunit for the proteasome 19S regulatory particle assemble and proteasome activation (Sokolova et al., 2015).

Together, this allowed us to formulate the hypothesis that SNA-dependent reduction in AMPK α 1 expression may be mediated by increased proteasome degradation mediated by increased activity of the 26S proteasome and that the 19S regulatory subunit PSMC5 could be a critical component.

3.4.2 AMPK α 1 protein degradation is regulated by proteasome activity

Therefore, to investigate whether the 26S proteasome controls AMPK α 1 protein level, we performed immunoblotting of AMPK α 1 from DRG neurons in culture and from DRG *ex vivo* after *in vitro* or *in vivo* delivery of the 26S proteasome inhibitor Bortezomib respectively. Indeed, Bortezomib administration enhanced AMPK α 1 protein expression both in culture and *ex vivo* (Figure 18A-D), suggesting that the 26S proteasome activity affects AMPK α 1 protein level.

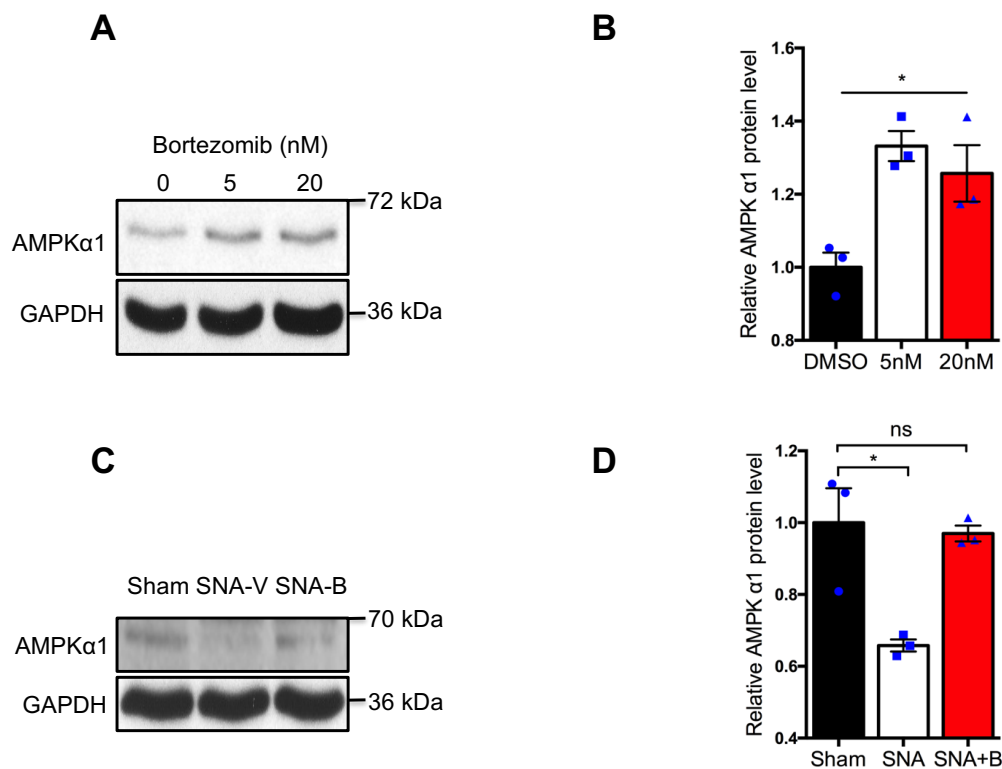


Figure 18. Proteasome activity controls AMPK α 1 expression

(A) Immunoblot shows AMPK α 1 expression in cultured DRG cells after incubation with different concentrations of Bortezomib at 6h.

(B) Quantification of (A). n=3 independent experiments. Relative AMPK α 1 expression level in Bortezomib group is normalized by GAPDH following versus that in DMSO group. Values represent means \pm SEM (*p < 0.05; Owo-Way ANOVA followed by Bonferroni test).

(C) Immunoblot shows AMPK α 1 expression in DRG neurons after intraperitoneal injection of Bortezomib (1mg/kg, 3 times i.p. injections per day) at 24h.

(D) Quantification of (C). n=3 independent experiments. Relative AMPK α 1 expression level is normalized by GAPDH following versus sham. Values represent means \pm SEM (*p < 0.05; ns: no significant; Owo-Way ANOVA followed by Bonferroni test).

3.5 PSMC5 forms a protein complex with AMPK α 1 to regulate AMPK α 1 expression

Next, we asked whether PSMC5 forms a protein complex with AMPK α by performing co-immunoprecipitation experiments and immunoblotting in DRG neurons. In line with our hypothesis, we found that AMPK α co-immunoprecipitated with PSMC5 (Figure 19).

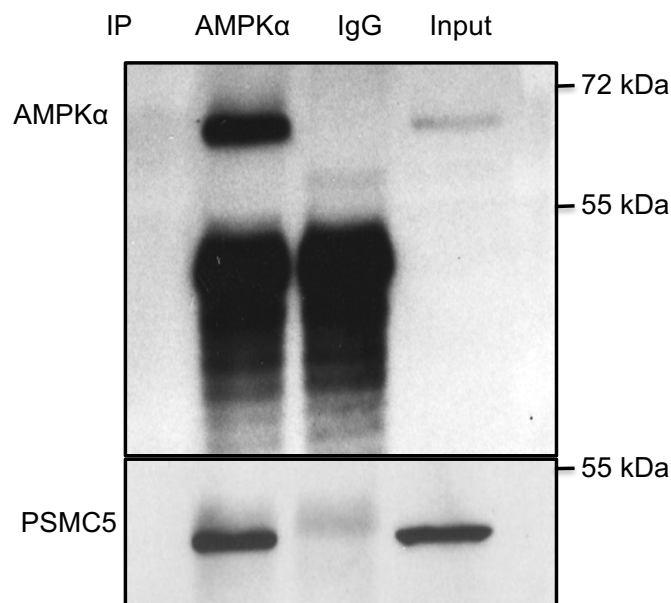


Figure 19. Immunoblot of AMPK α IP shows that AMPK α forms a complex with PSMC5

AMPK α IP was followed with AMPK α and PSMC5 immunoblot. IgG was used as control.

In order to confirm that PSMC5 is required for AMPK α 1 expression, we performed gene silencing of PSMC5 by doing transfection with PSMC5 siRNA or control siRNA in F11 DRG cell lines and measured AMPK α 1 protein expression by immunoblotting to find that AMPK α 1 was significantly up-regulated following PSMC5 silencing (Figure 20D, E). Next, we

electroporated primary cultured DRG neurons with the same siRNA against PSMC5 used in F11 DRG cell lines to verify whether it would inhibit neurite outgrowth. Indeed, we found that PSMC5 gene silencing inhibited neurite outgrowth in individual GFP positive neurons showing reduced PSMC5 expression (Figure 20A-C).

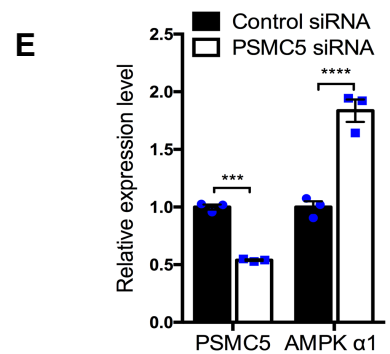
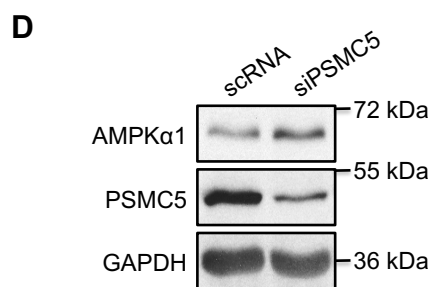
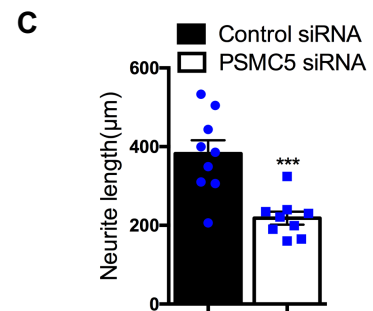
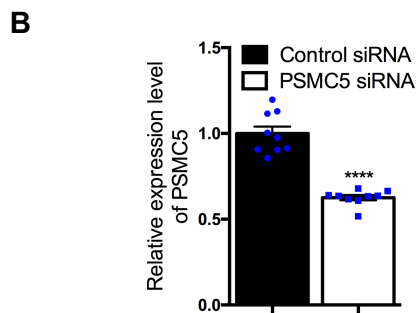
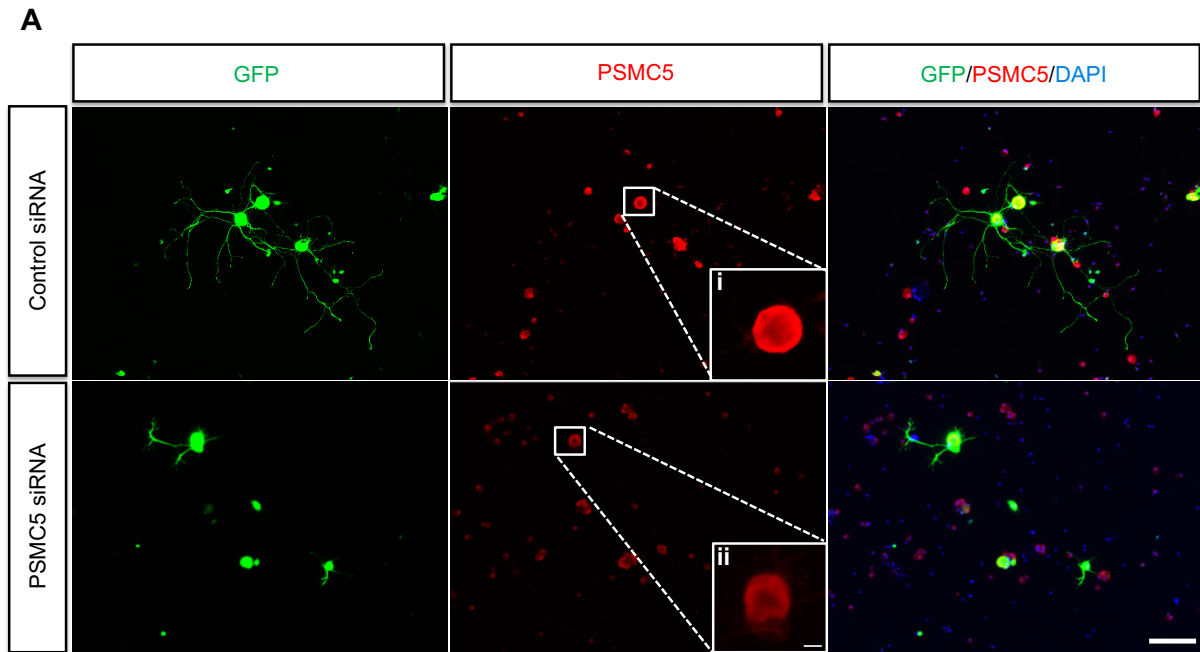


Figure 20. PSMC5 is required for AMPK α 1 degradation

(A) Representative neurite outgrowth images of cultured DRG neurons at 36h after electroporation with control siRNA, PSMC5 siRNA. Cells were stained with PSMC5, GFP and DAPI. Scale Bar; 200 μ m. A(i-ii), Scale Bar, 20 μ m.

(B) Quantification of PSMC5 expression of (A). n=3 independent experiments in triplicate. Relative PSMC5 expression level is quantified versus control siRNA. Values represent means \pm SEM (****p < 0.0001; Two- tailed test).

(C) Quantification average neurite length of (A). n=3 independent experiments in triplicate. Values represent means \pm SEM (**p < 0.001; Two- tailed test).

(D) Immunoblot shows PSMC5 and AMPK α 1 expression after transfection with control siRNA and PSMC5 siRNA in F11 cells.

(E) Quantification of (D). n=3 independent experiments. Relative protein expression level is normalized by GAPDH following versus control siRNA. Values represent means \pm SEM (**p < 0.001; ****p < 0.0001; Two-Way ANOVA followed by Bonferroni test).

Since it has been shown that PSMC5 activation in neurons depends upon phosphorylation at Serine 120 (S120) by Ca²⁺/calmodulin-dependent protein kinase II α (CaMKII α), which is activated after nerve injury (Bingol et al., 2010), we tested whether PSMC5 S120 phosphorylation would affect AMPK α 1 protein expression levels and DRG neurite outgrowth. To this end, we transfected F11 DRG cell lines with full length WT PSMC5, with PSMC5 phospho-mutant S120A, or PSMC5 phospho-mimetic S120D respectively. Immunoblotting revealed that PSMC5 S120D only significantly reduced AMPK α 1 protein level, suggesting that an active PSMC5 is required to downregulate AMPK α 1. Likely, in these culture conditions PSMC5 remains unphosphorylated since overexpression of WT or PSMC5 S120A do not have noticeable effects upon AMPK α 1 expression. This led to the prediction that PSMC5 S120D would promote DRG neurite outgrowth. Indeed, when we electroporated DRG neurons with PSMC5 WT or S120D, we found that cell expressing PSMC5 S120D but not WT, displayed enhanced neurite outgrowth (Figure 21A-C). Unfortunately, endogenous PSMC5 phosphorylation cannot be measured since p-specific antibodies are not available.

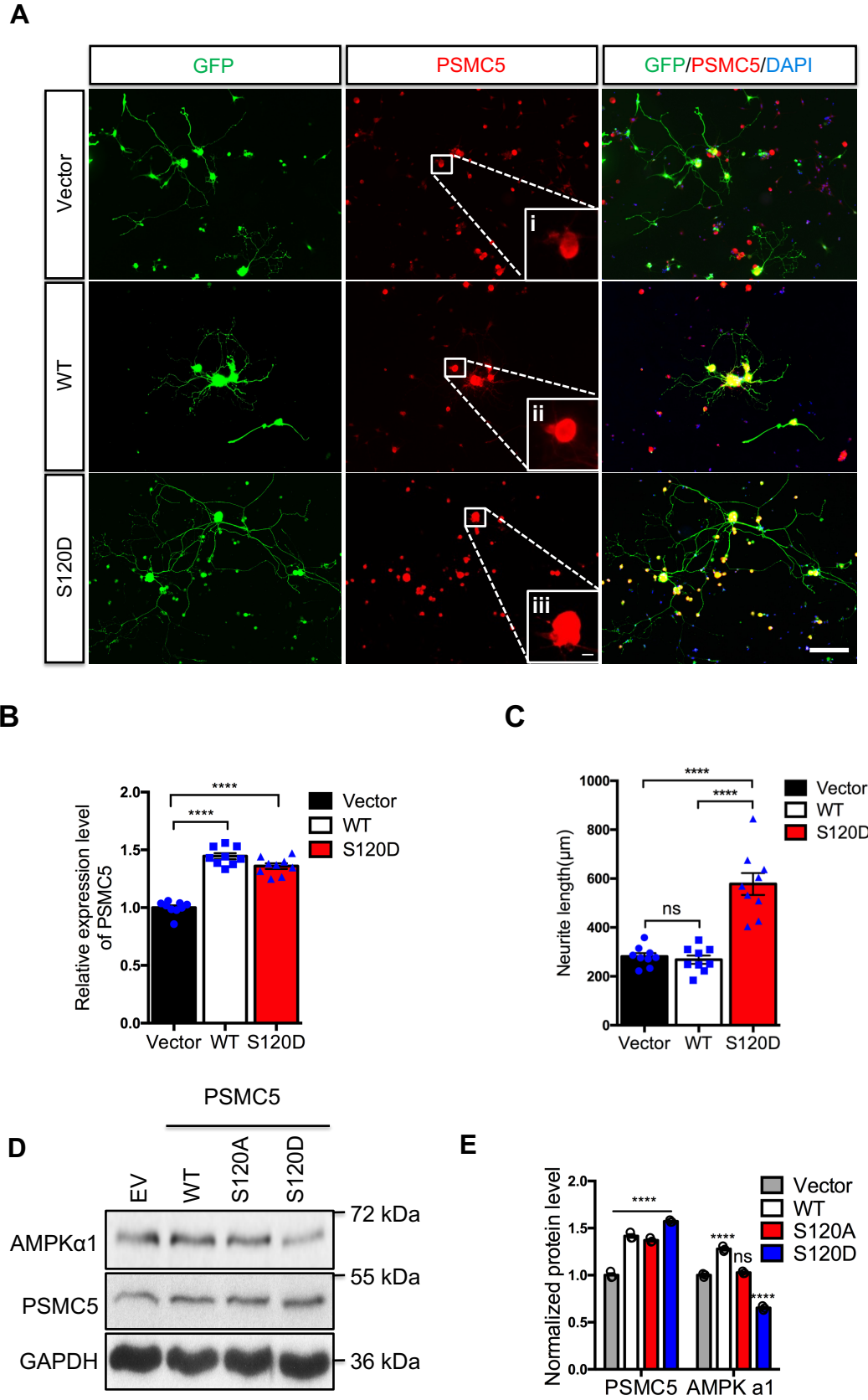


Figure 21. Phosphorylation of PSMC5 is required for AMPK α 1 degradation

(A) Representative neurite outgrowth images of cultured DRG neurons at 36h after electroporation with blank vector, PSMC5 WT and phospho-mimetic (S120D) plasmids. Cells were stained with PSMC5, GFP and DAPI. Scale Bar; 200 μ m, A(i-iii), Scale Bar; 20 μ m.

(B) Quantification of PSMC5 expression of (A). n=3 independent experiments in triplicate. Relative PSMC5 expression level is quantified versus empty vector. Values represent means \pm SEM (****p < 0.0001; One-Way ANOVA followed by Bonferroni test).

(C) Quantification of average neurite length of (A). n=3 independent experiments in triplicate. Values represent means \pm SEM (****p < 0.0001; ns: no significant, One-Way ANOVA followed by Bonferroni test).

(D) Immunoblot shows PSMC5 and AMPK α 1 expression after transfection with blank vector, WT, phospho-dead (S120A) and phosphor-mimetic (S120D) of PSMC5 plasmids at 48h in F11 cells.

(E) Quantification of (F). n=3 independent experiments. Relative protein expression level is normalized by GAPDH following versus empty vector. Values represent means \pm SEM (****p < 0.0001; ns: no significant, Two-Way ANOVA followed by Bonferroni test).

3.6 CaMKII α activation is required for SNA-dependent AMPK α 1 degradation

Previous studies have revealed that PSMC5 is phosphorylated at Serine 120 (S120) by Ca²⁺/calmodulin-dependent protein kinase II α (CaMKII α), which stimulates proteasome activation in neurons (Djakovic et al., 2012) and that is known to be activated after nerve injury (Bingol et al., 2010). Constitutively active T286D mutant (the autophospho-mimic form) of CaMKII α has been found sufficient to increase proteasome activity and phosphorylation of RPT6/PSMC5 (Djakovic et al., 2009).

Thus, we investigated whether SNA induced AMPK α 1 degradation is mediated by CaMKII α dependent proteasome activation. Adult mice were treated with CaMKII inhibitor KN-93 (12.5mg/kg) or KN-92 (12.5mg/kg), inactive analogue of KN-93, by intraperitoneal injection. L4-L6 DRG were collected 24h after SNA. Immunoblot showed up-regulated phosphorylation of CaMKII α by SNA and inhibition of CaMKII α activity blocked SNA induced AMPK α 1 degradation (Figure 22A-B). Moreover, overexpression of CaMKII α phospho-mimetic plasmid (T286D) reduced AMPK α 1 expression compared with WT and phospho-dead (T286A) plasmids in F11 DRG cells in vitro (Figure 22C, D). So, our data suggested that SNA induced activation of CaMKII α is required for proteasome mediated AMPK α 1 degradation. However, whether CaMKII α modulate AMPK α 1 expression upon injury in DRG neurons via phosphorylating PSMC5 deserves further investigation.

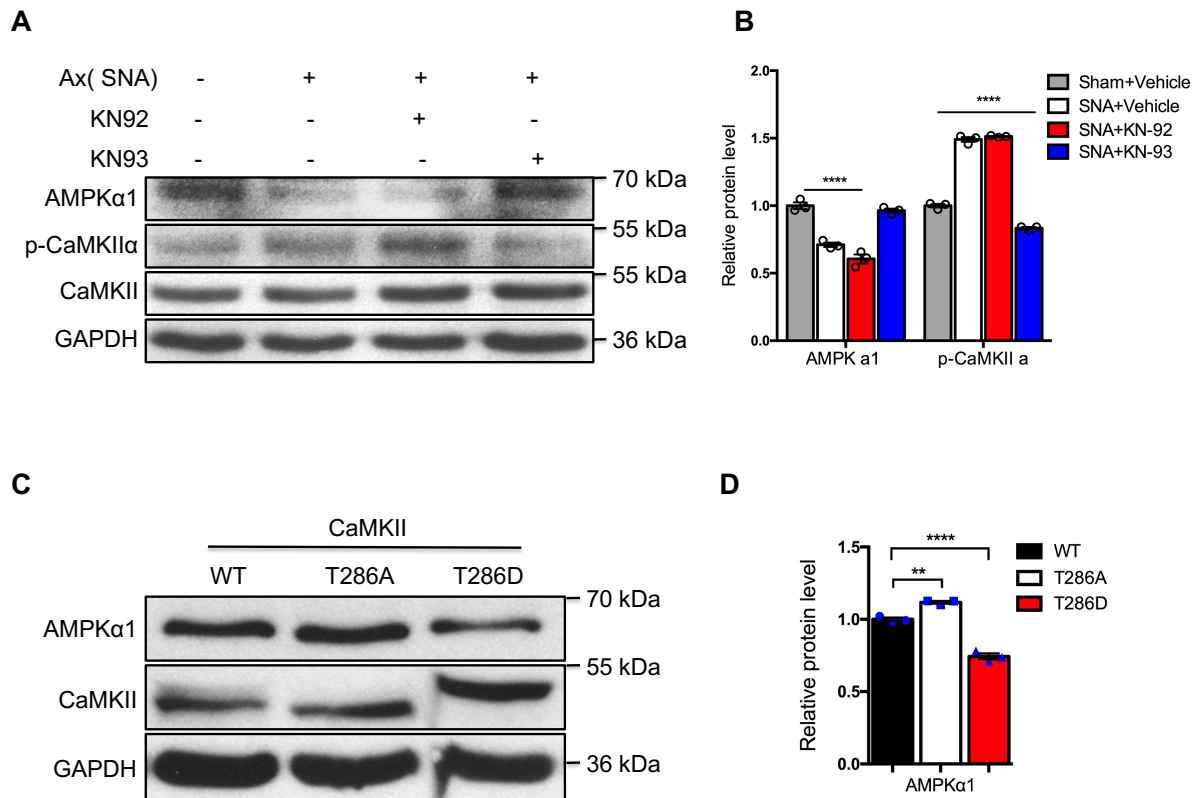


Figure 22. Phosphorylation of CaMKII α is required for SNA-reduced AMPK α 1 expression

(A) Immunoblot shows AMPK α 1 and p-CaMKII α expression level in L4-L6 DRG neurons after intraperitoneal injection of CaMKII inhibitor KN-93 (12.5mg/kg) and KN-92 (an inactive derivative of KN-93). The L4-L6 DRG neurons were collected 24h after SNA.

(B) Quantification protein expression of (A). n=3 independent experiments. Relative protein level is normalized by GAPDH following versus sham+vehiche. Values represent means \pm SEM (****p < 0.0001; Two-Way ANOVA followed by Bonferroni test).

(C) Immunoblot shows CaMKII and AMPK α 1 expression level after transfection with CaMKII α WT, T286A and T286D plasmids at 48h in F11 cells.

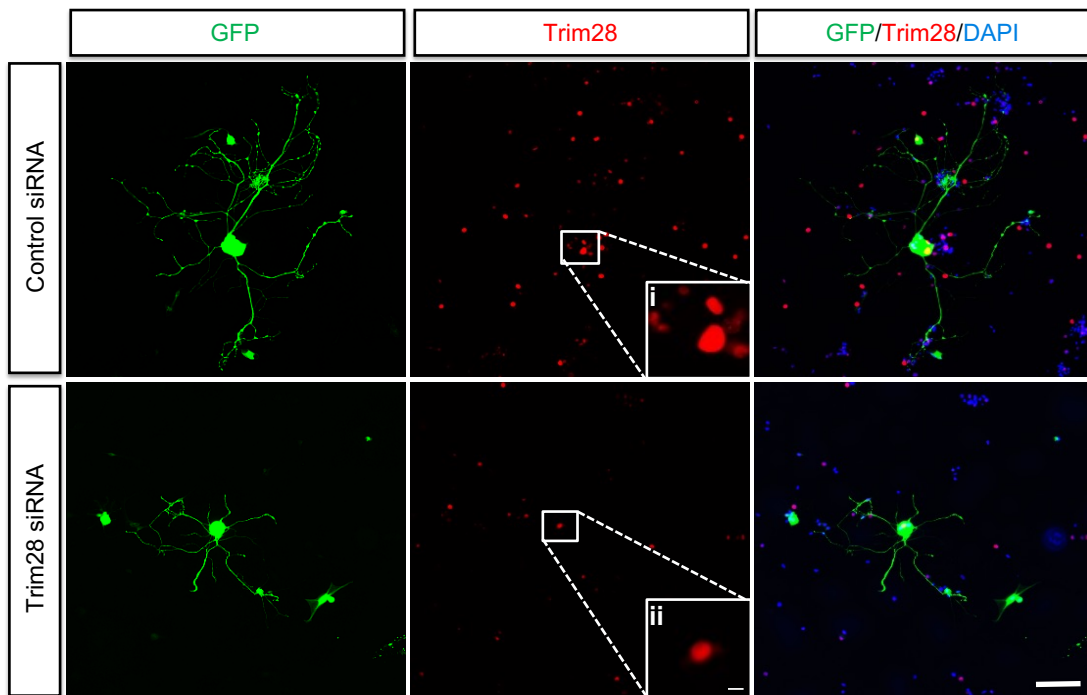
(D) Quantification of (C). n=3 independent experiments. Relative protein expression level is normalized by GAPDH following versus WT. Values represent means \pm SEM (**p < 0.01; ****p < 0.0001; Owo-Way ANOVA followed by Bonferroni test).

3.7 The E3 ligase Trim28 is involved AMPK α 1 degradation in DRG neurons after SNA

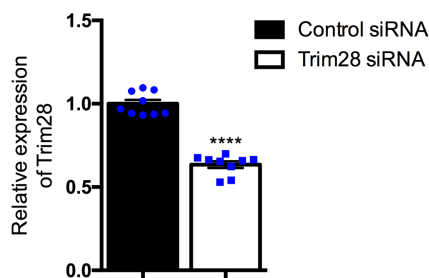
Although we found that the proteasome is involved in AMPK α 1 degradation, we have no idea about the ubiquitination of AMPK α 1 before it undergoes degradation by the proteasome. Tirm28, an E3 ligase, was reported to contribute to AMPK α 1 degradation in human cancer cells (Pineda et al., 2015). Therefore, we would like to know whether AMPK α 1 expression in DRG neurons is also mediated by Trim28. We transfected F11 DRG cells with Trim28 siRNA

and control siRNA respectively. Indeed, 48h after transfection, we found AMPK α 1 was upregulated after Trim28 silencing (Figure 23D, E). Next, we electroporated primary cultured DRG neurons with the same siRNA against Trim28 used in F11 DRG cell lines to verify whether it would inhibit neurite outgrowth. Indeed, we found that Trim28 gene silencing inhibited neurite outgrowth in individual GFP positive neurons showing reduced Trim28 expression (Figure 23A-C).

A



B



C

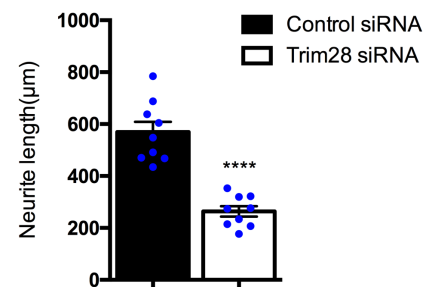




Figure 23. Trim28 is required for AMPK α 1 degradation

(A) Representative neurite outgrowth images of cultured DRG neurons at 36h after electroporation with control siRNA, Trim28 siRNA. Cells were stained with Trim28, GFP and DAPI. Scale Bar; 200 μ m. A(i-ii), Scale Bar, 20 μ m.

(B) Quantification of Trim28 expression of (A). n=3 independent experiments in triplicate. Relative Trim28 expression level is quantified versus control siRNA. Values represent means \pm SEM (****p < 0.0001; Two- tailed test).

(C) Quantification average neurite length of (A). Values represent means \pm SEM (***p < 0.001; Two- tailed test).

(D) Immunoblot shows Trim28 and AMPK α 1 expression after transfection with control siRNA and PSMC5 siRNA in F11 cells at 48h.

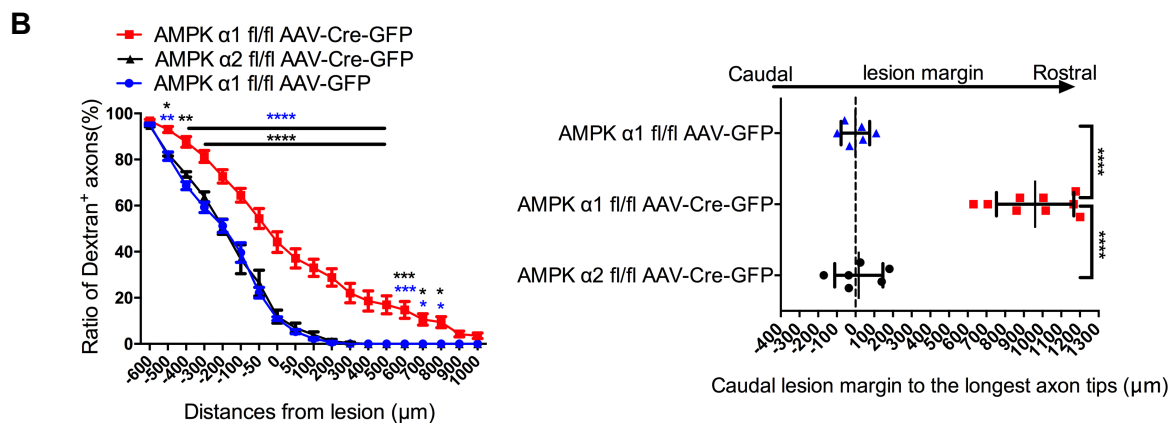
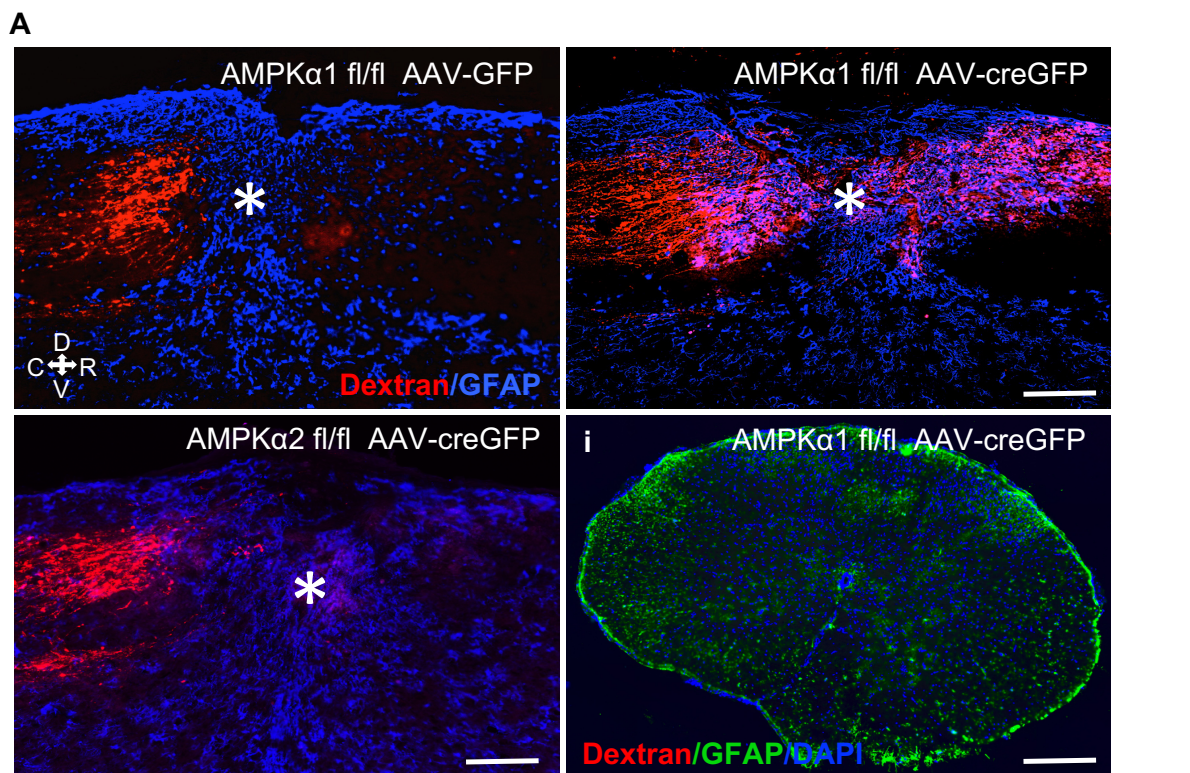
(E) Quantification of (D). n=3 independent experiments. Relative protein expression level is normalized by GAPDH following versus control siRNA. Values represent means \pm SEM (****p < 0.0001; Two-Way ANOVA followed by Bonferroni test).

However, we didn't find the direct combination of AMPK α 1 and Trim28 by immunoprecipitation (data not shown) which means that they may form complex indirectly by interacting with other adaptor proteins. Due to the ubiquitination is a transient and dynamic process, the measurement of ubiquitination level of AMPK α 1 in DRG neurons after SNA is not feasible at a single time point.

3.8 AMPK α 1 deletion promotes axonal regeneration and sensory recovery after SCI

Since bioinformatics analysis of proteomics and RNAseq data as well as experimental evidence so far suggested that AMPK might be a hub controlling regenerative signalling, we investigated whether *in vivo* genetic deletion of AMPK α 1 would enhance axonal regeneration across the inhibitory spinal cord environment. To this end, we injected the sciatic nerve of adult mice bilaterally with an AAV-cre-GFP or an AAV-GFP virus to delete AMPK α 1 in L4-L6 DRG neurons and 4 weeks later we performed a T9 spinal cord dorsal column crush injury. Five days before sacrificing the animals, at day 28 post-SCI, the axonal tracer dextran was injected in the

sciatic nerve, showing very highly percentage of expression in GFP positive transfected DRG (Figure 24F-H), to monitor axonal die-back and regeneration. Data analysis revealed that AMPK α 1 deletion reversed axonal die-back and promoted significant axonal regeneration past the lesion site. Interestingly, conditional deletion of AMPK α 2 did not affect axonal die-back or regeneration, suggesting that AMPK α 1 is specifically implicated in the regenerative phenotype (Figure 24A-C). AMPK α 1 deletion was validated by immunostaining followed with quantification (Figure 24D, E).



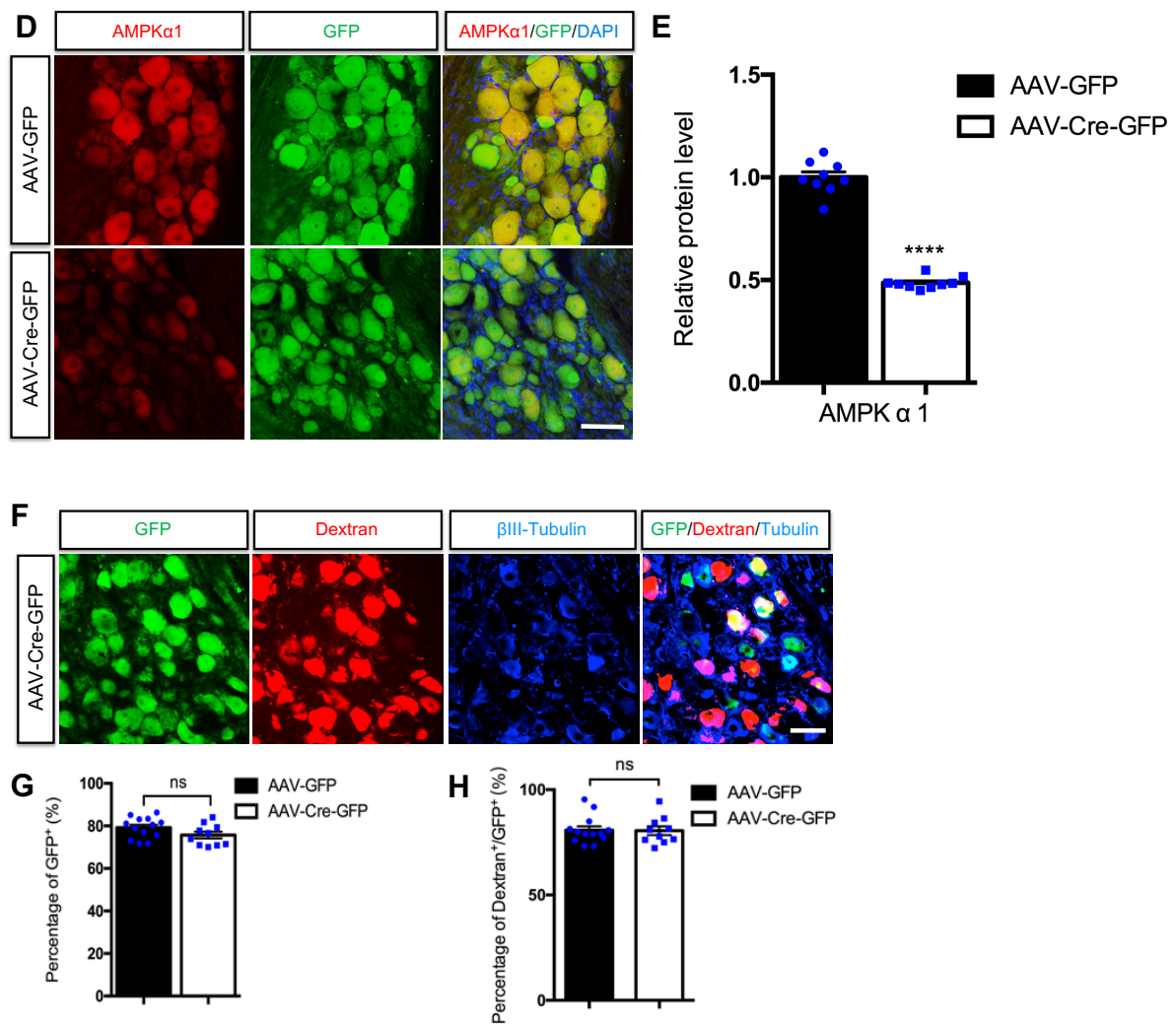


Figure 24. AMPK α 1 deletion promotes axonal regeneration after SCI

(A) Sample images of longitudinal spinal cord sections 4 weeks after SCI. Dorsal column axons are labeled by sciatic nerve injected Dextran. Asterisk indicates the lesion center. D; dorsal; V; ventral, C; caudal; R; rostral. Scale Bar; 200 μ m. Figure Ai, Fluorescence images of immunostaining for GFAP with Dextran and DAPI of spinal cord coronal section of AMPK α 1^{fl/fl} AAV-Cre-GFP at 8mm rostral to the lesion site showing the absence of spared dextran⁺ axons. Scale bar, 500 μ m.

(B) Quantification of regenerated axons. Blue asterisk indicates AMPK α 1^{fl/fl} AAV-Cre-GFP versus AMPK α 1^{fl/fl} AAV-GFP; black asterisk indicates AMPK α 1^{fl/fl} AAV-Cre-GFP versus AMPK α 2^{fl/fl} AAV-Cre-GFP. Values represent means \pm SEM (*p < 0.05; **p < 0.01; ***p < 0.001; ****p < 0.0001; Two-Way ANOVA followed by Tukey test; AMPK α 1^{fl/fl} AAV-Cre-GFP n=9 mice; AMPK α 1^{fl/fl} AAV-GFP n=6 mice; AMPK α 2^{fl/fl} AAV-Cre-GFP n=6 mice).

(C) Quantification of the distance from the caudal lesion margin to the longest dextran⁺ axon tips. Values represent means \pm SD (****p < 0.0001; Two-Way ANOVA followed by Tukey test; AMPK α 1^{fl/fl} AAV-Cre-GFP n=9 mice; AMPK α 1^{fl/fl} AAV-GFP n=6 mice; AMPK α 2^{fl/fl} AAV-Cre-GFP n=6 mice).

(D) Representative images of AMPK α 1 and GFP staining in DRG neurons sections after 4 weeks of AAV-GFP and AAV-Cre-GFP transfection. Scale bar, 50 μ m.

(E) Quantification AMPK α 1 level of (D). n=3 mice, 9 DRGs in total of each group. Values represent means \pm SEM (****p < 0.0001; Two-tailed test).

(F) Representative images of DRG neurons section from AAV-Cre-GFP group co-stained with GFP and Dextran. Scale bar, 50 μ m.

(G-H) Quantification of percentage of GFP⁺ and Dextran⁺ / GFP⁺ cells of both AAV-GFP and AAV-Cre-GFP groups. AAV-GFP, n=13 mice; AAV-Cre-GFP, n=10 mice. Percentage of GFP is calculated on GFP⁺ versus Tubulin⁺, percentage of Dextran⁺/GFP⁺ is calculated on Dextran⁺/GFP⁺ versus Tubulin⁺. Values represent means \pm SEM (ns: no significant; Two-tailed test).

Furthermore, we found that regenerating axons in mice that underwent AMPK α 1 deletion expressed pre-synaptic markers as shown by Dextran/VGlut1 co-labelling, including in close proximity to NeuN-positive neurons (Figure 25A).

We then asked whether conditional AMPK α 1 deletion in sensory DRG neurons leads to sensory recovery until 5 weeks after SCI by testing recovery of mechanoreception which was measured by performing Von Frey behaviour test. Sensorimotor test such as the Grid walk was also employed to discriminate whether recovery was limited to sensory function. Since dorsal column crush injury is mild compared with dorsal hemisection injury, so the locomotion impairment is not severe and cannot be detected easily by Grid walk, so the feasibility of this behaviour test for dorsal column crush injury model are different in different labs (Bradbury et al., 2002a; Kanagal and Muir, 2007, 2008). Indeed, we observed no effect upon the number of missteps on the Grid walk (Figure 25B), but we did find that conditional DRG AMPK α 1 deletion led to significant improvements in mechanoreception (Figure 25A). However, we found no differences in thermal nociception by performing the Hargraves test (Figure 25C) which indicated that the spinothalamic tract which transmits nociceptive signals to thalamus was intact after performing dorsal column crush.

Lastly, given the significant role of AMPK α 1 deletion in DRG neurons on axonal regeneration and functional recovery, we asked which regenerative signalling pathways are modulated by AMPK α 1 thereby promote axonal regeneration. To this end, we selected a number of candidates based upon merging previously published RAGs in DRG after sciatic nerve injury (Cho et al., 2015; Cho et al., 2013; He and Jin, 2016; Kone et al., 2014; Kwon et al., 2015; Ma and Willis, 2015), meanwhile the expression of some RAGs are regulate by AMPK α 1 deletion (Kone et al., 2014). To investigate whether the expression of these genes would depend upon AMPK α 1 expression in L4-L6 DRG neurons after SCI, we performed quantitative RT-PCR 24 hours following spinal cord injury after 4 weeks of AAV-cre-GFP mediated conditional deletion of AMPK α 1 by injecting the cre-GFP or control GFP virus in the sciatic nerve of AMPK α 1 floxed mice. Data analysis revealed that conditionally deleted AMPK α 1 in DRG display a significant increased expression of a number of key genes belonging to regenerative signalling pathways including c-jun, p53, BDNF, ATF3, Arg1, Fos, myc and IGF-1, while it had no effect upon HIF1a, CXCL12 and HDAC5 (Figure 26). As expected AMPK α 1 conditional deletion in DRG neurons led to changes in phosphorylation of well-defined protein targets including pACC and pERK and protein level of c-Jun (Figure 27). Thus, these data suggest that AMPK α 1 deletion induces multiple regenerative signalling pathways.

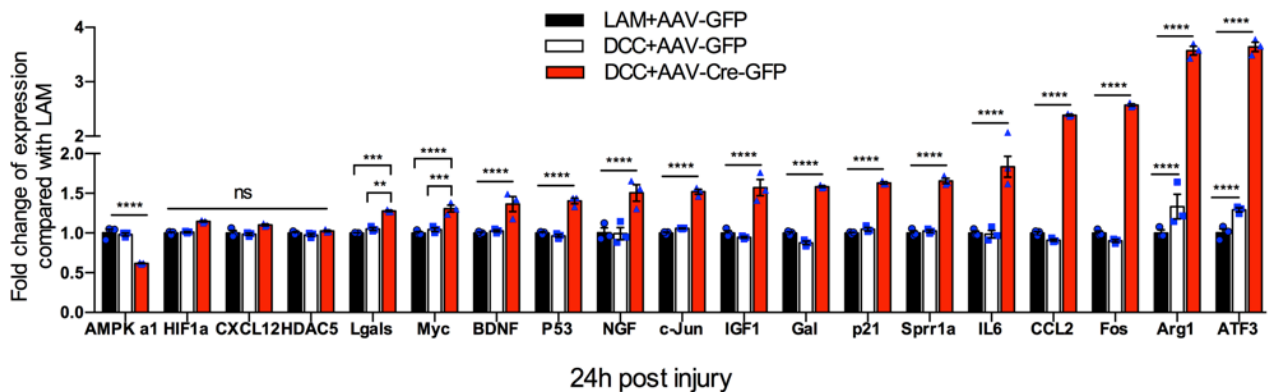


Figure 26. AMPK α 1 regulates the expression of multiple injury-induced RAGs

RT-PCR analysis the expression of some known RAGs 24h after SCI. AAV-GFP and AAV-Cre-GFP viruses are injected into sciatic nerve 4 weeks before injury. n=3 mice each group. Values represent means \pm SEM (**p < 0.01; ***p < 0.001; ****p < 0.0001; ns: no significant; Two-Way ANOVA followed by Tukey test).

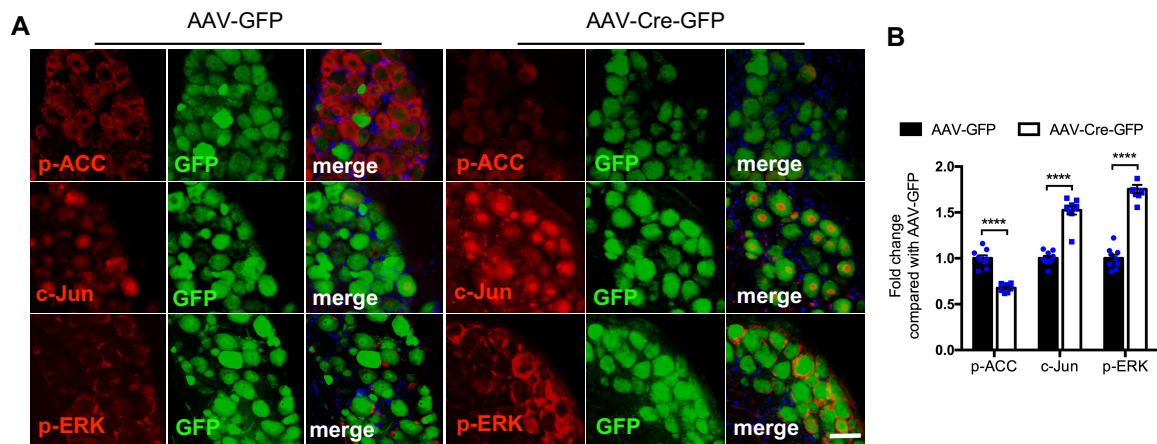


Figure 27. Immunostaining images show that AMPK α 1 regulates the expression of c-Jun and the phosphorylation of ERK and ACC

(A) Representative immunofluorescence images of p-ACC, c-Jun, p-ERK level after conditional deletion of AMPK α 1 in L4-L6 DRG neurons. DRG sections are stained with p-ACC, c-Jun, p-ERK together with GFP and DAPI. Scale bar, 50 μ m.

(B) Quantification of (A). n=3 mice. 9 DRGs in total of each group. Values represent means \pm SEM (****p < 0.0001; Two-Way ANOVA followed by Bonferroni test).

4. Discussion

4.1 Combined RNAseq in DRG and axoplasm proteomics bioinformatics analysis reveals a distinct injury response between peripheral and central axons injuries

Here, we performed combined RNAseq in DRG and axoplasm proteomics following sciatic nerve and dorsal column axotomy aimed to find the candidate central nodes and signaling pathways that are involved in axonal regeneration (Figure 8). First, we compared the proteins expression profile in axoplasm of both the peripheral and central branches prior to injury (Lam vs Sham). Interestingly, the peripheral and central projections had a very distinct molecular profile with 821 and 563 proteins were enriched in the axoplasm, respectively (Supplementary file 1,2). Functional analysis revealed that proteins in peripheral branch were mainly involved in cytoplasmic carbohydrates, amino acid and vitamin metabolism while proteins in central branch were mainly involved in energy production, mitochondrial metabolism (mainly TCA cycle), protein folding, cytoskeleton regulation (Figure 9 and Supplementary file 6,7). After, we compared the proteins and genes expression profiles in axoplasm and DRG after sciatic nerve and dorsal column axotomy via comparing with the mock controls. Not surprisingly, SNA elicited a robust proteins and genes expression changes compared with DCA (Figure 10A-C). Gene ontology analysis showed that differentially expressed proteins in axoplasm after SNA mainly participated in transcription regulation, cell adhesion, translation regulation and actin filament based movement, however, differentially expressed proteins after DCA were mainly involved in translation and mitochondrial structure (Figure 10D and Supplementary file 8). In order to have a better understanding of the signalling pathways in the “DRG axonal signalling unit” that are involved in axonal regeneration after injury, we did combined RNAseq and axoplasm proteomics analysis. The KEEG pathway analysis found that SNA enriched proteins mainly involved in regulation of actin cytoskeleton, metabolic pathways, insulin signalling pathway and several other regenerative pathways, while after DCA proteins were mainly involved in amino acid metabolism (Figure 12 and Supplementary file 9,10). Together, our data suggested that peripheral and central branch injury lead to a distinct response both in axoplasm and DRG.

4.2 AMPK is a novel regulator contributing to axonal regeneration

AMPK is a key energy sensor in cellular metabolism responding to stress signaling by enhancing catabolism, fatty acid production and glucose transport at the expenses of protein and fatty acid synthesis (Mihaylova and Shaw, 2011a). In most species, AMPK exists as a

heterodimer with a catalytic subunit α and two regulatory subunits β and γ . In mammals, there are two genes encoding the catalytic subunit α ($\alpha 1$ and $\alpha 2$), two genes encoding β ($\beta 1$ and $\beta 2$) and three genes encoding γ subunit ($\gamma 1$, $\gamma 2$ and $\gamma 3$) (Hardie, 2007). The α subunit contains an N-terminal catalytic domain that is followed by an auto-inhibitory domain (at least in vertebrates) and a C-terminal domain that mediates interaction with β and γ subunit (Chen et al., 2013; Hardie and Ashford, 2014; Xiao et al., 2011b). The β subunits have a carbohydrate-binding module (CBM) that leads AMPK to associate with glycogen particles (Hudson et al., 2003; Polekhina et al., 2003). The β subunit C-terminal domain (β -CTD) interacts with both α -CTD and γ subunit to form the heterodimer complex. The γ subunits have four tandem repeated sequences which are termed as CBS repeats (numbered as CBS1-CBS4) (Bateman, 1997). And two repeats assemble to form a Bateman domain (Kemp, 2004), with the ligands (such as ATP) binding site in the cleft between the repeats (Ignoul and Eggermont, 2005). The expression pattern of heterotrimers may differ across species. In human liver, $\alpha 1\beta 2\gamma 1$ is the predominant heterotrimer, but rat and dog liver mainly contain $\alpha 2\beta 1\gamma 1$ and $\alpha 1\beta 1\gamma 1$ respectively (Wu et al., 2013). In our DRG axoplasm, we found $\alpha 1$, $\alpha 2$, $\beta 1$, $\beta 2$, $\gamma 1$ and $\gamma 2$ subunits (supplementary file 11), but which AMPK heterotrimer is mainly represented is unknown and it deserves future research.

When the intracellular ATP level is low, ADP or AMP can bind to the γ subunit which leads to a conformational change that protects the phosphorylation of AMPK (Oakhill et al., 2011; Xiao et al., 2011a). The phosphorylation of Thr172 in α subunit is required for AMPK activation. AMPK can be activated by two classical pathways: one is LKB1 that is a tumor suppressor that activates AMPK in response to increased AMP, whereas CAMKK2 which seems to be involved in AMPK activation in neurons and T cells activates it in response to calcium increase (Anderson et al., 2008; Hawley et al., 2005; Shaw et al., 2004; Tamás et al., 2006). In addition, AMPK can be dephosphorylated by phosphatases PP2A, PP2C and PP1 (Garcia-Haro et al., 2010; Sanders et al., 2007; Tamura and Tsuiji, 1980). Glucose and lipid are the major source to store and supply energy in cells. AMPK promotes their breakdown and inhibits their synthesis and storage (catabolism) thereby increasing ATP level. AMPK has been found to potentially promote autophagy by inhibiting mTORC1 thereby it activates ULK1 (Kim et al., 2011). Besides the effects on cell growth and autophagy, recent studies suggest that AMPK may control cell polarity and cytoskeletal dynamics (Mirouse and Billaud, 2011).

The catalytic isoforms ($\alpha 1$ and $\alpha 2$) have distinct function and tissue localization although they are highly homologous. AMPK $\alpha 2$ appears to selectively localize in nucleus and its activation

is greatly dependent on AMP both in allosteric and upstream kinase (LKB1) activation (Sakamoto et al., 2005; Salt et al., 1998; Tzatsos and Tschlis, 2007). AMPK α is found mainly in neurons with much lower expression in astrocytes in the adult brain (McCullough et al., 2005) where the α 2 catalytic subunit is the predominant compared to α 1 (Turnley et al., 1999). In our DRG models, we found that AMPK α 1 mainly localizes in cytoplasm (Figure 15E). However, AMPK α 1 has been reported to localize in nucleus under some conditions (Lamia et al., 2009). Studies has reported that AMPK α 2 is induced by hypoxia in human glioma cells whereas AMPK α 1 does not change (Neurath et al., 2006). Moreover, glucose intolerance and reduced insulin sensitivity are observed in AMPK α 2 (-/-) mice, but no defect is found in AMPK α 1 (-/-) mice (Viollet et al., 2003a; Viollet et al., 2003b). It has been reported that the activity of AMPK is reduced in diabetes (Roy Chowdhury et al., 2012). Several studies have reported that activated AMPK reduces inflammation through inhibition of proinflammatory cytokine (Sag et al., 2008; Salminen et al., 2011). Administration of AMPK activator-metformin induces the phosphorylation of AMPK with the reduced expression of inflammatory cytokines (IL6, TNF- α , CRP) in DRG neurons of diabetic rat and increases motor nerve conduction velocities (MNCV, that is disturbed in diabetic neuropathy), which indicates that AMPK signaling plays a protective role in diabetic neuropathy potentially via an anti-inflammation effect (Hasanvand et al., 2016). However, IL6 has been reported to facilitate optic nerve regeneration upon informatory stimulation (Leibinger et al., 2013), in line with our RT-PCR data showing increased IL6 after AMPK α 1 deletion (Figure 26).

AMPK has been reported to promote catabolic and to inhibit anabolic metabolism (Mihaylova and Shaw, 2011b). After axotomy, injury signals will be retrogradely propagated to the neuron cell bodies, and neurons with regenerative capacity will shift metabolism status to anabolic metabolism to support new protein and lipid synthesis for axonal regrowth (He and Jin, 2016), which further indicates that AMPK signaling might be a negative regulator for axonal regeneration. In non-neuronal cells, mTOR and c-myc have been reported as the main regulators of anabolism, by regulating lipid synthesis, ribosome biogenesis, cell growth and proliferation (Dang, 2013). Indeed, overexpression of c-myc in combination with the activation of mTOR in RGCs, generates robust axonal regeneration (Belin et al., 2015), which suggests that modulating neuronal metabolic status is an important way to regulate neuronal intrinsic regenerative capacity.

Activation of AMPK in cell types other than neurons has been shown to inhibit the activity of several regenerative TFs including STAT3, CREB, and the histone acetyltransferase p300

involved in the regeneration programme (Horike et al., 2008; Nerstedt et al., 2010; Yang et al., 2001). In addition, a recent study found that AMPK can directly phosphorylate kinesin light chain 2 (KLC2) and inhibit axonal growth through prevention of PI3K localization at the axonal tip (Mihaylova and Shaw, 2011a). Interestingly, IGF1 signaling, recently shown to promote axonal regeneration by us and others (Duan et al., 2015; Joshi et al., 2015), is inhibited by AMPK activation (Ning and Clemmons, 2010). Therefore, these experimental evidences imply AMPK as a central inhibitory signalling hub for axonal regeneration. Indeed, we found that AMPK α protein is a central node of signalling pathways in protein networks after SNA (Figure 11A) and that combined RNAseq and proteomics KEGG pathway analysis showed that AMPK might control many regenerative pathways (Figure 13). Together, our data reveals that AMPK α 1 might be the main catalytic subunit involved in the inhibitory role in axonal regeneration. In addition, administration of AMPK inhibitor (Compound C) increased neurite outgrowth of cultured DRG neurons both on permissive and inhibitory substrates (Figure 16). Compound C (also known as dorsomorphin) a selective and reversible AMPK inhibitor, is found to induce dopaminergic axonal outgrowth via activating mTOR signaling pathway in an AMPK dependent way (Wakita et al., 2014). However, it also has been reported to inhibit BMP signals which are required for embryogenesis in zebrafish (Paul et al., 2008) and to promote neural differentiation of human induced pluripotent stem cells (iPSCs) (Zhou et al., 2010). Moreover, compound C is found as an anti-glioma agent in an AMPK-independent way by activating calpain/cathepsin pathway, inhibiting AKT signaling and mTORC1/C2, blocking cell cycle (Liu et al., 2014). Therefore, when compound C was used as an AMPK inhibitor in our neurite outgrowth experiment we cannot exclude that the effects might be partially independent on the inhibition of AMPK. Experiments with delivery of compound C in AMPK null neurons will be able to address this question. However, our bioinformatics analysis and further *in vivo* axonal regeneration and function recovery data do suggest that AMPK signals are inhibitory on axonal regeneration in DRG neurons.

4.3 SNA induced AMPK α 1 degradation is dependent upon the proteasome

In mammals, the proteasome that is mostly exclusively used as 26S proteasome contains a catalytic core subunit (CP, also known as 20S subunit) and one or two regulatory subunits (RP, also known as 19S subunit) which serves as a proteasome activator and recognises the ubiquitinated proteins to translocate them into the catalytic subunit for degradation (Coux et al., 1996; DeMartino and Gillette, 2007). Many researches demonstrate that the proteasome is phosphorylated at many sites in various of physiological and pathological processes although

the function of proteasome phosphorylation is still unclear (Guo et al., 2017). In order to understand the mechanisms that modulate AMPK α 1 expression upon SNA, we performed AMPK immunoprecipitation followed by mass spectrometry. Interestingly, we found an increased number of subunits of the 26S proteasome co-immunoprecipitating with AMPK α (Figure 17 and Supplementary file 11), suggesting that the proteasome may contribute to AMPK α protein expression. Indeed, *in vivo* and *in vitro* administration of the proteasome inhibitor Bortezomib showed increased AMPK α 1 expression (Figure 18). Therefore, we concluded that the degradation of AMPK α 1 following SNA was likely dependent on proteasome activity. Since protein network analysis identified PSMC5 as key connection node between AMPK α and the 26S proteasome we tested whether PSMC5 would form a direct complex with AMPK α (Figure 17). Indeed, AMPK α IP followed by PSMC5 immunoblot showed that these two proteins form a protein complex (Figure 19). PSMC5 has been reported to be a key 19S regulatory ATPase subunit for proteasome activity by modulating proteasome assembly (Sokolova et al., 2015). Additionally, PSMC5 is phosphorylated at Serine 120 (S120) by CaMKII α , which is required for PSMC5 activation (Schmidt and Finley, 2014). It has been reported that proteasome redistribution is controlled by neuronal activity (Bingol and Schuman, 2006). Moreover, the lost phosphorylation of PSMC5 (expression of S120A (phospho-dead) plasmid) blocks its accumulation at synapses (Djakovic et al., 2012).

Therefore, two hypotheses were proposed based on the previous discoveries and our AMPK IP MS analysis: 1. Whether peripheral injury induced AMPK α 1 degradation relies on the phosphorylation of PSMC5-S120? 2. Whether peripheral nerve injury induced degradation of AMPK α 1 in axoplasm of peripheral branch and L4-L6 DRG neurons depends on the peripheral injury stimulated proteasome activation and recruitment, that doesn't happen in central projecting axons and L4-L4 DRG neurons after spinal cord injury.

We found that silencing of PSMC5 or overexpression of phospho-mimetic plasmid (S120D) of PSMC5 blocked or promoted AMPK α 1 degradation with decreased or increased neurite outgrowth respectively (Figure 20A-C and Figure 21A-C). However, overexpression of WT PSMC5 didn't reduce AMPK α 1 expression and phospho-dead (S120A) did not affect AMPK α 1 expression (Figure 21D-E), which indicated that PSMC5 is likely not phosphorylated in our culture conditions. Whether SNA induces phosphorylation of PSMC5 is still unclear and deserves to be investigated. The lack of antibodies that recognise phospho-PSMC5 limits the feasibility of this experiment currently.

However, we did not find recruitment of PSMC5 after SNA in L4-L6 DRG neurons at 6h and 24h (data not shown), which suggests that that AMPK α 1 degradation induced after peripheral axotomy might depend on injury-dependent phosphorylation of PSMC5.

4.4 Calcium activated CaMKII α is necessary for SNA induced AMPK α 1 degradation

Injury induced calcium influx into axoplasm and soma is one of the first signals for axonal regeneration, including the activation of CaMKII α (Hasegawa et al., 2009; Tang et al., 2012a). CaMKII α contains an N-terminal catalytic domain, a regulatory domain (autoinhibitory domain) followed with a C-terminal association domain. The function of the autoinhibitory domain is to regulate the activity of this kinase. The autoinhibitory domain comprises regulatory phosphorylation sites, a calmodulin binding site, substrates binding sites and interaction sites for anchoring proteins. When the enzyme is inactive, the substrates binding sites domain binds to the catalytic domain thereby inhibits its activity. This kinase can be activated by direct binding of Ca²⁺/calmodulin (CaM) to its autoinhibitory domain which leads to the conformational change that exposes the catalytic domain and induces the phosphorylation of the threonine residue 286 (T286) in the autoinhibitory domain by a neighbouring subunit. This autophosphorylation can be kept even after disassociation of Ca²⁺/calmodulin (CaM) (Hudmon and Schulman, 2002; Irvine et al., 2006). It has been reported that autophosphorylation of CaMKII α enhances its binding to proteasome and promotes the proteasome to translocate to dendritic spines in vitro, but this scaffolding function is independent on CaMKII α kinase activity toward Rpt6-S120 (Bingol et al., 2010), however this phenomenon maybe differ in vivo. CaMKII α stimulates proteasome activity by phosphorylating proteasome subunit RPT6 on Serine120 (Bingol et al., 2010) and constitutively active T286D mutant (the autophospho-mimic form) of CaMKII α is sufficient to increase proteasome activity and phosphorylation of RPT6 (Djakovic et al., 2012; Djakovic et al., 2009). Therefore, we asked whether peripheral nerve axotomy induced calcium influx propagating to sciatic nerve and L4-L6 DRGs activates CaMKII α thereby phosphorylating PSMC5 that promotes proteasome activity to induce AMPK α 1 degradation.

Intraperitoneal administration of Ca²⁺/CaM competitor-KN-93 to pharmacological inhibition of CaMKII α activity was found to block SNA induced AMPK α 1 degradation in DRG neurons (Figure 22A-B). Moreover, the autophosphorylation of CaMKII α is required for AMPK α 1 degradation in vitro (Figure 22C, D). However, experiments concerning whether inhibition of calcium influx back propagating to DRG will affect AMPK α 1 expression after SNA are still

ongoing. And as mentioned above, PSMC5 is phosphorylated at serine 120 by CaMKII α , and whether the modulation of CaMKII α on AMPK α 1 expression occurs via regulating PSMC5 phosphorylation is unknown and will be investigated in future experiments.

4.5 The E3 ligase Trim28 is involved in AMPK α 1 degradation via ubiquitination-proteasome system

The ubiquitin-proteasome pathway is the major mode for intracellular protein degradation in cells (Rock et al., 1994). The majority of proteins that are doomed for degradation will be marked by a ubiquitin molecule, which provides a recognition signal for the 19S subunit of the proteasome. The protein ubiquitination process is completed through the participation of three enzymes: E1 (Ubiquitin-activating enzyme), E2 (Ubiquitin-conjugating enzyme) and E3 (Ubiquitin ligase). It should be noted that the specificity of ubiquitination is determined by the E3 ligase, which means each E3 enzyme or E3 multiprotein complex is specific to one or a few corresponding substrate proteins and E2 enzymes (Myung et al., 2001). Previous studies have revealed that AMPK α 1 degradation in cancer cells is mediated by a cancer specific ubiquitin ligase MAGE-A3/6-Trim28 protein complex (Pineda et al., 2015). Therefore, we asked whether in our DRG model, Trim28 is involved in SNA induced AMPK α 1 degradation, since Trim28 protein expression was found increased in the axoplasm after SNA. Indeed, we found that AMPK α 1 is upregulated after Trim28 gene silencing in F11 DRG cell lines (Figure 23D, E). Moreover, cultured DRG cells showed decreased neurite outgrowth after electroporation with Trim28 siRNA (Figure 23A-C). However, we didn't find Trim28 protein in our AMPK α IP MS data and which means that Trim28 maybe doesn't directly form a protein complex to regulate AMPK α 1 degradation. This conclusion was also validated by AMPK immunoprecipitation followed with WB *in vitro* (data not shown). Possibly the formation of this protein complex is transient as protein ubiquitination is a dynamic process that cannot be easily detected by immunoprecipitation at a single time point. This may also explain why the detection of AMPK α 1 ubiquitination level doesn't work in our hands due to these limitations.

4.6 Conditional deletion of AMPK α 1 promotes axonal regeneration and functional recovery after SCI

Finally, we investigated whether inhibition of AMPK α or deletion of AMPK α in DRG neurons would promote axonal regeneration and functional recovery after SCI *in vivo*. Since the high toxicity of compound C and its non-exclusive inhibitory role on AMPK activity, AMPK α conditional deletion was chosen as an optimal model in our *in vivo* experiments. We chose

AMPK α 1 and α 2 floxed mice and performed bilateral sciatic injection of AAV1-CAG-GFP or AAV1-CAG-cre-GFP virus that has very highly transfection efficiency in sensory neurons to conditional knockout AMPK α 1 or α 2 in L4-L6 DRGs 4 weeks before doing a T9-T10 dorsal column crush. Since AAV5-CMV-Cre-GFP virus has two promoters which significantly reduced the transfection efficiency in DRG neurons in our pilot experiment, we changed to use AAV1-CAG-cre-GFP that with a higher transfection efficiency and one promoter. Transfection efficiency was validated in Figure 24.

Our results showed that conditional deletion of AMPK α 1 but not α 2 in L4-L6 DRGs promoted axonal regeneration in the dorsal columns where the central branches of L4-L6 proprioceptive and mechanoreceptive neurons project (Figure 24-25). Furthermore, we found that regenerating axons in mice that underwent AMPK α 1 deletion expressed pre-synaptic markers as shown by Dextran/VGlut1 co-labelling, including in close proximity to NeuN-positive neurons (Figure 25A).

Behavioural test is an important factor to assess the efficacy of the treatment. However, functional deficits are mild after dorsal column crush, which makes the assessment of functional recovery after treatment difficult compared with dorsal hemisection injury. In order to evaluate whether conditional deletion of AMPK α 1 will promote functional recovery, here we performed Von Frey, Hargreaves and Gird walk for 35 days after injury. Von Frey is often used to evaluate the degree of the mechanical allodynia and hyperalgesia which are caused by spinal cord injury or peripheral nerve injury (Christensen et al., 1996; Hogan et al., 2004; Tsuda et al., 2003). This behavioural test is performed by using different calibrated filaments applying to the plantar surface of the forelimb or hind paw with a pressure to test the withdrawal response. However it has been reported that spinal cord injury causes the disconnected mechanoreceptive axon projections in dorsal column and induces tactile hyposensitivity with the higher threshold of paw withdrawal to the filament stimuli compared with basal level (Bradbury et al., 2002a; Demjen et al., 2004).

Indeed, we found the same phenomenon after T9 dorsal column crush, but deletion of AMPK α 1 promoted the mechanoreception recovery (Figure 25B). The Hargreaves test is used to assess thermal pain sensation in rodents such as rats and mice (Hargreaves et al., 1988). As after dorsal column crush, the spinothalamic tract which transmits nociception to thalamic should be intact, we didn't find any behavioural impairment on thermal pain sensation between AMPK α 1 deletion and control mice after injury (Figure 25D). Grid walk is also a behavioural test to assess the coordination of the sensory and motor function of forelimb and hind paw. In

our experiment, we did not see severe functional hind paw deficits after T9 dorsal column crush by Grid walk test (Figure 25C), which is consistent with that observed in some other experiments (Kanagal and Muir, 2007) (Kanagal and Muir, 2008).

Since our bioinformatics analysis indicated that AMPK controls many signaling pathways that are involved in axonal regeneration, we asked which signaling pathways are exactly regulated by AMPK α 1 deletion in L4-L6 DRG neurons thereby promotes axonal regeneration and functional recovery after SCI. After 4 weeks of AAV-cre or control AAV-GFP virus infection to conditional deletion AMPK α 1 in L4-L6 DRG neurons in AMPK α 1 floxed mice, we performed RT-PCR after SCI at 24h, our data demonstrated that deletion of AMPK α 1 upregulated genes that belong to regenerative signaling pathways including c-jun, p53, BDNF, ATF3, Arg1, Fos, myc and IGF-1, while it had no effect upon HIF1a, CXCL12 and HDAC5 (Figure 26). Therefore, our data directly indicates that AMPK α 1 plays an inhibitory role in axonal regeneration by regulating multiply regenerative pathways. AMPK has been found that to inhibit the p300 by phosphorylation of Ser89 (Zhang et al., 2011) and increased phosphorylation of JNK and STAT3 was found in Adipose tissue of AMPK α 1^{-/-} mice (Mancini et al., 2017), meanwhile increased phosphorylation of ERK was found in our DRG neurons after deletion of AMPK α 1.

4.7 A novel mechanism that involved in AMPK α 1 degradation after SNA in DRGs

Here, we propose a potential mechanism that regulated AMPK α 1 degradation via ubiquitination-proteasome system, which is shown as diagram in Figure 28.

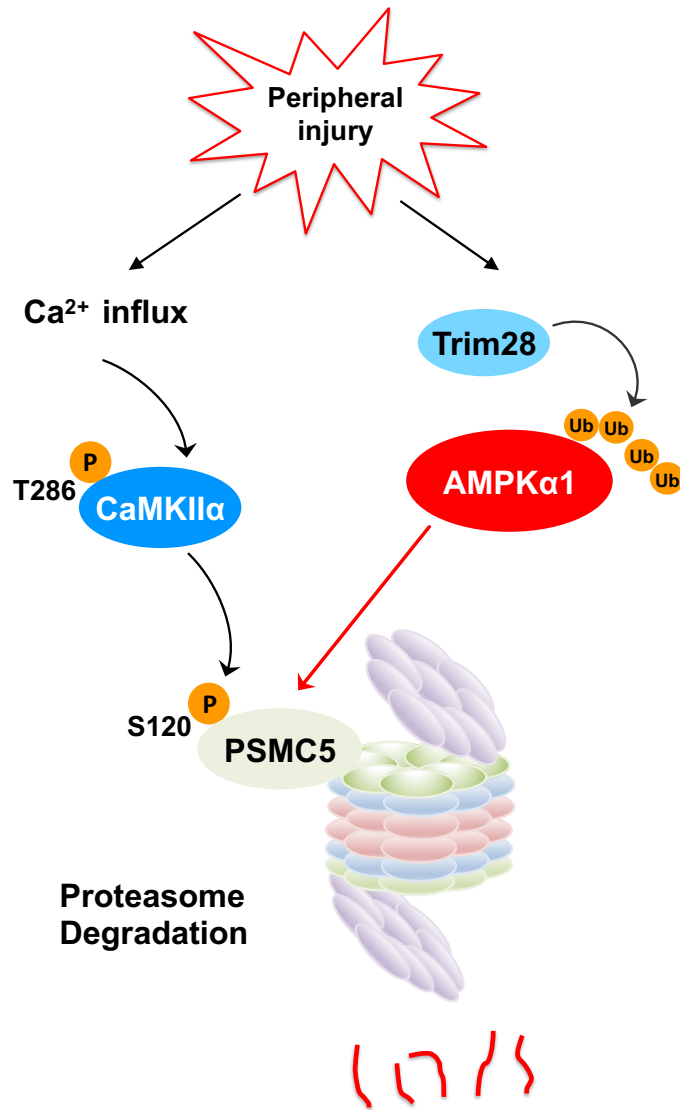


Figure 28. Mechanism diagram of AMPKα1 degradation following peripheral nerve injury

5. Outlook

While the peripheral branches of primary sensory neurons regenerate after injury, the central branches projecting into the spinal cord fail to regenerate after injury (Ramon y Cajal, 1928). The regenerative failure in CNS is attributed to inadequate intrinsic growth capacity (Fawcett, 1992) and an inhibitory extrinsic environment (Benfey et al., 1985; Fawcett and Asher, 1999; Fitch and Silver, 1997; Schwab and Bartholdi, 1996; Schwab and Caroni, 1988b). However, although progress has been made to promote CNS axonal regeneration to some extent, the proteins expression profile in the regenerative PNS branches and non-regenerative central branches and genes expression changes in DRG neurons after injury are still unclear.

Here, our data discovered very distinct axoplasmic proteins expression profiles between peripheral and central projections of L4-L6 DRG neurons in mock mice. Moreover, our proteomics and RNAseq data revealed that SNA elicits numerous protein and gene expression changes in both axoplasm and DRG neurons, whereas DCA has much more modest effects. Further, combined proteomics and RNAseq analysis discovered suggested AMPK as a new inhibitory hub to axonal regeneration. This finding suggests further investigation on the role of metabolism and related signaling pathways in axonal regeneration. An improved characterization of AMPK regulation after injury is also required. Additionally, the inhibition of AMPK in more clinically relevant models of spinal cord injury such as a rat spinal contusion are required to assess the full potential of AMPK inhibition in regeneration of motor fibers and in functional recovery.

6. References

- Abe, K., Chu, P.-j., Shirahata, A., Samejima, K., and Saito, H. (1997). Structural requirement for axonal regeneration-promoting effect of polyamines in cultured rat hippocampal neurons. *Brain research* 766, 281-284.
- Alilain, W.J., Horn, K.P., Hu, H., Dick, T.E., and Silver, J. (2011). Functional regeneration of respiratory pathways after spinal cord injury. *Nature* 475, 196.
- Anderson, K.A., Ribar, T.J., Lin, F., Noeldner, P.K., Green, M.F., Muehlbauer, M.J., Witters, L.A., Kemp, B.E., and Means, A.R. (2008). Hypothalamic CaMKK2 contributes to the regulation of energy balance. *Cell metabolism* 7, 377-388.
- Anderson, M.A., Burda, J.E., Ren, Y., Ao, Y., O'Shea, T.M., Kawaguchi, R., Coppola, G., Khakh, B.S., Deming, T.J., and Sofroniew, M.V. (2016). Astrocyte scar formation aids CNS axon regeneration. *Nature* 532, 195.
- Ard, M.D., Bunge, R.P., and Bunge, M.B. (1987). Comparison of the Schwann cell surface and Schwann cell extracellular matrix as promoters of neurite growth. *Journal of neurocytology* 16, 539-555.
- Bain, J., Plater, L., Elliott, M., Shpiro, N., Hastie, C.J., Mclauchlan, H., Klevernic, I., Arthur, J.S.C., Alessi, D.R., and Cohen, P. (2007). The selectivity of protein kinase inhibitors: a further update. *Biochemical Journal* 408, 297-315.
- Bareyre, F.M., and Schwab, M.E. (2003). Inflammation, degeneration and regeneration in the injured spinal cord: insights from DNA microarrays. *Trends in neurosciences* 26, 555-563.
- Bartsch, U., Bandtlow, C.E., Schnell, L., Bartsch, S., Spillmann, A.A., Rubin, B.P., Hillenbrand, R., Schwab, D.M.E., and Schachner, M. (1995). Lack of evidence that myelin-associated glycoprotein is a major inhibitor of axonal regeneration in the CNS. *Neuron* 15, 1375-1381.
- Bateman, A. (1997). The structure of a domain common to archaebacteria and the homocystinuria disease protein. *Trends in biochemical sciences* 22, 12-13.
- Belin, S., Nawabi, H., Wang, C., Tang, S., Latremoliere, A., Warren, P., Schorle, H., Uncu, C., Woolf, C.J., and He, Z. (2015). Injury-induced decline of intrinsic regenerative ability revealed by quantitative proteomics. *Neuron* 86, 1000-1014.
- Bellido, T., O'Brien, C.A., Roberson, P.K., and Manolagas, S.C. (1998). Transcriptional activation of the p21 waf1, cip1, sdi1 gene by interleukin-6 type cytokines a prerequisite for their pro-differentiating and anti-apoptotic effects on human osteoblastic cells. *Journal of Biological Chemistry* 273, 21137-21144.
- Ben-Yaakov, K., Dagan, S.Y., Segal-Ruder, Y., Shalem, O., Vuppalanchi, D., Willis, D.E., Yudin, D., Rishal, I., Rother, F., and Bader, M. (2012). Axonal transcription factors signal retrogradely in lesioned peripheral nerve. *The EMBO journal* 31, 1350-1363.
- Benfey, M., and Aguayo, A.J. (1982). Extensive elongation of axons from rat brain into peripheral nerve grafts. *Nature* 296, 150-152.
- Benfey, M., Büniger, U., Vidal-Sanz, M., Bray, G., and Aguayo, A. (1985). Axonal regeneration from GABAergic neurons in the adult rat thalamus. *Journal of neurocytology* 14, 279-296.
- Benowitz, L.I., and Yin, Y. (2007). Combinatorial treatments for promoting axon regeneration in the CNS: strategies for overcoming inhibitory signals and activating neurons' intrinsic growth state. *Developmental neurobiology* 67, 1148-1165.
- Benowitz, L.I., and Yin, Y. (2010). Optic nerve regeneration. *Archives of ophthalmology* 128, 1059-1064.

Benson, M.D., Romero, M.I., Lush, M.E., Lu, Q.R., Henkemeyer, M., and Parada, L.F. (2005). Ephrin-B3 is a myelin-based inhibitor of neurite outgrowth. *Proceedings of the national academy of sciences of the United States of America* *102*, 10694-10699.

Berry, M. (1982). Post-injury myelin-breakdown products inhibit axonal growth: an hypothesis to explain the failure of axonal regeneration in the mammalian central nervous system. *Bibliotheca anatomica*, 1.

Bingol, B., and Schuman, E.M. (2006). Activity-dependent dynamics and sequestration of proteasomes in dendritic spines. *Nature* *441*, 1144.

Bingol, B., Wang, C.-F., Arnott, D., Cheng, D., Peng, J., and Sheng, M. (2010). Autophosphorylated CaMKII α acts as a scaffold to recruit proteasomes to dendritic spines. *Cell* *140*, 567-578.

Blackmore, M.G., Wang, Z., Lerch, J.K., Motti, D., Zhang, Y.P., Shields, C.B., Lee, J.K., Goldberg, J.L., Lemmon, V.P., and Bixby, J.L. (2012). Krüppel-like Factor 7 engineered for transcriptional activation promotes axon regeneration in the adult corticospinal tract. *Proceedings of the National Academy of Sciences* *109*, 7517-7522.

Bomze, H.M., Bulsara, K.R., Iskandar, B.J., Caroni, P., and Skene, J.P. (2001). Spinal axon regeneration evoked by replacing two growth cone proteins in adult neurons. *Nature neuroscience* *4*, 38-43.

Bonilla, I.E., Tanabe, K., and Strittmatter, S.M. (2002). Small proline-rich repeat protein 1A is expressed by axotomized neurons and promotes axonal outgrowth. *Journal of Neuroscience* *22*, 1303-1315.

Bosse, F., Hasenpusch-Theil, K., Küry, P., and Müller, H.W. (2006). Gene expression profiling reveals that peripheral nerve regeneration is a consequence of both novel injury-dependent and reactivated developmental processes. *Journal of neurochemistry* *96*, 1441-1457.

Bosse, F., Küry, P., and Müller, H.W. (2001). Gene expression profiling and molecular aspects in peripheral nerve regeneration. *Restorative neurology and neuroscience* *19*, 5-18.

Bradbury, E.J., Moon, L.D., Popat, R.J., King, V.R., Bennett, G.S., Patel, P.N., Fawcett, J.W., and McMahon, S.B. (2002a). Chondroitinase ABC promotes functional recovery after spinal cord injury. *Nature* *416*, 636.

Bradbury, E.J., Moon, L.D., Popat, R.J., King, V.R., Bennett, G.S., Patel, P.N., Fawcett, J.W., and McMahon, S.B. (2002b). Chondroitinase ABC promotes functional recovery after spinal cord injury. *Nature* *416*, 636-640.

Bunge, R.P., Bunge, M.B., and Eldridge, C.F. (1986). Linkage between axonal ensheathment and basal lamina production by Schwann cells. *Annual review of neuroscience* *9*, 305-328.

Busch, S.A., Hamilton, J.A., Horn, K.P., Cuascut, F.X., Cutrone, R., Lehman, N., Deans, R.J., Ting, A.E., Mays, R.W., and Silver, J. (2011). Multipotent adult progenitor cells prevent macrophage-mediated axonal dieback and promote regrowth after spinal cord injury. *Journal of Neuroscience* *31*, 944-953.

Canning, D.R., McKeon, R.J., DeWitt, D.A., Perry, G., Wujek, J.R., Frederickson, R., and Silver, J. (1993). β -Amyloid of Alzheimer's disease induces reactive gliosis that inhibits axonal outgrowth. *Experimental neurology* *124*, 289-298.

Cao, Z., Gao, Y., Bryson, J.B., Hou, J., Chaudhry, N., Siddiq, M., Martinez, J., Spencer, T., Carmel, J., and Hart, R.B. (2006). The cytokine interleukin-6 is sufficient but not necessary to mimic the peripheral conditioning lesion effect on axonal growth. *Journal of Neuroscience* *26*, 5565-5573.

Case, L.C., and Tessier-Lavigne, M. (2005). Regeneration of the adult central nervous system. *Current biology* *15*, R749-R753.

Caspary, T., and Anderson, K.V. (2003). Patterning cell types in the dorsal spinal cord: what the mouse mutants say. *Nature Reviews Neuroscience* 4, 289-297.

Cavalli, V., Kujala, P., Klumperman, J., and Goldstein, L.S. (2005). Sunday Driver links axonal transport to damage signaling. *The Journal of cell biology* 168, 775-787.

Chen, L., Xin, F.-J., Wang, J., Hu, J., Zhang, Y.-Y., Wan, S., Cao, L.-S., Lu, C., Li, P., and Yan, S.F. (2013). Conserved regulatory elements in AMPK. *Nature* 498, E8.

Chen, M.S., Huber, A.B., van der Haar, M.E., and Marcus, F. (2000). Nogo-A is a myelin-associated neurite outgrowth inhibitor and an antigen for monoclonal antibody IN-1. *Nature* 403, 434.

Chierzi, S., Ratto, G.M., Verma, P., and Fawcett, J.W. (2005). The ability of axons to regenerate their growth cones depends on axonal type and age, and is regulated by calcium, cAMP and ERK. *European Journal of Neuroscience* 21, 2051-2062.

Chin, Y.E., Kitagawa, M., Su, W.-C.S., You, Z.-H., Iwamoto, Y., and Fu, X.-Y. (1996). Cell Growth Arrest and Induction of Cyclin-Dependent Kinase Inhibitor p21^{WAF1/CIP1} Mediated by STAT1. *Science*, 719-722.

Cho, Y., Shin, J.E., Ewan, E.E., Oh, Y.M., Pita-Thomas, W., and Cavalli, V. (2015). Activating injury-responsive genes with hypoxia enhances axon regeneration through neuronal HIF-1 α . *Neuron* 88, 720-734.

Cho, Y., Sloutsky, R., Naegle, K.M., and Cavalli, V. (2013). Injury-induced HDAC5 nuclear export is essential for axon regeneration. *Cell* 155, 894-908.

Christensen, M.D., Everhart, A.W., Pickelman, J.T., and Hulsebosch, C.E. (1996). Mechanical and thermal allodynia in chronic central pain following spinal cord injury. *Pain* 68, 97-107.

Cornbrooks, C., Carey, D., McDonald, J., Timpl, R., and Bunge, R. (1983). In vivo and in vitro observations on laminin production by Schwann cells. *Proceedings of the National Academy of Sciences* 80, 3850-3854.

Costigan, M., Befort, K., Karchewski, L., Griffin, R.S., D'Urso, D., Allchorne, A., Sitarski, J., Mannion, J.W., Pratt, R.E., and Woolf, C.J. (2002). Replicate high-density rat genome oligonucleotide microarrays reveal hundreds of regulated genes in the dorsal root ganglion after peripheral nerve injury. *BMC neuroscience* 3, 16.

Costigan, M., Mannion, R.J., Kendall, G., Lewis, S.E., Campagna, J.A., Coggeshall, R.E., Meredith-Middleton, J., Tate, S., and Woolf, C.J. (1998). Heat shock protein 27: developmental regulation and expression after peripheral nerve injury. *Journal of neuroscience* 18, 5891-5900.

Coux, O., Tanaka, K., and Goldberg, A.L. (1996). Structure and functions of the 20S and 26S proteasomes. *Annual review of biochemistry* 65, 801-847.

Cox, J., and Mann, M. (2008). MaxQuant enables high peptide identification rates, individualized pppb-range mass accuracies and proteome-wide protein quantification. *Nature biotechnology* 26, 1367-1372.

Cusimano, M., Biziato, D., Brambilla, E., Donegà, M., Alfaro-Cervello, C., Snider, S., Salani, G., Pucci, F., Comi, G., and Garcia-Verdugo, J.M. (2012). Transplanted neural stem/precursor cells instruct phagocytes and reduce secondary tissue damage in the injured spinal cord. *Brain*, 447-460.

Czeh, M. (2011). The Yin and Yang of Microglia. *Dev Neurosci* 33, 199-209.

D'mello, R., and Dickenson, A. (2008). Spinal cord mechanisms of pain. *British journal of anaesthesia* 101, 8-16.

Dang, C.V. (2013). MYC, metabolism, cell growth, and tumorigenesis. *Cold Spring Harbor perspectives in medicine* 3, a014217.

David, S., and Aguayo, A.J. (1981). Axonal elongation into peripheral nervous system “bridges” after central nervous system injury in adult rats. *Science* *214*, 931-933.

DeBellard, M.-E., Tang, S., Mukhopadhyay, G., Shen, Y.-J., and Filbin, M.T. (1996). Myelin-associated glycoprotein inhibits axonal regeneration from a variety of neurons via interaction with a sialoglycoprotein. *Molecular and Cellular Neuroscience* *7*, 89-101.

DeMartino, G.N., and Gillette, T.G. (2007). Proteasomes: machines for all reasons. *Cell* *129*, 659-662.

Demjen, D., Klussmann, S., Kleber, S., Zuliani, C., Stieltjes, B., Metzger, C., Hirt, U.A., Walczak, H., Falk, W., and Essig, M. (2004). Neutralization of CD95 ligand promotes regeneration and functional recovery after spinal cord injury. *Nature medicine* *10*, 389.

Deng, K., He, H., Qiu, J., Lorber, B., Bryson, J.B., and Filbin, M.T. (2009). Increased synthesis of spermidine as a result of upregulation of arginase I promotes axonal regeneration in culture and in vivo. *Journal of Neuroscience* *29*, 9545-9552.

Deumens, R., Bozkurt, A., Meek, M.F., Marcus, M.A., Joosten, E.A., Weis, J., and Brook, G.A. (2010). Repairing injured peripheral nerves: bridging the gap. *Progress in neurobiology* *92*, 245-276.

Di Giovanni, S., Knights, C.D., Rao, M., Yakovlev, A., Beers, J., Catania, J., Avantaggiati, M.L., and Faden, A.I. (2006). The tumor suppressor protein p53 is required for neurite outgrowth and axon regeneration. *The EMBO journal* *25*, 4084-4096.

Dickendesher, T.L., Baldwin, K.T., Mironova, Y.A., Koriyama, Y., Raiker, S.J., Askew, K.L., Wood, A., Geoffroy, C.G., Zheng, B., and Liepmann, C.D. (2012). NgR1 and NgR3 are receptors for chondroitin sulfate proteoglycans. *Nature neuroscience* *15*, 703-712.

Dimou, L., Schnell, L., Montani, L., Duncan, C., Simonen, M., Schneider, R., Liebscher, T., Gullo, M., and Schwab, M.E. (2006). Nogo-A-deficient mice reveal strain-dependent differences in axonal regeneration. *Journal of Neuroscience* *26*, 5591-5603.

Djakovic, S.N., Marquez-Lona, E.M., Jakawich, S.K., Wright, R., Chu, C., Sutton, M.A., and Patrick, G.N. (2012). Phosphorylation of Rpt6 regulates synaptic strength in hippocampal neurons. *Journal of Neuroscience* *32*, 5126-5131.

Djakovic, S.N., Schwarz, L.A., Barylko, B., DeMartino, G.N., and Patrick, G.N. (2009). Regulation of the proteasome by neuronal activity and calcium/calmodulin-dependent protein kinase II. *Journal of Biological Chemistry* *284*, 26655-26665.

Dornay, M., Gilad, V.H., Shiler, I., and Gilad, G.M. (1986). Early polyamine treatment accelerates regeneration of rat sympathetic neurons. *Experimental neurology* *92*, 665-674.

Dou, C.-L., and Levine, J.M. (1994). Inhibition of neurite growth by the NG2 chondroitin sulfate proteoglycan. *Journal of Neuroscience* *14*, 7616-7628.

Duan, X., Qiao, M., Bei, F., Kim, I.-J., He, Z., and Sanes, J.R. (2015). Subtype-specific regeneration of retinal ganglion cells following axotomy: effects of osteopontin and mTOR signaling. *Neuron* *85*, 1244-1256.

Enes, J., Langwieser, N., Ruschel, J., Carballosa-Gonzalez, M.M., Klug, A., Traut, M.H., Ylera, B., Tahirovic, S., Hofmann, F., and Stein, V. (2010). Electrical activity suppresses axon growth through Ca v 1.2 channels in adult primary sensory neurons. *Current Biology* *20*, 1154-1164.

Eng, L.F. (1985). Glial fibrillary acidic protein (GFAP): the major protein of glial intermediate filaments in differentiated astrocytes. *Journal of neuroimmunology* *8*, 203-214.

Fawcett, J.W. (1992). Intrinsic neuronal determinants of regeneration. *Trends in neurosciences* *15*, 5-8.

Fawcett, J.W., and Asher, R.A. (1999). The glial scar and central nervous system repair. *Brain research bulletin* *49*, 377-391.

Feng, X.-H., Zhang, Y., Wu, R.-Y., and Derynck, R. (1998). The tumor suppressor Smad4/DPC4 and transcriptional adaptor CBP/p300 are coactivators for Smad3 in TGF- β -induced transcriptional activation. *Genes & development* *12*, 2153-2163.

Fisher, D., Xing, B., Dill, J., Li, H., Hoang, H.H., Zhao, Z., Yang, X.-L., Bachoo, R., Cannon, S., and Longo, F.M. (2011). Leukocyte common antigen-related phosphatase is a functional receptor for chondroitin sulfate proteoglycan axon growth inhibitors. *Journal of Neuroscience* *31*, 14051-14066.

Fitch, M.T., and Silver, J. (1997). Glial cell extracellular matrix: boundaries for axon growth in development and regeneration. *Cell and tissue research* *290*, 379-384.

Fournier, A.E., GrandPre, T., and Strittmatter, S.M. (2001). Identification of a receptor mediating Nogo-66 inhibition of axonal regeneration. *Nature* *409*, 341.

Fu, S.Y., and Gordon, T. (1997). The cellular and molecular basis of peripheral nerve regeneration. *Molecular neurobiology* *14*, 67-116.

Gao, Y., Deng, K., Hou, J., Bryson, J.B., Barco, A., Nikulina, E., Spencer, T., Mellado, W., Kandel, E.R., and Filbin, M.T. (2004). Activated CREB is sufficient to overcome inhibitors in myelin and promote spinal axon regeneration in vivo. *Neuron* *44*, 609-621.

Garcia-Haro, L., Garcia-Gimeno, M.A., Neumann, D., Beullens, M., Bollen, M., and Sanz, P. (2010). The PP1-R6 protein phosphatase holoenzyme is involved in the glucose-induced dephosphorylation and inactivation of AMP-activated protein kinase, a key regulator of insulin secretion, in MIN6 β cells. *The FASEB Journal* *24*, 5080-5091.

Gaub, P., Joshi, Y., Wuttke, A., Naumann, U., Schnichels, S., Heiduschka, P., and Di Giovanni, S. (2011). The histone acetyltransferase p300 promotes intrinsic axonal regeneration. *Brain* *134*, 2134-2148.

Gaub, P., Tedeschi, A., Puttagunta, R., Nguyen, T., Schmandke, A., and Di Giovanni, S. (2010). HDAC inhibition promotes neuronal outgrowth and counteracts growth cone collapse through CBP/p300 and P/CAF-dependent p53 acetylation. *Cell death and differentiation* *17*, 1392.

Gensel, J.C., and Zhang, B. (2015). Macrophage activation and its role in repair and pathology after spinal cord injury. *Brain research* *1619*, 1-11.

Gey, M., Wanner, R., Schilling, C., Pedro, M.T., Sinske, D., and Knöll, B. (2016). Atf3 mutant mice show reduced axon regeneration and impaired regeneration-associated gene induction after peripheral nerve injury. *Open biology* *6*, 160091.

Gilchrist, M., Thorsson, V., Li, B., Rust, A.G., Korb, M., Kennedy, K., Hai, T., Bolouri, H., and Aderem, A. (2006). Systems biology approaches identify ATF3 as a negative regulator of Toll-like receptor 4. *Nature* *441*, 173.

Gordon, T., and Stein, R. (1982). Time course and extent of recovery in reinnervated motor units of cat triceps surae muscles. *The Journal of physiology* *323*, 307-323.

GrandPre, T., Nakamura, F., Vartanian, T., and Strittmatter, S.M. (2000). Identification of the Nogo inhibitor of axon regeneration as a Reticulon protein. *Nature* *403*, 439.

Guo, X., Huang, X., and Chen, M.J. (2017). Reversible phosphorylation of the 26S proteasome. *Protein & cell* *8*, 255-272.

Habib, A.A., Marton, L.S., Allwardt, B., Gulcher, J.R., Mikol, D.D., Högnason, T., Chattopadhyay, N., and Stefansson, K. (1998). Expression of the Oligodendrocyte-Myelin Glycoprotein by Neurons in the Mouse Central Nervous System. *Journal of neurochemistry* *70*, 1704-1711.

Hannila, S.S., and Filbin, M.T. (2008). The role of cyclic AMP signaling in promoting axonal regeneration after spinal cord injury. *Experimental neurology* *209*, 321-332.

Hanz, S., Perlson, E., Willis, D., Zheng, J.-Q., Massarwa, R.a., Huerta, J.J., Koltzenburg, M., Kohler, M., van-Minnen, J., and Twiss, J.L. (2003). Axoplasmic importins enable retrograde injury signaling in lesioned nerve. *Neuron* 40, 1095-1104.

Hardie, D.G. (2007). AMP-activated/SNF1 protein kinases: conserved guardians of cellular energy. *Nature reviews Molecular cell biology* 8.

Hardie, D.G., and Ashford, M.L. (2014). AMPK: regulating energy balance at the cellular and whole body levels. *Physiology* 29, 99-107.

Hargreaves, K., Dubner, R., Brown, F., Flores, C., and Joris, J. (1988). A new and sensitive method for measuring thermal nociception in cutaneous hyperalgesia. *Pain* 32, 77-88.

Hasanvand, A., Amini-khoei, H., Hadian, M.-R., Abdollahi, A., Tavangar, S.M., Dehpour, A.R., Semiei, E., and Mehr, S.E. (2016). Anti-inflammatory effect of AMPK signaling pathway in rat model of diabetic neuropathy. *Inflammopharmacology* 24, 207-219.

Hasegawa, S., Kohro, Y., Tsuda, M., and Inoue, K. (2009). Activation of cytosolic phospholipase A 2 in dorsal root ganglion neurons by Ca²⁺/calmodulin-dependent protein kinase II after peripheral nerve injury. *Molecular pain* 5, 22.

Hawley, S.A., Pan, D.A., Mustard, K.J., Ross, L., Bain, J., Edelman, A.M., Frenguelli, B.G., and Hardie, D.G. (2005). Calmodulin-dependent protein kinase kinase- β is an alternative upstream kinase for AMP-activated protein kinase. *Cell metabolism* 2, 9-19.

Hay, N., and Sonenberg, N. (2004). Upstream and downstream of mTOR. *Genes & development* 18, 1926-1945.

He, Z., and Jin, Y. (2016). Intrinsic control of axon regeneration. *Neuron* 90, 437-451.

Heinrich, P.C., Behrmann, I., Müller-Newen, G., Schaper, F., and Graeve, L. (1998). Interleukin-6-type cytokine signalling through the gp130/Jak/STAT pathway. *Biochemical journal* 334, 297-314.

Herdegen, T., Kummer, W., Fiallos, C., Leah, J., and Bravo, R. (1991). Expression of c-JUN, JUN B and JUN D proteins in rat nervous system following transection of vagus nerve and cervical sympathetic trunk. *Neuroscience* 45, 413-422.

Herdegen, T., Skene, P., and Bähr, M. (1997). The c-Jun transcription factor—bipotential mediator of neuronal death, survival and regeneration. *Trends in neurosciences* 20, 227-231.

Hille, B. (2001). *Ion channels of excitable membranes*, Vol 507 (Sinauer Sunderland, MA).

Hoffman, P.N. (2010). A conditioning lesion induces changes in gene expression and axonal transport that enhance regeneration by increasing the intrinsic growth state of axons. *Experimental neurology* 223, 11-18.

Hogan, Q., Sapunar, D., Modric-Jednacak, K., and McCallum, J.B. (2004). Detection of neuropathic pain in a rat model of peripheral nerve injury. *Anesthesiology: The Journal of the American Society of Anesthesiologists* 101, 476-487.

Höke, A. (2006). Mechanisms of Disease: what factors limit the success of peripheral nerve regeneration in humans? *Nature Reviews Neurology* 2, 448.

Horike, N., Sakoda, H., Kushiya, A., Ono, H., Fujishiro, M., Kamata, H., Nishiyama, K., Uchijima, Y., Kurihara, Y., and Kurihara, H. (2008). AMP-activated protein kinase activation increases phosphorylation of glycogen synthase kinase 3 β and thereby reduces cAMP-responsive element transcriptional activity and phosphoenolpyruvate carboxykinase C gene expression in the liver. *Journal of Biological Chemistry* 283, 33902-33910.

Hsu, J.-L., Huang, S.-Y., Chow, N.-H., and Chen, S.-H. (2003). Stable-isotope dimethyl labeling for quantitative proteomics. *Analytical chemistry* 75, 6843-6852.

Hudmon, A., and Schulman, H. (2002). Neuronal CA²⁺/calmodulin-dependent protein kinase II: the role of structure and autoregulation in cellular function. *Annual review of biochemistry* *71*, 473-510.

Hudson, E.R., Pan, D.A., James, J., Lucocq, J.M., Hawley, S.A., Green, K.A., Baba, O., Terashima, T., and Hardie, D.G. (2003). A novel domain in AMP-activated protein kinase causes glycogen storage bodies similar to those seen in hereditary cardiac arrhythmias. *Current biology* *13*, 861-866.

Ignoul, S., and Eggermont, J. (2005). CBS domains: structure, function, and pathology in human proteins. *American Journal of Physiology-Cell Physiology* *289*, C1369-C1378.

Irvine, E.E., von Herten, L.S., Plattner, F., and Giese, K.P. (2006). α CaMKII autophosphorylation: a fast track to memory. *Trends in neurosciences* *29*, 459-465.

Jenkins, R., and Hunt, S. (1991). Long-term increase in the levels of c-jun mRNA and jun protein-like immunoreactivity in motor and sensory neurons following axon damage. *Neuroscience letters* *129*, 107-110.

Johnson, P.W., Abramow-Newerly, W., Seilheimer, B., Sadoul, R., Tropak, M.B., Arquint, M., Dunn, R.J., Schachner, M., and Roder, J.C. (1989). Recombinant myelin-associated glycoprotein confers neural adhesion and neurite outgrowth function. *Neuron* *3*, 377-385.

Jones, L.L., Margolis, R.U., and Tuszynski, M.H. (2003). The chondroitin sulfate proteoglycans neurocan, brevican, phosphacan, and versican are differentially regulated following spinal cord injury. *Experimental neurology* *182*, 399-411.

Joshi, Y., S3ria, M.G., Quadrato, G., Inak, G., Zhou, L., Hervera, A., Rathore, K.I., Elnaggar, M., Cucchiari, M., and Marine, J.C. (2015). The MDM4/MDM2-p53-IGF1 axis controls axonal regeneration, sprouting and functional recovery after CNS injury. *Brain* *138*, 1843-1862.

Kamber, D., Erez, H., and Spira, M.E. (2009). Local calcium-dependent mechanisms determine whether a cut axonal end assembles a retarded endbulb or competent growth cone. *Experimental neurology* *219*, 112-125.

Kanagal, S.G., and Muir, G.D. (2007). Bilateral dorsal funicular lesions alter sensorimotor behaviour in rats. *Experimental neurology* *205*, 513-524.

Kanagal, S.G., and Muir, G.D. (2008). The differential effects of cervical and thoracic dorsal funicular lesions in rats. *Behavioural brain research* *187*, 379-386.

Kemp, B.E. (2004). Bateman domains and adenosine derivatives form a binding contract. *The Journal of clinical investigation* *113*, 182-184.

Kigerl, K.A., Gensel, J.C., Ankeny, D.P., Alexander, J.K., Donnelly, D.J., and Popovich, P.G. (2009). Identification of two distinct macrophage subsets with divergent effects causing either neurotoxicity or regeneration in the injured mouse spinal cord. *Journal of Neuroscience* *29*, 13435-13444.

Kim, J., Kundu, M., Viollet, B., and Guan, K.-L. (2011). AMPK and mTOR regulate autophagy through direct phosphorylation of Ulk1. *Nature cell biology* *13*, 132.

Kim, J.-E., Li, S., GrandPr3, T., Qiu, D., and Strittmatter, S.M. (2003). Axon regeneration in young adult mice lacking Nogo-A/B. *Neuron* *38*, 187-199.

Kone, M., Pullen, T.J., Sun, G., Ibberson, M., Martinez-Sanchez, A., Sayers, S., Nguyen-Tu, M.-S., Kantor, C., Swisa, A., and Dor, Y. (2014). LKB1 and AMPK differentially regulate pancreatic β -cell identity. *The FASEB Journal* *28*, 4972-4985.

Kottis, V., Thibault, P., Mikol, D., Xiao, Z.C., Zhang, R., Dergham, P., and Braun, P.E. (2002). Oligodendrocyte-myelin glycoprotein (OMgp) is an inhibitor of neurite outgrowth. *Journal of neurochemistry* *82*, 1566-1569.

Krause, T.L., Fishman, H.M., Ballinger, M.L., and Bittner, G.D. (1994). Extent and mechanism of sealing in transected giant axons of squid and earthworms. *Journal of Neuroscience* 14, 6638-6651.

Kwon, M.J., Shin, H.Y., Cui, Y., Kim, H., Le Thi, A.H., Choi, J.Y., Kim, E.Y., Hwang, D.H., and Kim, B.G. (2015). CCL2 mediates neuron–macrophage interactions to drive proregenerative macrophage activation following preconditioning injury. *Journal of Neuroscience* 35, 15934-15947.

Lamia, K.A., Sachdeva, U.M., DiTacchio, L., Williams, E.C., Alvarez, J.G., Egan, D.F., Vasquez, D.S., Juguilon, H., Panda, S., and Shaw, R.J. (2009). AMPK regulates the circadian clock by cryptochrome phosphorylation and degradation. *Science* 326, 437-440.

Lang, B.T., Cregg, J.M., DePaul, M.A., Tran, A.P., Xu, K., Dyck, S.M., Madalena, K.M., Brown, B.P., Weng, Y.-L., and Li, S. (2015). Modulation of the proteoglycan receptor PTP [sgr] promotes recovery after spinal cord injury. *Nature* 518, 404-408.

Lee, N., Neitzel, K.L., Devlin, B.K., and MacLennan, A.J. (2004). STAT3 phosphorylation in injured axons before sensory and motor neuron nuclei: potential role for STAT3 as a retrograde signaling transcription factor. *Journal of Comparative Neurology* 474, 535-545.

Lee-Liu, D., Edwards-Faret, G., Tapia, V.S., and Larraín, J. (2013). Spinal cord regeneration: Lessons for mammals from non-mammalian vertebrates. *Genesis* 51, 529-544.

Leibinger, M., Müller, A., Gobrecht, P., Diekmann, H., Andreadaki, A., and Fischer, D. (2013). Interleukin-6 contributes to CNS axon regeneration upon inflammatory stimulation. *Cell death & disease* 4, e609.

Lindwall, C., and Kanje, M. (2005). The role of pc-Jun in survival and outgrowth of developing sensory neurons. *Neuroreport* 16, 1655-1659.

Liu, K., Tedeschi, A., Park, K.K., and He, Z. (2011). Neuronal intrinsic mechanisms of axon regeneration. *Annual review of neuroscience* 34, 131-152.

Liu, L., Scolnick, D.M., Trievel, R.C., Zhang, H.B., Marmorstein, R., Halazonetis, T.D., and Berger, S.L. (1999). p53 sites acetylated in vitro by PCAF and p300 are acetylated in vivo in response to DNA damage. *Molecular and cellular biology* 19, 1202-1209.

Liu, X., Chhipa, R.R., Nakano, I., and Dasgupta, B. (2014). The AMPK inhibitor compound C is a potent AMPK-independent antiglioma agent. *Molecular cancer therapeutics* 13, 596-605.

Lu, P., Wang, Y., Graham, L., McHale, K., Gao, M., Wu, D., Brock, J., Blesch, A., Rosenzweig, E.S., and Havton, L.A. (2012). Long-distance growth and connectivity of neural stem cells after severe spinal cord injury. *Cell* 150, 1264-1273.

Lu, P., Woodruff, G., Wang, Y., Graham, L., Hunt, M., Wu, D., Boehle, E., Ahmad, R., Poplawski, G., and Brock, J. (2014). Long-distance axonal growth from human induced pluripotent stem cells after spinal cord injury. *Neuron* 83, 789-796.

Ma, C.H.E., Omura, T., Cobos, E.J., Latrémolière, A., Ghasemlou, N., Brenner, G.J., van Veen, E., Barrett, L., Sawada, T., and Gao, F. (2011). Accelerating axonal growth promotes motor recovery after peripheral nerve injury in mice. *The Journal of clinical investigation* 121.

Ma, T.C., Campana, A., Lange, P.S., Lee, H.-H., Banerjee, K., Bryson, J.B., Mahishi, L., Alam, S., Giger, R.J., and Barnes, S. (2010). A large-scale chemical screen for regulators of the arginase 1 promoter identifies the soy isoflavone daidzein as a clinically approved small molecule that can promote neuronal protection or regeneration via a cAMP-independent pathway. *Journal of Neuroscience* 30, 739-748.

Ma, T.C., and Willis, D.E. (2015). What makes a RAG regeneration associated? *Frontiers in molecular neuroscience* 8, 43.

Mancini, S.J., White, A.D., Bijland, S., Rutherford, C., Graham, D., Richter, E.A., Viollet, B., Touyz, R.M., Palmer, T.M., and Salt, I.P. (2017). Activation of AMP-activated protein kinase rapidly suppresses multiple pro-inflammatory pathways in adipocytes including IL-1 receptor-associated kinase-4 phosphorylation. *Molecular and cellular endocrinology* 440, 44-56.

Mantyh, P.W. (2006). Cancer pain and its impact on diagnosis, survival and quality of life. *Nature Reviews Neuroscience* 7, 797-809.

Mar, F.M., Bonni, A., and Sousa, M.M. (2014). Cell intrinsic control of axon regeneration. *EMBO Rep* 15, 254-263.

McCullough, L.D., Zeng, Z., Li, H., Landree, L.E., McFadden, J., and Ronnett, G.V. (2005). Pharmacological inhibition of AMP-activated protein kinase provides neuroprotection in stroke. *Journal of Biological Chemistry* 280, 20493-20502.

McKeon, R.J., Jurynech, M.J., and Buck, C.R. (1999). The chondroitin sulfate proteoglycans neurocan and phosphacan are expressed by reactive astrocytes in the chronic CNS glial scar. *Journal of Neuroscience* 19, 10778-10788.

McKeon, R.J., Schreiber, R.C., Rudge, J.S., and Silver, J. (1991). Reduction of neurite outgrowth in a model of glial scarring following CNS injury is correlated with the expression of inhibitory molecules on reactive astrocytes. *Journal of Neuroscience* 11, 3398-3411.

McKerracher, L.d., David, S., Jackson, D., Kottis, V., Dunn, R., and Braun, P. (1994). Identification of myelin-associated glycoprotein as a major myelin-derived inhibitor of neurite growth. *Neuron* 13, 805-811.

Menorca, R.M., Fussell, T.S., and Elfar, J.C. (2013). Peripheral nerve trauma: mechanisms of injury and recovery. *Hand clinics* 29, 317.

Mihaylova, M.M., and Shaw, R.J. (2011a). The AMP-activated protein kinase (AMPK) signaling pathway coordinates cell growth, autophagy, & metabolism. *Nature cell biology* 13, 1016.

Mihaylova, M.M., and Shaw, R.J. (2011b). The AMPK signalling pathway coordinates cell growth, autophagy and metabolism. *Nature cell biology* 13, 1016.

Mirouse, V., and Billaud, M. (2011). The LKB1/AMPK polarity pathway. *FEBS letters* 585, 981-985.

Moore, D.L., Blackmore, M.G., Hu, Y., Kaestner, K.H., Bixby, J.L., Lemmon, V.P., and Goldberg, J.L. (2009). KLF family members regulate intrinsic axon regeneration ability. *Science* 326, 298-301.

Moreau-Fauvarque, C., Kumanogoh, A., Camand, E., Jaillard, C., Barbin, G., Boquet, I., Love, C., Jones, E.Y., Kikutani, H., and Lubetzki, C. (2003). The transmembrane semaphorin Sema4D/CD100, an inhibitor of axonal growth, is expressed on oligodendrocytes and upregulated after CNS lesion. *Journal of Neuroscience* 23, 9229-9239.

Morgenstern, D.A., Asher, R.A., and Fawcett, J.W. (2002). Chondroitin sulphate proteoglycans in the CNS injury response. *Progress in brain research* 137, 313-332.

Myung, J., Kim, K.B., and Crews, C.M. (2001). The ubiquitin - proteasome pathway and proteasome inhibitors. *Medicinal research reviews* 21, 245-273.

Navarro, X., Vivó, M., and Valero-Cabré, A. (2007). Neural plasticity after peripheral nerve injury and regeneration. *Progress in neurobiology* 82, 163-201.

Nerstedt, A., Johansson, A., Andersson, C.X., Cansby, E., Smith, U., and Mahlapuu, M. (2010). AMP-activated protein kinase inhibits IL-6-stimulated inflammatory response in human liver cells by suppressing phosphorylation of signal transducer and activator of transcription 3 (STAT3). *Diabetologia* 53, 2406-2416.

Neumann, S., and Woolf, C.J. (1999). Regeneration of dorsal column fibers into and beyond the lesion site following adult spinal cord injury. *Neuron* 23, 83-91.

Neurath, K.M., Keough, M.P., Mikkelsen, T., and Claffey, K.P. (2006). AMP-dependent protein kinase alpha 2 isoform promotes hypoxia-induced VEGF expression in human glioblastoma. *Glia* 53, 733-743.

Ning, J., and Clemmons, D.R. (2010). AMP-activated protein kinase inhibits IGF-I signaling and protein synthesis in vascular smooth muscle cells via stimulation of insulin receptor substrate 1 S794 and tuberous sclerosis 2 S1345 phosphorylation. *Molecular endocrinology* 24, 1218-1229.

Oakhill, J.S., Steel, R., Chen, Z.-P., Scott, J.W., Ling, N., Tam, S., and Kemp, B.E. (2011). AMPK is a direct adenylate charge-regulated protein kinase. *Science* 332, 1433-1435.

Oertle, T., van der Haar, M.E., Bandtlow, C.E., Robeva, A., Burfeind, P., Buss, A., Huber, A.B., Simonen, M., Schnell, L., and Brösamle, C. (2003). Nogo-A inhibits neurite outgrowth and cell spreading with three discrete regions. *Journal of Neuroscience* 23, 5393-5406.

Parikh, P., Hao, Y., Hosseinkhani, M., Patil, S.B., Huntley, G.W., Tessier-Lavigne, M., and Zou, H. (2011). Regeneration of axons in injured spinal cord by activation of bone morphogenetic protein/Smad1 signaling pathway in adult neurons. *Proceedings of the National Academy of Sciences* 108, E99-E107.

Park, K.K., Liu, K., Hu, Y., Smith, P.D., Wang, C., Cai, B., Xu, B., Connolly, L., Kramvis, I., and Sahin, M. (2008). Promoting axon regeneration in the adult CNS by modulation of the PTEN/mTOR pathway. *Science* 322, 963-966.

Paul, B.Y., Hong, C.C., Sachidanandan, C., Babitt, J.L., Deng, D.Y., Hoyng, S.A., Lin, H.Y., Bloch, K.D., and Peterson, R.T. (2008). Dorsomorphin inhibits BMP signals required for embryogenesis and iron metabolism. *Nature chemical biology* 4, 33.

Perlson, E., Hanz, S., Ben-Yaakov, K., Segal-Ruder, Y., Seger, R., and Fainzilber, M. (2005). Vimentin-dependent spatial translocation of an activated MAP kinase in injured nerve. *Neuron* 45, 715-726.

Pineda, C.T., Ramanathan, S., Tacer, K.F., Weon, J.L., Potts, M.B., Ou, Y.-H., White, M.A., and Potts, P.R. (2015). Degradation of AMPK by a cancer-specific ubiquitin ligase. *Cell* 160, 715-728.

Polekhina, G., Gupta, A., Michell, B.J., van Denderen, B., Murthy, S., Feil, S.C., Jennings, I.G., Campbell, D.J., Witters, L.A., and Parker, M.W. (2003). AMPK β subunit targets metabolic stress sensing to glycogen. *Current biology* 13, 867-871.

Poliak, S., and Peles, E. (2003). The local differentiation of myelinated axons at nodes of Ranvier. *Nature Reviews Neuroscience* 4, 968-980.

Pouponnot, C., Jayaraman, L., and Massagué, J. (1998). Physical and functional interaction of SMADs and p300/CBP. *Journal of Biological Chemistry* 273, 22865-22868.

Puttagunta, R., Tedeschi, A., Sória, M.G., Hervera, A., Lindner, R., Rathore, K.I., Gaub, P., Joshi, Y., Nguyen, T., and Schmandke, A. (2014). PCAF-dependent epigenetic changes promote axonal regeneration in the central nervous system. *Nature communications* 5, 3527.

Qin, Q., Baudry, M., Liao, G., Noniyev, A., Galeano, J., and Bi, X. (2009). A novel function for p53: regulation of growth cone motility through interaction with Rho kinase. *Journal of Neuroscience* 29, 5183-5192.

Qiu, J., Cai, D., Dai, H., McAtee, M., Hoffman, P.N., Bregman, B.S., and Filbin, M.T. (2002). Spinal axon regeneration induced by elevation of cyclic AMP. *Neuron* 34, 895-903.

Raivich, G., Bohatschek, M., Da Costa, C., Iwata, O., Galiano, M., Hristova, M., Nateri, A.S., Makwana, M., Riera-Sans, L.s., and Wolfer, D.P. (2004). The AP-1 transcription factor c-Jun is required for efficient axonal regeneration. *Neuron* 43, 57-67.

Ramon y Cajal, S. (1928). Degeneration and regeneration of the nervous system.

Ramon y Cajal, S. (1991). Cajal's degeneration and regeneration of the nervous system (History of Neuroscience).

Rappsilber, J., Mann, M., and Ishihama, Y. (2007). Protocol for micro-purification, enrichment, pre-fractionation and storage of peptides for proteomics using StageTips. *Nature protocols* 2, 1896-1906.

Richardson, P., and Issa, V. (1984). Peripheral injury enhances central regeneration of primary sensory neurones. *Nature* 309, 791-793.

Richardson, P., Issa, V., and Aguayo, A. (1984). Regeneration of long spinal axons in the rat. *Journal of neurocytology* 13, 165-182.

Richardson, P., McGuinness, U., and Aguayo, A. (1980). Axons from CNS neurones regenerate into PNS grafts. *Nature* 284, 264-265.

Rock, K.L., Gramm, C., Rothstein, L., Clark, K., Stein, R., Dick, L., Hwang, D., and Goldberg, A.L. (1994). Inhibitors of the proteasome block the degradation of most cell proteins and the generation of peptides presented on MHC class I molecules. *Cell* 78, 761-771.

Roy Chowdhury, S.K., Smith, D.R., Saleh, A., Schapansky, J., Marquez, A., Gomes, S., Akude, E., Morrow, D., Calcutt, N.A., and Fernyhough, P. (2012). Impaired adenosine monophosphate-activated protein kinase signalling in dorsal root ganglia neurons is linked to mitochondrial dysfunction and peripheral neuropathy in diabetes. *Brain* 135, 1751-1766.

Sag, D., Carling, D., Stout, R.D., and Suttles, J. (2008). Adenosine 5'-monophosphate-activated protein kinase promotes macrophage polarization to an anti-inflammatory functional phenotype. *The Journal of Immunology* 181, 8633-8641.

Sakamoto, K., McCarthy, A., Smith, D., Green, K.A., Hardie, D.G., Ashworth, A., and Alessi, D.R. (2005). Deficiency of LKB1 in skeletal muscle prevents AMPK activation and glucose uptake during contraction. *The EMBO journal* 24, 1810-1820.

Salminen, A., Hyttinen, J.M., and Kaarniranta, K. (2011). AMP-activated protein kinase inhibits NF- κ B signaling and inflammation: impact on healthspan and lifespan. *Journal of molecular medicine* 89, 667-676.

Salt, I., Celler, J.W., Hawley, S.A., Prescott, A., Woods, A., Carling, D., and Hardie, D.G. (1998). AMP-activated protein kinase: greater AMP dependence, and preferential nuclear localization, of complexes containing the alpha2 isoform. *Biochemical Journal* 334, 177.

Salzer, J.L. (1997). Clustering sodium channels at the node of Ranvier: close encounters of the axon-glia kind. *Neuron* 18, 843-846.

Sanders, M.J., Grondin, P.O., Hegarty, B.D., Snowden, M.A., and Carling, D. (2007). Investigating the mechanism for AMP activation of the AMP-activated protein kinase cascade. *Biochemical Journal* 403, 139-148.

Scheib, J., and Höke, A. (2013). Advances in peripheral nerve regeneration. *Nature Reviews Neurology* 9, 668.

Schildhaus, N., Trink, E., Polson, C., DeTolla, L., Tyler, B.M., Jallo, G.I., Tok, S., and Guarnieri, M. (2014). Thermal latency studies in opiate-treated mice. *Journal of pharmacy & bioallied sciences* 6, 43.

Schmidt, M., and Finley, D. (2014). Regulation of proteasome activity in health and disease. *Biochimica et Biophysica Acta (BBA)-Molecular Cell Research* 1843, 13-25.

Schmitt, A.B., Breuer, S., Liman, J., Buss, A., Schlangen, C., Pech, K., Hol, E.M., Brook, G.A., Noth, J., and Schwaiger, F.-W. (2003). Identification of regeneration-associated genes after central and peripheral nerve injury in the adult rat. *BMC neuroscience* 4, 8.

Schnapp, B.J., and Reese, T.S. (1989). Dynein is the motor for retrograde axonal transport of organelles. *Proceedings of the National Academy of Sciences* 86, 1548-1552.

Schwab, M., and Caroni, P. (1988a). Rat CNS myelin and a subtype of oligodendrocyte in culture represent a nonpermissive neurite growth and fibroblast spreading substrate. *Journal of Neuroscience* 8, 2381-2393.

Schwab, M., and Thoenen, H. (1985). Dissociated neurons regenerate into sciatic but not optic nerve explants in culture irrespective of neurotrophic factors. *Journal of Neuroscience* 5, 2415-2423.

Schwab, M.E., and Bartholdi, D. (1996). Degeneration and regeneration of axons in the lesioned spinal cord. *Physiological reviews* 76, 319-370.

Schwab, M.E., and Caroni, P. (1988b). Oligodendrocytes and CNS myelin are nonpermissive substrates for neurite growth and fibroblast spreading in vitro. *Journal of Neuroscience* 8, 2381-2393.

Schwab, M.E., and Strittmatter, S.M. (2014). Nogo limits neural plasticity and recovery from injury. *Current opinion in neurobiology* 27, 53-60.

Seiffers, R., Mills, C.D., and Woolf, C.J. (2007). ATF3 increases the intrinsic growth state of DRG neurons to enhance peripheral nerve regeneration. *Journal of Neuroscience* 27, 7911-7920.

Shaw, R.J. (2009). LKB1 and AMP-activated protein kinase control of mTOR signalling and growth. *Acta physiologica* 196, 65-80.

Shaw, R.J., Kosmatka, M., Bardeesy, N., Hurlley, R.L., Witters, L.A., DePinho, R.A., and Cantley, L.C. (2004). The tumor suppressor LKB1 kinase directly activates AMP-activated kinase and regulates apoptosis in response to energy stress. *Proceedings of the National Academy of Sciences of the United States of America* 101, 3329-3335.

Shen, Y., Tenney, A.P., Busch, S.A., Horn, K.P., Cuascut, F.X., Liu, K., He, Z., Silver, J., and Flanagan, J.G. (2009). PTP σ is a receptor for chondroitin sulfate proteoglycan, an inhibitor of neural regeneration. *Science* 326, 592-596.

Silver, J., Schwab, M.E., and Popovich, P.G. (2015). Central nervous system regenerative failure: role of oligodendrocytes, astrocytes, and microglia. *Cold Spring Harbor perspectives in biology* 7, a020602.

Simmons, D., and Walsh, F. (2000). Inhibitor of neurite outgrowth in humans. *Nature* 403, 6768.

Simonen, M., Pedersen, V., Weinmann, O., Schnell, L., Buss, A., Ledermann, B., Christ, F., Sansig, G., van der Putten, H., and Schwab, M.E. (2003). Systemic deletion of the myelin-associated outgrowth inhibitor Nogo-A improves regenerative and plastic responses after spinal cord injury. *Neuron* 38, 201-211.

Skene, J., and Willard, M. (1981). Characteristics of growth-associated polypeptides in regenerating toad retinal ganglion cell axons. *Journal of Neuroscience* 1, 419-426.

Smith, R.P., Lerch-Haner, J.K., Pardinias, J.R., Buchser, W.J., Bixby, J.L., and Lemmon, V.P. (2011). Transcriptional profiling of intrinsic PNS factors in the postnatal mouse. *Molecular and Cellular Neuroscience* 46, 32-44.

Smith-Thomas, L.C., Fok-Seang, J., Stevens, J., Du, J.-S., Muir, E., Faissner, A., Geller, H.M., Rogers, J.H., and Fawcett, J.W. (1994). An inhibitor of neurite outgrowth produced by astrocytes. *Journal of Cell Science* 107, 1687-1695.

Sokolova, V., Li, F., Polovin, G., and Park, S. (2015). Proteasome activation is mediated via a functional switch of the Rpt6 C-terminal tail following chaperone-dependent assembly. *Scientific reports* 5.

Stout, R.D., and Suttles, J. (2004). Functional plasticity of macrophages: reversible adaptation to changing microenvironments. *Journal of leukocyte biology* 76, 509-513.

Sulaiman, O.A., and Gordon, T. (2003). Cellular and molecular interactions after peripheral and central nerve injury. *Biomedical Reviews* 14, 51-62.

Sun, F., Park, K.K., Belin, S., Wang, D., Lu, T., Chen, G., Zhang, K., Yeung, C., Feng, G., and Yankner, B.A. (2011). Sustained axon regeneration induced by co-deletion of PTEN and SOCS3. *Nature* 480, 372.

Tamás, P., Hawley, S.A., Clarke, R.G., Mustard, K.J., Green, K., Hardie, D.G., and Cantrell, D.A. (2006). Regulation of the energy sensor AMP-activated protein kinase by antigen receptor and Ca²⁺ in T lymphocytes. *Journal of Experimental Medicine* 203, 1665-1670.

Tamura, S., and Tsuiki, S. (1980). Purification and Subunit Structure of Rat - Liver Phosphoprotein Phosphatase whose Molecular Weight is 260000 by Gel Filtration (Phosphatase IB). *The FEBS Journal* 111, 217-224.

Tanaka, H., Yamashita, T., Asada, M., Mizutani, S., Yoshikawa, H., and Tohyama, M. (2002). Cytoplasmic p21Cip1/WAF1 regulates neurite remodeling by inhibiting Rho-kinase activity. *J Cell Biol* 158, 321-329.

Tang, Q., Bangaru, M.L.Y., Kostic, S., Pan, B., Wu, H.-E., Koopmeiners, A.S., Yu, H., Fischer, G.J., McCallum, J.B., and Kwok, W.-M. (2012a). Ca²⁺-dependent regulation of Ca²⁺ currents in rat primary afferent neurons: role of CaMKII and the effect of injury. *Journal of Neuroscience* 32, 11737-11749.

Tang, X., Davies, J.E., and Davies, S.J. (2003). Changes in distribution, cell associations, and protein expression levels of NG2, neurocan, phosphacan, brevican, versican V2, and tenascin-C during acute to chronic maturation of spinal cord scar tissue. *Journal of neuroscience research* 71, 427-444.

Tang, X., Skuba, A., Han, S.-B., Kim, H., Ferguson, T., and Son, Y.-J. (2012b). Sensory Nerve Regeneration at the CNS-PNS Interface. In *Basic Principles of Peripheral Nerve Disorders (InTech)*.

Taniuchi, M., Clark, H.B., Schweitzer, J.B., and Johnson, E. (1988). Expression of nerve growth factor receptors by Schwann cells of axotomized peripheral nerves: ultrastructural location, suppression by axonal contact, and binding properties. *Journal of Neuroscience* 8, 664-681.

Team, R.C. (2016). R: A language and environment for statistical computing [Computer software]. Vienna: R Foundation for Statistical Computing.

Tedeschi, A. (2011). Tuning the orchestra: transcriptional pathways controlling axon regeneration. *Frontiers in molecular neuroscience* 4.

Tedeschi, A., Dupraz, S., Laskowski, C.J., Xue, J., Ulas, T., Beyer, M., Schultze, J.L., and Bradke, F. (2016). The calcium channel subunit alpha2delta2 suppresses axon regeneration in the adult CNS. *Neuron* 92, 419-434.

Tedeschi, A., Nguyen, T., Puttagunta, R., Gaub, P., and Di Giovanni, S. (2009). A p53-CBP/p300 transcription module is required for GAP-43 expression, axon outgrowth, and regeneration. *Cell Death & Differentiation* 16.

Teng, F.Y.H., and Tang, B.L. (2006). Axonal regeneration in adult CNS neurons—signaling molecules and pathways. *Journal of neurochemistry* 96, 1501-1508.

Todd, A. (2002). Anatomy of primary afferents and projection neurones in the rat spinal dorsal horn with particular emphasis on substance P and the neurokinin 1 receptor. *Experimental physiology* 87, 245-249.

Tsao, B., Boulis, N., and Bethoux, F. (2012). Trauma of the nervous system, peripheral nerve trauma. *Bradley's neurology in clinical practice*, 984-1001.

Tsuda, M., Shigemoto-Mogami, Y., Koizumi, S., Mizokoshi, A., Kohsaka, S., Salter, M.W., and Inoue, K. (2003). P2X 4 receptors induced in spinal microglia gate tactile allodynia after nerve injury. *Nature* 424, 778.

Tsujino, H., Kondo, E., Fukuoka, T., Dai, Y., Tokunaga, A., Miki, K., Yonenobu, K., Ochi, T., and Noguchi, K. (2000). Activating transcription factor 3 (ATF3) induction by axotomy in sensory and motoneurons: A novel neuronal marker of nerve injury. *Molecular and Cellular Neuroscience* 15, 170-182.

Turnley, A.M., and Bartlett, P.F. (1998). MAG and MOG enhance neurite outgrowth of embryonic mouse spinal cord neurons. *Neuroreport* 9, 1987-1990.

Turnley, A.M., Stapleton, D., Mann, R.J., Witters, L.A., Kemp, B.E., and Bartlett, P.F. (1999). Cellular distribution and developmental expression of AMP-activated protein kinase isoforms in mouse central nervous system. *Journal of neurochemistry* 72, 1707-1716.

Tzatsos, A., and Tschlis, P.N. (2007). Energy depletion inhibits phosphatidylinositol 3-kinase/Akt signaling and induces apoptosis via AMP-activated protein kinase-dependent phosphorylation of IRS-1 at Ser-794. *Journal of Biological Chemistry* 282, 18069-18082.

Vabnick, I., and Shrager, P. (1998). Ion channel redistribution and function during development of the myelinated axon. *Developmental Neurobiology* 37, 80-96.

Viollet, B., Andreelli, F., Jørgensen, S.B., Perrin, C., Flamez, D., Mu, J., Wojtaszewski, J.F., Schuit, F.C., Birnbaum, M., and Richter, E. (2003a). Physiological role of AMP-activated protein kinase (AMPK): insights from knockout mouse models (Portland Press Limited).

Viollet, B., Andreelli, F., Jørgensen, S.B., Perrin, C., Geloën, A., Flamez, D., Mu, J., Lenzner, C., Baud, O., and Bennoun, M. (2003b). The AMP-activated protein kinase $\alpha 2$ catalytic subunit controls whole-body insulin sensitivity. *The Journal of clinical investigation* 111, 91-98.

Vogt, J., Traynor, R., and Sapkota, G.P. (2011). The specificities of small molecule inhibitors of the TGF β s and BMP pathways. *Cellular signalling* 23, 1831-1842.

Wakita, S., Izumi, Y., Nakai, T., Adachi, K., Takada-Takatori, Y., Kume, T., and Akaike, A. (2014). Staurosporine induces dopaminergic neurite outgrowth through AMP-activated protein kinase/mammalian target of rapamycin signaling pathway. *Neuropharmacology* 77, 39-48.

Wang, K.C., Koprivica, V., Kim, J.A., and Sivasankaran, R. (2002). Oligodendrocyte-myelin glycoprotein is a Nogo receptor ligand that inhibits neurite outgrowth. *Nature* 417, 941.

Weng, Y.-L., An, R., Cassin, J., Joseph, J., Mi, R., Wang, C., Zhong, C., Jin, S.-G., Pfeifer, G.P., and Bellacosa, A. (2017). An Intrinsic Epigenetic Barrier for Functional Axon Regeneration. *Neuron* 94, 337-346. e336.

Wu, J., Puppala, D., Feng, X., Monetti, M., Lapworth, A.L., and Geoghegan, K.F. (2013). Chemoproteomic analysis of intertissue and interspecies isoform diversity of AMP-activated protein kinase (AMPK). *Journal of Biological Chemistry* 288, 35904-35912.

Xiao, B., Sanders, M.J., Underwood, E., Heath, R., Mayer, F., Carmena, D., Jing, C., Walker, P.A., Eccleston, J.F., and Haire, L.F. (2011a). Structure of mammalian AMPK and its regulation by ADP. *Nature* 472, 230.

Xiao, B., Sanders, M.J., Underwood, E., Heath, R., Mayer, F.V., Carmena, D., Jing, C., Walker, P.A., Eccleston, J.F., and Haire, L.F. (2011b). Structure of mammalian AMPK and its regulation by ADP. *Nature* 472, 230.

Xiao, H.-S., Huang, Q.-H., Zhang, F.-X., Bao, L., Lu, Y.-J., Guo, C., Yang, L., Huang, W.-J., Fu, G., and Xu, S.-H. (2002). Identification of gene expression profile of dorsal root ganglion in the rat peripheral axotomy model of neuropathic pain. *Proceedings of the National Academy of Sciences* 99, 8360-8365.

Yang, H.-Y., Lieska, N., Shao, D., Kriho, V., and Pappas, G.D. (1994). Proteins of the intermediate filament cytoskeleton as markers for astrocytes and human astrocytomas. *Molecular and chemical neuropathology* 21, 155-176.

Yang, W., Hong, Y.H., Shen, X.-Q., Frankowski, C., Camp, H.S., and Leff, T. (2001). Regulation of Transcription by AMP-activated Protein Kinase PHOSPHORYLATION OF p300 BLOCKS ITS INTERACTION WITH NUCLEAR RECEPTORS. *Journal of Biological Chemistry* 276, 38341-38344.

Yudin, D., Hanz, S., Yoo, S., Iavnilovitch, E., Willis, D., Gradus, T., Vuppalachchi, D., Segal-Ruder, Y., Ben-Yaakov, K., and Hieda, M. (2008). Localized regulation of axonal RanGTPase controls retrograde injury signaling in peripheral nerve. *Neuron* 59, 241-252.

Yukawa, K., Tanaka, T., Takeuchi, N., Iso, H., Li, L., Kohsaka, A., Waki, H., Miyajima, M., Maeda, M., and Kikutani, H. (2009). Sema4D/CD100 deficiency leads to superior performance in mouse motor behavior. *Canadian Journal of Neurological Sciences* 36, 349-355.

Zhang, Y., Qiu, J., Wang, X., Zhang, Y., and Xia, M. (2011). AMP-activated protein kinase suppresses endothelial cell inflammation through phosphorylation of transcriptional coactivator p300. *Arteriosclerosis, thrombosis, and vascular biology* 31, 2897-2908.

Zheng, B., Ho, C., Li, S., Keirstead, H., Steward, O., and Tessier-Lavigne, M. (2003). Lack of enhanced spinal regeneration in Nogo-deficient mice. *Neuron* 38, 213-224.

Zhou, J., Su, P., Li, D., Tsang, S., Duan, E., and Wang, F. (2010). High-Efficiency Induction of Neural Conversion in Human ESCs and Human Induced Pluripotent Stem Cells with a Single Chemical Inhibitor of Transforming Growth Factor Beta Superfamily Receptors. *Stem Cells* 28, 1741-1750.

Zou, H., Ho, C., Wong, K., and Tessier-Lavigne, M. (2009). Axotomy-induced Smad1 activation promotes axonal growth in adult sensory neurons. *Journal of Neuroscience* 29, 7116-7123.

7. Appendix

7.1 List of Figures

AMPK	5' AMP-activated protein kinase	DRG	Dorsal root ganglion
RNA seq	RNA Sequencing	PSMC5	Proteasome 26S Subunit, ATPase 5
PNS iPSCs	Peripheral nervous system Induced pluripotent stem cells	CNS NGF	Central nervous system Nerve Growth Factor
cAMP	Cyclic adenosine monophosphate	PKA	Protein kinase A
HDAC5 STAT3	Histone Deacetylase 5 Signal transducer and activator of transcription 3	JNK RAGs	c-Jun N-terminal kinases Regeneration associated genes
GAP-43	Growth Associated Protein 43	CAP-23	brain abundant membrane attached signal protein 1
Arg1 SPRR1A	Arginase 1 Small Proline Rich Protein 1A	IL6 DLK-1	Interleukin 6 Delta Like Non-Canonical Notch Ligand 1
CSPGs	Chondroitin sulfate proteoglycans	DREZ	Dorsal root entry zone
MAG	Myelin-associated glycoprotein	Nogo	Reticulon-4
OMgp	Oligodentocyte myelin glycoprotein	Sema4D	Semaphorin4D
GFAP PTP σ	Glial fibrillary acidic protein Protein tyrosine phosphatases σ	ChABC LAR phosphatase	Chondroitinase ABC Leukocyte common antigen-related phosphatase
M1	Pro-inflammatory macrophages	M2	Anti-inflammatory macrophages
CCL2	C-C Motif Chemokine Ligand 2	KLFs	Krüppel-like transcription factors
Cacna2d2	Calcium Channel Subunit Alpha2delta2	c-Jun	AP-1 Transcription Factor Subunit
ATF3	Activating Transcription Factor 3	HIF-1 α	Hypoxia Inducible Factor 1 Alpha Subunit
SOX11	SRY-Related HMG-Box Gene 11	Smad1	SMAD Family Member 1
CREB	CAMP Responsive Element Binding Protein	CD44	Phagocytic Glycoprotein 1
Galanin	Galanin And GMAP Prepropeptide	Hsp27	Heat shock protein 27
AP1 Jund1 NF- κ B	activator protein 1 Transcription factor jun-D Nuclear Factor Kappa B Subunit 1	Fos Junb HDACs	Proto-oncogene c-Fos Transcription factor jun-B Histone Deacetylases

LIF	Leukemia Inhibitory Factor	CTNF	Ciliary Neurotrophic Factor
p21/Cip1/Waf1	Cyclin Dependent Kinase Inhibitor 1A	p53	Tumor Protein P53
CBP	CREB Binding Protein	PCAF	P300/CBP-associated factor
Coronin 1b	Coronin, Actin-Binding Protein, 1B	Rab13	Cell Growth-Inhibiting Gene 4 Protein
ROCK	Rho kinase	MDM4	Mdm2-Like P53-Binding Protein 3
MDM2	MDM2 Proto-Oncogene, E3 Ubiquitin Protein Ligase	BMP	Bone Morphogenetic Protein
Tet3	Ten-eleven translocation methylcytosine dioxygenases 3	SCI	Spinal cord injury
LC-MS/MS	Liquid chromatography tandem-mass spectrometry	CaMKII α	Ca ²⁺ /calmodulin-dependent protein kinase II
HBSS	Hank's Balanced Salt Solution	NGS	Normal goat serum
FBS	Fetal Bovine Serum	p-ACC	Phospho-Acetyl-CoA Carboxylase
qRT-PCR	Quantitative real-time PCR	F11	Rat embryonic dorsal root ganglion
NF-200 mTORC1	Neurofilaments 200 mammalian target of rapamycin complex 1	T9 PDL	Thoracic vertebrae 9 Poly-D-lysine
IP	Immunoprecipitation	p70S6K	ribosomal protein S6 kinase
LKB1	Serine/threonine-protein kinase STK11	p300	Histone acetyltransferase p300
KLC2	Kinesin light chain 2	CAMKK2	Calcium/calmodulin-dependent protein kinase kinase 2
IGF1	Insulin-like growth factor I	PI3K	phosphatidylinositide 3-kinases
CXCL12	C-X-C Motif Chemokine Ligand 12	Trim 28	Transcription intermediary factor 1-beta
BDNF	Brain-derived neurotrophic factor	ATF3	Cyclic AMP-dependent transcription factor ATF-3
Arg1 Myc	Arginase-1 Myc proto-oncogene protein	Fos HIF1a	Proto-oncogene c-Fos Hypoxia-inducible factor 1-alpha
IL6 CRP	Interleukin-6 cAMP-activated global transcriptional regulator CRP	TNF- α MAGE-A3/6	Tumor necrosis factor α Melanoma-associated antigen 3/6

7.2 List of Abbreviations

AMPK	5' AMP-activated protein kinase	DRG	Dorsal root ganglion
RNA seq	RNA Sequencing	PSMC5	Proteasome 26S Subunit, ATPase 5
PNS	Peripheral nervous system	CNS	Central nervous system
iPSCs	Induced pluripotent stem cells	NGF	Nerve Growth Factor
cAMP	Cyclic adenosine monophosphate	PKA	Protein kinase A
HDAC5	Histone Deacetylase 5	JNK	c-Jun N-terminal kinases
STAT3	Signal transducer and activator of transcription 3	RAGs	Regeneration associated genes
GAP-43	Growth Associated Protein 43	CAP-23	brain abundant membrane attached signal protein 1
Arg1	Arginase 1	IL6	Interleukin 6
SPRR1A	Small Proline Rich Protein 1A	DLK-1	Delta Like Non-Canonical Notch Ligand 1
CSPGs	Chondroitin sulfate proteoglycans	DREZ	Dorsal root entry zone
MAG	Myelin-associated glycoprotein	Nogo	Reticulon-4
OMgp	Oligodendrocyte myelin glycoprotein	Sema4D	Semaphorin4D
GFAP	Glial fibrillary acidic protein	ChABC	Chondroitinase ABC
PTP σ	Protein tyrosine phosphatases σ	LAR	Leukocyte common antigen-related phosphatase
M1	Pro-inflammatory macrophages	M2	Anti-inflammatory macrophages
CCL2	C-C Motif Chemokine Ligand 2	KLFs	Krüppel-like transcription factors
Cacna2d2	Calcium Channel Subunit Alpha2delta2	c-Jun	AP-1 Transcription Factor Subunit
ATF3	Activating Transcription Factor 3	HIF-1 α	Hypoxia Inducible Factor 1 Alpha Subunit
SOX11	SRY-Related HMG-Box Gene 11	Smad1	SMAD Family Member 1
CREB	CAMP Responsive Element Binding Protein	CD44	Phagocytic Glycoprotein 1
Galanin	Galanin And GMAP Prepropeptide	Hsp27	Heat shock protein 27
AP1	activator protein 1	Fos	Proto-oncogene c-Fos
Jund1	Transcription factor jun-D	Junb	Transcription factor jun-B
NF- κ B	Nuclear Factor Kappa B Subunit 1	HDACs	Histone Deacetylases

LIF	Leukemia Inhibitory Factor	CTNF	Ciliary Neurotrophic Factor
p21/Cip1/Waf1	Cyclin Dependent Kinase Inhibitor 1A	p53	Tumor Protein P53
CBP	CREB Binding Protein	PCAF	P300/CBP-associated factor
Coronin 1b	Coronin, Actin-Binding Protein, 1B	Rab13	Cell Growth-Inhibiting Gene 4 Protein
ROCK	Rho kinase	MDM4	Mdm2-Like P53-Binding Protein 3
MDM2	MDM2 Proto-Oncogene, E3 Ubiquitin Protein Ligase	BMP	Bone Morphogenetic Protein
Tet3	Ten-eleven translocation methylcytosine dioxygenases 3	SCI	Spinal cord injury
LC-MS/MS	Liquid chromatography tandem-mass spectrometry	CaMKII α	Ca ²⁺ /calmodulin-dependent protein kinase II
HBSS	Hank's Balanced Salt Solution	NGS	Normal goat serum
FBS	Fetal Bovine Serum	p-ACC	Phospho-Acetyl-CoA Carboxylase
qRT-PCR	Quantitative real-time PCR	F11	Rat embryonic dorsal root ganglion
NF-200	Neurofilaments 200	T9	Thoracic vertebrae 9
mTORC1	mammalian target of rapamycin complex 1	PDL	Poly-D-lysine
IP	Immunoprecipitation	p70S6K	ribosomal protein S6 kinase
LKB1	Serine/threonine-protein kinase STK11	p300	Histone acetyltransferase p300
KLC2	Kinesin light chain 2	CAMKK2	Calcium/calmodulin-dependent protein kinase kinase 2
IGF1	Insulin-like growth factor I	PI3K	phosphatidylinositide 3-kinases

8. Supplementary files

Supplementary file 1.

List of enriched proteins in peripheral and central projections without injury.

Label	Mean_LAMvsSham	Label	Mean_LAMvsSham
Pdhb	6.405268878	Pcbp2	-0.797110789
Snd1	5.387806048	Mob2	-0.797682543
Saa1	5.046083423	Marcks	-0.798008468
H1fx	4.246594952	Fbxo22	-0.79847883
Eno2	4.157270107	Ctnn	-0.799101558

Serpinf1	4.144654591	Sncb	-0.800161939
Crat	3.8925258	Ufc1	-0.804805994
BC026585	3.840530674	Pdlim5	-0.807092191
Fn3k	3.778008785	Prkch	-0.808890624
Thbs1	3.741088376	Rtkn	-0.81046812
Gfap	3.718956984	Dstn	-0.81126379
Serpina3a	3.688416154	Stk38l	-0.811604033
Pafah1b1	3.550369028	Sfn	-0.812334885
Dpp4	3.493751392	Sec31a	-0.815336573
Rpl4	3.387215713	Stat3	-0.815968067
Adam22	3.374345319	Sept6	-0.818367387
Aida	3.345281925	Gstm2	-0.820909558
Pa2g4	3.341423065	Ybx3	-0.822953409
Dnajc17	3.265181256	Anp32e	-0.825831736
Rplp0	3.258012383	Nudt3	-0.826040346
Hsd17b10	3.120424151	Sh3bgrl3	-0.826303137
Eif2s1	3.115494588	Tbc1d17	-0.828538565
Adh5	3.1091977	Zyx	-0.830138911
Vapb	3.067554609	Ywhag	-0.83193229
Lame3	3.062184908	Efhd2	-0.833513305
Aspa	3.057026397	Sod1	-0.834380218
Naa25	3.036675751	Ago2	-0.837232324
Serpine2	3.018798107	Gfpt2	-0.838356863
Psmc6	3.000759227	Bola1	-0.840198084
Capns1	2.977223289	Msra	-0.840946607
Acp5	2.907524769	Anxa11	-0.845975808
Dbt	2.895375764	Usp7	-0.847510561
Idh2	2.86517489	Pdxdc1	-0.850722426
Gulp1	2.864496567	Rap1gds1	-0.852074445
Krt222	2.853433672	Ahsg	-0.854004174
Plexd3	2.848621317	Ciapi1	-0.854046999
Vat1	2.837904599	Appl1	-0.855940197
Hadh	2.833304109	Tubb2a	-0.860764148
Erp44	2.801863942	Arf3	-0.861975785
Suclg1	2.784693762	Clint1	-0.864375246
Ckmt1	2.781060093	Ighg2c	-0.869686954
Naa10	2.773788434	Aldh1a7	-0.870795959
Tardbp	2.746879073	Srp72	-0.874895004
Yars	2.719550222	Uap1	-0.877512125
Vwal	2.700201265	Dbnl	-0.879065085
Actn2	2.689412176	Ptrf	-0.879574132
Ldb3	2.662993623	Faim	-0.87973452
Cyct	2.662540402	Sh3glb1	-0.880037244
Ckmt2	2.648373501	Eml2	-0.880507497
Dmd	2.632283045	Gnpda1	-0.882500138
Mybpc1	2.618084659	Actb12	-0.88275674

Hmgb2	2.5728229	Rheb	-0.883028506
Lims2	2.57238628	Eif3m	-0.883055528
Setd7	2.551676829	Strap	-0.883228579
Coro6	2.546231032	Ube2k	-0.884516726
Cabp1	2.518631875	Btf3l4	-0.885270453
Uba1	2.515830759	Gas7	-0.886711794
Rala	2.510061454	Aif1l	-0.888341472
Hapln1	2.499604842	Galk2	-0.893984044
Gm8394	2.46117857	Cpsf6	-0.895065458
Dlg3	2.460292433	Ube2v2	-0.897968225
Hmgb3	2.415670917	Ciao1	-0.899215349
Nup35	2.405167856	Vps26b	-0.903735079
Sept4	2.395083619	Spg20	-0.904215744
Edfl	2.3404191	Mri1	-0.904228894
Txnl1	2.33878021	Cops7a	-0.904277111
Zfp191	2.320914755	Cdk5	-0.906063024
Ralb	2.320528779	Ngp	-0.906659554
Itgb1	2.319135625	Cadps	-0.909243066
Nars	2.306172103	Ywhae	-0.909318784
Gnb2l1	2.29996596	Psme3	-0.913066659
Hadhb	2.279785772	Vtn	-0.916470815
Tsg101	2.278602601	Wdr44	-0.917209901
Pir	2.273291423	Nudt9	-0.918280365
Eef1d	2.267708392	Mical1	-0.918937897
Stxbp1	2.243133594	Ykt6	-0.920982219
Eif4a1	2.242444848	Sms	-0.921180218
Napb	2.242164012	Tbcb	-0.922597064
Mob4	2.234748565	Stub1	-0.926810877
Ccdc132	2.208571133	Lrp5	-0.928167893
Pgk2	2.202343895	Cbfb	-0.931060801
Ppp2ca	2.198302146	Camk1	-0.93362402
Pacs2	2.195947003	Akt1	-0.933910012
Hip1	2.194297544	Csrp1	-0.935635069
Arpc2	2.191864587	Purb	-0.936888938
Dhtkd1	2.184141491	Gstt1	-0.938118934
Nsfl1c	2.176744247	Ywhaz	-0.943849641
Uba1	2.16650355	S100a16	-0.944447556
Dtd2	2.127093799	Tatdn1	-0.946414364
Hspb8	2.117498103	Blmh	-0.947203833
Acadl	2.112964645	Pfn2	-0.947493727
Ppp1cc	2.106605404	Arf5	-0.94774088
Hdac3	2.099355023	Pggt1b	-0.947995724
P2rx7	2.09004484	Gmcs	-0.950100392
Parva	2.084893054	Psmc12	-0.95608161
Vdac1	2.079268583	Copa	-0.95758529
Sf3a2	2.07538722	Ifi47	-0.959934421

Elavl1	2.073095275	Pepd	-0.961442818
Myl10	2.069680428	Eif2s3x	-0.964728084
Hsd17b4	2.062320695	Psmc2	-0.967154174
Gnal	2.056753513	Rabggta	-0.96887765
Ddah1	2.052838852	Avil	-0.969454591
Cdc42ep1	2.049239256	Pfdn1	-0.970634012
Thumpd1	2.042981087	Gab1	-0.971204829
Prdx3	2.033559575	Gstm5	-0.972938629
Hp	2.023697418	Phpt1	-0.972948284
Pdha1	2.010031889	Tbcc	-0.973088428
Ide	1.999466998	Bid	-0.974102348
Ganab	1.989870832	Cpxm2	-0.974717458
Mdh1	1.974390859	Tubb6	-0.976255702
Dtd1	1.963928165	Ppp1r2	-0.977102318
Pf4	1.956695552	Tjp3	-0.978339654
Oxr1	1.952906468	Stard10	-0.980048637
Chmp4c	1.946823518	Atp6v1d	-0.980294369
Sod2	1.933469246	Cdc3711	-0.981115428
Rps2	1.930927941	Sdc4	-0.981256445
Atp5d	1.930516012	Hint1	-0.981636022
D10Jhu81e	1.930509789	Arhgef16	-0.983152025
Lama1	1.927928335	Gmps	-0.983810662
Vasp	1.923083587	Abhd14b	-0.983915925
Rnh1	1.920684503	Fbxl15	-0.98535334
Dnajc6	1.919050708	Cdh19	-0.985439901
Fermt3	1.913111535	Snapin	-0.988409314
Apoe	1.908229665	Rnf14	-0.989534011
Plekhd1	1.882164198	Bcat1	-0.992026799
Acat1	1.881971543	Atg4b	-0.992162282
Vash1	1.879155733	Cpne1	-0.992831192
Cct3	1.864617583	Txndc9	-0.996830523
Rpl32	1.863637194	Comt	-0.999344434
Nfasc	1.863289404	Pea15a	-1.000963629
Tbc1d10b	1.862612734	Commmd9	-1.000997806
Etfb	1.850218627	Sec24c	-1.002843749
Otud6b	1.848180395	Anpep	-1.002896515
Wwp1	1.833341178	Gbe1	-1.003537647
Etfa	1.826887071	Mdp1	-1.004073064
Wasl	1.816522234	Sar1a	-1.005041775
Pou2f1	1.805588741	Crip2	-1.005640246
Drp2	1.798968371	Rad23b	-1.006811
Tmod1	1.790986714	Myom2	-1.009193718
Pip4k2b	1.788798314	Diras2	-1.009670752
Pin4	1.788553795	Ifit3	-1.010066664
Vdac2	1.786426143	Fnbp1	-1.013244774
Sarnp	1.785772252	Tbc1d13	-1.014967313

Sept2	1.783680237	Ankrd13d	-1.016391949
Acaa2	1.780278597	Prepl	-1.018546604
Fga	1.778896466	N6amt2	-1.018780175
Gpm6a	1.777507425	Txndc17	-1.019295241
Aars	1.773285646	Txn1	-1.019519989
Dld	1.758494208	Nub1	-1.021371929
Hspd1	1.754522773	Grcc10	-1.024285056
Atp1b1	1.749794335	Ift22	-1.025478663
Lmnb2	1.747051874	Cstb	-1.02930176
Ech1	1.743256792	Pzp	-1.030507048
Mgea5	1.73759824	Pvalb	-1.030910157
Psmd11	1.725818459	Sri	-1.032738506
Mybbp1a	1.72428895	Capza1	-1.036434875
Atp1a2	1.722252354	Lmnb1	-1.039011963
Map7d2	1.713228218	Actn1	-1.039921524
Actr10	1.71095234	Itpa	-1.040170389
Ppp1r7	1.708231759	Gpc4	-1.041434316
N4bp2l1	1.705629549	Tsnax	-1.041523411
Nebi	1.70464543	Ngly1	-1.041946907
Ppib	1.700093599	Ube2z	-1.042580648
MacroD2	1.698099365	Tln1	-1.046243409
Pspc1	1.698015074	Gnai2	-1.046745623
Got2	1.696205768	Nid2	-1.047074366
Sntb1	1.694218339	Xpo7	-1.048224246
Ccdc124	1.692915887	Rbbp9	-1.048388385
Txndc5	1.692460838	Osbpl3	-1.051719209
Pdcd10	1.691956876	Blvrb	-1.052509986
Ina	1.681703851	Drg2	-1.055199481
Bzw2	1.677374166	Gipc1	-1.056824672
Adap2	1.664268744	Nampt	-1.060127536
Sf3a1	1.65961226	Dhx9	-1.060323276
Pnkp	1.651169358	4930533O14Rik	-1.061751888
Map4	1.645934404	Lypla2	-1.066307135
Cdh1	1.643053787	Npepps	-1.067012881
Smad4	1.642363889	Lgals3	-1.068715147
Ctnnd1	1.629773786	Gsta4	-1.069099846
Fkbp3	1.629759919	Stmn1	-1.069651569
Hkdc1	1.628110261	Hpcal1	-1.073388445
Ttc38	1.624212949	S100a9	-1.07398824
Plp1	1.620885954	Gnpda2	-1.075932159
Dynlt3	1.618026986	Ddt	-1.076852852
Dnajc9	1.613891686	Gng2	-1.07781897
C1qb	1.611363857	Hspa2	-1.080104496
Flot1	1.60832683	Sncg	-1.08251634
Gm9833	1.606761672	Sh3bgrl	-1.083509041
Sypl	1.590985539	Myh14	-1.083659813

Sult1a1	1.574816725	Anks1	-1.08564613
Smarcc2	1.573024721	Pygl	-1.088313149
Naa20	1.572632099	Cmpk1	-1.092715752
Dnajc8	1.567043012	Stk3	-1.094446863
Decr1	1.566438923	Aco1	-1.094984076
Gm9774	1.565588207	Igbp1	-1.096746063
Pacsin2	1.554921157	Thop1	-1.099159868
Fgf13	1.553652904	Hrsp12	-1.100172796
Gripap1	1.547369217	Tbc1d15	-1.10068242
Cggbp1	1.543964989	Tgfb1	-1.10321987
Cyb5r3	1.541260829	Gnao1	-1.106389062
Eif1b	1.536251109	Gstt2	-1.10682951
Golim4	1.534187441	Arl2	-1.110579521
Hmgn5	1.53304101	Ube2l3	-1.111029036
Eno1b	1.524138923	Deptor	-1.115295721
Serpinh1	1.521877599	Brk1	-1.117619643
Lrrc57	1.517801941	Arl3	-1.118012861
Aldh2	1.516112307	Csrp2	-1.118639209
Hnrnpa1	1.515717923	G6pdx	-1.121793668
Lgi3	1.507931855	Park7	-1.122936043
Bzw1	1.500706149	Adsl	-1.124744891
Hspb1	1.493727009	Rabgap1	-1.128058622
Gm4978	1.489979639	Klkb1	-1.128191636
Ssb	1.48654627	Clic1	-1.131745966
Vapa	1.481399678	Pkn1	-1.13438622
Nfib	1.480995874	Rufy1	-1.13481638
G3bp2	1.478339386	Pgm3	-1.136147712
Ctnna3	1.476357926	Ap2m1	-1.138007908
Hspe1	1.472784035	Aip	-1.138568548
Sparc	1.467673103	Flnb	-1.140336259
Fam98b	1.465505525	Mapk14	-1.141655888
Tssc1	1.463793119	Ckm	-1.142359103
Pelo	1.461508509	Anp32a	-1.145290465
Tma7	1.460413072	Fhl2	-1.145760002
Cd82	1.457853612	Ighg3	-1.150533487
Pitpna	1.454044767	Ttll12	-1.152689004
Eif1	1.453990431	Qprt	-1.152729514
Tagln3	1.451020826	Mien1	-1.153364383
Vps36	1.450356481	Dffa	-1.153541796
Dag1	1.442536236	Pts	-1.15371169
Phf24	1.434213437	Psme2b	-1.157264766
Lcp1	1.432569787	Chorde1	-1.157478447
Eif2a	1.431105405	Acss2	-1.159808319
Dpysl2	1.430882133	Ppcs	-1.16071716
Rab5c	1.429958877	Ywhab	-1.162499753
Zbed5	1.429825568	Farsb	-1.165406138

Endod1	1.425361953	Csk	-1.16845824
Mthfd1	1.419864337	Mif	-1.168847077
Atf1	1.416756812	Tubb4a	-1.168853304
Dlst	1.414366929	Gca	-1.170788084
Eif4a3	1.409529987	Gmfb	-1.172921935
Fen1	1.409269935	Psmc9	-1.175068466
Pdpc1	1.407294791	Ankfy1	-1.177062797
Fgb	1.393326233	Prune	-1.180837722
Zfp207	1.3901172	Sugt1	-1.187416931
Hist1h1c	1.388801036	Psmf1	-1.189997418
Eif3c	1.382221788	Acly	-1.190860338
Sept3	1.380283291	Capn1	-1.193302968
Pdap1	1.375547048	Nckap1	-1.194411274
Hdgfrp3	1.368830637	Cspg4	-1.196332182
Vat11	1.365365046	6430548M08Rik	-1.198165261
Stx7	1.363303091	Crip1	-1.20026332
Cct5	1.356802666	Acat2	-1.201823953
Snrpa	1.355794574	Glrx	-1.204695192
Ckap5	1.352793145	Abca9	-1.208593139
Psmc1	1.341741865	Prkca	-1.208621896
C1qc	1.34021021	Impact	-1.213499194
Hnrnpu	1.335186679	Igkv1-122	-1.216192942
Pde1a	1.330557939	Fth1	-1.218131734
Ndufa4	1.329459092	Sorbs1	-1.221644943
Dhrs1	1.328268695	Carhsp1	-1.22219472
Prkab1	1.326674412	Stam	-1.224765779
Ptbp2	1.324631002	Agfg2	-1.229012371
Ilf2	1.324360404	Rfk	-1.232563563
Gstk1	1.321484398	Arhgef10	-1.233507907
C1qa	1.315869361	Serpib6a	-1.233756951
Dtna	1.315699852	Rpl5	-1.239341491
Rpl12	1.315631778	Camk1d	-1.244924528
Bud31	1.31485834	Lypla1	-1.245811236
Hspa4	1.314771857	Frmc8	-1.246454187
Snrpb2	1.313327775	Igkc	-1.256160541
Col14a1	1.310109661	Gmppb	-1.258566346
Sept5	1.305282071	Fkbp1a	-1.261178066
2610002M06Rik	1.302297258	Diras1	-1.262667463
Efnb1	1.299450613	Myg1	-1.266278055
Nefm	1.293074525	Psmc1	-1.267163052
Atp1b3	1.289658845	Cotl1	-1.267365388
Cnrip1	1.286848107	Eml1	-1.268635393
Tgm2	1.286786248	Apex1	-1.271216534
Api5	1.28579534	Pex5l	-1.271772126
Idh1	1.28477234	Col5a3	-1.271803352
Cd200	1.282760899	Gnb2	-1.275527651

Hsd17b7	1.281323802	Ppm1b	-1.283302611
1700080E11Rik	1.280785472	Asrgl1	-1.28332198
Metap1	1.277778628	Tagln	-1.283867004
Sept9	1.275753369	Prmt5	-1.284489184
Nudt21	1.272351232	Vps4b	-1.286011293
Gabarapl2	1.2635918	Asl	-1.286517528
Cops4	1.263465468	Hnmt	-1.28713154
Prx	1.262260836	Adk	-1.288148445
Clta	1.261214395	Ugp2	-1.289032259
Mag	1.253858654	Cmpk2	-1.290191954
mt-Co2	1.248395485	Nt5c	-1.292374333
M6pr	1.245554406	Atg7	-1.293107996
Aco2	1.242785588	Rnf114	-1.295615999
Dnaja2	1.241223704	Pfdn5	-1.295712311
Slc9a3r2	1.2333673	Atcay	-1.297433556
Hcfc2	1.224533048	Cstf2	-1.29885394
Maged1	1.216927722	Mybph	-1.301528394
Sptbn2	1.209313599	Atxn10	-1.302396022
Atp4a	1.206645622	Sh3glb2	-1.304350956
Nek7	1.20499785	Cbr1	-1.304840309
Mpp2	1.20158281	Crlf3	-1.305391959
Parvb	1.199306035	Etf1	-1.305985277
Hars	1.198014558	Guk1	-1.307195934
Tcp1	1.196378424	Dcun1d2	-1.309901806
Pcnp	1.195714348	S100a10	-1.316454191
Col1a1	1.193401397	Lap3	-1.318417595
Ptn	1.1922162	1700037H04Rik	-1.328579634
Fsd1	1.192180318	Glr3	-1.331061883
Cnpy2	1.189328394	Psmg1	-1.333503498
Cacnb3	1.188703114	Aldh1a3	-1.334676273
Rpl27a	1.188684787	Tpm2	-1.33469301
Rgcc	1.182408927	Gstp2	-1.340571817
Prps1	1.178170941	Uap111	-1.344487105
Gabarapl1	1.174340237	Iqgap3	-1.345489551
Rps26	1.173608525	Snx1	-1.345534773
Vps52	1.172825793	Aamdc	-1.346941802
Slc3a2	1.169909881	Aprt	-1.350846502
Calr	1.168872321	Npepl1	-1.355452428
Syn1	1.167061636	Ptpn11	-1.357068987
Itih4	1.165959264	Phgdh	-1.359497229
Nrcam	1.161393892	Ephx2	-1.359507467
Gm8973	1.157815647	Ppp2r5a	-1.361910073
Dusp15	1.156136274	F2	-1.36300613
Tomm34	1.154789595	Nit2	-1.364704145
Uchl5	1.150989569	Mvd	-1.367441855
Mat1a	1.14859592	Snx7	-1.368437579

Syncrip	1.144548657	Dhdh	-1.369907437
Eif2s2	1.13552864	Adprh	-1.370957557
Hexa	1.130523682	Frzb	-1.376407359
Spr	1.125055221	Rad23a	-1.381499486
Sfpq	1.123330095	Fam188a	-1.384447589
Ddx39b	1.121310638	Fabp3	-1.391732831
Lrpap1	1.121199256	Hs1bp3	-1.392162147
Caskin1	1.115362817	Atp6v1h	-1.396909384
Colla2	1.104853381	Hspbp1	-1.398270028
Tppp	1.10266898	Tbc1d9	-1.399069499
Rpl13a-ps1	1.102068814	Galk1	-1.400699525
Dync1i2	1.099166822	Haghl	-1.403171184
Hsp90b1	1.098603128	Nutf2	-1.411836346
Gjc3	1.096653565	Nudcd3	-1.415627462
Prph	1.093993901	Ggt5	-1.421786059
Npm1	1.091275884	Flna	-1.427858647
Gpm6b	1.077914238	Apip	-1.430675597
Lbp	1.075024094	Nif3l1	-1.430702122
Prnp	1.073061231	Pef1	-1.439484258
Rrbp1	1.069339489	Slc2a1	-1.444036834
Dync1i1	1.066337139	Sat2	-1.447626194
Bcas1	1.063775345	Lzic	-1.448553657
Hist1h2bc	1.063629498	Ighv1-12	-1.449749198
Parp3	1.061177175	Uprt	-1.456111799
Vps51	1.051116277	Bola2	-1.456937278
Stag3	1.049703853	Nudt2	-1.461244204
Gna12	1.049523218	Snca	-1.461920255
Sowahc	1.048575474	2700060E02Rik	-1.466406653
Pdia6	1.048443848	Capn2	-1.467901025
Ubl3	1.047801488	Cops7b	-1.476004759
Bicd1	1.045740602	Pgm1	-1.478730146
Rpl31	1.039561781	Isoc1	-1.482595759
Atp5h	1.035540086	Tmsb4x	-1.483150799
Yaf2	1.030247033	Lxn	-1.483915612
Map7d1	1.027866536	Ak1	-1.483958898
Cd81	1.019754174	Cntf	-1.485268026
Ogdh	1.019635553	Ywhaq	-1.485470723
Calu	1.019243255	Fscn1	-1.489009041
Prkesh	1.013509702	Ttc9	-1.490867131
Ctnnb1	1.012343405	Srsf5	-1.491419791
Rpl28	1.011945155	Mtpn	-1.494782193
Nono	1.006196245	Oplah	-1.501299974
Cd93	1.005470015	Tkt	-1.502709812
Fgf14	1.005427335	Acyp1	-1.506041719
Pdia4	1.003983341	Gk	-1.509207057
Tnxb	1.001584017	Uros	-1.509911714

Wdr82	0.999902821	Ufm1	-1.512536001
Mvp	0.998554316	Nhlrc2	-1.51300547
Rps10	0.995883773	Srp68	-1.513612906
Epb4112	0.995285636	Gamt	-1.517614405
Lgals9	0.995163653	Rangap1	-1.522198138
Map1lc3a	0.990419716	Cav1	-1.53169556
Rpl34	0.988382484	Col15a1	-1.533738744
Alyref	0.986687002	Ndrgr4	-1.536910648
Psmd14	0.982528391	Acaca	-1.53730168
At1l	0.976808229	Prkar2a	-1.539580583
Sgcd	0.970352786	Prep	-1.539882257
Rpl24	0.967553721	Stk39	-1.541978198
Vps53	0.964605769	Gm10116	-1.54821268
Cct8	0.963293836	Hmgcs1	-1.555936991
Lamp1	0.962074649	Gnb3	-1.563859551
Dync1li2	0.959803476	Ppp3cb	-1.564106489
Tpi1	0.957058099	Napg	-1.571967835
Ehd4	0.957047473	Fn1	-1.572529382
Rpl23a	0.954583486	Urod	-1.580827516
Pacsin3	0.954319633	Sgtb	-1.585910359
Cltb	0.954306772	Lactb2	-1.590177514
Arhgap17	0.951283577	Uba6	-1.59242108
Adrbk1	0.947602007	Casq1	-1.593300257
Trim28	0.946851509	Arih1	-1.599225293
Adh1	0.944522621	Cndp2	-1.605233351
Actr1a	0.941335877	Hspg2	-1.606069616
Ctnnal1	0.9376738	Tipr1	-1.607290404
Sh3bgrl2	0.931582568	Ube2r2	-1.610706443
Mapt	0.931026271	Carns1	-1.611159358
Map6	0.930327551	Gdi2	-1.614447651
Ddx6	0.92489991	Fam129a	-1.615814174
Atp5f1	0.924521439	Naalad2	-1.617930802
Slc44a1	0.924480033	Gsn	-1.623305399
C4bp	0.9236817	Pip4k2a	-1.627668347
Stxbp6	0.922511976	Gsr	-1.629010924
Rap1b	0.921175682	Fabp5	-1.639045115
Brap	0.919325722	Arhgdia	-1.640437019
Cdh2	0.919135984	Fasn	-1.640742421
Stx12	0.916226248	Ighg2b	-1.645411409
Ppp6r1	0.914021465	Asna1	-1.649870246
Nmt1	0.913018983	Gng12	-1.650450491
Enah	0.909352304	Acyp2	-1.654938815
Thyn1	0.908411893	Pgam2	-1.655551182
H2-Q7	0.906972368	Atxn3	-1.660784924
Rps6	0.90571882	Setd3	-1.661583072
Hint3	0.904000033	Klc3	-1.663028495

Mybpc3	0.902875239	Prdx5	-1.668091447
Snf8	0.898762729	Myh9	-1.668361343
Dnm3	0.896592914	Scrn3	-1.668633838
Mpp1	0.893409394	Tbc1d10a	-1.673965717
Rpl37a	0.889614508	Ecm1	-1.678656607
Amph	0.886633049	Kng1	-1.69474862
Ndrg1	0.884745762	Gpt	-1.703498142
Stx1b	0.883339207	Acot7	-1.706257408
Plcb1	0.881028431	Tpm2	-1.708732678
Bsg	0.879327649	Ppm1f	-1.71038225
Snrpd1	0.877326991	Cuta	-1.712780912
Nefl	0.870318917	Gnai3	-1.716861936
Baiap2	0.86959424	Myh10	-1.718807555
Dctn6	0.868786481	Ppp1r1b	-1.723600983
Puf60	0.867398915	Adprh2	-1.729277128
Glud1	0.866078214	Abce1	-1.731408969
Erp29	0.861832274	Polr3g	-1.732010251
Bag3	0.859883343	Lims1	-1.732064885
Palm	0.852893685	Nit1	-1.735803809
Cadm3	0.852823148	Gda	-1.737909484
Dync1li1	0.851466515	Gclc	-1.738709013
Chmp2a	0.848767666	Lcmt1	-1.739317682
Ddx5	0.848597869	Myo1c	-1.739701561
Gpd1	0.848199788	Aldh7a1	-1.743536009
Rap1a	0.848127599	Cnn3	-1.754816483
Cat	0.844826957	Ddc	-1.759222347
Eif3i	0.844748045	Selo	-1.770730919
Tspan8	0.843976635	Arhgdib	-1.776769617
Zc3h15	0.840277472	Aacs	-1.778565676
Dctn4	0.836203576	Des	-1.779308953
Mcts1	0.829546854	Capg	-1.780450662
Eif4g2	0.825874274	Sord	-1.782516687
Mapre3	0.823378919	Snx5	-1.784485439
Pdia3	0.822609368	Snx2	-1.785514726
Cct7	0.818427159	Padi2	-1.785992514
Cntn2	0.817169429	Ugdh	-1.788201573
Actr1b	0.815370705	Set	-1.791927374
Ap2b1	0.811329558	Ppp2r5d	-1.797615982
Arhgap44	0.809184965	Wdfy1	-1.802800016
Pin1	0.804527402	Echs1	-1.807879289
Rab5a	0.802803392	Renbp	-1.81266038
Aimp2	0.802415854	Ass1	-1.817170239
Rcc2	0.800438137	Lgals1	-1.820885089
Cct6b	0.796031547	Eif4e	-1.822620363
Cd151	0.79321212	Nt5e	-1.828605297
Farsa	0.791307601	Nedd8	-1.832785777

Lin7c	0.785748643	Pafah1b2	-1.83387864
Pdcl3	0.784427926	Pnpo	-1.83598862
Sema7a	0.783957296	Cfb	-1.840586664
Capza2	0.77983629	Itih2	-1.841333185
Cmtm5	0.778894976	Ptgr2	-1.841625255
Brsk1	0.778417461	Cdkn2c	-1.847713804
Napa	0.777765529	Adssl1	-1.849543811
Spin1	0.773893654	Sae1	-1.849975895
Wdr61	0.768307101	Tra2a	-1.850763996
Itga7	0.767190623	Arrb1	-1.858827584
Ap1m1	0.765760998	Pmm1	-1.859420022
Map1s	0.754525034	Sept7	-1.861830004
Ncl	0.75430731	Cbx1	-1.861843748
Tpd52	0.751971354	Anxa7	-1.864911989
Kras	0.749890364	Ubqln1	-1.871294724
Smc3	0.748777311	Mtap	-1.872116537
Tial1	0.748110293	Stambp	-1.872176121
Mthfsd	0.747416164	Pygm	-1.874653097
Uso1	0.746935537	Akr1a1	-1.8781928
Ostf1	0.735344729	Ptgr1	-1.878610772
Oard1	0.730056719	Nol3	-1.8791024
Cct4	0.721370886	Uba3	-1.879967336
Actn3	0.720838221	St13	-1.897362379
Magoh	0.717512823	Flot2	-1.89912999
Elmo1	0.716497101	Snrpn	-1.90262303
Rtn1	0.715807647	Ang	-1.916323417
Srl	0.711318261	Ubxn1	-1.919725375
Dctn3	0.707143739	Atox1	-1.920163909
Strbp	0.706111645	Sh3bp1	-1.922079722
Dctn5	0.703952818	Stip1	-1.929380913
Tppp2	0.69991094	Pdlim1	-1.940932116
Itgb4	0.695099451	Pcbd1	-1.952072068
Ptbp1	0.693841677	Xpnpep1	-1.952457321
P4hb	0.690163948	Bgn	-1.953585632
Mdh2	0.689924178	Sgta	-1.954999177
Rps24	0.689214901	Atg3	-1.959661991
Rab2a	0.686368178	Dnajb2	-1.966686946
Zc2hc1a	0.684448888	Nans	-1.970016875
Eef1b2	0.682152206	Anxa2	-1.973450771
Cd9	0.680896116	Tra2b	-1.973881446
Dynlrb1	0.677015453	Swap70	-1.989472805
Rdx	0.675990555	Tsta3	-1.998250343
Ppa1	0.667602603	Abi3bp	-2.006210803
Ola1	0.666398991	Selenbp1	-2.006451067
Map1b	0.664834308	C9	-2.008654056
Sirpa	0.664038475	Prpsap1	-2.00947863

Rpl9	0.660830387	Gstz1	-2.00995771
Denr	0.659609858	Eif3d	-2.016620161
Smc1a	0.659318943	Lipe	-2.02792102
Rab35	0.657554091	Vps26a	-2.029377381
Fgg	0.655418867	Aldh1a1	-2.03366669
Rtn4	0.65537936	Fam114a1	-2.039342118
U2af2	0.653718297	Pnp	-2.045442637
Doc2b	0.651371232	S100a8	-2.048595665
Slc44a2	0.650383137	Adipoq	-2.052435234
G3bp1	0.646242426	Bcap31	-2.0556734
Sbspon	0.643965813	Papss1	-2.064668444
Snx3	0.642267453	Alad	-2.068402814
Pddc1	0.641384371	Armc6	-2.068663513
Mras	0.639715795	Psmc5	-2.070123962
Rps7	0.636202174	Hnrnpf	-2.070388997
Rps20	0.63155498	Serpinf2	-2.070878209
Rhob	0.628813989	Islr	-2.071570963
Sec13	0.626321993	Gbp7	-2.071918141
Hsph1	0.607636557	Ywhah	-2.080077457
Manf	0.600900461	Ipo5	-2.088221758
Canx	0.598244666	Cfi	-2.095225005
Abi1	0.588926742	Ppt1	-2.097096088
Drg1	0.586220889	Ppp2r2a	-2.101211578
Fsd11	0.585901842	Gsto1	-2.103039776
Hist2h2ab	0.574689994	Naprt	-2.111985719
Cirbp	0.57127348	Plg	-2.118659745
Cc2d1b	0.566688737	Ilk	-2.120878393
Ap1b1	0.563430666	Rnase4	-2.122533226
Cdc42ep4	0.56192323	Hdhd2	-2.131249407
Map2k4	0.540848323	Thbs4	-2.146264536
Ndrp3	0.53112627	Cops2	-2.152974034
Hmox1	0.529494126	Gclm	-2.158785708
Sgce	0.526872846	Galm	-2.167502625
Prkaca	0.509172787	Prpsap2	-2.169098674
Myl12a	0.502755016	Hrg	-2.175534647
Ppp2cb	0.499634584	Tpmt	-2.179506168
Psmc10	0.497612319	Pak3	-2.181031501
Ehd3	0.434470139	Fdps	-2.197150437
Metap2	0.425648331	Cbr3	-2.205821702
Cope	0.408901347	Mtmt6	-2.206731504
Cdv3	0.37234051	Hspa1b	-2.211023522
Hnrnp3	0.371749386	Twf2	-2.215434065
Grhpr	0.358660774	Dcun1d1	-2.223065681
Ruvbl1	0.354761463	Prkag3	-2.227201819
Araf	0.353684677	Prkar2b	-2.227482185
Rbmx11	0.340115772	Gpc6	-2.22768078

Ccdc25	0.327535463	Arpin	-2.244080475
Fn3krp	0.270396949	Scrn1	-2.24666291
Paics	0.203322125	Ctbp1	-2.259929559
Coro1c	0.171870242	Plin3	-2.268722926
Pcolce	0.155707829	Vcl	-2.270402816
Pip4k2c	0.068131497	Eef1g	-2.277205311
Ybx2	-0.02785393	Gart	-2.277217427
Cops5	-0.045347901	Pgls	-2.281273872
Snrpa1	-0.080338542	Capzb	-2.28246393
Ufd11	-0.090178357	Apoa1bp	-2.28695385
Acot2	-0.105366525	Ddb1	-2.296986468
Col4a1	-0.149426946	Ctps2	-2.297724966
Stxbp1	-0.159825082	2210016F16Rik	-2.297856827
Sdcbp	-0.207741393	Dcxr	-2.302644953
Rpl7	-0.234531078	Srsf9	-2.314346054
Carkd	-0.271891017	Psmc3	-2.318782864
Rpl19	-0.272950294	Bpnt1	-2.321159983
Ggps1	-0.317246852	Serpina1c	-2.322988169
Cfap36	-0.330940171	Pls3	-2.331940058
Ahcy	-0.338086373	Itih3	-2.339426126
1700009N14Rik	-0.355129284	Pdlim4	-2.343470012
Coro1a	-0.373469299	Rnpep	-2.355439288
Adss	-0.380336795	Irgq	-2.357962256
Kif5b	-0.391588064	Pfdn6	-2.362634193
Slc9a3r1	-0.410386911	Dnpep	-2.365517184
Fam49b	-0.421579864	Fbln5	-2.369873472
0610037L13Rik	-0.436738844	Tpm4	-2.370192512
Actr3	-0.446737095	Akr7a5	-2.37901331
Fnta	-0.46260491	Serpina1d	-2.38833289
Git1	-0.497068848	Mb	-2.388845248
Pycrl	-0.497569554	Cryl1	-2.390356937
As3mt	-0.502245625	Csad	-2.392565976
Pcbp1	-0.524951823	Prkcdbp	-2.394224638
Mpi	-0.532678446	Bpgm	-2.39811433
Anxa3	-0.53992871	Atp6v1a	-2.400433236
Bag1	-0.561883924	Rilpl1	-2.402652785
Arhgef7	-0.57002522	Gale	-2.408165986
Rpl10a	-0.581026543	Gmpr2	-2.410065376
Pklr	-0.593040592	Chat	-2.4163804
Ranbp1	-0.598129841	S100b	-2.426471425
Uchl1	-0.608158797	Cryz	-2.439625812
Mgll	-0.611610537	Th	-2.452097027
Ahcyl2	-0.611770497	Pmm2	-2.456024012
Ptges3	-0.612828041	Mat2b	-2.469649324
Nsun2	-0.621199878	Dcps	-2.48324249
Fkbp1b	-0.629100708	Cd34	-2.485179864

Plcb3	-0.630739524	4931406C07Rik	-2.492947159
Hnrnpc	-0.633669269	Thtpa	-2.495925558
Syn2	-0.635327977	Ipo7	-2.499045587
Gm5160	-0.639505881	Dbi	-2.503076611
Qdpr	-0.641747755	Serpinc1	-2.510180427
Gpi1	-0.644249282	Echdc1	-2.517037159
Col18a1	-0.646191911	Gng5	-2.517070231
Chmp5	-0.649347342	Entpd2	-2.51710466
Rps21	-0.654980487	Pter	-2.521467974
Cyth3	-0.655742299	Ppp1cb	-2.5305773
Ehd2	-0.655784501	Vcan	-2.540970192
Gga1	-0.656760036	Dym	-2.542326595
Eif4h	-0.658337161	Scfd1	-2.555656598
Clip2	-0.660006248	Mug1	-2.560933665
Tmod3	-0.660545914	Ttr	-2.5665438
Fbxo2	-0.662152226	Wash1	-2.568898105
Srm	-0.670392636	Inmt	-2.573020288
Nudt5	-0.670654878	Pafah1b3	-2.580980741
Plekhb1	-0.675371313	Hagh	-2.588026522
Gpc1	-0.676034597	Uchl3	-2.601226408
Prdx1	-0.676062772	Gc	-2.603643796
Psm4	-0.67670867	Taldo1	-2.605108369
Myl6	-0.677662513	Psm3	-2.609947706
Hprt	-0.679168368	Pgam1	-2.620994789
Ppp1ca	-0.681129608	Eif3j1	-2.622583566
Inpp1	-0.682877556	Eno3	-2.642218501
Gspt1	-0.683147771	Myh8	-2.642271992
C3	-0.684000221	Tigar	-2.64646092
Bcam	-0.68826407	Mfap5	-2.647969638
Dock7	-0.69435709	Impa1	-2.66468704
Snx4	-0.696817631	Pten	-2.665244903
Prdx2	-0.696989899	Arhgap1	-2.673299574
Tax1bp3	-0.697069221	Ckap4	-2.70227066
Mvk	-0.697686479	Rela	-2.705710639
Mapre2	-0.698865745	Ace	-2.7242657
Pla2g16	-0.706132867	Psm7	-2.727656753
Dusp3	-0.706168072	Postn	-2.72819432
Arf4	-0.706909952	Trf	-2.740921988
Vars	-0.707576425	Steap3	-2.745931489
Cul5	-0.708451021	Hebp2	-2.772436568
Sumo2	-0.710652536	Crkl	-2.784305823
Orm1	-0.712244124	Itih1	-2.786683356
Cfl1	-0.712616519	Serpina3k	-2.790968339
Wbp2	-0.712628651	Dpep1	-2.794572247
Tprgl	-0.712640846	Anxa6	-2.814750852
Dnm11	-0.717729073	Nqo2	-2.825110464

Nme2	-0.719149357	Raly	-2.837425859
Lgalsl	-0.720404598	Pgm2l1	-2.839948606
Nploc4	-0.722189686	Gimap4	-2.85586429
Ncdn	-0.724064067	Hpx	-2.877435275
Dnajb4	-0.725209592	Twf1	-2.882512429
Tns1	-0.727658014	Clic4	-2.898768455
Uba2	-0.732729148	S100a6	-2.909033106
Cs	-0.734907481	S100a13	-2.913432244
Palmd	-0.736371986	Gbp3	-2.91774595
Nae1	-0.736773377	Ubash3b	-2.926806179
Atp6v1g1	-0.739031223	Serpina1c	-2.934689146
Gpcpd1	-0.739321302	Ppp2r4	-2.937792136
Ahsa1	-0.742761025	Nqo1	-2.963358706
Rpsa	-0.743447694	Crot	-3.000547924
Pdcd5	-0.74548411	Pithd1	-3.017935931
Glod4	-0.746522791	Crabp1	-3.041192357
Arpc1b	-0.747427485	Aldh9a1	-3.050854003
Rpl3	-0.74846067	Serpina1b	-3.055312605
Ptms	-0.74944229	Pgd	-3.066424332
Tom1	-0.751321693	Myh4	-3.073645626
Pygb	-0.752754835	Ighg1	-3.083689818
Casp6	-0.752979763	Bag5	-3.128913397
C4b	-0.757513621	Ddah2	-3.161634543
Ube2t	-0.759706676	Prosc	-3.167174967
Pcna	-0.761121165	Dctn2	-3.195939645
Txnrd1	-0.762243327	Psmg7	-3.204729678
Tjp1	-0.76473743	Wwc2	-3.221641639
Pdxk	-0.765309701	Ces1f	-3.236346695
Fgf1	-0.768494782	Enoph1	-3.257637974
Cda	-0.771457086	Serpina1e	-3.292056518
Sorbs2	-0.773542598	Calb2	-3.32679942
Ube2h	-0.773877131	Gbp2	-3.329148743
Ncald	-0.778836213	Lta4h	-3.44311173
Trmt112	-0.779030272	Akr1b10	-3.572539345
Gget	-0.780422615	Gmpr	-3.703229907
Lpp	-0.780493229	Iah1	-3.741288541
Camk2a	-0.781226922	S100a4	-3.749418886
Rpe	-0.789058973	S100a11	-3.802006546
Pebp1	-0.792215542	Afm	-3.803279443
AI837181	-0.792561905	Fabp4	-3.811923073
Snta1	-0.795053055	Akr1b3	-3.885497896
Cand1	-0.795589594	Ctsz	-3.909115525
Zfand2b	-0.796171096	Psat1	-4.342848622

Supplementary file 2.

List of differential expressed axoplasmic proteins in peripheral projection after sciatic nerve injury.

label	Mean_SNAvsSham	label	Mean_SNAvsSham
Chil3	2.404548215	Gmms	-0.417442943
Tnc	1.99395124	Adssl1	-0.425011028
Arg1	1.951169798	Hrsp12	-0.439397905
Lcn2	1.674484233	Asrgl1	-0.444696271
Thbs1	1.646028367	Casq1	-0.450020753
Ybx2	1.625433371	Cyfip1	-0.450192524
Spock2	1.552934178	Gpi1	-0.462188056
Lspl	1.493529691	Ap2a2	-0.468095193
Serpina3a	1.482191533	Dnajb4	-0.473856501
Hp	1.474782567	Nqo1	-0.482536825
Ctss	1.468814519	Kif27	-0.487166841
Fga	1.412295594	Pygm	-0.488585629
Ckap4	1.397721625	Gart	-0.508584702
Gap43	1.397500049	Flnc	-0.509836887
Mnda	1.391751684	Aspa	-0.520520221
Ear1	1.390334538	Psm3	-0.527661221
Ccl6	1.377701934	Ap2a1	-0.528972515
Yy1	1.372105623	Ctps2	-0.529581985
Fgb	1.322363602	Plekhb1	-0.55610453
Fgg	1.318352285	Eif3c	-0.557053171
Igf2bp2	1.289466067	Nckap1	-0.559354609
Hcls1	1.229659566	Comt	-0.563083775
S100a8	1.217185476	Egflam	-0.565702721
Pglyrp1	1.200531737	Cadps	-0.566065245
Psap	1.161912799	Nedd4	-0.567587347
Itih4	1.13910733	Nrd1	-0.573107375
Tnxb	1.136248158	Arhgap5	-0.57392594
Sf3a2	1.121362553	Vwal	-0.576207496
Hmgb2	1.086697045	Drg2	-0.580240895
S100a9	1.069502833	Acss2	-0.58037249
Dpt	1.050745715	Pygl	-0.589828863
Lgals3	1.049309653	Rpl6	-0.594905967
Camp	1.048756892	Gstm1	-0.595371442
Mlec	1.043906882	Copa	-0.5989398
Gripap1	1.032654717	Nploc4	-0.604723615
Stmn3	1.02888942	Dpep1	-0.608325256
Tmpo	1.01932624	Prkca	-0.612696162
Hist1h4j	1.014203872	Cul4b	-0.613797918
Col6a2	1.013942652	Ifi47	-0.617700183
F2	1.008527221	Cdc42bpb	-0.622003402

Gabpa	0.974930708	Glipr2	-0.624471862
H3f3b	0.974516045	Myo18a	-0.625515975
Fermt3	0.972251213	Wasf2	-0.626149553
Hmox1	0.966698884	Xpnp1	-0.633206247
Npc2	0.965403336	Prdx6	-0.638213039
Nfyc	0.964431707	Capg	-0.638984176
Hmgn5	0.963875406	Srp68	-0.640496609
Ldb3	0.956105724	Entpd2	-0.641636186
Snrnp70	0.934618536	Rps17	-0.642934836
Aatk	0.933158495	Pygb	-0.645737178
Snap25	0.928485909	Hnrnpul2	-0.64801316
Parvb	0.924571104	Rpl23	-0.649298567
Stmn2	0.923318088	Naa16	-0.65001008
Col28a1	0.912925174	Gcn111	-0.659035837
Apoh	0.886972764	Git1	-0.661240171
Was	0.886282435	Dpysl4	-0.666599506
Hdac3	0.886144734	Iah1	-0.668523782
Gm4788	0.883342725	Cltc	-0.668657183
Aldh2	0.877141838	Sf3b1	-0.671116792
Clu	0.861548829	Iqgap2	-0.671139316
Smarcc2	0.860762214	Nt5e	-0.67136247
Atp1b1	0.856054656	Myh14	-0.671456626
AI607873	0.855895646	Chat	-0.672827203
Htatip2	0.827754796	Capn1	-0.672998569
Pspc1	0.826475351	Steap3	-0.680105542
Th	0.816398018	Aldh1a1	-0.681400099
Glg1	0.801485186	Rbbp9	-0.688948601
Rplp1	0.800613231	Arhgef7	-0.689570354
Ndrp4	0.799709203	Gbp7	-0.692127508
Cd93	0.796943497	Eml1	-0.692239924
Lgals9	0.79056729	Ap2m1	-0.694037232
Prune2	0.786624887	Hnrnpu	-0.696882095
Mybbp1a	0.784502204	Ppm1g	-0.697940101
Myl9	0.781104695	Rps13	-0.699175513
Ccdc124	0.780500626	Prkaa2 or 1	-0.699273821
Fubp3	0.770429037	Osbpl3	-0.699987486
L1cam	0.770236832	Gstt1	-0.700327016
Srsf4	0.762112374	Pgm1	-0.70220601
Serpinf1	0.758928472	Hmgb1	-0.718973095
Edf1	0.757995429	Osbp	-0.720180025
Cadm4	0.754150865	Prkacb	-0.726436607
Ddc	0.74912618	Rpl9	-0.728962749
Mxra8	0.734297852	Ddx42	-0.733975633
Ctsd	0.729746061	Acot2	-0.734838996
Snx30	0.729032393	Ddx17	-0.735670352
App	0.724459377	Prkcd	-0.736832675

Kctd8	0.717269556	Fasn	-0.747674833
Dhrs4	0.715884031	Nub1	-0.750696197
Ptpn6	0.713701561	Srr	-0.750828308
Cfap36	0.708825425	Eif3a	-0.751318132
Bicd1	0.705853425	Flna	-0.751520276
Pdia6	0.699856589	Rtcb	-0.753556178
Rab3a	0.698699632	Ttc37	-0.755652636
Ccdc92	0.690312461	Iqgap3	-0.759273401
Ubl7	0.687913434	Ephx2	-0.761798491
Rplp2	0.68781822	Acaca	-0.772875712
Syn2	0.686598361	Pgm211	-0.781229552
Acat1	0.682199646	Jup	-0.784428061
Lyz2	0.675808151	Arhgap35	-0.784751061
Caprin1	0.667977736	Hspa1b	-0.785327477
Dctn2	0.663802949	Hectd1	-0.787742437
U2af1	0.659672191	Rps16	-0.789124762
Apoe	0.658666732	Rpl15	-0.791577413
Mcam	0.656818688	Ap1m1	-0.794623665
Arhgdib	0.649532688	Rock2	-0.799139947
Prnp	0.648604837	Smc1a	-0.801767218
Dab2	0.639601103	Aco1	-0.807014272
Cadm3	0.638728895	Ap1g1	-0.826756644
Doc2b	0.638547859	Dnm3	-0.828756633
Plcx3	0.629769622	Asap1	-0.841718177
Sept11	0.628856214	Hspg2	-0.847285633
Ctsb	0.626260182	Myh9	-0.853313484
Ppib	0.622180269	Rnpep	-0.855594723
Hnrnpa2b1	0.622067923	Rfk	-0.867326374
Pcna	0.619691305	Vps45	-0.878358003
Dynlrb1	0.617147852	Tln1	-0.884187253
C4bp	0.612575161	Vps53	-0.886328065
Nono	0.608275533	Cdk6	-0.890786679
Atf1	0.607996002	Rps4x	-0.891142805
Ndr3	0.606059634	Gnl1	-0.893269838
Sod2	0.605081028	Dhx9	-0.894668546
Coro1a	0.601289098	Myh10	-0.900985837
Phf24	0.599021764	Smoc2	-0.909723012
Fgf13	0.595854666	Cul3	-0.911653497
Sf3a1	0.593445637	Itih5	-0.91545379
Sept6	0.581116069	Mink1	-0.916735069
Cdh2	0.578147304	Oplah	-0.921030443
Ptprf	0.576460883	Cyfp2	-0.924793134
Fus	0.573856399	Dync1h1	-0.930419488
Igfbp7	0.572914769	Eprs	-0.935425744
Cntnap2	0.57217722	Snx2	-0.942147937
Psmb10	0.569671752	Abca6	-0.944190712

Dtd2	0.569274122	Myo1c	-0.949209098
Thbd	0.565929493	Usp8	-0.951200654
Ctsc	0.556394046	Sec23a	-0.953144496
Btf3	0.555862308	Vars	-0.957636335
Sf3b2	0.552636944	Gbp9	-0.959325638
Lbp	0.550111487	Dip2c	-0.961777763
Hspd1	0.547020019	Rpl18	-0.975585213
Chl1	0.546172621	Rps25	-0.991881897
Col6a3	0.535536496	Prepl	-1.017563503
Dynlt1c	0.533397122	Lrrc47	-1.019070179
Ywhag	0.531965568	Abca8b	-1.025551032
Erp44	0.528410827	Crabp1	-1.051486422
Psmb8	0.524239769	Rabep2	-1.057320336
Calr	0.523986689	Flnb	-1.058048798
Manf	0.523142946	Snx1	-1.080142955
Cdh1	0.511139476	Rpl17	-1.110512961
Etfp	0.510468265	Rpl28	-1.121416353
Rbbp4	0.500970149	Fabp7	-1.126710444
Pa2g4	0.497406517	Eftud1	-1.127139755
Hspa5	0.49661535	Emc8	-1.134002651
Epha2	0.490377451	Ckmt2	-1.134735849
Hexa	0.490233137	Rps23	-1.150415483
Kcnab2	0.488744325	Acly	-1.154042472
Trim28	0.488386176	Ddx1	-1.156319819
Pafah1b1	0.48046684	Atp2a1	-1.179758878
Sfpq	0.466828248	Eif3d	-1.180066587
Ltf	0.447317712	Sec31a	-1.183334972
Ank2	0.440941742	Abca9	-1.22662305
Syn1	0.417909608	Rpl35	-1.255071096
Hspa14	0.394425463	Nf1	-1.280384509
Sept3	0.390704551	Pls3	-1.287506905
Sept8	0.343863876	Lars	-1.296817701
Atp5b	0.31821494	Chadl	-1.309669058
Serbp1	0.313807693	Slc25a4	-1.365891002
Pitpnc1	0.308626721	Rpl35a	-1.458764937
Eno3	0.278017895	Myo5a	-1.468622648
Sept9	0.264743528	Ubash3b	-1.48385343
H2-Q7	0.243703483	Rpl13a-ps1	-1.485344079
Pgam2	0.237862582	Rpl7	-1.51988083
Sept2	0.202951439	Ppie	-1.521660764
Sept5	0.064510847	Thrap3	-1.547803364
Calu	-0.030684751	Actbl2	-1.575297706
Got2	-0.098802109	Rpl21	-1.588313236
Rps15	-0.272505157	Smad2	-1.594233736
Agl	-0.333611938	Rpl18a	-1.835262064
Mybpc3	-0.339623113	Hnrnp1l	-1.879071253

Dync1li1	-0.344718026	Rpl10	-1.903272086
Vdac2	-0.357493944	Rpl8	-1.988433017
Vps52	-0.380118849	Ttn	-2.770178371
Hdgfrp2	-0.391804552	Svip	-3.751553019
Myom2	-0.398311538	Ctsz	-4.271892241

Supplementary file 3.

List of differential expressed axoplasmic proteins in central projection after spinal cord injury.

label	Mean_DCA vs Lam	label	Mean_DCA vs Lam
Ctsz	3.56540782	Ogdh	-0.573661
Tbc1d15	2.6876041	Serpina1d	-0.5770469
Ablim3	1.83477015	Atp1b1	-0.6244634
Pcp4l1	1.73488414	Cndp2	-0.6334101
Rpl8	1.46565357	Trim3	-0.6340729
Ccdc43	1.46090522	Lman2	-0.6407383
Svip	1.11143053	Ckmt2	-0.6418153
Chmp1a	1.10587587	Tmpo	-0.6566509
Chmp3	0.98574285	Elmo1	-0.6605454
Alyref	0.81450943	Dazap1	-0.6646165
Stat5b	0.80208118	Tppp	-0.6666419
Psmc1	0.77605025	Ezr	-0.6679762
Rpl18	0.68402154	Aimp1	-0.6703283
Gm4978	0.6435627	Aldh7a1	-0.6717901
Psmf1	0.62822147	Hspe1	-0.6770718
Mpz	0.61651559	Pfkl	-0.6834427
Rps6	0.61522587	Acp5	-0.7105367
Gnpda2	0.60894839	Spint1	-0.7114785
Birc3	0.56178501	Ptgds	-0.7168077
Rpl6	0.54904497	Rdx	-0.7254503
Rplp1	0.49604171	Slc25a3	-0.7333653
Rps2	0.48431267	Hars	-0.7541913
Psmc2b	0.48093641	Tra2b	-0.7621285
2610002M06Rik	0.41755158	Dnajb1	-0.7735011
Fntb	0.41694713	Gna12	-0.7739069
S100b	0.29768231	Rnf14	-0.7851447
Dnm1	0.0081366	Nsf	-0.887002
Hip1	-0.2569861	Fermt2	-0.9006933
Cul3	-0.3688945	Gars	-0.9041448
Col2a1	-0.4386275	Ugp2	-0.9143234
Pacs2	-0.4538012	Abat	-0.9304452
Epb42	-0.4609538	Pacsin3	-0.9583567
Aco2	-0.4767873	Ccdc50	-0.9654752

Gnao1	-0.4894393	Ddx6	-1.030508
Kctd12b	-0.4993833	Dlst	-1.0532864
Ruvbl1	-0.522961	Aldh2	-1.0835263
Saa1	-0.5267223	Myl10	-1.1485213
Sept6	-0.5579586	Oat	-1.2007672
Serpina1e	-0.5591164	Chid1	-1.3843374
Ltf	-0.5708244	Nsdhl	-1.7470472

Supplementary file 4.

List of differential expressed genes in L4-L6 DRGs after sciatic nerve injury (SNA vs sham

Gene Name	logFC	Gene Name	logFC	Gene Name	logFC
Saa1	3.6646	Slc25a40	0.38037	Lpin2	-0.38641
Cd207	3.6106	Dnttip2	0.37982	Gpr22	-0.38646
Npy	3.2743	Bet11	0.3796	Atp5g1	-0.3867
Cckbr	3.0924	Rab11fip5	0.37921	Sema4b	-0.38676
Ankrd1	2.8735	Pdf	0.37902	Bcr	-0.38691
Fgf3	2.8517	Brd2	0.3785	Gpr137	-0.38806
Sprr1a	2.8037	Bud31	0.37796	Golim4	-0.38806
Serpine1	2.7962	Spsb4	0.37753	Kcnip3	-0.3889
Saa2	2.762	Slc2a3	0.3764	Tpgs2	-0.38955
Gpr151	2.7373	Pfn2	0.37638	Lgi3	-0.38989
Procr	2.7119	Zbtb38	0.37623	Cntn3	-0.39047
Tmem88b	2.7037	Zfand5	0.37586	Scn10a	-0.39076
Atf3	2.6237	Polr3h	0.37584	Top3b	-0.39081
Gadd45a	2.5958	Zfp839	0.37564	Rabac1	-0.39084
Bambi-ps1	2.5725	Agtrap	0.37523	Pfkm	-0.39103
Areg	2.5548	Ppp1r18	0.3745	Grb14	-0.39143
Il6	2.4861	Alyref	0.37416	Spg7	-0.39163
Rin1	2.4657	Spef1	0.37387	Colla2	-0.39208
Serpinb1c	2.4292	Nifk	0.37358	Unc5c	-0.39233
Flrt3	2.3221	C2cd2	0.37331	Pde4dip	-0.3926
Gm5152	2.2192	D11Wsu47e	0.37317	Slitrk4	-0.39276
Slc6a4	2.1806	2610001J05Rik	0.37317	Magi1	-0.39301
Speer4b	2.1109	Zfp874a	0.37289	Cyp2j12	-0.39338
Gfap	2.0953	Hmgcs1	0.37288	Trim3	-0.39385
Mchr1	2.0802	Sys1	0.37274	Lrrtm2	-0.39386
Aim2	2.0233	Srsf5	0.37256	Mvb12b	-0.39454
Sox11	1.9454	Cnbp	0.37202	Mink1	-0.39481
Sema6a	1.9412	Znhit3	0.3716	Atxn2	-0.39485
Chrna5	1.8928	Slc2a1	0.37153	AU040320	-0.39487
Plaur	1.8348	Fgl2	0.37027	Pcyox11	-0.39509
Gm266	1.8008	Sf3b6	0.36985	Fam173b	-0.39527
Pmaip1	1.7775	2010012O05Rik	0.36957	Hdgfrp2	-0.39538

Tehh	1.775	Ccdc38	0.36936	Mpp2	-0.39572
Fst	1.7652	Txnrd1	0.36934	Entpd6	-0.39646
Smim3	1.7564	Nmd3	0.36922	Naa60	-0.39753
Ccl7	1.7491	Chp2	0.36858	Fmn11	-0.39764
Rnd1	1.7438	Lsm14b	0.36849	Ragef2	-0.39775
Ecel1	1.74	Slc16a1	0.36747	Limk1	-0.39814
Igfbp3	1.7395	Rnf181	0.36721	Dip2a	-0.39825
A630023A22Rik	1.7254	Gm16731	0.36719	Nod1	-0.39858
Tnfrsf12a	1.7246	Tfe3	0.36565	4930412C18Rik	-0.39861
Colec10	1.7231	Rnh1	0.36458	Wiz	-0.39882
Gm12250	1.6968	Zfp687	0.36447	Sorcs3	-0.39885
Rasl11a	1.6966	Nptx2	0.36428	Ptprs	-0.39886
Gm4952	1.6868	Lipo1	0.36302	Tom112	-0.39929
Tmc1	1.6597	Trmt10c	0.36281	Pla2g6	-0.3998
Mcoln2	1.6567	Chl1	0.36247	Fam53b	-0.39989
Ano7	1.6325	Slc7a5	0.36218	St3gal5	-0.39992
Pla2g2d	1.624	Tub	0.36198	Plekha6	-0.40018
Bhlhe22	1.6198	Trmt6	0.36161	Igsf8	-0.40038
Steap1	1.5903	Chchd2	0.36154	Dhx30	-0.40068
Gm9905	1.5889	Mettl7a3	0.36136	BC023829	-0.40115
Vash2	1.5886	Tob2	0.3613	Atp1a3	-0.40126
Tpbg	1.5738	Cd1d1	0.36091	Spire2	-0.40181
Sox9	1.5646	Snx10	0.36048	Zbtb20	-0.40193
C230012O17Rik	1.5628	Gesh	0.36038	Mcm3ap	-0.40235
Slfn9	1.5518	Calcr1	0.36021	Ksr1	-0.40244
Oacyl	1.5485	Fastkd3	0.36004	Mrpl44	-0.40261
Adcyap1	1.5298	Zpr1	0.35961	Vps18	-0.40319
Cebpdl	1.5254	Cyb561d1	0.3595	St8sia1	-0.40326
Cited2	1.5251	Tmem41b	0.35949	Rusc2	-0.4034
Ccl12	1.5231	Zfp46	0.3594	Mrps9	-0.40344
Tusc1	1.5147	C1qbp	0.3588	Tesk1	-0.40353
Gal	1.5088	Ythdf2	0.35863	Pitpnm2	-0.40449
Lrrc15	1.5021	Frmd8	0.35845	Pgbd5	-0.40453
Slamf1	1.502	Plp1	0.35839	Gnb2	-0.405
Csf1	1.4986	Sbds	0.35813	Rgs3	-0.40515
Msh6	1.4983	Myo1a	0.35793	Alg1	-0.40594
Uck2	1.497	Cln8	0.35792	Agl	-0.40601
Sectm1b	1.4916	Arf2	0.35791	Btrc	-0.40647
Trim15	1.4811	Etf1	0.35772	Stard9	-0.40752
Ccl8	1.4801	Hoxb5	0.35709	Usp54	-0.40757
Stmn4	1.4686	Pdcd5	0.3563	Zfp286	-0.40776
Frat2	1.461	Crebzf	0.35611	Ints3	-0.40785
Phlda1	1.4578	Cspg5	0.3561	Chd2	-0.40785
Itpr1	1.4564	Cnst	0.35586	Ubr4	-0.40806
Serp1b1a	1.4273	Ttyh1	0.35478	Tep1	-0.4087
Saa3	1.4177	Pla2g3	0.35471	Acaa2	-0.40902

A930012O16Rik	1.4166	Rab8b	0.35454	Mgat4a	-0.40914
Srxn1	1.4124	Hoxb9	0.35448	Nim1k	-0.40925
1700084C01Rik	1.408	Rps2	0.35444	Gsn	-0.40945
Lrrc10b	1.4078	Aph1a	0.35422	Focad	-0.40978
Lmo7	1.4056	Rhov	0.3535	Ttll5	-0.40985
Star	1.3918	Nop14	0.35334	Glg1	-0.41049
Satb2	1.3858	Dazap1	0.35333	Pi4ka	-0.41077
Tifa	1.3696	Csrnp2	0.35308	Ank2	-0.41135
Zfp367	1.3586	Zfand2a	0.35305	Phactr1	-0.41172
Gm4841	1.3585	Pgp	0.35247	Cd97	-0.41239
Sez6l	1.3567	Pkd1l3	0.35134	Mrpl4	-0.41282
E130012A19Rik	1.3509	Impdh2	0.34997	Gdpd5	-0.41283
AW011738	1.3459	Slc39a14	0.34988	Crip2	-0.41295
Mir17hg	1.3356	Nip7	0.34961	Tenm1	-0.41342
Olf920	1.3349	Cdk4	0.34937	Dzip1	-0.41356
Creb3l4	1.3343	Rnf11	0.34912	Pfk1	-0.41391
2310039H08Rik	1.3159	Bbs5	0.34888	6430573F11Rik	-0.41447
Fhad1	1.3059	Col16a1	0.34844	Cys1	-0.41456
Iigp1	1.2967	Pdpn	0.34831	Ncor1	-0.4149
Dancr	1.2938	Tsc22d1	0.34818	Iqsec2	-0.41588
C1qtnf9	1.2866	Cstf2t	0.34808	Agk	-0.41623
Fam227a	1.2841	Snip1	0.34777	Nxpe3	-0.41644
Adam8	1.2668	Scyl3	0.34763	Dock3	-0.41668
Jun	1.264	Rprm	0.3476	Clstn3	-0.41686
Mmp16	1.2636	Lrig1	0.34754	Map2k2	-0.41689
Ifi205	1.2578	Ehd1	0.34742	St5	-0.41695
Rnf122	1.2576	Tmem167b	0.34738	Klhl32	-0.41749
Txk	1.2543	Slc37a1	0.3473	Rbfox3	-0.41765
Ikzf4	1.2526	Nmi	0.34691	Fam149a	-0.4179
Hao1	1.2517	Gm12352	0.34683	Rgs11	-0.41817
BC023105	1.2475	Pfkfb3	0.34672	Hrasls	-0.41827
Ifit1	1.2388	Rnd3	0.34671	Ap2a1	-0.41849
Timp1	1.2321	Gm17130	0.34645	Ip6k1	-0.4186
Socs3	1.2219	Utp3	0.34633	Ten2	-0.41867
Ell3	1.218	Amd1	0.34626	Ccm2	-0.41916
Shisa9	1.2173	Arpc2	0.34606	Rasgrp1	-0.41963
Mex3a	1.217	Hn1	0.3458	Fryl	-0.41975
Rgs20	1.2091	Nudt16	0.34553	Elmod3	-0.4198
2810408A11Rik	1.2035	Tgfa	0.34508	Fbxw7	-0.42011
Col6a5	1.2031	Cox18	0.34464	Zdhhc8	-0.42021
Tmem184a	1.1999	A330050F15Rik	0.34463	Acad11	-0.42117
Spag8	1.1842	Csnk1g3	0.34381	Sema7a	-0.42145
Camk1	1.1816	Insig1	0.34352	Rnf216	-0.42163
Ifi204	1.1677	Mat2a	0.34309	Gramd1b	-0.42203
Zfp772	1.1662	Fam171b	0.34298	Fars2	-0.42209
Tubb6	1.1633	Ifitm3	0.34239	Gpr26	-0.42219

Rassf10	1.1623	Fam136a	0.34146	Ndufv3	-0.42225
Mstn	1.1616	Rab31	0.34138	Fam126b	-0.42226
Qrfpr	1.1597	Mief1	0.34109	Dis3l2	-0.42303
2010003K11Rik	1.1551	Gas5	0.34078	Sssca1	-0.42311
Foxd3	1.1542	Mageh1	0.34008	Ralgapb	-0.42318
Liph	1.1536	Spcl1	0.33998	Myo1d	-0.42342
AA987161	1.1529	Klf16	0.33997	Zmiz2	-0.42358
Chac1	1.1434	Daxx	0.33971	Erc1	-0.42402
Bex4	1.1395	Ppp1r15b	0.33934	Mpst	-0.42424
Ch25h	1.1368	Mcur1	0.33897	Fbxo41	-0.42477
Gm15035	1.1363	Bak1	0.33845	Gas6	-0.42493
Sox7	1.1347	Zxdc	0.33831	Ift172	-0.42533
Fosl1	1.1345	Akirin1	0.33824	Gm5069	-0.42535
Mx1	1.1342	Abhd5	0.33734	Fam98c	-0.42565
Gm14273	1.1291	Nufip1	0.33705	Fntb	-0.42567
Arc	1.1282	Fem1c	0.33668	Acaca	-0.42586
Rras2	1.1245	Nr2c2ap	0.33637	Abcb8	-0.42612
Tph1	1.1229	Arl6ip1	0.33623	Mrpl45	-0.42724
A730056A06Rik	1.1113	Rela	0.33569	Ptov1	-0.42742
Gm14057	1.1124	Swsap1	0.33557	Lrrc49	-0.42836
Tuba1c	1.1106	Sfrp1	0.33535	Med24	-0.42858
Shh	1.1086	Gtf2a1	0.33507	Ephx1	-0.42878
Snhg1	1.1076	Hspa5	0.33482	Ctnnb1l	-0.42925
Csrnp1	1.106	Rab33b	0.33403	Eya3	-0.42945
Nfil3	1.1029	Rnf44	0.3334	Ubap2	-0.42948
Fam111a	1.1026	Pa2g4	0.33324	Abtb2	-0.42956
Itgae	1.0995	Cdyl	0.33323	Fibin	-0.42964
Tmem43	1.0931	Gtpbp2	0.33275	Huwe1	-0.42985
Btnl5-ps	1.0914	Pag1	0.33138	Gfod1	-0.42996
Dnajb3	1.0882	Gm16279	0.33133	Ciz1	-0.43023
Mycn	1.0834	Ddx10	0.33049	Fxyd7	-0.43028
Klf6	1.0827	Polr1e	0.33018	Pdcd11	-0.43063
Mboat4	1.0757	Rpl12	0.32986	Tenm2	-0.4309
Serpinb5	1.0754	Naa25	0.32961	B230217O12Rik	-0.43092
Tmem74b	1.074	Pvrl3	0.32951	Gm17029	-0.43098
Rasef	1.0704	Ube2g1	0.32915	Fxr2	-0.43101
Gm26708	1.0683	Phf23	0.32893	Slc6a17	-0.43123
Mx2	1.0659	Tmx1	0.32893	Ambra1	-0.43155
Rhoq	1.0606	Prkab2	0.32885	Mtcl1	-0.43169
Ppp1r36	1.0593	Nudt4	0.32817	Tmem150b	-0.43258
Glis3	1.0591	Pnrc2	0.32752	Ap1b1	-0.43266
Kctd11	1.058	Itgb1	0.32698	Kenq5	-0.43286
Mex3d	1.0579	Ahcy	0.32632	Frs3	-0.43314
Usp18	1.0578	Rasgrf2	0.32577	Pkd1	-0.43388
Slc44a5	1.0564	Ebp	0.32535	Tcf20	-0.43432
Exoc3l2	1.0556	Ube2e1	0.3253	Inadl	-0.43433

Rps19-ps3	1.0538	Jak2	0.32512	Hertr2	-0.43461
5330438D12Rik	1.0533	Atf5	0.32453	Atp13a2	-0.43489
Cdt1	1.0531	Ofd1	0.32428	Slc19a1	-0.43502
Cd14	1.0522	Zbtb33	0.32425	Csnk1g2	-0.43526
Cebpb	1.0519	Samhd1	0.32418	Pigo	-0.43547
Mocs3	1.0437	Rab39	0.32409	Eml2	-0.43593
S1pr2	1.039	Syt12	0.32359	Pomt1	-0.43636
Higd1b	1.0371	2810403A07Rik	0.32347	Mad111	-0.43637
9230105E05Rik	1.0338	Tdg	0.32302	Lrp1	-0.43668
Dusp1	1.0337	Sqle	0.32285	Sbf2	-0.43679
Fcgr1	1.0322	Set	0.32274	Lamtor4	-0.43694
Gm12976	1.0321	Cars	0.32266	Fxyd2	-0.437
Ifrd1	1.0316	Caprin2	0.32258	Sfswap	-0.43739
Myc	1.0288	Anp32b	0.32196	Sh2d3c	-0.43787
Prr15	1.0271	Tmem79	0.32195	Tenc1	-0.43793
Dnali1	1.0225	Srp14	0.32186	Srrm2	-0.43824
Casp6	1.0212	Tax1bp3	0.3216	Aco2	-0.43902
2700046G09Rik	1.0176	P4ha3	0.32115	Rgs8	-0.43911
Ip6k3	1.0164	Zfp37	0.32026	Acsbg1	-0.43937
Zbp1	1.0138	Ddx3x	0.32017	Grin1	-0.43939
Fam210b	1.0088	Cdv3	0.31931	Slco5a1	-0.43993
Bhlhe41	1.0055	Gm16973	0.31834	Cad	-0.43998
Pim1	1.005	Itgb8	0.31809	Pigz	-0.44021
Rsad2	1.0045	Fam129b	0.31798	Vstm2a	-0.44058
Nts	1.002	Taf7	0.31766	Cntnap4	-0.4407
Arid5a	0.99339	Clic1	0.31762	Prrg1	-0.44174
Ptgdr2	0.99107	Med8	0.31683	Stk32c	-0.44175
Frmd8os	0.98739	Pex5	0.31672	Zswim8	-0.44177
Fam60a	0.98527	Hspa12b	0.31669	Cryab	-0.44249
Fosl2	0.98188	Klhl21	0.31639	Hcn3	-0.4435
Gm16277	0.97971	Rchy1	0.31636	Ache	-0.4436
Zfp697	0.963	Tysnd1	0.31559	C2cd3	-0.44375
Ccdc96	0.96069	Tyw5	0.3155	Asic1	-0.4439
St6galnac4	0.96012	Gm26631	0.3155	Gne	-0.44398
Sdc1	0.95662	Calml4	0.3154	Wdr4	-0.44502
Gm26617	0.95484	Usp38	0.31524	Ap2b1	-0.4454
Gm4425	0.95342	Nt5e	0.31399	Exoc4	-0.4467
Tes	0.95107	Dnajc2	0.31389	Trim45	-0.44693
Ppp1r3d	0.95053	Siah1a	0.31386	Pigb	-0.44721
Cd3eap	0.94932	Rgag4	0.3131	Pnpla6	-0.44832
Mir22hg	0.94275	Brat1	0.31183	Mgat1	-0.44854
Kank4os	0.94137	Ypel5	0.31085	Lrrc16b	-0.44958
Ets2	0.94047	Abcb10	0.31067	Amph	-0.4496
Sap30bpos	0.93944	Prr13	0.31064	Arhgap24	-0.45207
4930455G09Rik	0.93832	Zfp251	0.31028	Hivep1	-0.45218
Gm715	0.93512	Gnai3	0.31006	Sipa111	-0.45262

Epb4.114a	0.93466	Bmi1	0.3099	Tmem131	-0.45307
Tmem30b	0.93392	Ccdc174	0.30966	Svop	-0.45308
Gm13483	0.93354	Psma4	0.309	Pacsin1	-0.45323
Fam110a	0.932	Tlcd1	0.30899	Dcakd	-0.45375
Npy1r	0.93182	Suv39h1	0.30883	Abcc5	-0.45379
Ugdh	0.93167	Wipfl	0.30849	Caskin1	-0.45398
Lrtm2	0.93137	Lrrc47	0.30844	Abcb4	-0.45414
E230013L22Rik	0.93085	07-Mar	0.30826	Car10	-0.45434
Lce6a	0.93085	Pak1ip1	0.3082	Slc10a7	-0.45469
Marcks11	0.92834	Serinc5	0.30816	Iglon5	-0.45489
mt-Tt	0.92795	Apex1	0.30815	Nat9	-0.45548
Zbtb42	0.92707	Fxyd3	0.30808	Fchsd1	-0.45552
Gm20204	0.92554	Slc35e3	0.30743	B3galt1	-0.45614
Gm14866	0.92378	Srp9	0.30649	1700071M16Rik	-0.4564
Usp27x	0.92271	Ii10rb	0.30644	Atg101	-0.45647
Fam181b	0.92184	Rmnd1	0.30596	Depdc5	-0.45746
Arhgef15	0.92168	Mien1	0.30583	Mrgprd	-0.45909
Aif1	0.92081	Rraga	0.30476	Gm11739	-0.45938
Dnah10	0.91754	Fbxw11	0.30387	Fgf9	-0.45941
Gm15743	0.91754	Sdccag3	0.30334	Etfb	-0.45981
Vgf	0.91623	Pfn1	0.30302	Gm12371	-0.46017
Slc29a2	0.91613	Clpx	0.30272	R3hdm2	-0.46078
Pvr	0.91407	Plod3	0.30247	Thop1	-0.46103
F630040K05Rik	0.9115	Slc36a4	0.30229	Med25	-0.46146
Gm15655	0.90799	Necap2	0.30166	Gprc5c	-0.46151
1700109H08Rik	0.90372	Snapc2	0.30138	Galnt10	-0.46157
Tet3	0.90362	Golt1b	0.30116	Ccl27a	-0.46178
Gm16093	0.90311	Dr1	0.29942	Coro1a	-0.4621
4632434I11Rik	0.90176	Ano6	0.29927	Rnf32	-0.4623
Shisa2	0.90174	Cdr2	0.29871	Abcd2	-0.46258
Oasl1	0.90004	Rwdd2b	0.29833	Ube2o	-0.46271
Zfp36	0.89981	Dnajc7	0.29822	Rxrg	-0.46276
Irx3	0.89801	Dcaf10	0.29776	Fam73b	-0.46305
Mapkbp1	0.89621	Grk6	0.29766	Gpr162	-0.46319
9130230N09Rik	0.89404	Pde12	0.29737	Tesc	-0.46433
Gm10638	0.89261	M6pr	0.29725	Nol4	-0.46475
Smad1	0.89158	Eif4e2	0.29702	Ntng1	-0.46519
Itpkc	0.89069	05-Mar	0.29676	Arhgap27	-0.46548
Midn	0.88992	Abce1	0.29654	Bcl7c	-0.46582
Otud1	0.88979	Pigm	0.29562	Tab1	-0.466
Sik1	0.88807	Hnrnpf	0.29467	Angell1	-0.46623
Irgm1	0.8879	Pop4	0.29435	Tceal3	-0.46715
Gm16034	0.88696	Xbp1	0.29425	Eepd1	-0.46745
Fndc4	0.88579	Tmem120a	0.29318	Arhgef4	-0.46748
Akr1b8	0.88536	Pgam5	0.29317	Ar	-0.46778
Hmgb3	0.88439	Dnajb9	0.2927	Slc6a11	-0.4686

Gm15050	0.88426	Mrto4	0.29207	Gna12	-0.46892
Tnfrsf1b	0.88357	Htra2	0.29147	Hs3st2	-0.46893
Trib1	0.88318	0610031J06Rik	0.29142	Srprb	-0.46919
Coil	0.88312	Rab23	0.29135	Sirt3	-0.4693
Srrm4os	0.87978	Cltb	0.29111	Parm1	-0.46995
Sepn1	0.8771	Zrsr2	0.29057	Zfp423	-0.4704
Gfra1	0.87444	Tspyl1	0.28951	Cadm3	-0.47136
Sh3bp2	0.87295	Larp1b	0.28897	Usp20	-0.4719
Hoxa4	0.86968	Crot	0.28855	Setd1a	-0.47212
Lgals3	0.86703	Gm26649	0.28817	Brsk1	-0.47236
Tnfrsf10b	0.86574	Zfp451	0.28808	Ttc3	-0.47266
Gadd45g	0.86463	Psme2	0.28801	Armc9	-0.47298
Gpr119	0.86328	U2af1	0.28785	Prlr	-0.47309
Ell2	0.86174	Pik3cb	0.28777	Vgll4	-0.47328
Gm14257	0.85961	Gm14325	0.28721	Mgrn1	-0.47346
Ccr5	0.85741	Nme1	0.28692	Epyc	-0.47404
Cx3cr1	0.85628	Sh3glb1	0.28655	Dagla	-0.47438
Tgif1	0.85623	Ldhd	0.28652	6430571L13Rik	-0.47529
Lrat	0.85595	Zc3h7a	0.28589	Fbln7	-0.47534
Nabp1	0.85328	Fam76a	0.28584	Tpcn1	-0.47603
9330160F10Rik	0.85151	Hdgf	0.28582	Hdac5	-0.47621
Gm13688	0.85092	Iars	0.28556	Pgf	-0.47625
Stx11	0.85051	Nhp211	0.28542	Cntfr	-0.47662
Mafb	0.84996	Tapbp	0.28536	Cacng5	-0.47703
Kcne3	0.84989	Wdr43	0.28483	Prune2	-0.47746
Tnip2	0.84907	Ufd11	0.28476	Ror2	-0.4775
A130051J06Rik	0.84903	Exoc5	0.28436	Tdp1	-0.47768
Gm26643	0.84747	Akirin2	0.28427	Cacna2d2	-0.47794
Ier5	0.83846	2410004B18Rik	0.28406	Gfra2	-0.47811
Bach1	0.83659	Mib1	0.28366	Apc2	-0.47928
Gm11549	0.83608	Basp1	0.28335	Nsf	-0.47933
Gm16170	0.83429	Abhd17c	0.28207	Bmpr1b	-0.4795
Gm3510	0.83429	Tnfrsf21	0.28153	Cdk2ap2	-0.47998
Avpr1a	0.83227	Ric8	0.28141	Plekhf1	-0.4807
Fgf4	0.83217	Camk2n2	0.28101	Mta3	-0.48085
Fcnb	0.83109	Cdc42ep2	0.28019	Tmco6	-0.48129
Gm15756	0.83063	Mob1b	0.2801	Clstn1	-0.48154
Galnt6	0.83049	Cinp	0.27971	Ubac2	-0.4817
Gpr3	0.82853	Gars	0.27946	Dock6	-0.48178
Gm7534	0.82745	Nsg1	0.2784	Mrgpra2b	-0.48346
Pklr	0.82653	Rbm43	0.27794	Epb4.1	-0.4837
Adamts1	0.8262	Myo1h	0.27783	Larp6	-0.48381
Slc25a24	0.82556	Klf13	0.27772	Pld3	-0.48476
Cd63	0.82418	Csgalnact1	0.27713	Prrxl1	-0.48485
Tm4sf1	0.82295	Lrrc8a	0.27671	Bcas3	-0.48654
Pre1	0.8224	Se5d	0.27633	Actn4	-0.48657

Cd44	0.8212	Sgtb	0.27632	Ablim2	-0.48688
E130317F20Rik	0.8182	Sav1	0.27585	Gsg11	-0.48727
Gabra5	0.81817	Serp1	0.27573	3110056K07Rik	-0.48768
Ifi44	0.81683	Las11	0.27558	Epha7	-0.48779
Hist1h1d	0.81376	Hax1	0.27529	Cachd1	-0.48806
Lck	0.81376	Ogfr	0.27524	Polr1a	-0.48825
Scpep1os	0.81353	Stam	0.27497	Jdp2	-0.48881
Cdkn1a	0.8134	Srsf3	0.27458	Tmc3	-0.48918
Scpep1	0.81303	Kitl	0.27417	Mapre3	-0.48926
Mex3b	0.81289	Csdc2	0.27261	Phgdh	-0.4895
Dbp	0.81191	Osbpl8	0.27246	Vwa5b2	-0.4898
Dusp7	0.81183	Srsf6	0.27242	Plekha4	-0.48997
Tas1r3	0.81044	Zfp110	0.27197	Ppp1r12b	-0.49026
Soat2	0.81024	Tubb2b	0.27173	Atp9b	-0.49039
Ptp4a1	0.80828	Gnl3	0.27139	Numa1	-0.49208
Fos	0.80798	Trp53inp2	0.27122	Aifm3	-0.49235
Ccl2	0.80718	Gpsm1	0.27118	Rps15	-0.49369
Fjx1	0.80648	Trappc5	0.27037	Apba2	-0.49417
Itk	0.80274	Dek	0.27002	Pde4d	-0.49596
Gm20496	0.80184	Tspyl2	0.26977	Phka2	-0.49607
Vangl2	0.80105	Bdh1	0.26921	Kcnh7	-0.4963
Csf2rb2	0.80091	Pank2	0.26905	Strada	-0.49685
Gm14446	0.80075	Trp53inp1	0.26889	Cnpy3	-0.49693
Cyp1b1	0.80058	Dvl1	0.26874	Deaf1	-0.49697
AI467606	0.79822	Fam115a	0.26848	Mcrs1	-0.49751
Rtp4	0.79671	Wdr77	0.26829	Gm16172	-0.4977
Wnt5b	0.79619	Nras	0.26783	4930452B06Rik	-0.49834
Gm9866	0.78996	Dhx32	0.26768	Pias4	-0.49877
Draxin	0.7899	Triap1	0.26764	Cystm1	-0.49888
Gm17711	0.78878	Rock2	0.2674	Hecw1	-0.4991
Il17ra	0.78823	Stx12	0.26723	Kif19a	-0.49952
Inca1	0.78705	Erc2	0.26698	Dgkz	-0.49956
Gm13846	0.78666	Tmem129	0.26623	Micu1	-0.50041
Itga7	0.7859	Ube2i	0.2659	Smarca4	-0.50099
Fam196a	0.78433	Ttc39c	0.26586	Creb311	-0.50129
4833418N02Rik	0.78335	Gorasp1	0.2657	Pde4a	-0.50159
Nrip1	0.78297	Lhfpl2	0.26551	Kcnj12	-0.50191
Fads3	0.78098	Zfp954	0.26522	Herc2	-0.50273
Tmem98	0.78044	Ube2d1	0.26458	Plcb3	-0.5028
Hdx	0.78001	Dgkq	0.26445	Mab2112	-0.50293
Btg2	0.77928	Tmcc3	0.26425	Ednra	-0.50379
Abca1	0.77891	Nbea	0.26405	Tnrc6b	-0.50429
Casp3	0.77764	Ran	0.26392	Wasf3	-0.50453
Bdnf	0.77761	Clic4	0.26363	Cnnm1	-0.50469
Wisp1	0.77696	Seh11	0.2632	Mertk	-0.50491
Igtp	0.77637	Fam32a	0.26283	Rail	-0.50498

Ccdc60	0.77586	Eif1ad	0.26254	Rap1gap	-0.50512
Myo19	0.7742	Fam124a	0.26231	Dpp6	-0.50547
Myadm	0.7738	Ptp4a2	0.26122	Det1	-0.50579
Nmnat3	0.77228	Tbl1xr1	0.26086	Cnih2	-0.50612
Arl16	0.77016	Samd10	0.2608	Chd6	-0.50623
Zbtb46	0.7691	Snupn	0.26047	Pik3r2	-0.5063
Azin1	0.76879	Mex3c	0.26	Pak4	-0.50658
Pkib	0.76863	Zfp639	0.25946	Isl2	-0.50732
Mrfap1	0.76636	Mrps7	0.25942	Arhgap35	-0.50749
Prkcdbp	0.76612	Ctdsp2	0.25837	Otoa	-0.50821
Pik3cg	0.76585	Nceh1	0.25829	Fam20a	-0.50824
Tmem173	0.76499	Slc17a6	0.25808	Kcnn2	-0.51064
Rasd1	0.76301	Cmip	0.25788	Dos	-0.51144
Zfp655	0.76197	Fbxl3	0.25726	Olfm2	-0.51205
Scd4	0.76184	Lgi4	0.25703	Robo1	-0.51213
Msr1	0.75951	Nlgn2	0.25678	Ank1	-0.51216
Phox2a	0.75951	Psmc4	0.25635	Kcnn2	-0.51226
C230021G24Rik	0.75705	Trim35	0.25598	Brinp2	-0.51239
Gpr19	0.75554	Cnot6	0.25488	Gtf3c1	-0.51246
Clec4n	0.75336	Schip1	0.25465	Mroh1	-0.51319
Crem	0.7526	Fnde3a	0.25384	Luzp1	-0.51373
Adora2b	0.75194	Samd8	0.25369	Eml6	-0.51419
Atg9b	0.75189	Hnrnpu	0.25336	Trrap	-0.51467
Ms4a6d	0.7516	Efnal	0.25319	Lmln	-0.51533
Fbxl22	0.74994	Zmat2	0.25256	Scaf1	-0.51536
A630052C17Rik	0.74964	Dclk1	0.25238	Tomm40	-0.51537
Btg1	0.74856	Gtpbp4	0.25213	Ubl7	-0.51541
Acpt	0.74799	Psme4	0.25146	Krba1	-0.51567
Eif5	0.7465	Eif3b	0.25141	Urgcp	-0.51691
Apln	0.74555	Nus1	0.25136	Mbp	-0.51732
Gm15706	0.7428	Psmd8	0.25071	Mark2	-0.51864
Gpr85	0.74268	Gna13	0.25023	Calhm2	-0.5194
Pou3f1	0.74159	Psme3	0.25019	Fn1	-0.51946
Gm12346	0.73926	Glul	0.24979	P4htm	-0.52081
Ppp1r15a	0.739	Rer1	0.24968	Sesn3	-0.52087
Gnpnat1	0.73857	Tcta	0.24915	Gaa	-0.52136
Odc1	0.73854	Sdcbp	0.24858	Ckb	-0.52155
Mesdc1	0.73798	Ssr3	0.2482	Agap3	-0.52188
Best1	0.73781	Adam19	0.24814	Trpc4ap	-0.52191
Slc7a3	0.73633	Map1lc3b	0.24772	Otud3	-0.52242
Fadd	0.73594	Thumpd1	0.24711	Rnf166	-0.52313
Cish	0.73578	Stk16	0.24709	Mt3	-0.5236
Zfp36l2	0.73438	Cops5	0.24671	Il16	-0.52383
Mrgbp	0.73429	Fuca2	0.24645	Ndufa11	-0.52387
Cbx2	0.73134	Zdhhc2	0.24466	Olfm3	-0.52423
Pde7a	0.72986	H2-D1	0.24461	Sptbn5	-0.52445

Gm7340	0.72747	Cebpg	0.24449	Penxl2	-0.5247
Parp16	0.72329	Aen	0.24434	Xylt2	-0.52591
Gm4285	0.72174	Epc2	0.24425	Eya2	-0.52592
Plin2	0.72008	Vstm5	0.24384	Tubg1	-0.52762
Gem	0.71914	Haus2	0.24315	Adgb	-0.5292
Gm5531	0.71762	Tmem168	0.24272	Podxl2	-0.5299
Galnt3	0.71761	Rbpj	0.24261	Esrrg	-0.53152
Kcnmb4os2	0.71581	Ldlr	0.2421	Rbks	-0.53223
Nlrc5	0.71479	Ppp1cb	0.24166	Ncdn	-0.53281
Rsad1	0.71146	Oxsr1	0.24142	Cc2d1a	-0.53342
Tmem159	0.71093	Psm12	0.24066	Tagln3	-0.53366
Rrs1	0.70989	Lin7c	0.24027	Nup214	-0.53375
Mareks	0.70962	Bod1	0.24002	Hsf1	-0.53398
Gm12043	0.7095	BC017643	0.23987	Gm16755	-0.53456
Tnik	0.70875	Rae1	0.23947	Sf3a2	-0.5346
Trib3	0.70538	Ist1	0.23911	Srsf4	-0.53472
Dok5	0.7047	Ctnn	0.23692	Ren3	-0.53534
Zfp784	0.7045	Sec22b	0.23691	Gm26840	-0.53582
Slc26a8	0.70297	Tiparp	0.23643	Stim1	-0.53587
Gnpda2	0.70213	Esf1	0.23625	Col9a2	-0.53621
Aim1	0.70051	Klhl7	0.23586	Skor2	-0.53675
Pxdc1	0.70047	Arl6ip5	0.23541	Mst1r	-0.53866
Gbp3	0.69965	Vps4b	0.23534	Fndc5	-0.53967
Rbm15b	0.69779	Dnajb6	0.23513	B3galt5	-0.54002
Mapk6	0.69709	Tbc1d19	0.2342	Hs3st1	-0.54025
Klf10	0.69536	Ptpn12	0.23376	Omg	-0.54077
4930586N03Rik	0.69465	Cnppd1	0.23338	Lamb2	-0.54094
Hotairm1	0.69395	Mapk14	0.23173	Nwd2	-0.54098
Il13ra1	0.69166	Tagln2	0.23115	Myh10	-0.54287
Dgat1	0.69139	Plaa	0.23108	Chd5	-0.54311
C5ar1	0.68799	Impact	0.23099	Mapk8ip3	-0.54476
Il1r1	0.68774	Rbm18	0.23079	Slc27a3	-0.54491
Hr	0.68744	Sap30bp	0.23054	Dclk2	-0.54535
Heca	0.68562	Eif5a	0.2304	Zmat5	-0.54589
Btbd19	0.68529	Bmpr1a	0.23039	Rasgrp4	-0.54629
Man1a	0.68479	Acat2	0.22916	Rhbdd3	-0.54635
Mir3082	0.68339	Kat5	0.22905	Slc25a29	-0.54636
Parp3	0.68294	Tor1aip2	0.22531	Rasgrf1	-0.54672
Uck2	0.68033	Cnih4	0.22461	Hip1	-0.54699
Gm10762	0.68026	Ndr2	0.22257	Bcl2l1	-0.54707
Fhl3	0.68025	Ugcg	0.22197	Apol8	-0.54837
D3Bwg0562e	0.68009	Surf4	0.22166	Gm26673	-0.54871
Lat2	0.67955	Ttc19	0.22135	2810455O05Rik	-0.54882
Wnt5a	0.67944	Ppef1	0.21961	Arhgef1	-0.54892
A730085K08Rik	0.67884	Tpm3	0.21891	Atp8a2	-0.54935
Tmig1	0.67778	Cd59a	0.21839	Tmem143	-0.54944

Gm9962	0.67761	Nude	0.21769	Fsd1	-0.54998
Fam107b	0.67628	Tspan13	0.2176	Dcaf4	-0.55257
Dynlt1f	0.67494	Tpd52l2	0.21691	Chst12	-0.5526
Gbp2	0.6741	Rala	0.21683	B3gat1	-0.55265
4930500J02Rik	0.67175	Chmp7	0.21602	Pkn1	-0.55277
Acvr1	0.67114	Tbc1d20	0.21589	Cables1	-0.55316
Zxdb	0.67016	Cry2	0.21543	Chrm2	-0.55363
Pthlh	0.6686	Men1	0.21407	Nup188	-0.55453
Geh1	0.66841	Naa35	0.21385	Gmpr	-0.5562
Tepp	0.6683	Rars	0.21277	Armc6	-0.55639
Plcd1	0.66788	Stard4	0.21247	Ogdh	-0.55642
Dffb	0.66659	Atad1	0.21241	Ncln	-0.55659
Mafk	0.66523	Ppp2cb	0.21099	Baiap2l1	-0.55703
Hnrnpa0	0.66377	Sms	0.2104	Chrna6	-0.5574
Fkbp1	0.66276	Slc25a46	0.21014	Pnpla7	-0.55794
Slc41a2	0.66209	Asns	0.21001	Cox10	-0.55812
Chst2	0.66195	Ythdf1	0.20915	Lurap11	-0.5587
Irf7	0.66176	Wdr26	0.20775	Raly	-0.55921
Cmtm3	0.65954	Vps26a	0.20452	Adap1	-0.55931
H2-Q4	0.65931	Rac1	0.20237	Kndc1	-0.55939
Pip5k1l	0.65926	Ormdl3	0.20132	Etv1	-0.55982
Gm26894	0.65784	Sumo3	0.1978	Hmha1	-0.56105
Rhoc	0.65784	Map6	0.19759	Asphd2	-0.56282
Rcc1	0.65783	Atp6v0b	0.19646	Dapk2	-0.5629
Plek2	0.65691	Arl8a	0.19447	Vps72	-0.5649
Bend5	0.65446	Zdhhc3	0.19422	Myo1e	-0.56564
Snhg3	0.65412	Eif3g	0.19143	Mbd3	-0.5665
Fam53c	0.65398	Tmem65	0.18997	Evl	-0.56722
Nt5dc2	0.65314	Nek9	-0.19648	B3gnt1l	-0.56864
Hhip12	0.65101	Nqo2	-0.20037	Psd	-0.56892
1700016P03Rik	0.65006	Cyhr1	-0.20471	Polr2f	-0.56924
Ube2q2	0.65003	Fam120b	-0.20474	Tsfm	-0.56937
Nkain1	0.64897	Coa5	-0.20544	Uaca	-0.56976
Prkab1	0.64817	Exoc3	-0.20548	Gm16754	-0.57017
Arhgap42	0.6481	Fam114a2	-0.20894	Kif21b	-0.57032
Pigf	0.64802	Ldb2	-0.21048	Rps26	-0.57035
Bloc1s4	0.64579	Cbx5	-0.21112	Shank1	-0.57144
B230219D22Rik	0.64395	Amz2	-0.21213	Slc9a5	-0.57154
Plekho1	0.64355	Phtf1	-0.21373	Ankrd55	-0.57175
Ccdc162	0.64275	Cc2d1b	-0.21519	Camta2	-0.57238
Carhsp1	0.64197	Evi5	-0.21721	Ndufa8	-0.57255
Gp1bb	0.64189	Rhobtb2	-0.22097	Slc25a10	-0.57292
Gpr133	0.64161	Gyg	-0.22257	Rhbdf2	-0.57338
Ccdc711	0.64158	Osbp19	-0.22366	Chchd10	-0.57358
Gm24082	0.64149	Stoml2	-0.22413	Ldhb	-0.57415
Tnfaip6	0.6388	Bad	-0.22523	Fkbp5	-0.57466

Ggct	0.6385	Brsk2	-0.22613	Tmem205	-0.57476
Tlcd2	0.63754	Atg4b	-0.22637	Lingo1	-0.57504
St6galnac2	0.63752	Cox15	-0.22838	Ragef5	-0.57535
Zfp583	0.63748	Hdac11	-0.22851	Galnt5	-0.57544
Cers6	0.63688	Lrp3	-0.22884	Rbck1	-0.57626
Egr2	0.63486	Akt2	-0.23055	Nup210	-0.57703
Gm17300	0.63442	Mgat4b	-0.23088	Mrgpra3	-0.57714
Srrm4	0.63382	Rgl1	-0.23126	Arhgef11	-0.57755
Hist1h1c	0.63362	Nbl1	-0.23218	Itgb4	-0.57765
Ly6a	0.63292	Smarca2	-0.23284	Tbc1d31	-0.5784
Abracl	0.63251	Tubgcp4	-0.23292	Aip	-0.57848
Fam214b	0.6322	Trak1	-0.2336	Bnc2	-0.57862
AA414768	0.63177	Ndr3	-0.23377	Myadml2	-0.57932
Kif22	0.63094	Usp25	-0.23481	Mgp	-0.57945
Tnk1	0.62994	Btbd3	-0.23521	Prdm10	-0.57984
Gm26880	0.6292	Lipa	-0.23562	Syk	-0.58008
1700019G17Rik	0.62843	Tmcc2	-0.23765	Lrrc45	-0.58026
Glipr2	0.6274	Ptprf	-0.23812	Palm	-0.58028
Gm13033	0.6268	Rims1	-0.23822	Mif	-0.58073
5430417L22Rik	0.62662	Arsb	-0.23823	Dapk3	-0.58209
Rab35	0.62625	Hexa	-0.2384	Zfp804a	-0.58226
Zfp580	0.626	Dpp10	-0.23857	Agap2	-0.58286
Syt4	0.62599	Opa1	-0.24033	Dtnb	-0.58342
Psmb8	0.62533	Inf2	-0.2408	Tmem180	-0.58348
Atf4	0.62463	Gnai1	-0.2411	BC005764	-0.58413
Gm26879	0.62426	Arhgef9	-0.24128	D630003M21Rik	-0.58432
Adamts8	0.62274	Sppl3	-0.24264	Pcx	-0.58481
Atp1b2	0.62273	Atrn	-0.24388	Gm26702	-0.58657
Parp9	0.62267	Kcnmb1	-0.24438	Herc1	-0.58722
2410006H16Rik	0.62182	Gba2	-0.24476	Cdh18	-0.58811
Rnf19b	0.62143	Ngfr	-0.24554	Gria2	-0.58973
Gjb2	0.62009	Frm4a	-0.24571	Gm15800	-0.58992
Gm8773	0.6193	Ttc7b	-0.24605	Fry	-0.59092
Nanos1	0.61924	Aldh2	-0.24661	Heatr5a	-0.59116
1500017E21Rik	0.61858	Slc35f1	-0.24715	Hspg2	-0.59223
Stom	0.61599	Paqr7	-0.24749	Heatr5b	-0.59362
Fcgr2b	0.61428	Zdhc21	-0.24816	Pnkd	-0.59363
Rmnd5b	0.61428	Gabrg2	-0.24932	Cacna1h	-0.59381
Wnt7a	0.61367	Actr3b	-0.25131	Pcdh18	-0.59575
Socs2	0.61274	Atg9a	-0.25144	Tnk2	-0.59598
Erich6	0.6114	Hjurp	-0.25218	Wdte1	-0.59795
Gm14005	0.61099	Fam19a2	-0.25373	Prrc2a	-0.5989
Riok3	0.61091	Tmem25	-0.25384	Oprl1	-0.59894
Ddx5	0.61062	Tmem150c	-0.25414	A3galt2	-0.60103
Ktn1	0.61057	2310022B05Rik	-0.25416	Ppp1r37	-0.60225
Sesn2	0.609	Ppp1r1c	-0.25424	Clec2l	-0.6034

Slc4a8	0.60886	Mpdz	-0.25446	Tln2	-0.60389
Zc3hav1	0.60879	Nsmaf	-0.25481	Snd1	-0.60443
1700066B19Rik	0.60671	Strip1	-0.25523	Jph3	-0.60541
Ctxn2	0.60597	Sh3gl2	-0.25597	Smad9	-0.60548
Eid2	0.60585	Ube3c	-0.25618	Abhd14a	-0.60569
Ifit2	0.60479	Iqsec1	-0.25737	Gm996	-0.60577
Gm15522	0.60365	Dcun1d2	-0.25836	Rdh12	-0.60674
Phf13	0.60318	Lap3	-0.25872	Osbp110	-0.60768
Glyat	0.60096	Hdhd2	-0.25912	D130043K22Rik	-0.60877
1810026J23Rik	0.59971	Ckmt1	-0.25953	Lrrn2	-0.60878
Guf1	0.59917	Snx25	-0.25988	Pex6	-0.60922
Gbp6	0.59814	Sltn	-0.26026	Tk1	-0.60933
Stk17b	0.59585	Tuse5	-0.26042	Cep250	-0.6096
Hes1	0.59499	Bbs2	-0.26212	Mef2c	-0.61043
Snhg4	0.59459	Clint1	-0.26233	Mgst3	-0.61063
Nfkbiz	0.59426	Atg4c	-0.26239	Lmnb2	-0.61106
Il18	0.59292	Fbxo21	-0.26274	Fam222a	-0.61233
D130007C19Rik	0.59273	Susd4	-0.26308	Wipf3	-0.61304
Otop1	0.59208	Ccdc181	-0.26394	Chchd6	-0.6132
Zfp28	0.59154	Mapk10	-0.26476	Map3k10	-0.61365
Flt3l	0.59116	Ddx17	-0.26592	Pcdh7	-0.61404
Hsd17b7	0.59029	Snx27	-0.26604	Dctn1	-0.61416
Dnase1l3	0.58935	Adsl	-0.26672	Wdr25	-0.6155
Herc6	0.58926	Pck2	-0.26686	Kalrn	-0.61581
Coq10b	0.58908	Rps6ka2	-0.26728	Pex14	-0.6165
Irgm2	0.58907	Ipo11	-0.26729	Atp6v0c	-0.61704
E130309F12Rik	0.58865	Tgfb1l1	-0.26737	Galnt18	-0.61741
Fam83h	0.58818	Enox1	-0.26753	Gm26564	-0.6181
Clec4a1	0.58792	Chgb	-0.26761	Dlgap3	-0.61817
Bst2	0.58761	Chn1	-0.26802	Slc2a8	-0.62106
Rap2b	0.58705	Cbx6	-0.26826	Fam189a1	-0.62116
Ggta1	0.58667	Arhgef10l	-0.26833	Otud7a	-0.62155
Snhg6	0.58663	P4ha1	-0.26867	D930015E06Rik	-0.62193
Kti12	0.58662	Ap3s2	-0.26874	Cntnap2	-0.62318
Hoxd8	0.58658	Klhl5	-0.26883	Lpcat4	-0.62322
Pim3	0.58631	Pcdh1	-0.26892	Apoe	-0.62364
Abhd17b	0.58616	Slc25a19	-0.26899	6430550D23Rik	-0.62408
Sac3d1	0.58596	Map7	-0.27006	Syt3	-0.62427
Stk32a	0.58584	Snx3	-0.27026	Panx2	-0.62456
Slc39a1	0.58529	Csmd1	-0.27045	Cntn6	-0.62571
Angptl2	0.58514	Prkar2b	-0.27075	Dnase2a	-0.62572
Rdh10	0.58461	Usp11	-0.27081	Grik5	-0.62574
Sertad1	0.58416	Sec14l1	-0.27129	Uqcr10	-0.62596
Cnbd2	0.58346	Tvp23a	-0.27144	Tonsl	-0.62625
St8sia2	0.58176	Pak3	-0.27247	Cul9	-0.62761
Cfl1	0.58153	Gm26883	-0.27311	Adck5	-0.62927

Rps6ka1	0.58144	9330159F19Rik	-0.27315	Map3k13	-0.63035
Gm26778	0.58127	Plcd4	-0.27316	Mum111	-0.63149
Tmem158	0.57919	Mtx3	-0.27339	Rps29	-0.63188
Gprin1	0.57816	Asic3	-0.27398	Myh14	-0.63281
Ddx28	0.57776	Lman21	-0.27405	Banp	-0.63316
Rnase4	0.57678	Cdk5rap2	-0.27475	Colq	-0.63436
Map7d1	0.57614	Abr	-0.27511	Sema3f	-0.63585
Oasl2	0.5758	Phtf2	-0.27627	Cyp27a1	-0.636
Acot1	0.57533	Nfia	-0.27651	Camk1g	-0.63669
Tle3	0.57525	Prkcq	-0.27694	Akr7a5	-0.63783
Gm16033	0.57499	Tars2	-0.27748	Abhd17a	-0.63845
Myd88	0.57368	Klhl20	-0.27784	Zbtb48	-0.63932
Cep112os2	0.57338	Trappc10	-0.27832	Kcnj8	-0.63982
Gpr153	0.57088	Ppm11	-0.27871	Cactin	-0.6407
Serpina3i	0.56868	N28178	-0.27893	Ankrd11	-0.64071
Psmel	0.56615	Vt1a	-0.27998	Pik3r5	-0.64292
Doc2b	0.56577	Mcu	-0.28016	Gpr123	-0.64295
Arf6	0.56547	Faah	-0.28028	Mfge8	-0.64381
Tpt1	0.5653	Ankrd27	-0.28032	Gm12592	-0.64544
Eif4e	0.56524	Aatk	-0.28048	Chst8	-0.64554
Tmem154	0.5649	Nrxn2	-0.28074	Ankrd34c	-0.64709
Fgfr11	0.56323	Trpc6	-0.28092	Tmem132e	-0.64718
Micall1	0.56258	Rab3ip	-0.28102	Tmem109	-0.64722
Surf6	0.56254	Ehmt2	-0.28211	Spock1	-0.64776
Ccdc172	0.5625	Itm2c	-0.28297	Scrib	-0.6489
Rest	0.56233	Numb	-0.28335	Tppp3	-0.65123
Ckap4	0.56198	Sharpin	-0.28358	Myo5b	-0.65134
Prokr2	0.5614	Grik4	-0.28377	Lrrk1	-0.65181
Myo10	0.56007	Eif3k	-0.28388	Nrg1	-0.65225
Omp	0.55951	Lin7a	-0.28393	Mast2	-0.65261
Ttpal	0.55925	Anks1	-0.28423	Gon4l	-0.65272
Medag	0.55895	Dnajc6	-0.28471	Htr4	-0.65689
Arxes1	0.55837	Gm4980	-0.28472	Gm14290	-0.65757
Zfp703	0.55827	Pot1a	-0.28472	Apbb1	-0.65801
Scai	0.55725	Mllt3	-0.28489	Zer1	-0.66084
Mrpl36	0.5571	Strbp	-0.28505	Comp	-0.66163
Zfp747	0.55639	Vps33a	-0.28517	Fam193b	-0.66265
Ptma	0.55612	Prdm12	-0.28522	Trappc9	-0.66367
4833424O15Rik	0.55576	Mmp15	-0.28545	Hhat	-0.66445
Inhbb	0.5552	Syn2	-0.28581	Hdac4	-0.66552
S100a11	0.55495	Nucb1	-0.28597	Ints1	-0.66572
Med22	0.55381	Tnrc6c	-0.28641	1700021J08Rik	-0.66605
Nr2f2	0.55299	Slc29a4	-0.28655	Grm4	-0.66652
Eif1	0.55152	1700037C18Rik	-0.28697	Gm765	-0.66685
Cxadr	0.55047	Ppcdc	-0.28714	Tjap1	-0.66695
Tpm4	0.5483	Tbc1d1	-0.28776	Nell2	-0.66707

Zbtb3	0.54482	Thrsp	-0.28787	Tceb2	-0.66757
Zfp948	0.54479	Fam168a	-0.28825	Ppp1r16a	-0.66806
Ctu1	0.54445	Tgfb3	-0.28887	Arntl	-0.66855
Rhebl1	0.54365	Elp2	-0.28925	Ttc9b	-0.67084
Cybrd1	0.54333	Megf8	-0.28933	Zfp341	-0.67085
Pisd-ps1	0.54235	Pex51	-0.28957	Hoxb6	-0.67085
Irf2bpl	0.54232	Pik3cd	-0.28977	Fbp2	-0.67106
BC022687	0.54213	Stip1	-0.28999	Zfp13	-0.67161
Birc5	0.542	2900011O08Rik	-0.29026	Lin7b	-0.67505
Pnlip	0.54193	Tceanc2	-0.29078	Gpr156	-0.67524
Them4	0.54176	Sptb	-0.29086	Ankrd13d	-0.67721
Slc1a4	0.54168	Snph	-0.29089	Dad1	-0.6776
Slc1a2	0.54104	Bcl7a	-0.29168	Slc25a25	-0.67787
Fgf11	0.541	Mgat3	-0.29168	Kcnab2	-0.67796
Map10	0.54063	Kcnip1	-0.2923	Rpusd1	-0.67864
Rora	0.54001	Akt3	-0.29235	Pdlim7	-0.67967
Kpna2	0.53919	Adck2	-0.29249	Armc2	-0.68103
4933428G20Rik	0.53904	Epn2	-0.29283	Sik2	-0.68185
Cstb	0.53833	Cpt1c	-0.29291	Gm14493	-0.682
Tecta	0.53801	Abca7	-0.29363	Rpap1	-0.68235
Fam150b	0.53753	Bai3	-0.29375	Boc	-0.68492
Lipt2	0.536	Prpf40b	-0.29405	Slc9a1	-0.68565
Zbed4	0.53516	Dcaf8	-0.29426	Gpx2	-0.68566
Cbln2	0.53511	Abhd6	-0.29462	Sfi1	-0.68566
Atp8b1	0.53437	Pex11b	-0.29473	Scn1a	-0.68597
Ypel4	0.53337	Wdr7	-0.29477	Spn	-0.68608
Lrrc19	0.53333	Add1	-0.29482	Clrn1	-0.6884
Sft2d3	0.53129	Tmtc1	-0.29488	Kctd16	-0.68928
4632433K11Rik	0.53089	Akap9	-0.2949	Timm13	-0.68953
Sdf211	0.52993	Als2	-0.29495	Gm20529	-0.6903
Plau	0.52993	Poc5	-0.29547	Il17rc	-0.69097
Rdh13	0.52908	Galm	-0.29556	Tcf7l1	-0.69148
Ccdc86	0.52884	Cntn1	-0.29648	Ldlrad4	-0.69234
Gimap4	0.52833	Cyth1	-0.29727	Myl4	-0.69336
Acy1	0.52792	Tbc1d32	-0.29738	Pstpip1	-0.69345
Nhlrc1	0.52645	Mrrf	-0.29768	5830417I10Rik	-0.6947
Slc30a1	0.52598	Nsd1	-0.29786	Tnxb	-0.69478
Nox4	0.52563	Top1mt	-0.29798	Gm53	-0.69494
Galnt4	0.52479	Impdh1	-0.29851	Gen1	-0.69613
Cln5	0.52437	Ppp2r4	-0.29856	Ndufa2	-0.69737
Maff	0.52319	Cpne4	-0.2986	L3mbtl1	-0.69851
Esd	0.52257	Kcnip2	-0.29869	Caln1	-0.69926
Gdpd3	0.52125	Osbp16	-0.2993	Perm1	-0.70058
Trmt13	0.51965	Bear3	-0.29947	Pcnx13	-0.70189
Cd24a	0.51939	Nudt12	-0.29955	Bmp6	-0.70212
Ezr	0.51919	Map3k5	-0.29955	Ftsj2	-0.70475

Pcnx	0.5188	Peak1	-0.29966	Lrrn1	-0.70498
Eif1b	0.5187	Xk	-0.29967	Abhd15	-0.70604
Podxl	0.51779	1700021K19Rik	-0.29971	Tmem196	-0.70658
Fcrls	0.5175	Dmtn	-0.30038	Wnk2	-0.71085
Lins	0.51671	Ppp6r3	-0.30061	Rbm20	-0.71096
Zik1	0.51647	Ankrd29	-0.30098	Trem12	-0.71213
Uap1	0.51611	Nfic	-0.30103	Clrn2	-0.71333
2310047M10Rik	0.51599	Tle1	-0.30119	Gbfl	-0.71414
Rccd1	0.51541	Dip2c	-0.30119	Gm16551	-0.71422
Arg2	0.51534	Jakmip1	-0.3012	Htr3b	-0.71432
Sdr42e1	0.51505	Kcnd1	-0.30144	Lrrc32	-0.71492
Golga7	0.51387	Map2k5	-0.30146	Ernm	-0.71718
Fam167a	0.51319	Rpa1	-0.30182	Mrap2	-0.71801
Baz1a	0.5129	Slc25a38	-0.30214	Mrps11	-0.71826
Slc6a19	0.51237	Dcaf5	-0.3023	Ddc	-0.72174
B3galt6	0.51225	Arhgef17	-0.3025	Mok	-0.72361
Aaed1	0.51202	1810058I24Rik	-0.30266	Slitrk3	-0.7253
Tcf19	0.51195	Pde2a	-0.30274	Gm21992	-0.72574
Cirbp	0.51142	Pknox2	-0.30279	Insrr	-0.7273
Mcl1	0.51044	Mgll	-0.30313	Slc8a2	-0.72764
Hspa2	0.50813	Epb4.111	-0.30319	Aars2	-0.72928
Gm9917	0.50727	Srrm3	-0.30333	Pelo	-0.73053
Neto2	0.50663	Pcdh10	-0.30341	Sppl2b	-0.73062
Znrf3	0.50591	Mlxip	-0.30415	mt-Ta	-0.731
Sla2	0.50589	Rab36	-0.30435	6030419C18Rik	-0.73126
Anks1b	0.50518	Ampd2	-0.30555	Shf	-0.73134
Slc39a6	0.50482	Fchsd2	-0.30623	Fam221a	-0.73185
Gm12841	0.50421	Zfp532	-0.30624	Ccm2l	-0.73185
Pcgf5	0.50395	Clip2	-0.30687	Igf1r	-0.73209
Plekha3	0.50371	Fam185a	-0.30708	Arhgap39	-0.73371
Slc23a2	0.50344	Meis2	-0.30775	Ncor2	-0.73394
Arxes2	0.50328	Plekhdl	-0.30805	Dgkh	-0.7372
Nfkbia	0.50259	Pepd	-0.30846	Sgsm3	-0.73801
Elmsan1	0.50228	Dedd	-0.30849	Fam196b	-0.73867
C4b	0.50171	Zfp365	-0.30866	Mast1	-0.73938
Phf11d	0.5014	Dbnnd1	-0.30903	Shroom3	-0.73955
Micall2	0.50103	Mapre2	-0.30908	Gm13562	-0.74223
Gpr146	0.50062	Arhgef6	-0.30939	Ankrd34a	-0.74247
Psmb9	0.50049	Papss1	-0.30987	Ssbp4	-0.74296
Mtus2	0.50026	Tmcc1	-0.31012	Sema5b	-0.74329
Loxl2	0.49983	Wdsub1	-0.31019	Sncaip	-0.74371
Tmem243	0.49728	Hk1	-0.31022	Tmem108	-0.74395
Cenpl	0.49708	Asna1	-0.31121	Syne4	-0.74398
Lcmt2	0.49706	Klhl22	-0.31228	Acacb	-0.74463
Mgat2	0.49661	Fgfr1	-0.31251	D630044L22Rik	-0.74487
Spata13	0.49641	Slc25a12	-0.31307	Gal3st1	-0.74526

Slc38a1	0.49637	Neol	-0.31319	Ephb6	-0.74581
Nfyb	0.49596	Efr3a	-0.31373	Chpf	-0.74636
Mrc1	0.49522	Lsamp	-0.31375	Fam69b	-0.74651
Gm26716	0.49521	Rtn2	-0.31439	Nbas	-0.74721
Hs2st1	0.49452	Atg16l1	-0.31452	Unc79	-0.74839
Tmbim1	0.49444	Sympk	-0.31464	Eps8l2	-0.74987
Ankrd33b	0.49309	Lamc1	-0.31544	Ntrk3	-0.75194
Gm13889	0.49287	Rcc2	-0.3155	Mgat5	-0.75226
Nek6	0.49204	Gm26518	-0.31561	Chodl	-0.7526
Wsb1	0.49202	L1cam	-0.31569	Cabin1	-0.75332
Cyp4f14	0.49199	Cmc2	-0.31575	Bekdha	-0.75345
Sphk1	0.49195	Rab4a	-0.3159	Rnf180	-0.75444
Slc6a8	0.49185	Rell2	-0.31698	Wdfy4	-0.75481
Hddc3	0.49157	Ube3b	-0.31699	2310067B10Rik	-0.75593
Gm6548	0.49101	Gpbp111	-0.31702	Fcho1	-0.75662
Tnfaip1	0.48997	Plec	-0.31791	Rnf208	-0.75711
Cd302	0.4899	Rabl6	-0.31826	Igfbp2	-0.75763
Ppp4r4	0.48973	Wbscr17	-0.31901	Ndufb7	-0.75782
Pgm1	0.48962	Ctnnd2	-0.31921	Btbd2	-0.75822
Mob3c	0.489	Trim37	-0.31939	Gm26517	-0.75934
Arhgef2	0.48893	Katnb1	-0.31947	Hal	-0.76406
Slc35f6	0.48873	Utrn	-0.3197	Zfp523	-0.76511
Zswim4	0.48846	Dpp9	-0.32023	Osbp17	-0.76587
H3f3b	0.48839	Pcbp3	-0.32027	Dst	-0.76727
Rassf1	0.48823	Tmem178b	-0.32051	Fam195a	-0.76794
Snhg5	0.48818	1110037F02Rik	-0.32081	Pmfbp1	-0.76808
Timm8a1	0.48799	Spats2l	-0.32091	Abhd8	-0.76979
Rcan1	0.48691	Lrba	-0.32108	Bambi	-0.77068
Rims4	0.48671	Prpf8	-0.32133	Ndufs7	-0.77099
Mfhas1	0.48632	Scn11a	-0.32157	Hp	-0.77105
Rpl39	0.48614	Gtf2h4	-0.32174	Inpp5j	-0.77319
Armxc5	0.48612	Dok4	-0.32202	Uqcr11	-0.77523
Ube2j2	0.48597	Rnf219	-0.32211	Pde4d	-0.77702
Blcap	0.48574	Tdrd7	-0.32226	Hhatl	-0.77763
2610524H06Rik	0.48549	Asb6	-0.32228	Hs3st6	-0.78046
Itgav	0.48478	Nckipsd	-0.32276	Isoc2a	-0.78111
Nod2	0.48457	Dlg4	-0.32308	Rplp1	-0.78171
Nxpe4	0.48374	Bcl2	-0.32342	Naa10	-0.78191
Tob1	0.48289	Ablim3	-0.32374	Rita1	-0.78191
Kbtbd3	0.48262	Ncald	-0.32374	Smyd1	-0.78199
Snx30	0.48232	Tmem72	-0.32408	Mib2	-0.78212
Zfp629	0.48151	Snrk	-0.32417	Sptbn4	-0.78242
Hnfla	0.48122	Kcns3	-0.32434	Gm10532	-0.78559
Slc10a6	0.48104	Carm1	-0.32435	Impa2	-0.7885
Tex40	0.48083	Trpc3	-0.32468	Gtpbp6	-0.78866
Nedd1	0.4807	Grik1	-0.32488	Gm16235	-0.79074

Trafd1	0.48058	Gamt	-0.32489	Chrn3	-0.79304
Amotl2	0.48048	Sorl1	-0.32554	Plekhh3	-0.79595
Rbm3	0.47805	Tmem63b	-0.32563	Atp1a1	-0.79764
Slc22a23	0.47782	Ift122	-0.32593	Irf4	-0.80018
Plscr2	0.4769	Kank1	-0.32624	Pou6f2	-0.80018
Cd200	0.47662	Rap1gap2	-0.32632	Cdh15	-0.80155
Cxcl12	0.47606	Cobl	-0.32647	Lrp5	-0.80247
Pde1c	0.47582	4933411K20Rik	-0.32693	Rpusd3	-0.80504
Gm16740	0.47581	Asic2	-0.32713	Ccdc124	-0.80601
Fam26e	0.47519	1700037H04Rik	-0.32771	Ccr10	-0.80658
Ovca2	0.47454	Gpr125	-0.32774	Zfp524	-0.81124
Cd38	0.47365	Pcyt1b	-0.32802	3000002C10Rik	-0.81259
Wbp5	0.47284	Arhgdia	-0.32812	Dpf3	-0.81414
Prosl	0.47275	Maea	-0.32814	Psmg3	-0.81641
Ddx21	0.47206	Rps6kc1	-0.32819	Bai1	-0.81678
Dynll2	0.47185	Myo5a	-0.32822	Tfeb	-0.81858
Six1	0.47175	Zfp142	-0.32915	1700040D17Rik	-0.81999
Gm26658	0.47154	Plekhm2	-0.32924	Gm7457	-0.82176
Plp2	0.47153	Vps13a	-0.32929	Prrt3	-0.82186
Lonrf1	0.47077	Tti1	-0.32932	Prr15l	-0.82196
Ankrd13a	0.47074	Rere	-0.32934	Cdh12	-0.82322
Csf2rb	0.46952	Kcnk2	-0.32938	Nkain3	-0.82355
4930451E10Rik	0.46836	Wrap73	-0.32941	Unc5b	-0.8256
Irf9	0.46759	Sh3bp5l	-0.32962	8030453O22Rik	-0.82809
Herc4	0.46682	Baz1b	-0.32966	Chrna7	-0.83072
Dnajb5	0.46667	Kens1	-0.32978	Tagap	-0.83109
Eaf1	0.46571	Tmem255a	-0.32998	Rassf6	-0.83882
Prosc	0.46564	Ak5	-0.33008	Cacna1e	-0.83921
H2-K1	0.46538	Them6	-0.33026	Gm16083	-0.83977
Dazap2	0.46512	Nisch	-0.33029	Crybb1	-0.84061
Fastkd5	0.46452	Slc9a9	-0.33055	Dgkg	-0.8407
Gtf2ird1	0.46398	Cul7	-0.33078	Map3k7cl	-0.84118
Oser1	0.4635	Mbd5	-0.33087	Pou2af1	-0.84606
Ier3	0.46315	Slc35c2	-0.33091	Kcnh5	-0.84695
Nat14	0.46274	Itgb5	-0.33158	Prr12	-0.84773
Erf	0.46239	Rtn4rl1	-0.3318	Cd79a	-0.85109
F8a	0.46185	Dym	-0.3323	C8g	-0.85296
2310036O22Rik	0.46184	Ift80	-0.33235	Ndufa7	-0.85332
Gnl2	0.46147	Apba1	-0.33265	Fn3k	-0.85716
Zfp281	0.46115	Anapc5	-0.33302	Acta2	-0.86287
Hbegf	0.46093	Slc38a10	-0.33325	1500012K07Rik	-0.86377
Pfdn4	0.46062	Camk2b	-0.33382	Gm5859	-0.86869
Eef1b2	0.46056	Csk	-0.33382	Trerf1	-0.86869
Ppif	0.46028	Trib2	-0.33439	Snta1	-0.86985
Cd274	0.45993	Rassf4	-0.33456	Rin3	-0.87276
Cetn4	0.45895	Mettl16	-0.33567	Kirrel3	-0.87378

Slc35g2	0.45793	Sv2b	-0.3357	Gal3st3	-0.87473
Atp6ap2	0.45786	Pcdhgc5	-0.33571	Fam13a	-0.87879
Cnksr3	0.45772	Snrnp200	-0.33622	Nr1h3	-0.88262
Slc25a20	0.45713	Lhfp14	-0.33623	Cdkl4	-0.88384
Ahr	0.45702	Dync1h1	-0.33626	Rtn4r	-0.88529
Zfp667	0.45657	Hadha	-0.33678	Vwc2l	-0.88607
Nfe2l2	0.45549	Ppfia3	-0.33686	Cpm	-0.88656
Rap1b	0.45541	Zfyve9	-0.33736	Plin4	-0.89529
Jund	0.45469	Unc119	-0.33743	Grin2d	-0.89569
Polr3d	0.45385	Tyrp1	-0.33749	D930019O06Rik	-0.89574
Cyb561	0.45324	Csrnp3	-0.33754	Gm13629	-0.89621
Vsig10	0.45234	Cog4	-0.33827	Rag1	-0.8965
Cacna2d1	0.45213	9430015G10Rik	-0.33839	9330162012Rik	-0.89907
Rnd2	0.45211	Ifngr1	-0.3387	Ssc5d	-0.9022
Nr4a1	0.45181	Trappc8	-0.33904	Fbxo40	-0.90326
Sh2b3	0.45151	Clstn2	-0.3396	Frmpd1	-0.90343
Nav2	0.4493	Smap2	-0.33962	Gm5581	-0.90362
Hnrnpab	0.44918	Soga3	-0.3398	Vps13c	-0.90407
2900026A02Rik	0.44904	Plekhg3	-0.33988	Klrg2	-0.90497
Tuba1a	0.44876	Prex1	-0.34012	Gm26804	-0.90875
Hnrnpdl	0.44876	Gm7271	-0.34026	Adcy9	-0.91166
Pop5	0.44871	Lcp1	-0.34061	Shd	-0.91385
1110038B12Rik	0.44868	Map3k4	-0.34063	4930453O03Rik	-0.91603
Syt12	0.44858	Ccdc141	-0.34089	Cidea	-0.91677
Kdm2b	0.44832	Adrbk1	-0.34099	Kcnk18	-0.91727
Sco2	0.44782	Cgnl1	-0.34108	Lpar5	-0.91754
Emc6	0.44777	Tmem229b	-0.34122	Sf3b5	-0.91901
Ptpn2	0.44716	Cdo1	-0.34175	Eefsec	-0.92033
Sbno2	0.4471	Fbxo31	-0.342	Hrh2	-0.92133
Hipk4	0.44708	Sap130	-0.34204	Lrmp	-0.92175
Glrx5	0.44629	Man2c1	-0.3422	Gm10676	-0.92353
Litaf	0.44604	Rgl2	-0.34226	Gm16861	-0.92429
Plekhf2	0.44577	Slc9a3r2	-0.3426	Gck	-0.92478
Tpx2	0.44537	Rrbp1	-0.34285	Mospd3	-0.92531
Enc1	0.44454	Are1l	-0.34334	Sars2	-0.92587
Ifih1	0.44445	Parvb	-0.34338	Zdhhc22	-0.92729
Ripk2	0.4442	Kank4	-0.34367	Ankrd9	-0.93051
Zfp593	0.44336	Ptger1	-0.34377	Vstm2b	-0.93438
Clp1	0.4431	Ift46	-0.34418	Ptk7	-0.93555
1700019L03Rik	0.44284	Ppp6r2	-0.34426	Gm15759	-0.93602
Tinf2	0.44284	Vwa8	-0.34438	Lrrc31	-0.93621
Bloc1s3	0.44157	Gtf2i	-0.3445	Ccdc64	-0.93803
Tomm22	0.44145	Tsen15	-0.34496	Bzrap1	-0.93804
Spry2	0.44133	Zhx3	-0.34496	Ndst4	-0.94537
Repin1	0.44132	Rcsd1	-0.34497	Tpgs1	-0.94627
Wnt9a	0.44058	Srgap2	-0.34509	Trappc6a	-0.94681

Tmc7	0.44045	Prkca	-0.34514	Rapgef1l	-0.94928
Txnrd3	0.44036	Gabbr2	-0.34557	Kcnb1	-0.95183
Pnp	0.4396	Mpnd	-0.34575	D10Bwg1379e	-0.95288
Csnk1e	0.43922	Dock10	-0.34575	Gm17178	-0.95775
Ufsp1	0.43909	Flad1	-0.34619	Capn15	-0.9587
Cldn25	0.43884	Chga	-0.34628	Zfp385a	-0.95991
Srsf2	0.4388	Sos1	-0.34634	Nudt12os	-0.96087
Rpp38	0.43857	Aldh7a1	-0.34639	Card11	-0.96117
Nox1	0.43739	Fam189a2	-0.34684	Wdr16	-0.96174
Plekho2	0.43713	Sorbs3	-0.34691	Dscam	-0.96396
Mospd1	0.43663	2210018M11Rik	-0.34693	Unc5a	-0.96429
Dynll1	0.43657	Nf1	-0.34697	Klc3	-0.96688
Il4ra	0.43651	Ccser2	-0.34699	Gm17509	-0.96929
Yeats4	0.43578	Rnf123	-0.34708	Lrnf4	-0.96937
Cdc42se1	0.43568	Rltpr	-0.34734	Dgki	-0.97806
Hmgb1	0.43564	Oscp1	-0.34741	Sert1	-0.98016
Lactb2	0.435	Reps1	-0.34801	Hif3a	-0.98092
Gcc1	0.43486	Unc80	-0.34807	Nphp4	-0.9823
Stat2	0.43464	Phrf1	-0.34829	Kifc1	-0.98729
Cib1	0.43449	Jarid2	-0.34838	Ushbp1	-0.98934
Arl4c	0.43329	Gpaa1	-0.34852	Foxj1	-0.99006
Ing2	0.43315	Cep350	-0.34856	Jag2	-0.99108
Rdh11	0.43307	Amigo3	-0.34915	Rec8	-0.99135
Mrpl43	0.43288	Ica1	-0.34932	Slc16a14	-0.99345
Lymr2	0.4324	Tro	-0.34936	Gm6994	-0.9936
Gpr137b	0.43165	Uqcre1	-0.3495	D630008O14Rik	-0.99748
4732487G21Rik	0.43161	Ppargc1a	-0.34955	Grid2ip	-1.0063
Gm16153	0.4313	Trappc11	-0.35006	Gm26794	-1.0093
Jtb	0.42982	Herc3	-0.3505	Pold1	-1.01
Arv1	0.42947	Gpr155	-0.35055	Adora2a	-1.0142
Nudcd2	0.42928	Mettl7a1	-0.35107	Papln	-1.0151
Tgs1	0.4289	Hivep2	-0.35138	Ptchd2	-1.0176
H2-T23	0.42862	Klhl8	-0.35161	Iqej	-1.0184
Metap1	0.42856	Extl2	-0.35167	Eno4	-1.02
Hif1a	0.42833	Srebf2	-0.35194	Dpys	-1.0209
Cnot11	0.4281	Unc45a	-0.35219	Foxp4	-1.021
Zfp664	0.42809	Heatr6	-0.35254	1810024B03Rik	-1.022
Pdcl3	0.42803	Glb1l2	-0.3528	Mpo	-1.0231
Ptrf	0.4272	Ppp1r13b	-0.35293	Gm16845	-1.033
Gent2	0.42697	Thra	-0.35316	Rhag	-1.0381
Ubxn8	0.42689	Dab2ip	-0.35326	Abcc8	-1.0388
Noc4l	0.42632	Tacc2	-0.35333	Chad	-1.0427
Irf5	0.42594	Pelp1	-0.35358	Actg2	-1.0449
Mettl23	0.42548	Haghl	-0.35388	Plcx3	-1.0527
Acsl4	0.42527	Ctdspl	-0.35389	Slc9a3	-1.0538
Yes1	0.42523	Fmo5	-0.35428	AI118078	-1.056

Galns	0.42389	Myo18a	-0.35434	2010300C02Rik	-1.0582
Mfsd7b	0.42323	Atp5d	-0.35441	Acap1	-1.0591
Rhob	0.42298	Rptor	-0.35448	Irs3	-1.0612
Pole3	0.4226	Zfp651	-0.35488	3425401B19Rik	-1.0632
Elmod1	0.42096	Bckdhb	-0.35491	Rtn4rl2	-1.0703
Ndel1	0.4199	Pik3r4	-0.35515	Cbl	-1.0715
Gm16701	0.41983	Gga1	-0.35564	Lct	-1.0721
B2m	0.41981	Mmp24	-0.35574	Kctd19	-1.0733
Mtss1	0.41956	Tubg2	-0.35588	Gm10543	-1.0757
P2rx5	0.41919	Chn1os1	-0.35599	Bcas1os2	-1.0786
Tmem251	0.41894	Scrn1	-0.35633	Dok3	-1.0822
Xaf1	0.41868	Ppp6r1	-0.35657	Dact2	-1.0844
Ticam1	0.41804	Fkbp8	-0.35721	Esrra	-1.0871
Maz	0.41748	Abcb9	-0.35782	Siah3	-1.0889
Irf1	0.41718	Ppfia4	-0.35804	Gm14862	-1.0946
Hoxc10	0.41716	Mprip	-0.35807	B3gnt8	-1.0952
Slc11a2	0.41644	Zdhhc1	-0.35834	Spib	-1.0968
Tmem150a	0.41637	Pard3	-0.35839	Gm15337	-1.1026
Txndc15	0.41617	Rims3	-0.35925	Eln	-1.1075
Elk3	0.4161	Peli3	-0.35967	Kcnb2	-1.1076
Mthfd2	0.41593	Plxnd1	-0.35969	Hspbp1	-1.1085
2700081O15Rik	0.41543	Magi3	-0.3598	Itga11	-1.1182
Rcor3	0.41488	Aplp2	-0.36041	Gabrb2	-1.1209
Nop58	0.41472	Def6	-0.36042	Tmprss9	-1.1229
AI464131	0.41445	Arsg	-0.36049	Gm13609	-1.1229
Arhgap23	0.41443	Htr3a	-0.36079	4930566F21Rik	-1.1229
Rab24	0.41408	Arhgef3	-0.36126	Ackr4	-1.1239
Dclk3	0.41298	Ckap5	-0.36129	Exoc3l	-1.127
Cdk17	0.41248	Tomm6os	-0.3613	A330008L17Rik	-1.1319
Eif2ak2	0.41205	Btbd9	-0.36163	Bnc1	-1.1327
Osbp2	0.41191	Dync1i1	-0.36187	Gm6410	-1.1462
Sat2	0.41161	Cnr1	-0.3622	Prtn3	-1.1616
Eif1a	0.41142	Nedd4	-0.36232	Lrrc24	-1.1619
Hmgn1	0.41111	Grin3a	-0.36241	Gm13425	-1.163
Cyth2	0.41056	Pip5k1c	-0.36242	Tlx3	-1.165
Ado	0.41015	Ano3	-0.36259	Gm14597	-1.1693
Fam134b	0.41012	Nxpe2	-0.3627	Wfdc2	-1.1701
9530027J09Rik	0.40999	Acin1	-0.36295	Vstm2l	-1.1752
Eps8	0.40994	Rab11fip3	-0.36313	Gm16108	-1.1762
Plscr4	0.40985	Galnt14	-0.36333	Il17re	-1.1783
Vegfa	0.40984	Neur14	-0.36369	Till9	-1.1793
Pcbp1	0.40978	Naccl	-0.36371	4932443L11Rik	-1.1794
Dnajc25	0.40977	Gatsl2	-0.36426	Alk	-1.1838
Zbtb6	0.4092	Fam81a	-0.36479	Plk5	-1.1851
Ndst1	0.40806	Abcg1	-0.36486	Scx	-1.188
Fiz1	0.40799	Lphn2	-0.3652	1810012K08Rik	-1.1883

Pdlim4	0.40789	Rnpep	-0.36562	Ptchd1	-1.1906
Hspb1	0.40721	Amacr	-0.3657	Cdh6	-1.206
Plekha7	0.40701	Pls1	-0.36574	Wscd2	-1.216
Ccdc112	0.40641	Bag6	-0.36582	Prdm6	-1.2173
Eif4a1	0.40569	Slc7a4	-0.3663	Ltbp4	-1.2191
Ndnf	0.40531	Psen2	-0.36644	Nckap51	-1.2237
Tmed5	0.4043	Sec31a	-0.36689	Kcnj11	-1.2254
H2afx	0.40408	Tubb5	-0.36747	Lrfn1	-1.2305
Klf11	0.40385	Slc25a22	-0.36752	Igsf21	-1.2323
Chst1	0.40338	Aox1	-0.36774	Bfsp2	-1.2389
Nppb	0.40293	Zmat4	-0.36786	Slc16a5	-1.2458
Arhgap33	0.40266	Phlpp1	-0.3681	Klhl36	-1.2475
A730081D07Rik	0.40081	Man1a2	-0.36818	D430001F17Rik	-1.2512
Mfap31	0.40029	Brinp1	-0.36842	Gm11769	-1.2543
Ppp4r1	0.39993	Ncoa1	-0.3687	Bcl9l	-1.2595
Zfp637	0.39967	Itfg3	-0.36902	Klhl33	-1.2617
Phykpl	0.39876	Raver1	-0.3693	Whrn	-1.2628
Paip2	0.39838	Sptbn2	-0.36963	Kcna2	-1.2645
Plscr3	0.39764	Filip1	-0.36966	Fam78a	-1.268
Slc41a1	0.39727	Cdh5	-0.36967	Trpv4	-1.268
Lix1	0.39665	Ntrk1	-0.36979	Kcnj4	-1.2701
Shc2	0.39611	Gcn111	-0.37003	Gm26775	-1.2711
Ehd4	0.39605	Zzef1	-0.37006	Gm15462	-1.2711
E130218I03Rik	0.39599	Abhd12	-0.3701	Gm15336	-1.272
Nsmce1	0.39567	Sh3glb2	-0.3714	Oprd1	-1.2727
Bag5	0.39553	Scn8a	-0.37142	Zfp109	-1.2761
Gm17122	0.39516	Ptprd	-0.37152	Gm15475	-1.2811
1700025G04Rik	0.3949	Loh12cr1	-0.37198	Nrg2	-1.2822
Gorab	0.3948	Pcsk7	-0.37218	Lrrc4b	-1.2875
Cam1	0.3946	Abca2	-0.37262	Adra1b	-1.2898
Sfxn3	0.39416	Zbtb40	-0.37267	Gm15411	-1.2955
Stac	0.39377	Pth1r	-0.37368	A230005M16Rik	-1.298
Gm17690	0.39295	Wdfy3	-0.37388	Grrp1	-1.3073
Erlin1	0.39269	Kcnj3	-0.3739	Zim1	-1.3201
B3gnt1	0.39256	Yeats2	-0.3742	Oprm1	-1.3214
0610009E02Rik	0.39249	Zfyve28	-0.37452	Hes5	-1.3302
Pgrmc1	0.39235	Mdn1	-0.37454	Gm14164	-1.3322
S100a4	0.39223	Adra2c	-0.37455	0610039K10Rik	-1.3332
Ext2	0.39222	Kcnh6	-0.37482	4921514A10Rik	-1.3359
Limd1	0.39186	Bod11	-0.37616	Cox16	-1.353
Gm13563	0.39093	Rnf19a	-0.37623	Dnah6	-1.3533
Trim13	0.39082	Htr7	-0.37635	Gm16538	-1.3605
Slc30a4	0.39041	Ethel	-0.37645	Rpl36	-1.3686
H1f0	0.39023	Adam11	-0.37685	Lrrc9	-1.3733
Dhps	0.39012	Fam193a	-0.37691	Uchl1	-1.3806
Mgl2	0.39009	Ankrd17	-0.37745	Gm26788	-1.3819

Nop56	0.39002	Cby1	-0.37747	Slc22a6	-1.3835
Reck	0.39	Tfdp2	-0.37773	Gm6981	-1.3902
Epb4.114b	0.38945	Pnpla3	-0.37813	Gm16564	-1.4011
Slitrk2	0.38911	Ppie	-0.37829	Tnk2os	-1.4111
Steap4	0.38905	Rab40c	-0.3786	Klf12	-1.4161
Myeov2	0.38899	Cacng2	-0.37889	Slc38a4	-1.4245
Abcg2	0.3882	Frmpd4	-0.37905	Gm26613	-1.4326
Rcl1	0.38804	Snx11	-0.37946	Fbl11	-1.4488
Yrde	0.38725	Golgb1	-0.37956	Scrn2	-1.4501
Pcsk1	0.38719	Tkt	-0.37977	Tmem121	-1.4776
Nrarp	0.38705	Caskin2	-0.38034	H1fx	-1.5358
Tshz1	0.38696	Ttc21b	-0.38048	Gm16159	-1.5359
Htr1a	0.38695	Ccdc74a	-0.38064	Pesk1n	-1.5626
Fam19a4	0.38689	Rnf157	-0.38139	Kcnk12	-1.5895
Fads1	0.38667	Hsf4	-0.38166	Emilin1	-1.6081
Tmtc4	0.38652	Slc36a1	-0.38175	Gm16240	-1.6105
Atp6v1g2	0.38606	Tm9sf4	-0.38191	4930442H23Rik	-1.6583
Ankrd28	0.38479	Tanc2	-0.38208	Hopxos	-1.6665
Ly6c1	0.38396	Chd8	-0.38208	Zbtb16	-1.6684
Panx1	0.38366	Syt2	-0.38229	Ccdc88b	-1.698
Gm26718	0.3835	Mccc2	-0.38233	Gm1667	-1.7607
Ube216	0.38341	Tnrc6a	-0.38352	Ccdc85b	-1.7793
Fbxo30	0.38322	Ccnd3	-0.38396	Proser2	-1.7836
Serpina3n	0.38309	Pwwp2b	-0.38411	Ntf3	-1.8287
Rfc5	0.3829	Prkcz	-0.38463	C1ql4	-1.8507
Tsc22d2	0.38198	Pin1	-0.38474	Cox6a2	-1.8897
Slbp	0.38165	Itga4	-0.38497	Uchl1os	-1.9554
Zfp68	0.38142	Ogfr11	-0.38526	Hoxa6	-2.0301
Med7	0.38117	Ptpm	-0.38539	Gm11175	-2.1226
Idi1	0.38106	Nfasc	-0.38552	Ckm	-2.2338
Otud4	0.38094	Coro2b	-0.38616	Dpm3	-2.2467
Elf1	0.38069	Epn1	-0.38633	Myh4	-2.2819
				A930016O22Rik	-2.5567

Supplementary file 5.

List of differential expressed genes in L4-L6 DRGs after Dorsal column axotomy (DCA vs Lam)

Gene Name	logFC	Gene Name	logFC	Gene Name	logFC
Capn11	2.3403	Micu1	0.43977	Synpo	-0.39355
Trim63	2.0601	Zfp821	0.43922	Tox2	-0.3939
Ccdc85b	2.0094	Edf1	0.43697	Ly6a	-0.39439
H1fx	1.9972	Btbd2	0.43558	Oasl2	-0.39495
Kenk12	1.9668	Slc25a29	0.43512	Mettl23	-0.3966

Rpl36	1.7032	Jdp2	0.43402	Laptm5	-0.39691
Uchl1os	1.6986	Sh3tc2	0.43287	Irs1	-0.39766
Etnppl	1.669	Hsf1	0.43155	Bhlhe41	-0.39799
Hopxos	1.5858	Rasgrp4	0.43138	Plekha7	-0.39883
Adra1d	1.5153	Tagln3	0.4302	Ubqln2	-0.40126
Gm16564	1.502	Gpr162	0.42899	Tmc7	-0.4024
Plin4	1.4601	Ambra1	0.42871	C1ra	-0.40288
Gm11769	1.4313	Mad111	0.42744	Gm9747	-0.4031
Col2a1	1.3623	Prre2a	0.42609	Nrep	-0.40366
Slc9a3	1.268	Mrpl4	0.42581	Rsad1	-0.40536
Dpm3	1.2589	Actn4	0.42455	Cstf2t	-0.40553
Slit3	1.2441	Lmf1	0.4238	Uck2	-0.406
D430001F17Rik	1.2393	Cabin1	0.42166	Ccnd1	-0.40693
Chad	1.2211	Slc22a18	0.41934	Hnrnpdl	-0.40706
Klhl36	1.2173	Scaf1	0.4191	Ado	-0.40919
Gm14597	1.1991	Cul9	0.41853	Tmem261	-0.41157
Gm2895	1.1987	Cope	0.41803	Hbegf	-0.41188
Capn15	1.1837	Kdm4b	0.41797	Ubiad1	-0.41217
4921514A10Rik	1.1733	Gmpr	0.4161	Ppapdc2	-0.41283
Pcdh15	1.171	Rplp0	0.4155	Gm16551	-0.41434
Gm12868	1.1533	Aspser1	0.41495	Cbx8	-0.41957
Gm15337	1.1516	Pola2	0.4147	Rdh10	-0.42265
Gm13748	1.1357	Eif3h	0.41467	Fosl2	-0.42398
Gm27010	1.1357	Acbd4	0.41437	Fcgr2b	-0.4243
Tmc1	1.1229	Palm	0.41432	2700081O15Rik	-0.42611
Gm15821	1.1211	Psmb3	0.41414	Mxd3	-0.42624
Cyp4f18	1.113	Galnt16	0.41373	Midn	-0.42708
1700003F12Rik	1.1107	Fam195b	0.4137	Fbxo27	-0.42919
Gm17178	1.0878	Ntmt1	0.41281	Thap11	-0.42958
Tbxa2r	1.0829	Frmpl1	0.41186	Rem2	-0.43163
Tmem254b	1.0804	Clec2l	0.41183	Lum	-0.43325
Park2	1.0788	Bcam	0.41169	Pdik11	-0.43387
Cldn14	1.0763	Asb6	0.4053	Rras2	-0.43441
Foxs1	1.066	Apc2	0.40402	Ctsh	-0.43528
Dchs1	1.0623	Git1	0.40344	Galns	-0.43574
Grrp1	1.0564	Mvb12a	0.40194	Tmem173	-0.43647
6030443J06Rik	1.0564	2210018M11Rik	0.40015	Mgl2	-0.4402
4933428G20Rik	1.0525	Ccdc101	0.39955	Ptma	-0.44022
Gm17552	1.051	Abtb1	0.39824	C1s1	-0.44435
Klhl34	1.0407	Rpl26	0.39772	Tmem198b	-0.44626
Proser2	1.031	Hcn3	0.39764	Ttc30b	-0.44662
Slco1a6	1.031	Xpo6	0.39666	Sco2	-0.44714
Neurl2	1.0134	Dos	0.39634	Arxes1	-0.44783
Pold1	1.0062	Sbf2	0.3962	Bloc1s3	-0.44822
Syngap1	0.99722	Evc2	0.39515	C2cd4c	-0.45174
Atf3	0.99721	Polr2e	0.39424	Fiz1	-0.4518

Ovol1	0.99389	Gnb2	0.3937	Col6a3	-0.45441
Gm20529	0.99028	Mpnd	0.39347	Hipk4	-0.45635
Chit1	0.98729	Uaca	0.39341	Pou4f1	-0.45674
Gck	0.98666	St3gal3	0.3924	Ccl6	-0.45723
4930404N11Rik	0.98558	Chst12	0.39151	Lepr	-0.45759
Znhit2	0.98295	Tubg1	0.39111	Hspa8	-0.45906
Gm16982	0.97651	Ranbp3	0.3908	Eid2	-0.46121
Bcas1os2	0.96997	Ctc1	0.38966	Ppp1r26	-0.46175
Trpv4	0.96804	Dnal4	0.38695	Zfhx3	-0.46223
Bcl9l	0.93963	Tubgcp2	0.38693	Ptprc	-0.46232
Gm7701	0.92561	Tsc22d4	0.38679	Btg2	-0.47441
A930005H10Rik	0.92306	Cxx1a	0.38662	Pnma1	-0.4776
Zdhhc22	0.92018	Cnpy3	0.38634	Cxcl12	-0.47893
Atad3aos	0.91532	Lox	0.38556	Rbm15b	-0.48347
Cited1	0.91351	Med25	0.38249	Actb	-0.48428
Hoxb5os	0.91192	Wdr38	0.38242	Pdgfa	-0.48432
Ubt1	0.91127	Zswim8	0.38134	Mcl1	-0.48472
Gm10231	0.89297	Ppm1g	0.38084	Cd93	-0.48692
Zfp652os	0.88835	Gpr19	0.38073	Tgfb1	-0.48916
Cpn1	0.88181	Asl	0.37941	Hoxb8	-0.49031
Ndufb7	0.87947	Pnpla2	0.37881	Chd3os	-0.49056
Tnrc18	0.87874	Zfp11	0.37754	Wnt6	-0.49331
Zfp524	0.87745	Lrwd1	0.37753	Ctu1	-0.49372
Klc3	0.87469	Gipc1	0.37645	Col8a1	-0.49556
Tpgs1	0.87352	Fxyd1	0.37548	Megf11	-0.49635
Ttc18	0.86347	Ndufb8	0.37459	Ccr2	-0.49789
Gm11946	0.86227	Zfand2b	0.37435	Cxxc5	-0.50034
AB041806	0.86206	Gm15441	0.37331	Nlrc5	-0.50155
Ii25	0.85645	Cern4l	0.37299	Trim34a	-0.50255
Bekdha	0.85535	Btbd9	0.37292	Gm26982	-0.50462
Trappc6a	0.85324	Myh14	0.37285	Fgf11	-0.50556
Bai2	0.8454	Ankrd13b	0.37269	Mcm3	-0.50654
B230206L02Rik	0.82888	Sap130	0.3715	Gm15884	-0.51033
Nle1	0.82511	Slc38a6	0.37124	Igdcc4	-0.51098
Nphp4	0.82488	Atp5d	0.37092	Dynll2	-0.51191
Foxp4	0.82395	Tnip1	0.36961	Parp3	-0.5125
Myh7b	0.81599	Tkt	0.3692	Hmgn2	-0.51443
Dpep1	0.81309	Till11	0.36783	Trim30a	-0.51578
Dnah3	0.80648	Tubb5	0.36709	Ss18l1	-0.51758
Apba3	0.80328	Spg7	0.367	Cdk2	-0.51847
Gm15991	0.79546	Hyi	0.36335	Emp1	-0.51982
Mei1	0.79505	Flywch1	0.36329	Nr2f2	-0.52063
Gtpbp6	0.79337	Wdr81	0.36323	H2-Ab1	-0.52303
Gm26596	0.7885	Ncam1	0.36305	Spata25	-0.52349
Aldh16a1	0.78155	Gm17029	0.36281	Srsf2	-0.52349
Ankrd9	0.77995	Rnf31	0.3621	Irf2bpl	-0.53154

Kcnj4	0.77394	Gga1	0.36139	Nanos1	-0.53273
Fam171a2	0.76974	Phldb1	0.36068	Hoxb7	-0.53399
Dyrk1b	0.76565	Numa1	0.36028	Marcks	-0.53902
Polr2f	0.76319	Dcaf6	0.35475	Myo19	-0.54138
1700021J08Rik	0.76023	Rabac1	0.35396	Repin1	-0.54312
Ccdc57	0.76001	Sec13	0.35374	Hnrnpa0	-0.54313
Gm12592	0.75612	Lmf2	0.35356	Apold1	-0.54493
Ndufa7	0.75426	Pik3r2	0.35196	Sdf2l1	-0.54756
Gpr62	0.74798	Itpr3	0.35029	Mesdc1	-0.54934
Bola2	0.74786	Rit1	0.34837	Thbd	-0.55078
Ggnbp1	0.74413	Zdhhc1	0.34817	Slc13a4	-0.55145
Uqcr11	0.73978	Fkbp8	0.34749	Shh	-0.55216
Ccdc124	0.73821	Dtd1	0.34695	Aldh1a3	-0.555
Snta1	0.73797	Crip1	0.34576	Npr1	-0.55588
Lrp5	0.72794	Uqcr1	0.345	Nrarp	-0.55659
Gm2694	0.72627	Spire2	0.34387	Flt3l	-0.55713
Acads	0.71988	Brms1	0.34385	Marcks1l	-0.55824
D630003M21Rik	0.71585	Ctnnb1	0.34337	Ankrd34a	-0.5604
Zbtb49	0.71482	Pomgnt2	0.34278	Irgm1	-0.56136
Lrrc24	0.71345	Hdac5	0.34238	Padi2	-0.5622
Zbtb17	0.71038	Trpc4ap	0.34206	Bcl11b	-0.56418
Psd	0.70963	Ints9	0.34186	B3galt2	-0.56814
Cntn5	0.70826	Vps11	0.34038	Pla2g4a	-0.5713
Pias4	0.69922	Flot1	0.3398	Jund	-0.57174
Isoc2a	0.69266	Vps51	0.33949	Hoxa5	-0.57309
Gm16861	0.68963	Asna1	0.33864	Rrs1	-0.57459
Ak8	0.6798	Urod	0.33654	Ctss	-0.57783
Exosc5	0.67961	Zdhhc18	0.33652	Sfrp4	-0.58404
Ube4bos3	0.6779	Asphd2	0.33539	Col5a1	-0.58406
Chchd6	0.67556	Cuedc2	0.33511	H2afj	-0.58462
Taf1c	0.67547	Gsn	0.33334	Hoxaas2	-0.59386
Dad1	0.67498	Eif2b2	0.33324	Pabpn1	-0.59788
Tmem132a	0.67204	Fbxo42	0.33014	Lrrn4cl	-0.60075
Gm20650	0.66713	Ciz1	0.32797	Sla	-0.60409
Ppan	0.66691	Ankrd54	0.32621	Lrp8os3	-0.60821
Ndufs7	0.66645	Stoml1	0.32587	Ccm2l	-0.61579
Ntsr2	0.66432	Tmem222	0.32544	Ifi44	-0.61756
1700101I11Rik	0.66199	Golgb1	0.32482	Sectm1b	-0.6179
Fbxl6	0.66189	Katnb1	0.32184	Tnk1	-0.62173
Ttc9b	0.66173	Prkrip1	0.32181	Ccdc142	-0.62181
Mif	0.65965	Abca2	0.32109	Cd302	-0.62246
Sptbn5	0.65926	Arhgef28	0.32102	Lipt2	-0.62443
Tonsl	0.65388	Epn1	0.31963	Klk5	-0.62611
Rasl11a	0.65101	Tbc1d7	0.319	Egr2	-0.62851
Slc8a2	0.64992	Phgdh	0.31882	Per2	-0.62898
Fdxr	0.64943	Supt5	0.31779	Esrp2	-0.63548

Eps8l2	0.64798	Pfkl	0.317	Efnb3	-0.63562
Gm20511	0.64754	Stmn4	0.31665	5330438D12Rik	-0.63575
Gm11149	0.64578	Hepacam	0.31564	Aif1	-0.63844
Mok	0.64498	Pmm1	0.31502	Ciita	-0.64193
Lrln2	0.64438	4930506C21Rik	0.31492	Slc11a1	-0.64367
Gm16754	0.63854	Pold4	0.31351	Ppp1r3d	-0.64725
Ces	0.63825	Rnf121	0.31338	Krt10	-0.64869
Mks1	0.63474	Man2c1	0.31072	Adra2a	-0.64968
Zfp13	0.63222	Nol12	0.3102	Ier5	-0.65064
Ercc1	0.63218	Slc38a10	0.30949	Hotairm1	-0.6557
Atp6v0c	0.62817	Prx	0.30818	Kcng1	-0.65927
Trpm4	0.62568	Bcan	0.30785	Frat2	-0.65969
Pgls	0.62507	Pomgnt1	0.30528	Mex3b	-0.65973
Mzt2	0.62004	Ndufs8	0.30456	Pcdhb22	-0.66071
Rps9	0.61966	Sarm1	0.30407	Fut4	-0.66193
Rpl8	0.61946	Eif3d	0.3011	Fos	-0.66274
Mill2	0.61667	Ipo13	0.30087	Zfp36l2	-0.66341
9430069I07Rik	0.61433	Syndig11	0.29756	Tmc5	-0.66482
Grik5	0.61411	Slc25a38	0.29702	Bloc1s4	-0.67034
Gpx2	0.60892	Stk25	0.29349	Perm1	-0.67371
Ptpru	0.60884	Ddx49	0.29208	Siglec1	-0.67381
A730011C13Rik	0.60762	Prpf40b	0.29088	Gbp2	-0.67527
Timm13	0.60697	Sgip1	0.28789	AY074887	-0.67575
Atox1	0.60637	Mpc1	0.28671	Klf2	-0.67645
Ndufa13	0.60304	Cdk5rap2	0.28622	Ebf2	-0.67951
Rnf180	0.60154	Arhgap19	0.28433	Igfbp5	-0.68182
Ppp1r16a	0.60132	Vwa8	0.28385	Clec4a3	-0.68538
Zmat5	0.59987	Rogdi	0.28181	Zfp36	-0.68841
Abhd14a	0.59953	Tenc1	0.27848	Cebpb	-0.69136
Pex14	0.59755	Ncmap	0.27724	Kpna2-ps	-0.69339
Fam163a	0.59736	Sh3glb2	0.27603	Strc	-0.6975
Rps15	0.59413	Csdc2	0.27567	Shmt1	-0.69752
Gm20748	0.594	Rabl6	0.27449	Tmem88b	-0.70887
Otud3	0.58944	Slc27a1	0.26878	Egr1	-0.71401
Comp	0.58662	Gabarapl1	0.26581	Zfp503	-0.71427
Pnpla7	0.58637	Scn1b	0.26539	Inhbb	-0.71452
Tmem219	0.58449	Arfgap1	0.2647	Foxd3	-0.72228
Dlgap3	0.58273	Nelfe	0.26332	Cpa3	-0.73212
Scrib	0.57712	Rpl7a	0.26198	Pou3f1	-0.73493
Podxl2	0.57665	Ass1	0.26062	Dbnnd2	-0.73539
D030047H15Rik	0.57644	Vps33a	0.25689	Mrfap1	-0.74016
Rhbdf1	0.57466	Wdr18	0.25135	AW011738	-0.74223
Prodh	0.569	Pck2	0.24291	Bmp2	-0.74633
Mfsd10	0.56846	Nup93	0.24232	Bmyc	-0.7486
Chia1	0.56717	Prkcz	0.23493	Six5	-0.75271
Khk	0.56511	Ndufv1	0.23466	1700007L15Rik	-0.75336

Prdm10	0.56088	Rgs3	0.22743	Rftn1	-0.75657
Eml2	0.56069	Grik1	0.21666	Hes1	-0.75974
Cc2d1a	0.55585	Cul1	0.2082	Gm26532	-0.78151
Abhd8	0.55575	Spred1	-0.20917	Ccdc78	-0.78471
Mt3	0.55104	Klhl9	-0.20932	D730003I15Rik	-0.79287
Kif19a	0.54683	Trib2	-0.22499	Pmp2	-0.80043
Slc29a2	0.54461	Fam102b	-0.22834	Plac8	-0.80103
Mgst3	0.54386	Hnrnph1	-0.23204	Lrat	-0.8016
4930556J24Rik	0.54361	Vapb	-0.23508	Tef7	-0.80529
Tmem204	0.54063	Ubqln4	-0.23931	2810433D01Rik	-0.80673
Wrap53	0.5399	Tmbim1	-0.2466	Csf2ra	-0.80821
Mast2	0.53984	Iah1	-0.24905	Zbp1	-0.81227
Bcat2	0.53527	Efnb2	-0.25573	Shb	-0.8182
Mon1a	0.53519	Hnrnpl	-0.26488	4930469K13Rik	-0.81955
Nme6	0.53487	Aldh4a1	-0.26542	Lat2	-0.82409
Rpl18	0.53486	Phf2011	-0.26641	Ctgf	-0.82938
Gm11537	0.53234	Ehbp111	-0.27293	Il1rn	-0.84061
Tmem143	0.52943	1810014B01Rik	-0.27515	Cma1	-0.84415
Mbp	0.52887	C530008M17Rik	-0.27536	Cbln1	-0.84475
Arhgap39	0.52709	Gm17122	-0.27624	Ccdc22	-0.84627
Bcl7c	0.52592	Slc35f6	-0.2792	Itgal	-0.84712
Polr2i	0.51903	Ppp1r15b	-0.27948	Cd209a	-0.84939
Acacb	0.51829	Ndufaf1	-0.28834	Gm15506	-0.86158
Sirt3	0.51789	Amd1	-0.28929	Scarf2	-0.86347
Abhd17a	0.51776	Pcbp1	-0.29254	Gm15035	-0.87509
Thop1	0.51728	Tmem100	-0.29365	Dnd1	-0.88443
Rpusd1	0.51568	Rcan2	-0.29375	Fhl3	-0.88542
Il34	0.51504	Stat2	-0.30039	Rgs9bp	-0.89217
Tom1	0.51503	Gm26716	-0.30144	Fgfr3	-0.89391
Wdte1	0.51498	Klf16	-0.30207	Cebpa	-0.89681
Ptov1	0.51372	Trp53inp2	-0.30355	2810430I11Rik	-0.89951
Josd2	0.5132	Rfc5	-0.3059	Cebpd	-0.90354
Tmem205	0.51288	Ahr	-0.30832	Smad6	-0.90514
C630016N16Rik	0.51216	Bri3bp	-0.31107	Ccl2	-0.90732
Arhgef11	0.51104	Tuba1b	-0.31472	Ttc16	-0.90772
Gm11457	0.50924	Tle3	-0.31506	Tmie	-0.9188
Fars2	0.50659	Srd5a1	-0.31673	Fam129c	-0.92277
Sirt6	0.50472	Fastkd3	-0.31741	Il5	-0.92478
Ccm2	0.50351	Tpm4	-0.31781	Ldlrap1	-0.92498
Pcx	0.50268	Atp6v1g2	-0.31808	Oxtr	-0.92787
Ifrd2	0.50205	Tysnd1	-0.31858	Hspa1b	-0.92918
Plekhm2	0.50029	Cchcd2	-0.32239	Foxc1	-0.93133
Zfp444	0.4985	Bola3	-0.32322	Tmem30b	-0.93212
Stmn2	0.49793	Kin	-0.33156	Gad1	-0.94137
Dennd1a	0.49692	Emc6	-0.33168	Wt1	-0.94928
Hmgcs2	0.4965	Lyn	-0.33301	Igha	-0.95995

Mapk8ip3	0.49579	Ctsc	-0.33315	Tmem184a	-0.96444
Aars2	0.49462	Samd4	-0.33334	Gm26892	-0.97398
Xrcc1	0.49396	Irf1	-0.33371	Wnt4	-0.97554
Zfp523	0.4936	Yeats4	-0.33858	Edn3	-0.98545
Nenf	0.49241	Hoxb5	-0.33897	Aoc2	-0.99403
Mvd	0.49125	Sema4g	-0.34036	Galnt12	-1.02
3010026O09Rik	0.49061	Arhgef15	-0.34081	Xlr3b	-1.0373
Tsfm	0.48971	Ndn	-0.34082	Itgae	-1.0403
Pip5k11	0.48949	Ttpal	-0.34178	Accs1	-1.0455
Lamb2	0.4886	Rsrp1	-0.34343	Hist1h1d	-1.059
Cyp4f39	0.48818	Gm9917	-0.34348	Stc1	-1.061
Map3k10	0.48697	Trim8	-0.34396	Rph3al	-1.0699
Rpl41	0.48554	Fam217b	-0.34679	Foxd1	-1.0772
Ube2s	0.48436	Igfbp4	-0.34696	Tspan32	-1.0935
Rpl4	0.48323	Sfrp1	-0.34766	Cxcl14	-1.0947
Tap2	0.48258	Appl2	-0.34786	Aplnr	-1.0953
Tbc1d25	0.48175	Prmt8	-0.3491	Gm12319	-1.0956
Rps18	0.48083	D17H6S53E	-0.34964	Oas2	-1.0964
Bcas3	0.47921	Litaf	-0.35089	Dll3	-1.1059
Il16	0.47736	Postn	-0.35321	Fam84a	-1.1333
GpnmB	0.46952	Gldn	-0.35333	Rin1	-1.1333
Smtn	0.4684	Pgp	-0.35497	Bhlhe22	-1.1769
Mast1	0.46838	Tyw3	-0.35523	Tmem86b	-1.2049
Pacs1	0.46808	Mtss1	-0.35739	Ptgdr2	-1.2097
Kcnn4	0.46401	Ndufb2	-0.35895	Ces1d	-1.227
Pi4k2a	0.4639	S1pr2	-0.36194	E230013L22Rik	-1.2505
Ten1	0.46312	Col15a1	-0.36261	Apln	-1.2605
Dctn1	0.45883	Dolk	-0.36334	Prss8	-1.2858
Nrg1	0.45745	Itpr1l1	-0.37189	Ip6k3	-1.2858
Sorbs3	0.45644	Vegfa	-0.37449	Asgr1	-1.2858
Smim3	0.4549	Gm16731	-0.37466	Foxc2	-1.3019
Dis3l2	0.4544	6430571L13Rik	-0.37819	Ky	-1.3196
Myl6	0.45207	H2afz	-0.38029	Gm14057	-1.3785
Hvcn1	0.45111	Exoc8	-0.38038	Apobec2	-1.3865
Ifitm10	0.44949	Spry4	-0.38107	Kcnk6	-1.3996
Hps4	0.44934	Nptx1	-0.38199	Phf19	-1.4704
Prss36	0.44825	Plk3	-0.38632	Tfcp2l1	-1.4887
Rims2	0.44597	Fgl2	-0.38676	AY036118	-1.4962
Fsd1	0.4458	Kcnc1	-0.38684	Mir17hg	-1.5252
Mbd3	0.44367	Cmtm3	-0.38735	Mss51	-1.5652
Mvk	0.44253	Dab2	-0.38846	Saa2	-1.9406
Zdhxc8	0.44	Gcc1	-0.39044	Rn7sk	-1.9897
Bcl2l1	0.43991	Slc39a1	-0.3917		

Supplementary file 6.

Gene Ontology of the first 5 ranked categories of the proteins enriched in the peripheral branch (p-value < 0.01).

Category	Term	-Log10 (pvalue)
CC	cytosol	4.304582
CC	extracellular region	3.388346
MF	peptidase inhibitor activity	3.482213
MF	enzyme inhibitor activity	2.944919
MF	intramolecular transferase activity	2.351698
MF	carboxylesterase activity	2.006527
MF	metallopeptidase activity	2.002999
BP	hexose metabolic process	4.825867
BP	monosaccharide metabolic process	4.465709
BP	vitamin metabolic process	4.311108
BP	cellular amino acid derivative biosynthetic process	4.38452
BP	nitrogen compound biosynthetic process	4.275343

Supplementary file 7.

Gene Ontology of the first 5 ranked categories of the proteins enriched in the central branch (p-value < 0.01).

Category	Term	-Log10 (pvalue)
CC	mitochondrial part	5.989123
CC	mitochondrial membrane	4.953733
CC	intracellular organelle lumen	4.438462
CC	organelle inner membrane	4.434637
CC	endoplasmic reticulum part	4.143938
MF	structural molecule activity	2.644809
MF	unfolded protein binding	2.356349
MF	intramolecular oxidoreductase activity	2.224285
MF	protein disulfide isomerase activity	2.224285
BP	cellular respiration	2.8366
BP	protein folding	2.740285
BP	generation of precursor metabolites and energy	2.571205
BP	microtubule cytoskeleton organization	2.257202
BP	cell division	2.212619

Supplementary file 8.

Gene Ontology of categories of the proteins upregulated in the peripheral branch after SNA (p-value < 0.01)

Category	Term	-Log10 (pvalue)
MF	carbohydrate binding	6.27424547
BP	regulation of transcription	4.327572225
BP	cell adhesion	4.168192354
BP	regulation of RNA metabolic process	3.8333266
CC	intracellular organelle lumen	3.787784834
BP	regulation of transcription, DNA-dependent	3.767438428
CC	organelle lumen	3.744861958
BP	response to wounding	3.585053145
BP	transcription	3.065756128
MF	sugar binding	2.874116809
BP	chemotaxis	2.669738824
CC	synapse	2.482311744
BP	neuron development	2.170021241
CC	synaptic vesicle	2.12224036

Gene Ontology of categories of the proteins downregulated in the peripheral branch after SNA (p-value < 0.01)

Category	Term	-Log10 (pvalue)
CC	ribosome	6.003346603
BP	translation	5.018834692
MF	ATP binding	3.710958106
MF	structural molecule activity	3.623715062
MF	adenyl nucleotide binding	3.533563984
MF	nucleoside binding	3.447132452
MF	ribonucleotide binding	3.377785599
CC	ribonucleoprotein complex	3.098694438
MF	motor activity	3.018773725
BP	actin filament-based movement	2.879723719
MF	ATPase activity	2.618438721
MF	nucleotide binding	2.588477906
CC	non-membrane-bounded organelle	2.476584382
BP	actin filament-based process	2.456472297
CC	cytosolic ribosome	2.074101517

Gene Ontology of categories of the differentially expressed proteins in the central branch after DCA (p-value < 0.01)

Category	Term	-Log10 (pvalue)
CC	ribosome	3.981381974
MF	structural constituent of ribosome	3.854693276
CC	ribonucleoprotein complex	2.699549681
BP	regulation of cell cycle	2.285294381
MF	structural molecule activity	2.231197496
BP	regulation of mitotic cell cycle	2.097281956
CC	mitochondrial lumen	2.146758912
CC	mitochondrial matrix	2.146758912

Supplementary file 9.

Enriched KEGG pathways (pvalue < 0.1) of the differentially expressed genes and proteins, in DRG and axoplasm after SNA

Term	-Log10 (pvalue)
Regulation of actin cytoskeleton	2.290923
Arginine and proline metabolism	2.064402
Insulin signaling pathway	1.77654
Neurotrophin signaling pathway	1.456849
Ribosome	1.29397
Starch and sucrose metabolism	1.253727
Fc gamma R-mediated phagocytosis	1.17251
Type II diabetes mellitus	1.167008
ABC transporters	1.139686
Jak-STAT signaling pathway	1.121999
Adipocytokine signaling pathway	1.088898
MAPK signaling pathway	1.05904
Pyruvate metabolism	1.026108
Melanoma	1.024136
Apoptosis	1.000132

Supplementary file 10.

Enriched KEGG pathways (pvalue < 0.1) of the differentially expressed genes and proteins, in DRG and axoplasm after DCA

Term	-Log10 (pvalue)
Ribosome	2.42609
Arginine and proline metabolism	1.897588

Butanoate metabolism	1.410039
beta-Alanine metabolism	1.241175
Valine, leucine and isoleucine degradation	1.129763

Supplementary file 11.

Protein list of AMPK α IP-mass spec after SNA and Sham compared with IgG

AMPK IP		
1.5 fold change		
Log2 > 0.58 ,log2 < -0.58		
SNA vs IgG		
Protein name	log2.Ratio.H.L.normalized.forward	log2.Ratio.H.L.normalized.reverse
Prkag2	9.42481714	-3.48860888
Ahnak	8.767787198	-8.483968711
Prkag1	8.085233429	-4.493101568
Psm8	6.645730475	-3.038598927
Psmc6	6.570447751	-4.560574731
Psmc2	6.275714808	-6.176576709
Psm11	6.135021758	-3.751484594
Psm2;Gm5422	6.042972583	-3.224047661
Psmc1	5.819872517	-3.681732913
Psmc5	5.497165246	-3.162169757
Prkab2	5.446984012	-4.279451848
Ppap2b	5.384913231	-2.526493604
Psm13	5.24587591	-4.549856647
Prkaa1	4.462837601	-3.439872024
Psm1	4.2124137	-2.313512919
Psm5	4.032806145	-2.321062737
Psm3	3.994308175	-4.01730024
Psmc4	3.93593114	-5.803735416
Psm6	3.924479992	-3.560166258
Psm7	3.808590988	-3.92690918
Prkab1	3.52656966	-1.67134733
Psm12	3.406672716	-2.719946395
Prkaa2	3.303634645	-4.342444135
Gphn	3.275781841	-2.937657202
Crmp1	3.153708072	-4.005272575
Rbms3;Rbms1	2.887174302	-5.531289492
Hspa4	2.675183626	-3.331452398
Cpsf1	2.628633634	-4.769964265
Rpl37a	2.610038557	-2.221623189
S100a10	2.600008027	-2.859247516

Psmc3	2.503323291	-4.053278122
Rps4x;Rps4l;Gm15013	2.388823247	-2.114847378
Rpl27	2.271604956	-2.275786313
Rps11	2.252930296	-1.833927324
Rps15a	2.153740494	-1.788564097
Rpl10a	2.123997204	-1.964939203
Rpl9	2.113300436	-1.486731613
Psm14	1.983312871	-3.357832636
Rbfox3;Rbfox2;Rbfox1	1.97019104	-2.208494292
Pura	1.835641165	-1.593398026
Rps3a1;Rps3a	1.814878504	-1.460846153
Fxr1	1.804301423	-1.703454492
Rplp0;Gm8730	1.763709007	-1.773096941
Rpl17	1.759837596	-1.902389203
LLRep3;Rps2;Gm18025;Gm6576;Gm8225;Gm5786;Gm10653	1.750349241	-1.594530372
Rpl30	1.731487392	-1.975283173
Rps16	1.718175283	-1.73082319
Sdha	1.68853847	-1.611843534
Rpl8	1.686612577	-1.896629934
Ahnak2	1.663663412	-1.79816543
Rpl12;Gm16519	1.643902355	-1.558431534
Rpl13	1.641823444	-1.716813093
Pabpc1	1.598079306	-1.715959736
Rpl23a	1.579083579	-1.759649031
Cnp	1.572356136	-1.391152917
Purb	1.563597463	-1.742699665
Rps13	1.534360472	-1.851625516
FAM120A	1.491083454	-0.954724794
Hist2h4;Hist1h4a	1.480988873	-1.491348241
Hspa8	1.433119698	-1.616215541
Rps8	1.425674135	-2.687520693
Anxa2	1.419808529	-1.956291542
Rps3	1.399936681	-1.474773006
Hnrnpd	1.398514552	-1.973865681
Pcbp2;Pcbp3	1.393251437	-1.580310105
Gm9493;Rps7	1.390777727	-1.83933792
Upf1	1.378678078	-1.045223005
Rpl3;Rpl3	1.33187716	-1.361601738
Rps14;rps14	1.329468079	-1.482452173
Rpl27a	1.268913416	-2.174491136
Rps18;Gm10260	1.230817842	-1.31423025
Elavl2	1.167807495	-1.14963261

Ywhah	1.052137623	-1.329522196
Epb4.1l2;Epb41l2	1.038646881	-0.757671884
Hspa5	1.036116453	-1.358158064
Hspa9	1.033581579	-1.184293423
Gm10036;Rpl11;Gm5093	0.995520699	-1.337557489
Hsp90aa1	0.954717448	-0.757745063
Slc25a5	0.944708548	-0.625088505
Rpl28	0.912113305	-1.085588556
Rps19	0.901108243	-1.161136955
Hnrnpk;Gm7964	0.881194737	-1.134413697
Ywhaq	0.855591108	-1.241304538
Prdx1	0.836004895	-1.265726099
Eef1a2	0.747859985	-0.859011989
Serbp1	0.745108226	-1.315378721
Ywhag	0.726918386	-1.02414974
Dpysl2	0.666574824	-1.124157042
Atp5c1	0.653426952	-0.732691935
Tpi1	0.607484193	-0.8633886
Hsp90ab1	0.600079412	-0.677541091

SHAM vs IgG

Protein name	log2.Ratio.H.L.normalized.forward	log2.Ratio.H.L.normalized.reverse
Prkag2	8.749400182	-3.062866566
Psmc5	8.733828833	-2.860923485
Psmc1	8.6370233	-2.757598708
Ahnak	8.00365845	-5.722876963
Prkag1	7.75141016	-3.756584388
Ppap2b	7.376602952	-3.565810018
Rbms3;Rbms1	6.578516105	-3.738370501
Psmc2	5.753283616	-5.651957988
Psmc4	5.736415462	-4.196911866
Psmc3	5.390702074	-3.694545382
Prkab2	4.511910749	-4.188127866
Crmp1	4.36429227	-2.618207205
Psmd13	4.023787614	-3.552731856
Psmd2;Gm5422	4.000991512	-3.044657435
Cpsf1	3.997653714	-2.480115955
Prkaa2	3.990864122	-3.734044691
Psmd7	3.854993017	-3.857134382
Rpl27	3.679311189	-2.868700269
Rbfox3;Rbfox2;Rbfox1	3.63784206	-2.522923705
Psmd5	3.399171094	-2.265067152
Rpl27a	3.252809222	-2.442614419

Rps24	3.202809492	-2.591092533
Pgam5	3.199845065	-2.367061785
Psmc6	3.113667165	-3.096159598
Psmd4	3.113400462	-2.876201392
Rpl18a	3.016425003	-0.650747968
Rpl8	2.876133814	-2.494840763
Gphn	2.854813541	-2.777541628
Psmd1	2.798423845	-2.29938273
Prkaa1	2.75332641	-3.163074065
Rps8	2.721438285	-2.269442641
Rps11	2.678545212	-2.149248574
Slc25a1	2.618778978	-1.627894829
Hist2h4;Hist1h4a	2.594978428	-1.397486109
Hspb1	2.593282053	-2.270973722
Rpl9	2.552622992	-2.347765927
Rps9	2.544707931	-0.793081765
Rps4x;Rps4l;Gm15013	2.532840574	-2.091786579
Rpl10a	2.507058837	-2.39775218
Psmd11	2.465870012	-4.054859788
Rpl3	2.415569395	-2.192776988
Ahnak2	2.355495579	-2.410581651
Rpl37a	2.291190964	-1.989363364
Rpl17	2.182755851	-1.714775355
Rpl35a	2.175588471	-0.898242364
Psmd6	2.165107985	-2.931370459
Anxa2	2.155813984	-2.011529802
Rpl6;Gm5428	2.117528824	-2.384734384
Rpl24	2.115832299	-2.233108062
Rps13	2.094573898	-2.082224559
Gm9493;Rps7	2.070354978	-1.812080265
Rpl28	2.022154722	-1.075854496
Rpl5	2.020057652	-2.252157197
Rpl23a	1.993819258	-2.160233859
Rpl21	1.993348292	-2.700403651
Upf1	1.943546308	-1.526992432
Rplp0;Gm8730	1.931456141	-1.768567592
Rps18;Gm10260	1.898982227	-1.624154275
Ddx3y;D1Pas1;Ddx3x	1.871883066	-0.668661666
Hspa4	1.867856938	-3.166178862
Rps17	1.847676272	-2.077893512
Rpl31	1.836489726	-2.095419565
Rpl13	1.822934048	-0.685709516
Rpl12	1.770490792	-1.768715064

Hspa8	1.769390919	-1.607220989
Hsp90aa1	1.755101219	-1.17299399
FAM120A	1.747172537	-1.468970444
Hspg2	1.739848103	-0.799570979
Rps14;rps14	1.736994448	-1.713024252
Rps3a1;Rps3a	1.732225777	-1.774034124
Cnp	1.729835517	-1.415576206
Rps6	1.72320904	-1.415845635
Rps15a	1.698440756	-1.724134745
Rps2;Gm6576;Gm5786;Gm18025;LLRep3;Gm8225	1.618943383	-1.10547323
Rpsa	1.614332928	-0.634016378
Pcbp3	1.608241513	-1.199984361
Rps16	1.581495871	-1.826130617
Gm10036;Rpl11;Gm5093	1.576377015	-1.756867155
Rps3	1.544831552	-1.351074441
G3bp2	1.541118304	-1.163817315
Pabpc1	1.531518705	-1.235789746
Pura	1.524113838	-1.665797879
Prdx1	1.456963812	-1.535749966
Rps19	1.397857712	-1.503813791
Ywhah	1.3934162	-1.836604321
Rpl30	1.335940529	-1.949143114
Prx	1.326997465	-0.855614213
Psm12	1.318634995	-1.698388943
Fmr1	1.263815654	-1.501973853
Rps5	1.26141046	-0.997405483
Ldha	1.258760107	-0.806997899
Ywhag	1.240802778	-0.910528968
Hbbt1;Hbb-bs;HBB1;Hbb-b1	1.239275826	-1.388128873
Purb	1.238481171	-1.89009122
Atp5c1	1.235972083	-1.352584171
Tecr	1.22718656	-1.354095484
Dpysl2	1.186246986	-1.534537424
Hsp90ab1	1.177407578	-1.122208642
Rpl15;Gm10020	1.173703117	-1.323804819
Eef1a2	1.162467868	-0.984845019
Prkab1	1.160016608	-3.097887821
Hnrnpm	1.117096566	-1.683020169
Elavl2	1.105074594	-1.315845549
Psm14	1.100103022	-2.705005853
Tpi1	1.09369538	-1.911207098
Fxr1	1.082021269	-1.24814213

Hnrnpd	1.064951812	-2.121800441
Hspa5	1.041383179	-1.225699982
Hnrnpab	1.012926174	-0.671669027
Rps20	0.932590365	-1.246600844
Eef1a1	0.881821213	-0.95042499
Hadha	0.770617647	-0.780165476
Rpl14;Rpl14-ps1	0.718526026	-1.40789942
Rtcb	0.712023431	-0.993436265
Hnrnpk;Gm7964	0.69706208	-0.87450759
Sdha	0.682573297	-2.106001047
Gja1	0.60767356	-0.656808243

Acknowledgements

This work was carried out during the years 2013-2017 at the Hertie Institute for Clinical Brain Research, Center of Neurology, University of Tübingen.

First of all, I owe my deepest gratitude to my supervisor, Prof. Simone Di Giovanni, without his guidance, encouragement and financial support, this work would hardly have been complete. I am also deeply grateful to my family, especially my husband, Dr. Luming Zhou, who gives me the greatest help and support on my work and life. Moreover, I would like to thank my Advisory Board Committee members, Dr. Jing Hu and Dr. Andrea Wizemann for their professional advice and supervision. I am also very grateful to Prof. Philipp Kahle for the assessment of my thesis and Dr. Jonas Neher for his attendance in my graduation defense.

Furthermore, I am grateful to Dr. Ilaria Palmisano, Elisabeth Serger, Dr. Anja Freiwald, Dr. Radhika Puttagunta and all collaborators for their contribution to my work.

Lastly, I would like to thank Chinese Scholarship Council, Hertie Institute and Graduate Training Centre of Neuroscience, University of Tübingen, for providing financial supports on my work, international conferences as well as life maintenance.

Curriculum Vitae

Guiping Kong

Personal Information:

University of Tübingen
Hertie Institute for Clinical Brain Research
Otfried-Müller-Straße 27
72076 Tübingen
Germany
E-mail address: guipingkong0804@gmail.com

Education:

- | | |
|------------------|---|
| 09.2013- Present | PhD student in Laboratory for Neuro Regeneration and Repair, Hertie Institute for Clinical Neuroscience, University of Tübingen, and Graduate Training Centre of Neuroscience, Tübingen, Germany.
Supervisor: Prof. Dr. Simone Di Giovanni |
| 09.2009- 06.2012 | Master of Chemicobiology, Metabolic Disease Research Center, School of Pharmaceutical Science, Xiamen University, Fujian, China.
Supervisor: Prof. Dr. Zhongxian Lv |
| 09.2005- 06.2009 | Bachelor of Biotechnology, School of Life Science, Qufu Normal University.
Supervisor: Dr. Xiangyong Peng |

Experience:

- | | |
|------------------|---|
| 01.2013- 05.2013 | Research assistant (part time) in Center for Plant Molecular Biology, University of Tuebingen, Germany. |
| 02.2009- 07.2009 | Research assistant in College of Life Science, Qufu Normal University, Jining, P.R.China. |

Awards

- | | |
|------------|--|
| 2013- 2016 | Doctoral Scholarship of China. |
| 04. 2012 | Scholarship of scientific research of School of Pharmaceutical Science, Xiamen University. |
| 2009- 2012 | Master scholarship of School of Pharmaceutical Science, Xiamen University. |

2006- 2008 Bachelor scholarship of School of Life Science, Qufu Normal University.

Conference presentations

12. 2016 Kong G. AMPK controls the regenerative programme of DRG sensory neurons after injury. Society of Neuroscience 2016. San Diego, CA, US.
11. 2016 Kong G. AMPK controls the regenerative programme of DRG sensory neurons after injury. NeNa 17th conference. Schramberg, Germany.

Publications

Arnau Hervera*, Luming Zhou*, Ilaria Palmisano, Eilidh McLachlan, **Guiping Kong**, Thomas Hutson, Matt C Danzi, Vance P. Lemmon, John L. Bixby, Andreu Matamoros-Angles, José Antonio del Río, Kirsi Forsberg, Francesco De Virgiliis, Dina P. Matheos, Janine Kwapis, Marcelo A. Wood, Radhika Puttagunta, Simone Di Giovanni. Reactive oxygen species regulate axonal regeneration through the release of exosomal NADPH oxidase 2 complexes into injured axons. *Nature cell Biology* (Published online: 12.2.2018).

Dongping Liu ^{a+}, **Guiping Kong** ^{a+}, Quan Cheng Chen ^a, Guanghui Wang^a, Jie Li ^a, Yang Xu ^a, Ting lin ^a, Yingpu Tian ^a, Xiaokun Zhang ^{a,b}, Xinsheng Yao ^{a,c}, Gensheng Feng ^{a,d}, Zhongxian Lu ^{a,*}, Haifeng Chen ^{a,*}. Fatty acids as natural specific inhibitors of the proto-oncogenic protein Shp2. *Bioorganic & Medicinal Chemistry Letters* 21 (2011) 6833–6837.
**These authors contributed equally to this work.*

Yanyan Bu ^{a,+}, Tao Shi ^{b,+}, Minghui Meng ^{a,+}, **Guiping Kong** ^a, Yingpu Tian ^a, Quancheng Chen ^b, Xinsheng Yao ^{b,c}, Gensheng Feng ^{a,d}, Haifeng Cheng ^{b,*}, Zhongxian Lu ^{a,*}. A novel screening model for the molecular drug for diabetes and obesity based on tyrosine phosphatase Shp2. *Bioorganic & Medicinal Chemistry Letters* 21 (2011) 874–878.

Jia Hu,^[a] Jie Wu,^[a] Cong Li,^[a] Ling Zhu,^[a] Wei Yun Zhang,^[a] **Guiping Kong**,^[b] Zhongxian Lu,^{*[b]} and Chaoyong James Yang^{*[a]}. A G-Quadruplex Aptamer Inhibits the Phosphatase Activity of Oncogenic Protein Shp2 in vitro. *ChemBioChem* 2011, 12, 424–430.